NASA CR-143668

EARTH OBSERVATORY SATELLITE SYSTEM DEFINITION STUDY

REPORT NO. 3: DESIGN/COST TRADEOFF STUDIES

- Appendix E: EOS Program Supporting System
- Part 1: System Trade Studies No. 1 through 8

(NASA-CR-143668) EARTH OBSERVATORY SATELLITE SYSTEM DEFINITION STUDY. REPORT NO. 3: DESIGN/COST TRADEOFF STUDIES. APPENDIX E: EOS PROGRAM SUPPORTING SYSTEM. PART 1: SYSTEM TRADE STUDIES NO. 1 (Grumman

N75-15714

Unclas

G3/18 09251

GRUMMAN

EARTH OBSERVATORY SATELLITE SYSTEM DEFINITION STUDY

REPORT NO. 3: DESIGN/COST TRADEOFF STUDIES
- **Appendix E: EOS Program Supporting System**
- **Part 1: System Trade Studies No. 1 through 8**

Prepared For

NATIONAL AERONAUTICS AND SPACE ADMINISTRATION

GODDARD SPACE FLIGHT CENTER

GREENBELT, MARYLAND 20771

Prepared By

GRUMMAN AEROSPACE CORPORATION

BETHPAGE, NEW YORK 11714

NAS 5-20520

September 1974

CONTENTS

------

*System Trade Study No.

5/5

SYSTEM TRADE
STUDY NO. 1

GRUMMAN

TRADE STUDY REPORT

TITLE	TRADE STUDY REPORT NO. 1
ORBITAL ALTITUDE SELECTION	WBS NUMBER

See Report No. 1, Orbit/Launch Vehicle Trade-Off Studies and Recommendations

PREPARED BY	GROUP NUMBER & NAME	DATE	CHANGE LETTER
			REVISION DATE
APPROVED BY			PAGE 1-1

SYSTEM TRADE
STUDY NO. 2

GRUMMAN

TRADE STUDY REPORT

TITLE	TRADE STUDY REPORT NO. 2
LAUNCH VEHICLE SELECTION	WBS NUMBER

See Report No. 1, <u>Orbit/Launch Vehicle Trade-Off Studies and Recommendations</u>

PREPARED BY	GROUP NUMBER & NAME	DATE	CHANGE LETTER
			REVISION DATE
APPROVED BY			PAGE 2-1

*GAC 3711

SYSTEM TRADE
STUDY NO. 3

TITLE	TRADE STUDY REPORT NO. 3
Shuttle Compatibility	WBS NUMBER 1.2.1.4.4

Purpose: The purpose of this study is to identify the design requirements and associated cost impacts for using the Shuttle for EOS delivery, and the additional impact of achieving full compatibility for resupply and retrieval. At this point in the study, the intent is to provide a preliminary assessment of these impacts and identify areas for further analyses.

Summary: A preliminary assessment of the design and cost impact of configuring the EOS for Shuttle compatibility in delivery, retrieval, and resupply modes has been completed for the entire mission model, Table 3-1. Assuming that each spacecraft was initially delivered by a conventional launch vehicle, the minimum functional requirements, associated design changes, and incremental spacecraft weight and cost impacts were estimated for EOS compatibility with each of the potential Shuttle utilization modes. Analyses during this study phase emphasized the impact on the EOS flight hardware.

Conclusions and Recommendations: Based on the results of analysis to date, EOS-Shuttle compatibility can be realized with reasonable spacecraft weight and cost penalties. Inherent Shuttle capabilities are adequate to meet the requirements of all missions except E and F. Mission E (Tiros O) may be accommodated by either an EOS orbit transfer capability or a Tug. The Tug appears to be the only viable approach to satisfying the Mission F (SEOS) requirements. Excluding the Orbit Transfer Subsystem (OTS) assumed for Mission E, Shuttle delivery and retrieval compatibility add only about 40 lb to spacecraft weight while the addition of mechanisms to enable on-orbit replacement of spacecraft modules and assemblies results in a weight impact of about 200 lb. for resupply. Cost impacts range

PREPARED BY B. Sidor	GROUP NUMBER & NAME	DATE 7/17/74	CHANGE LETTER
			REVISION DATE
APPROVED BY			PAGE 3-1

SPACECRAFT	INITIAL LAUNCH VEHICLE	INITIAL LAUNCH DATE	MISSION CHARACTERISTICS	
			ALTITUDE (n. mi)	INCLINATION (deg)
EOS-A	DELTA 2910	'79	366	98
EOS-A'	DELTA 2910	'80	366	98
EOS-B	DELTA 3910	'81	366	98
EOS-B'	DELTA 3910	'82	366	98
EOS-C	TITAN IIIB/SSB	'80	366	98
EOS-D	DELTA 2910	'81	324	90
EOS-E	TITAN IIIB/SSB	'82	915	103°
EOS-F	TITAN III C7/ TE 364-4	'81	19323	0°
SHUTTLE DEMO	SHUTTLE	'80	160	28.5

Table 3 - 1
Mission/Traffic Model

from a low of $287K non-recurring/$69K recurring for Delivery to $2111K/$464K for Resupply. The OTS, peculiar to Mission E, adds significantly to the impact on spacecraft weight and cost.

Addition of Shuttle compatibility provisions for any mode do not result in exceeding the performance capabilities of the launch vehicles assumed for initial delivery.

In-flight verification of EOS-Shuttle compatibility, requiring the availability of a Shuttle Demonstration Model spacecraft is considered necessary for only the Resupply mode. Deployment and retrieval techniques do not differ significantly from conventional spacecraft.

Cost and Weight Summary: Table 3-2 summarizes the cost and weight impacts of configuring each EOS mission concept for compatibility with Shuttle delivery, retrieval, and resupply modes. Cost and weight impacts for Mission E include the Orbit Transfer Subsystem (OTS) unique to this mission. Exclusive of the OTS, the weight impact is 42, 45, and 192 lb for the three Shuttle modes respectively. Recurring costs are quoted for a single spacecraft only. The marked jumpin costs for resupply reflect the addition of module replacement mechanisms to the spacecraft, qualification of the Systems Qualification Spacecraft for in-flight verification of resupply techniques, and associated Engineering-type activities.

TABLE 3 - 2 SHUTTLE COMPATIBILITY IMPACT SUMMARY

IMPACT PARAMETER	MISSION								SHUTTLE MODE		
	A	A'	B	B'	C	D	E	F	DELIVER	RETRIEVE	RESUPPLY
COST ($K)											
Non-Recurring	X	X	X	X					287	680	2039
					X	X			287	680	2111
							X		587	980	2390
								X	287	680	1996
Recurring	X	X	X	X					69	195	430
					X	X			69	195	464
							X		189	435	445
								X	69	195	410
WEIGHT (LB)	X	X	X	X					42	45	183
					X	X			42	45	203
							X		590	1634	1781
								X	42	45	171

Discussion:

Introduction:

This study addresses the impact of developing the EOS to be physically compatible with the Shuttle delivery, retrieval, and resupply modes. The full impact of Shuttle utilization is the combination of design, operational, and program considerations which is to be addressed in the next study increment in the Shuttle Interface/Utilization Study (Book 6). This study, then, provides a preliminary indication of one aspect of the broader utilization question, that of design compatibility.

Groundrules, Guidelines, and Assumptions:

The study was conducted in accordance with the following constraints:

a. All missions in the mission model (Table 3-1) are to be considered.

b. All missions are delivered initially by the launch vehicle cited in Table 3-1.

c. All missions are continued through the Shuttle operational era making each a candidate for Shuttle compatibility.

d. Baseline modular subsystems for all EOS concepts

e. Baseline current Shuttle-based EOS Flight Support System (FSS) definition

f. Baseline Module Exchange Mechanism (MEM) resupply concept

g. Potential Shuttle utilization modes are limited to:

- o Delivery only
- o Delivery plus retrieve
- o Delivery plus retrieve plus resupply

h. For mission F only, a Tug, having payload interface characteristics identical to the Titan IIIC7/TE 364-4, is assumed.

i. The minimum requirements for Shuttle compatibility are defined.

These constraints will be re-assessed for follow-on study activities.

Approach:

For this study phase, emphasis was placed on physical impact on basic spacecraft design. Instruments and operations were considered only to the extent that they influenced the basic spacecraft. The overlying philosophy applied was that each mission spacecraft was designed for initial delivery on a conventional launch vehicle and, therefore, Shuttle compatibility provisions were in addition to, rather than in lieu of, basic design characteristics. Potential Shuttle utilization modes were considered in order of increasing complexity (i.e. Deliver, Retrieve, and then Resupply).

Development of compatibility impact estimates was a three-step process. First, the functional requirement increments for each mode were identified for each of three areas; EOS Spacecraft Design, Instrument and Operations. For convenience, the spacecraft was addressed in five groupings of related functions:

- Communications and Data Handling
- Electrical Power
- Attitude Control
- Structure/Mechanical/Thermal
- Propulsion
  - The propulsion group includes Reaction Control, Orbit Adjust, and Orbit Transfer functions as required by the individual missions.

Functional differences between an EOS spacecraft designed for conventional launch vehicle delivery only and one configured for Shuttle compatibility in each projected Shuttle utilization mode were identified for each program area. These requirements are summarized in Table 3-3. The requirements are additive, unless otherwise noted, since each successive Shuttle utilization mode includes the preceding modes (i.e. Delivery, Delivery plus Retrieval, Delivery plus Retrieval plus Resupply). For example, the Propulsion (item 1.5) requirement to provide for pressure relief (No. 1) applies to all modes. Requirement 2, applicable to Mission E only, imposes a transfer capability to mission orbit for Delivery and adds transfer back to Shuttle orbit for Delivery and Resupply. Requirement 3 applies only to Resupply.

As shown in Fig. 3-1, the Shuttle has a capability of 9600 lb for the 366 n.mi altitude and 98° inclination for missions A-C, with close to 20,000 lb for Mission D (324 n.mi and 90°). For these missions, Shuttle capability is adequate to meet EOS demands. Missions E (915 n.mi., 103° and F (19323 n.mi, 0°), however, both require performance significantly in excess of Shuttle capabilities. Both missions can be accommodated by projected Tug capabilities and Mission E could be satisfied by a moderately sized kick stage integral to the EOS. An integral kick stage does not appear practical for Mission F. For comparison purposes, the requirements for Mission E include the kick stage while Mission F assumes the Tug. Due to the status of Tug definition at this time, the interfaces between it and EOS have been assumed to be identical to those of the initial launch vehicle, the Titan IIIC7/TE 364-4.

ORIGINAL PAGE IS OF POOR QUALITY

TABLE 3 - 3

SHUTTLE COMPATIBILITY - REQUIREMENTS IMPACT

CONSIDERATION	MISSION APPLICATION								REQUIREMENT			REMARKS
	A	A'	B	B'	C	D	E	F	DELIVER	RETRIEVE	RESUPPLY	
1. EOS S/C DESIGN												
1.1 Comm & Data Handling	X	X	X	X	X	X	X	X	1. Provide for immediate relay to the Orbiter crew, readout of EOS parameters critical to Shuttle system and range safety operations while the EOS is attached to or in the vicinity of the orbiter			
									2. Provide for command override of critical EOS functions by the Orbiter crew while attached to or in the vicinity of the Orbiter.			
									3. Provide for relay of EOS/Instrument status data through the Orbiter while attached to or in the vicinity of the Orbiter			During EOS operation near Orbiter the Orbiter may occlude EOS antenna line-of-sight to ground stations.
										4. Provide for stowing dish antennas		
											5. Provide for on-orbit replacement of dish antennas.	
1.2 Electrical Power	X	X	X	X	X	X	X	X	1. Provide for 24 hr stay in Orbiter prior to deployment	1. Same plus provide for 24 hr. stay in Orbiter after recovery	1. Same plus provide for sustained power during servicing	Assumed worst case condition
										2. Provide for stowing solar arrays	2. Same 3. Provide for interruption and restoration of wiring runs among S/C and Instrument modules.	

ORIGINAL PAGE IS
OF POOR QUALITY

TABLE 3 - 3 (cont)

SHUTTLE COMPATIBILITY - REQUIREMENTS IMPACT

CONSIDERATION	MISSION APPLICATION								REQUIREMENT			REMARKS
	A	A'	B	B'	C	D	E	F	DELIVER	RETRIEVE	RESUPPLY	
1.2 Electrical Power(cont)	X	X	X	X	X	X	X	X			4. Provide for on-orbit replacement of solar arrays	
											5. Provide for on-orbit replacement of power module	
										6. Provide for sustaining power with non-operating solar arrays		Assumes arrays retracted for ease of SAMS acquistion
1.3 Attitude & Control	X	X	X	X	X	X	X	X			1. Provide for on-orbit replacement of ACS module	
										2. Provide back-up attitude hold capability		For fail-safe operation in vicinity of Orbiter and on-orbit survivability.
1.4 Structure/Mechanical/Thermal	X	X	X	X	X	X	X	X	1. Provide for Shuttle induced ascent and abort re-entry loads	1. Same plus provide for descent and landing loads		
									2. Provide for Shuttle ascent and abort re-entry induced environment	2. Same plus provide for descent and landing induced environment		
									3. Provide attachment to FSS cradle			
									4. Provide for mating to FSS docking/deployment platform			
									5. Provide for acquisition by SAMS			
											6. Provide for on-orbit detachement/attachment of replaceable assemblies/modules	

TABLE 3 - 3 (cont)

SHUTTLE COMPATIBILITY - REQUIREMENTS IMPACT

CONSIDERATION	MISSION APPLICATION								REQUIREMENT			REMARKS
	A	A'	B	B'	C	D	E	F	DELIVER	RETRIEVE	RESUPPLY	
1.9 Propulsion	X	X	X	X	X	X	X	X	1. Provide for propellant tank pressure relief			
							X	X	2. Provide for EOS transfer from parking orbit to mission orbit	2. Same plus provide for transfer from mission orbit to Orbiter parking orbit.		Integral EOS capability required only if Tug is unavailable
	X	X	X	X	X	X	X	X			3. Provide for on-orbit replacement of propulsion module	EOS Pneumatics, OAS, and/or OTS, as needed for mission, contained in common module
2.0 INSTRUMENTS	X	X	X	X	X	X	X	X		1. Provide for retraction of all deployable elements		
											2. Provide for on-orbit replacement of Instrument modules/assemblies	
3.0 OPERATIONS 3.1 Flight Operations	X	X	X	X	X	X	X	X			1. Provide for in-flight demonstration of EOS servicing/resupply	Assumes that deployment and retrieval technique demonstrated with prior S/C
									2. Provide for pre-deployment checkout of EOS systems/subsystems and Instruments			
										3. Provide for on-orbit survival in excess of mission design life		Contingent upon outcome of design life/resupply study

TABLE 3 - 3 (cont)

SHUTTLE COMPATIBILITY REQUIREMENTS IMPACT

CONSIDERATIONS	MISSION APPLICATION								REQUIREMENTS			REMARKS
	A	A'	B	B'	C	D	E	F	DELIVER	RETRIEVE	RESUPPLY	
3.2 Ground Operations	X	X	X	X	X	X	X	X	1. Provide for pre-launch integration of EOS with shuttle			
										2. Provide for ground handling of landed EOS		
										3. Provide for ground-based refurbishment of EOS sub-system and Instrument modules and assemblies		
										4. Provide for replacement EOS modules/assemblies		
									5. Provide for integrated EOS-Shuttle flight scheduling			
									6. Provide for integrated EOS-Shuttle mission planning			
									7. Provide for voice-data communications between EOS and Shuttle operations control centers			

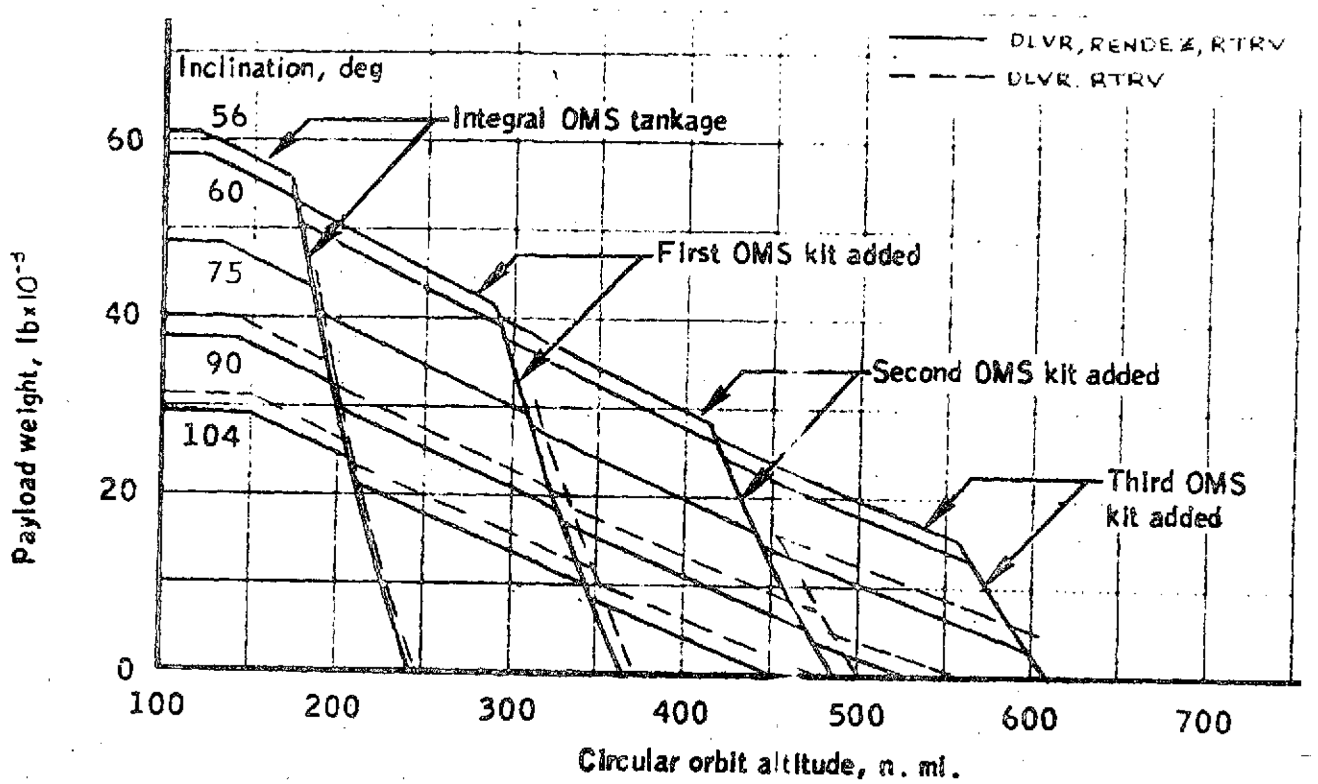

- VAFB

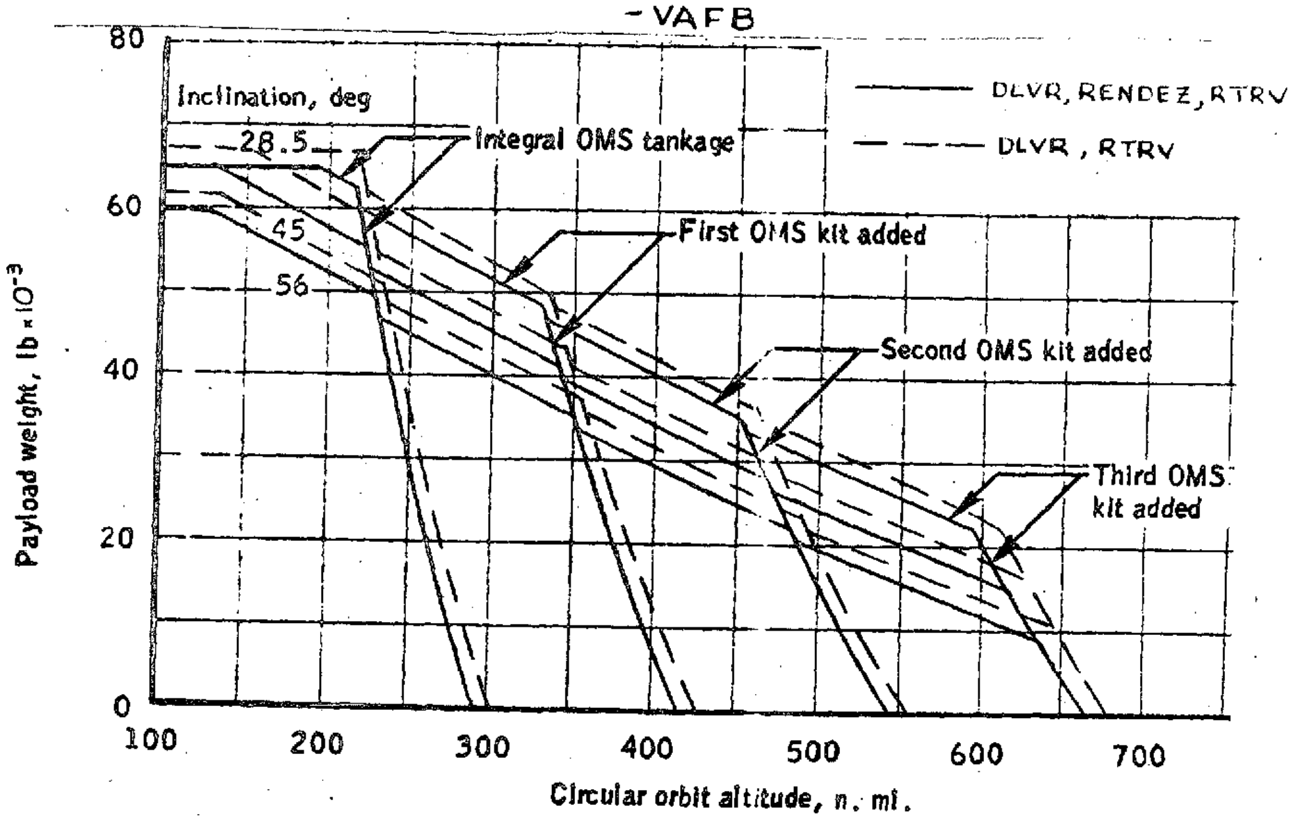

- KSC -

FIGURE 3 - 1 SHUTTLE PAYLOAD WEIGHT vs CIRCULAR ALTITUDE

The second step of the process was to identify the design implications of each additional functional requirement. Table 3-4 lists the visible design changes resulting from the requirements. The format of Tables 3-3 and-4 are identical to permit direct correlation between requirement and design change. No changes have been defined for the Ground Operations requirements since the changes are dependent upon a number of programmatic issues, including flight interval and overall program definition, which will have a profound influence on resultant impacts. The assumed availability of Tug for Mission F results in no unique design implications for that mission.

The final step in the process was to estimate the weight and cost impact of each design change on the EOS program. In Table 3 - 5, the weight increment, and associated non-recurring and recurring costs for achieving Shuttle compatibility for one EOS spacecraft are estimated for each projected Shuttle utilization mode. Two significant points are evident in the table:

a. The difference between weight impacts for "Deliver" and "Retrieve" modes is insignificant.

This is the result of using the baseline FSS concept which utilizes the same equipment for either deployment or retrieval. For deployment only arrangements which dispense with the FSS cradle and docking/deployment table could conceivably reduce spacecraft impact. The major effect of such an approach however, would be to reduce the ancillary equipment requirements which necessitate the FSS. The significance of this effect is contingent upon whether or not an EOS would be developed to support Shuttle-borne spacecraft other than EOS.

TABLE 3 - 4

SHUTTLE COMPATIBILITY - DESIGN IMPLICATIONS

CONSIDERATION	MISSION APPLICATION								DESIGN			REMARKS
	A	A'	B	B'	C	D	E	F	DELIVER	RETRIEVE	RESUPPLY	
1. <u>EOS S/C DESIGN</u> 1.1 Comm & Data Handling	X	X	X	X	X	X	X	X	1. Add a hardwire interface including a separable connection, capable of: a. Transmitting selected C&W signals b. Receiving selected commands	1. Add a make/break/make connector to "Deliver" design		Basic EOS software is designed to process the same data for nominal mission operations. Flagging C&W conditions has insignificant impact.
									2. RF Interface No impact			RF interface reqmt. is met by EOS-ground implementation of baseline system.
									3. Data/Cmd Relay see item 1			
										4. Antenna Stowage Add retraction mechanism to all antennas extending beyond allowable P/L envelope		Basic S/C antennas are fixed. Instrument Mission Peculiar deployable antennas have not been assessed.
											5. Antenna Replacement a. Add structural attach/release mechanisms b. Add power disconnects c. Add signal disconnects	Assumes that required provisions will be incorporated in mission peculiar equipment so no impact has been defined.
1.2 Electrical Power	X	X	X	X	X	X	X	X	1. Attach to Orbiter a. Add disconnect b. Add switching assembly			
										2. Stow Arrays a. Baseline roll-up concept b. Add reversing to drive motors. c. Add stowage latches		
											3. Convert from manual to automatic connector mating.	Connector requirements identified in individual design areas are compiled in this item. Assumes that Instruments come appropriately equipped.

TABLE 3 - 4 (cont)

SHUTTLE COMPATIBILITY - DESIGN IMPLICATIONS

CONSIDERATION	MISSION APPLICATION								DESIGN			REMARKS
	A	A'	B	B'	C	D	E	F	DELIVER	RETRIEVE	RESUPPLY	
1.2 Electrical Power (cont)	X	X	X	X	X	X	X	X			4. Replace Arrays a. Add structural attach/ release mechanisms b. Add power disconnect c. Add signal disconnect	
											5. Replace Power Module a. Replace disconnect b. Add structural attach/ release mechanisms	
										6. Sustaining Power No impact		Battery assemblies in baseline design provide 40-120 amp-hrs dependent upon mission
1.3 Attitude Control	X	X	X	X	X	X	X	X			1. Replace Module a. Add structural attach/ release mechanisms b. Add signal disconnects c. Add power disconnects	Replace provisions required for both ACS module and 3-axis magnetometer
										2. Back-Up Attitude Control [illegible] • ± 1° • ± 1°/sec		For Orbiter safety during EOS recovery
1.4 Structure/Mechanical/ Thermal	X	X	X	X	X	X	X	X	1. Loads No impact	1. Loads No impact		a. Design load conditions for Delta more stringent for ascent b. Descent and Landing loads less stringent than ascent plus abort
									2. Environment a. Qualify structure and equipment to higher acoustic levels			Impact undefined

TABLE 3 - 4 (cont)

SHUTTLE COMPATIBILITY - DESIGN IMPLICATIONS

TRADE STUDY REPORT 3

WBS NUMBER 1.2.1.4.4

CONSIDERATION	MISSION APPLICATION								DESIGN			REMARKS
	A	A'	B	B'	C	D	E	F	DELIVER	RETRIEVE	RESUPPLY	
1.4 Structure/Mechanical/ Thermal (cont)	X	X	X	X	X	X	X	X	3. FSS Cradle a. Add attach/release fittings at selected points on upper bulkhead b. Qualify structure for cantilevered mounting at upper bulkhead			a. Full circumference transition ring vs discrete attach fittings is currently under study b. Pick-up for conventional launch vehicle is at lower bulkhead
									4. FSS Docking/Deployment Platform a. Add four passive docking probes to lower bulkhead b. Add power disconnect c. Add comm disconnect			b/c. Optimum arrangement of connectors to accommodate S/C - Orbiter configuration in stowed, attached to docking/deployment table, and rotated modes is subject to study
									5. SAMS Interface Add passive attach fitting to upper bulkhead			Assuming that the cradle attach fittings will accommodate manipulator pick-up, there is no impact.
											6. MEM Interface Add attach/release latches compatible with MEM module handling fixture to all replaceable modules/assemblies	- All latches identified for individual design areas are compiled in this item - Simplified latch mechanism offers potential simplification of current MEMS design

TABLE 3 - 4 (cont)

SHUTTLE COMPATIBILITY - DESIGN IMPLICATIONS

CONSIDERATION	MISSION APPLICATION								DESIGN			REMARKS
	A	A'	B	B'	C	D	E	F	DELIVER	RETRIEVE	RESUPPLY	
1.5 Propulsion	X	X	X	X	X	X	X	X	1. Pressure Relief a. Add GN_2 pressure relief assembly to propellant tank pressurant storage b. Add GN_2 vent to Orbiter P/L bay.			
							X		2. Orbit Transfer a. Add SRM's to raise apogee from 300n mi to 915n mi b. Add SRM's to circularize at 915n mi	2. Orbit Transfer a. Same plus add SRM to lower apogee from 915n mi to 300n mi and circularize		Mission F utilizes a Tug. Interfaces are assumed consistent with initial launch vehicle requiring no additional provisions
	X	X	X	X	X	X	X	X			3. Replace Module a. Add structural attach/release mechanisms b. Provide unobstructed lateral motion c. Add signal/power disconnects	
2. INSTRUMENTS	X	X	X	X	X	X	X	X		1. Appendage Retraction Not considered at this time		For this phase of study, only the latch mechanisms have been considered
											2. Replace Instruments a. Provide structural attach/release mechanisms	

ORIGINAL PAGE IS OF POOR QUALITY

TABLE 3-4 (cont)

SHUTTLE COMPATIBILITY - DESIGN IMPLICATIONS

TRADE STUDY REPORT 3

WBS NUMBER 1.2.1.4.4

CONSIDERATION	MISSION APPLICATION								DESIGN			REMARKS
	A	A'	B	B'	C	D	E	F	DELIVER	RETRIEVE	RESUPPLY	
3. OPERATIONS 3.1 Flight Operations	X	X	X	X	X	X	X	X			1. Shuttle Demo a. Reconfigure ground qualification spacecraft for flight status b. Qualify demo model for flight	
									2. In-Flight Checkout No impact			Combination of AOP, Shuttle-based system, and ground support is adequate
										3. Survival a. Add RCS vlv redundancy b. Add backup attitude sensing (see ACS)		Based on prior experience on OAO and ERTS, consumables sized for design life will be adequate
3.2 Ground Operations	X	X	X	X	X	X	X	X	Not Defined	Not Defined	Not Defined	Impact on ground ops is a function of flight frequency, number of spacecraft, etc. It will be addressed in the upcoming Shuttle Utilization analysis.

TABLE 3 - 5

SHUTTLE COMPATIBILITY IMPACT ASSESSMENT

CONSIDERATION	MISSION								DELIVER			RETRIEVE			RESUPPLY		
	A	A'	B	B'	C	D	E	F	WT (lb)	COST ($K) NON-REC	COST ($K) RECUR	WT (lb)	COST ($K) NON-REC	COST ($K) RECUR	WT (lb)	COST ($K) NON-REC	COST ($K) RECUR
COMM & DATA HANDLING																	
o C & W Interface	X	X	X	X	X	X	X	X	2	Insig	Insig	2	Insig	Insig	2	Insig	Insig
ELECTRICAL POWER																	
o Solar Array Stow	X	X	X	X	X	X	X	X				1	74	2	1	74	2
o Module Interface Connectors/Receptacles	X	X	X	X	X	X	X	X							53	157	90
ATTITUDE CONTROL																	
o Analog Processor	X	X	X	X	X	X	X	X				1	55	40	1	55	40
STRUCT/MECH/THERM																	
o Cradle Attach Fittings	X	X	X	X	X	X	X	X	36	126	61	36	126	61	36	126	61
o Dock/Deploy Table Probes	X	X	X	X	X	X	X	X	2	8	3	2	8	3	2	8	3
o Latches/Pins																	
- Basic S/C	X	X	X	X	X	X	X	X							38	138	65
- Instruments	X	X	X	X											26	94	44
					X										43	155	73
						X									46	166	78
							X								36	130	61
								X							18	65	31

TABLE 3 - 5 (cont)

SHUTTLE COMPATIBILITY IMPACT ASSESSMENT

CONSIDERATION	MISSION								DELIVER			RETRIEVE			RESUPPLY		
									WT	COST ($K)		WT	COST ($K)		WT	COST ($K)	
	A	A'	B	B'	C	D	E	F	(LB)	NON-RECUR	RECUR	(LB)	NON-RECUR	RECUR	(LB)	NON-RECUR	RECUR
o Rollers/Tracks																	
- Basic S/C	X	X	X	X	X	X	X	X							14	51	24
- Instruments	X	X	X	X											7	25	12
					X										10	36	17
						X									7	25	12
							X								6	22	10
								X							3	11	5
o Propulsion																	
- Pressure Relief	X	X	X	X	X	X	X	X	2	33	5.4	2	33	5.4	2	33	5.4
- Redundant S/O Vlv	X	X	X	X	X	X	X	X				1	0	3.5	1	0	3.5
- Kick Stage							X		548	300	120	1589	300	240	1589	300	240
SHUTTLE DEMO MODEL	X	X	X	X	X	X	X	X							N/A	265	N/A
SYSTEM ENG'G & INTEG	X	X	X	X	X	X	X	X	-	120	0	-	224	0	-	428	0
REL & QUAL	X	X	X	X	X	X	X	X	-	0	0	-	160	80	-	320	80
TOTAL	X	X	X	X					42	287	69	45	680	195	183	2039	430
					X				42	↓	↓	45	↓	↓	203	2111	464
						X			42			45			203	2111	464
							X		590	587	189	1634	980	435	1781	2390	445
								X	42	287	69	45	680	195	171	1996	410

b. Mission variations, other than the OTS for Mission E, are visible only in the Structural/Mechanical/Thermal area for "Resupply".

The impact variations result from the different complements of Instruments carried on each mission with associated variations in the number of latches, rollers, tracks, and wiring disconnects required. Basic spacecraft (i.e., subsystem) impacts are constant increments to initial designs.

The resultant EOS mass properties, combined with corresponding FSS and MEM equipment, are compatible with the Shuttle c.g. restrictions. Figure 3-2 shows the range of c.g.'s for Missions A and C for the Shuttle utilization modes considered.

Follow On Effort:

As previously stated, the analysis of Shuttle compatibility to date has considered baseline FSS and MEM concepts. In addition, the analyses were limited to consideration of visible physical impact and by the current level of design definition. Follow-on efforts during the next study increment will consist of the following:

a. Refined Weight/cost impacts

b. Shuttle utilization mode variation effects resulting from on-going design life/resupply interval studies.

c. Alternate resupply concept effects

-SAMS

-EVA

-IVA

d. Associated impacts on Operations, Instruments, Shuttle, and FSS.

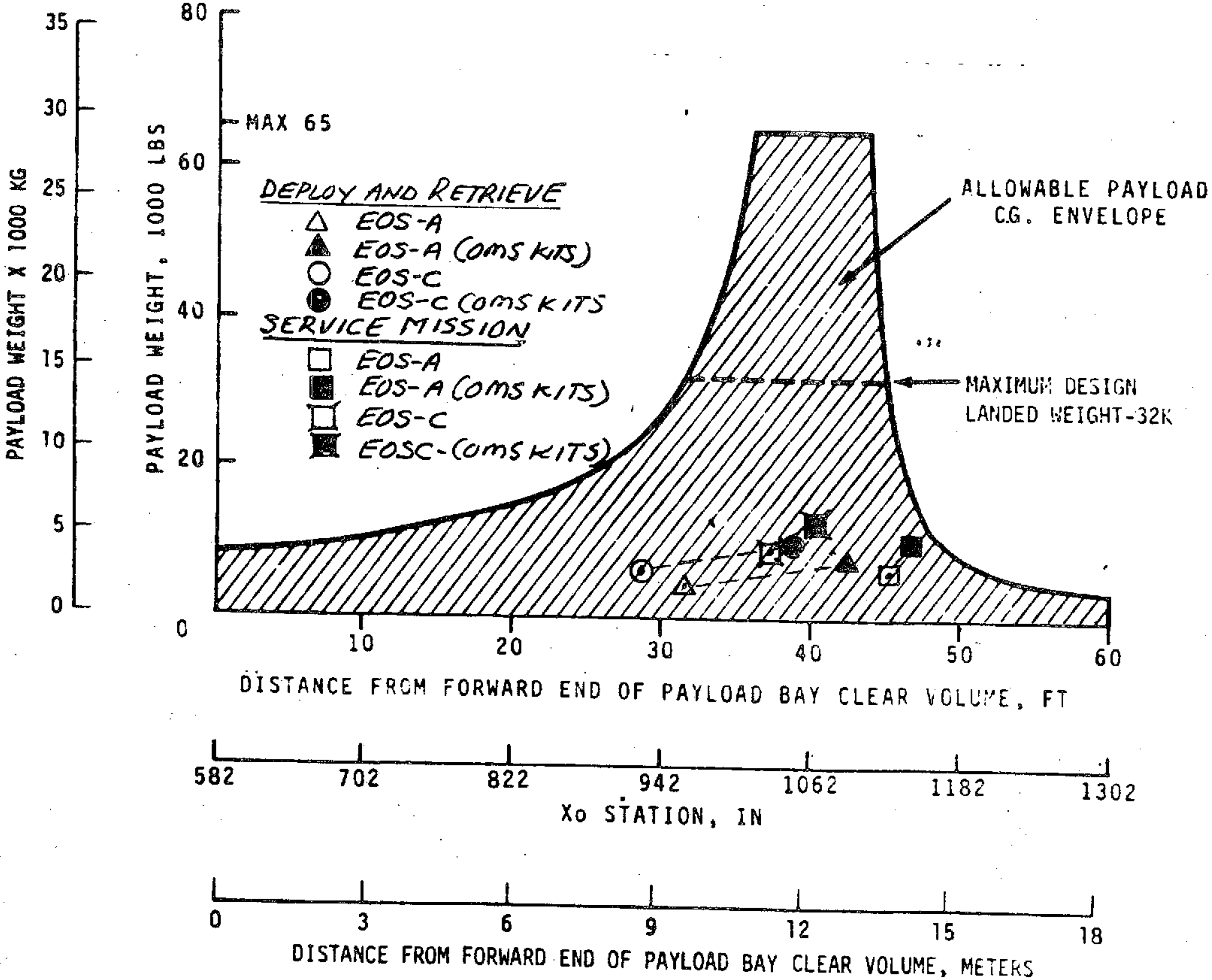

Figure 3 - 2 EOS LONGITUDINAL C.G. ENVELOPE

- EVA
- IVA

d. Associated impacts on Operations, Instruments, Shuttle,and FSS

References

The Shuttle Compatibility Study was conducted on the basis of results of on-going EOS study activities and the following reference decuments:

a. JSC 07700, Volume XIV, Revision B, "Space Shuttle System Payload Accommodations," dated 21 December 1973

b. RI Report SD73-SA-0099, "Quarterly Report, EOS Flight Support System Definition Study", dated 16 July 1973 (SOW Ref 1.4.2)

c. SPAR/DSMA Report, "Phase II Preliminary Report, Design Definition Studies of Special Purpose Manipulator System for Earth Observatory Satellites," dated January 1974. (SOW Ref. 1.4.3)

GRUMMAN

TRADE STUDY REPORT

TITLE	TRADE STUDY REPORT NO.
6.4 INSTRUMENT APPROACH	WBS NUMBER 1.2.1.1

Purpose:

a) To evaluate the competitive point designs provided for the proposed instruments; thematic mapper, high resolution pointing imager, synthetic aperture radar, and passive multichannel microwave radiometer.

b) To evaluate overall system designs applicable to the EOS-A instrument package.

c) To evaluate the utility, reliability, and costs related to each sensor point design proposed for EOS-A sensors.

d) To provide an evaluation of the available data collection system and recommendations to increase its utility when used on EOS if applicable.

e) To provide designs compatible with later EOS missions with regard to the follow-on instruments and to identify the operational and cost impacts of providing this capability.

Summary:

During the course of the study, a broad range of considerations were addressed in selecting the most useful, reliable and high growth potential instrument designs and data handling concepts.

Because of direction received during the study and the continual development of the various TM and HRPI point designs during the study, effort was concentrated on the further evolution of the TM and HRPI, relative to the ERTS multi-spectral scanner, and their various configurations and utilizations in the EOS-A mission.

The result of these studies are as follows:

1. No single point design is considered optimum in the form proposed by the suppliers.

2. The object plane scanner as a class offers significant growth potential relative to the EOS baseline without significant weight growth.

3. Spectral band selection by filtration techniques offers significantly better growth potential than does the spectrometer (dispersion) approach.

4. The reduction in preamplifier noise by cooling down to 200°K promises performance improvements for silicon detectors even

PREPARED BY	GROUP NUMBER & NAME	DATE	CHANGE LETTER A
J. T. Fulton			REVISION DATE
APPROVED BY J. R. Fragola			PAGE 4-1

in Band 1, which makes them highly competitive with photomultiplier tubes.

5. The lower cost, higher reliability, simpler design, lighter weight and higher growth potential of an all solid state detector array make this the preferred approach even if a slightly larger telescope aperture is felt necessary to meet minimum S/N ratio requirements.

6. In examining overall system performance, further definition of the system instantaneous field of view (SFOV) suggests further definition of the optimum sampling ratio may be appropriate. A major cost trade is involved.

7. Both 6 and 7 bit data encoding was examined. No significant cost or performance trade could be discovered. Therefore, the choice of 7 bit encoding is concurred with.

8. There are significant economies in obtaining the TM and HRPI from the same supplier due to a possible commonality factor as high as 80%.

9. An "advanced" TM has been defined which can provide a 330 KM swath at 27 meters resolution, provide an output at 80 meters completely compatible with and providing a backup to the operational MSS, and providing a pseudo-HRPI output covering a selectable 35 kilometer swath at 30 meters. Both the MSS backup and pseudo-HRPI signal would be compatible with the present DOI and planned low costs ground stations. (LOGS).

10. DELETED

11. As the land resources mission (LRM) matures, the desirability of obtaining stereo coverage will increase and a ±50 N.M. drift in the orbit repeat cycle prior to orbit adjust will become a preferred orbit. Furthermore, the use of ground control points in isolated or distant areas will become prohibitively expensive.

All of the studies associated with the instruments assumed a nominal satellite altitude of 680 kilometers.

E. 2. 1 External Input Considerations
ORBITAL MECHANICS IN THE GEOID

The potential performance of the instruments and data reconstruction equipment is highly dependent upon the adequacy with which all systematic errors effecting the data can be determined and factored out. These sources of error and also various allowable variations are discussed in this section.

The basic geometry of these discussions is shown in figures E.2.4-1 to 5

There are a number of instrument-vehicle errors which distort the transmitted imagery relative to the geoid:

1. Errors in the local vertical of the instrument; roll, pitch and yaw and their deviations.
2. Errors in the scan angle of the instrument from the expected value.
3. Errors in the vehicles altitude from the expected ephemeris.
4. Errors in the vehicle velocity from the nominal.

On top of these errors are a group of distortions due to the:

1. rotation of the earth
2. inclination of the orbit and
3. precession of the orbit which complicate the data reduction.

The general goal of the EOS program is to minimize the uncontrollable errors and to remove the controllable errors from the data channel as early as possible. The goal would be creation of "maps" with an uncontrolled error of under 10 meters. The above performance would be done preferably without ground control points.

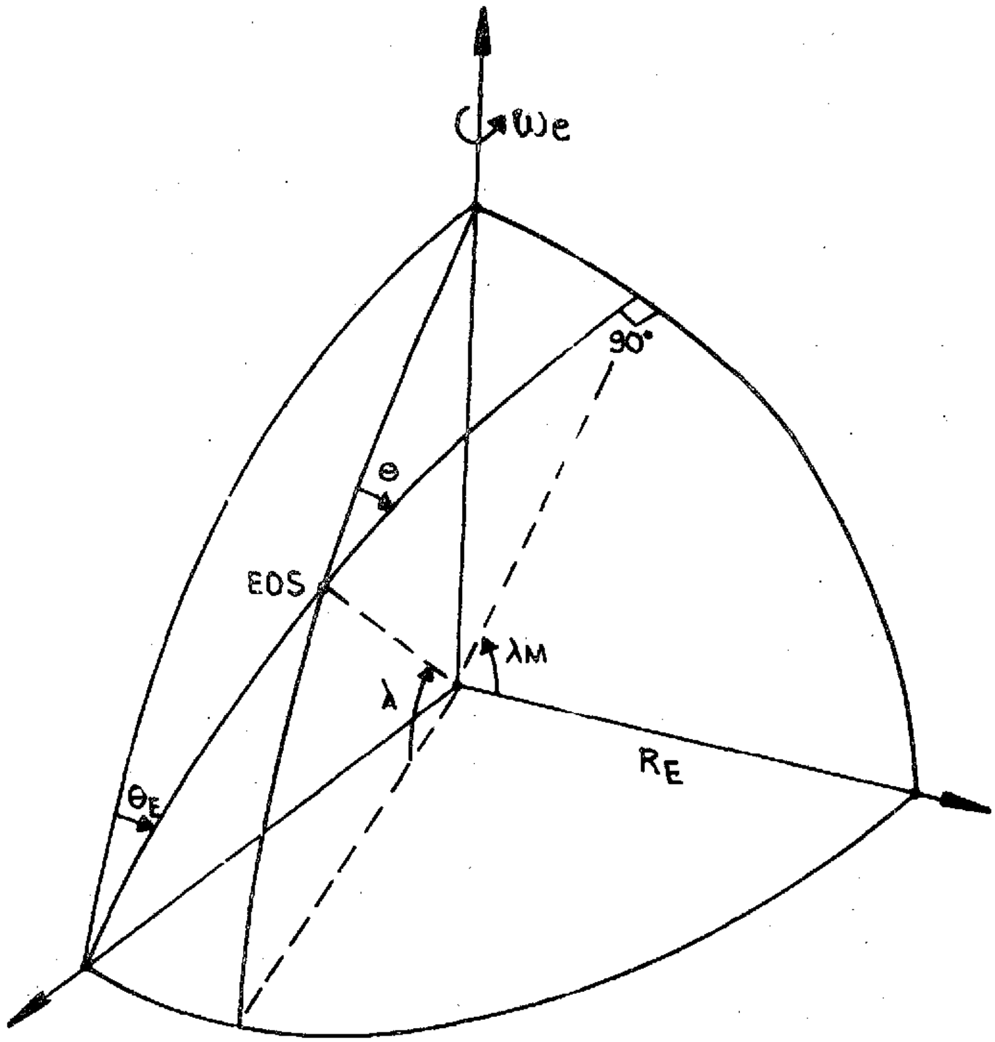

Fig. 4-1 EOS Orbit Geometry

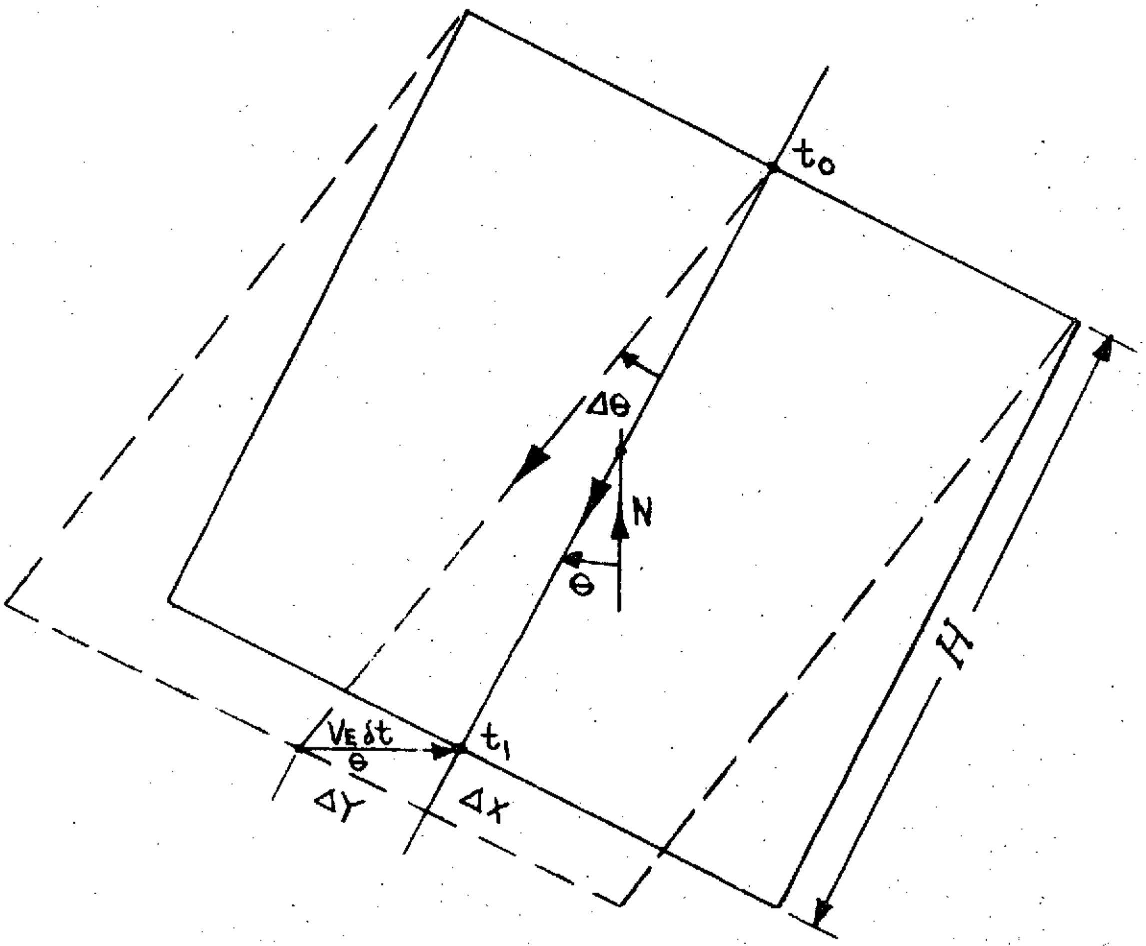

$$\Delta X = V_E \ \delta t \ \cos\theta$$

$$\Delta X = V_E \ \delta t \ \sin\theta$$

WHERE: V_E = NOMINAL VELOCITY OF EARTH SURFACE

$= R_E \omega_E \cos\lambda$

$\delta t = t_1 - t_o$ = SCAN TIME OF FRAME

Fig. 4-2 Planar EOS Image Geometry

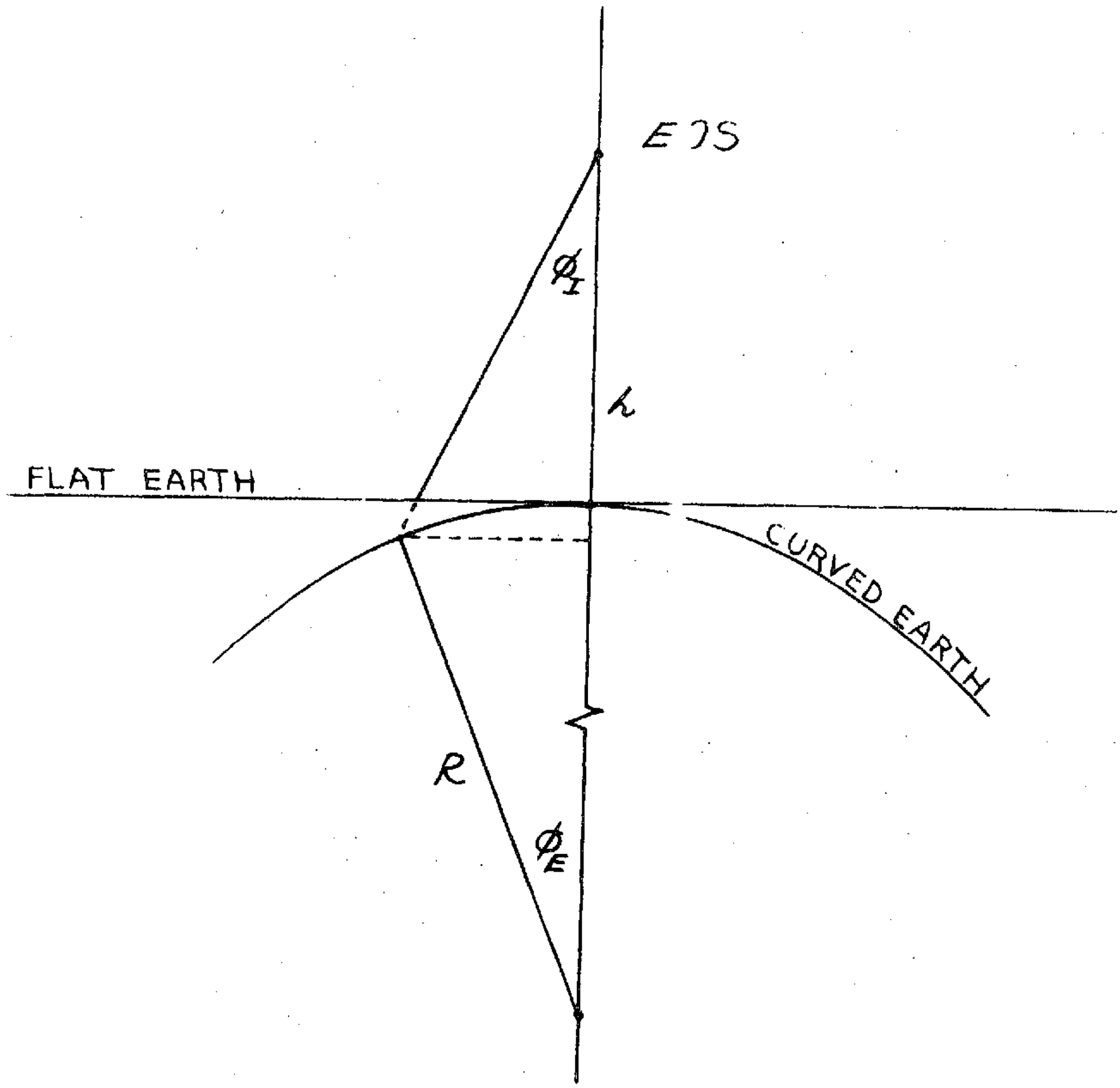

Fig. E. 4-3 Effect of Earth Radius on Scan Geometry

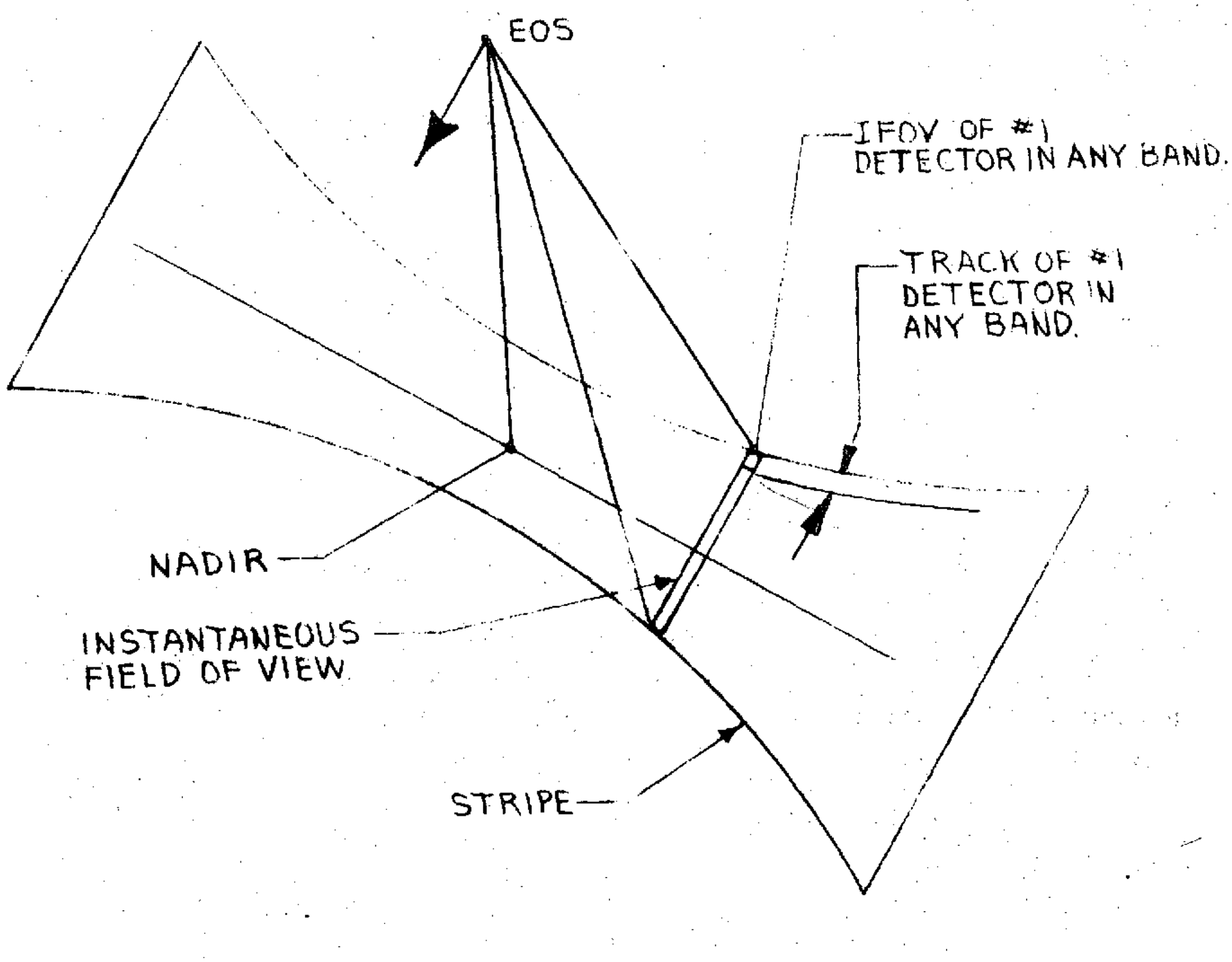
EOS
IFOV OF #1
DETECTOR IN ANY BAND.
TRACK OF #1
DETECTOR IN
ANY BAND.
NADIR
INSTANTANEOUS
FIELD OF VIEW
STRIPE

E-1

Fig. E. 4-4

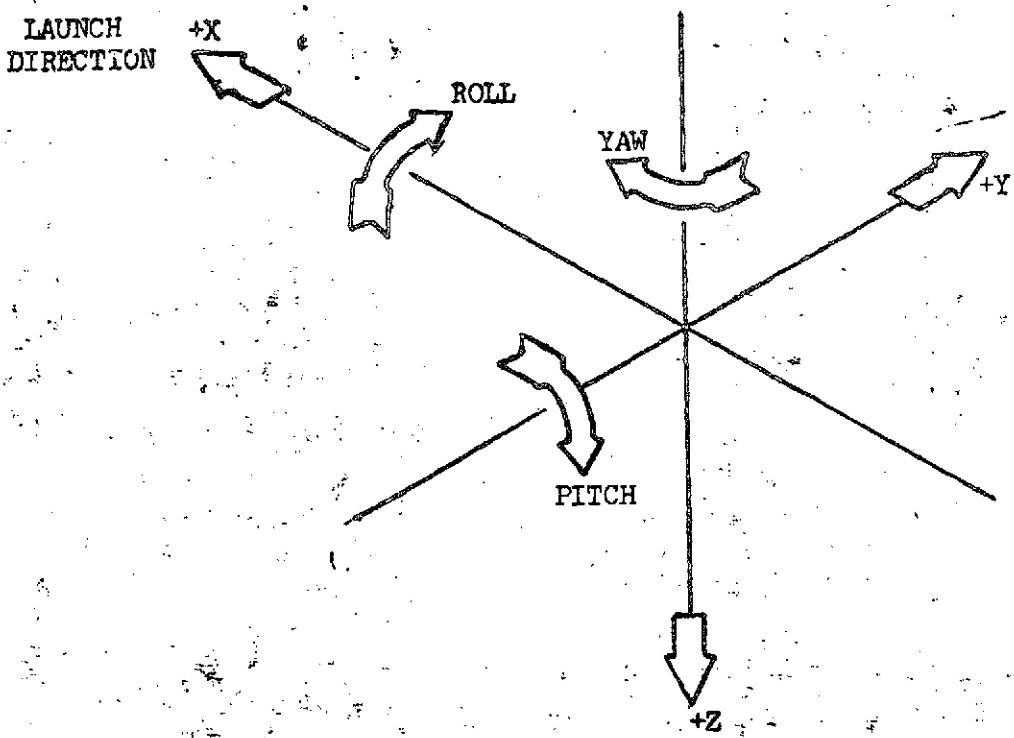

Fig. 4-5 Spacecraft Coordinate System

Critical to creation of data to the above accuracy is an accurate knowledge of the local vertical of the instrument primarily the thematic mapper. The RMS error in the location of the nadir point is needed to at least ± 30 meters or better, one IFOV, from the nominal altitude of 680 kilometers. The important constituents of this RMS value are primarily four:

1. The roll angle of the spacecraft from nonimal.
2. The pitch angle of the spacecraft from nominal.
3. The along track ephemeris error of the spacecraft.
4. The cross track ephemeris error of the spacecraft.

Thus the instrument line of sight is needed, in pitch and roll to ± 3 arc seconds or better.

Similarly, the position of the satellite along its track should be known to better than ± 30 meters at a nadir velocity of approximately 6800 meters per second. Therefore, the vehicle clock should be available, for transmission with the data, at an accuracy of ± 5 milliseconds. The corrected ephemeris would also be needed to this accuracy in order to determine the in track and lateral position error of the vehicle.

As the thematic mapper scans out to the side the effective ground field of view increases. Along the in track direction, the increase as given by the secant of the angle $\bar{\phi}_x$. In the cross track direction, it is given by the square of the secant.

For a non-flat earth, these distortions are somewhat greater but for scan angles of less than ± 30 degrees the increases are negligible.

The position of the area on the geoid scanned during a given time interval may not be the expected area due to a number of distortions. Besides the roll and pitch errors discussed earlier, the vehicle yaw error becomes prominent in this context. The position error for a flat earth is given by $h \sin \phi_I \sin \phi_{yaw}$. This error increases rapidly with scan angle ϕ_I. To maintain this error below $\pm$ 30 meters at 680 KM and 5° $= \phi_I$, ϕ_{yaw} must be below $\pm$ 530 microradians ($\pm$ 2 minutes of arc).

Figure 3 illustrates in elementary form the geometry of the scanning problem, particularly for the non-conical scanners. The goal of the program is to generate maps of the earth's surface which correctly display data with respect to its correct position on the geoid, data is presented linearly with respect to position S. From a design point of view, the output of the scanners themselves should be linear with respect to S if at all possible to minimize the amount of data processing required later in the system.

Clearly ϕ_E, the angle between the scanned point and the nadir, is linearly related to the distance S. A similar linear relationship cannot be obtained from a location outside of the geoid except by an approximation applicable over a limited angle ϕ_I. The desired function for ϕ_I is:

$$\phi_I = \text{arc tan} \frac{\text{Sin } S/R}{\text{COS } S/R \left[-1 + \frac{1 + 680/R}{\text{COS } S/R} \right]}$$

which is linear in S for small values of S/R, where the paranthesis is negligible.

At $S = 0$, $\phi_I = \frac{R}{680} \phi_E$.

At $S = \pm 92.5$ kilometers, $\phi_I = \frac{R}{680} \phi_E$

to better than one part in 10^4. At $S = \pm 165$ kilometers, ϕ_I still equals

$[R/680]\,\phi_E$ to at least one part in 10^4 also. One part in 10^4 is one IFOV in 300 kilometers (± 150 kilometers).

Thus a scanner which scans linearly with ϕ_I will provide a final map which is linear in S to within one IFOV over the desired scanning swath.

To scan linearly in ϕ_I and achieve an accuracy of 0.1 IFOV ($1:10^5$), without correction, the scan angle would have to be limited to $\phi_E = 0.27°$ or $\phi_I = \pm 2.5255°$, a swath width of only ± 30 kilometers.

Thus correction or compensation is likely to be required.

The TE scanner employs a unique characteristic of a reflective optical system to provide this compensation. By proper choice of nodal points in their optical system, a curved focal plane is obtained for a flat object plane. By adjusting the radius of their scan wheel to equal the radius of curvature of the image, a scan which is linearly related to ϕ_I can be achieved. Following final choice of nominal flight altitude, it is possible to adjust the nodal points of the optical design to achieve a scan linear in S. Whether it is possible to manufacture the optical system to the desired accuracy, specifying radii of curvature to about $1:10^5$ has not been determined but it is questionable.

The Hughes linear scanner is not intrinsically linear in ϕ_I or S and will require considerable additional design analysis by Hughes before any possibility of a sufficiently linear output to avoid digital correction on the ground can be confirmed.

An additional problem with the geometry of the linear object plane scanner is the likelyhood that both the east to west and west to east scans will be employed. Since neither of these scans is intrinsically linear in ϕ or S or to each other without compensation or correction, the breadboard of this design should be expanded to evaluate and/or demonstrate what level of linearity could be achieved in this respect.

The accurate scanner of Honeywell exhibits a negligible intrinsic error in scan linearity with ground position assuming the residual roll and pitch errors of the vehicle are acceptable and the yaw error is small. For excessive pointing errors, the accurate scanner becomes very difficult to correct.

As more detectors are used simultaneously to scan a single stripe, the outer detectors are further removed from the center detector which scans a great circle through nadir. These outer detectors exhibit a scan distortion as shown in figure 4 . The graph shows the tradeoff between the number of detectors and the scan angle for a given position error.

The actual shape of the area mapped on the geoid with a perfect scanner of negligible scan and attitude errors can be described in terms of three additional errors; orbit inclination skew, earth rotation skew, and scan time skew.

The required orbit inclination of a long life span synchronous satellite results in a nadir flight path which is skewed with regard to the UTM grid by an angle which varies with lattitude, ranging from 9° at the equator to 90° at the lattitude equal to the orbit inclination.

In addition, earth rotation during scan causes two further skews. The first causes the rectilinear scan of the overall sensor to become rhomboid when transferred to the geoid. The finite time required for a single detector to scan a single line also causes the line to be warped on the geoid by the earth's rotation.

Each of these three skews is sufficiently large to require ground processing to correct prior to reduction of the data to UTM based maps.

Table 4-1 summarizes the system mapping errors showing the desired and the expected errors on both a pre-and post processing basis. The methods of processing to achieve this are examined elsewhere.

TABLE 4-1 Summary of Desired and Expected Errors on Preprocessing and Post Processing

	Desired	Typical Before Processing	Expected After Processing
• Position Errors			
- Sensor Pointing Error	45×10^{-6} Radians	TBD	TBD
- In Track Position Error	30 Meters		
- Lateral Position Error	30 Meters		
- On Board Clock Error	5 Milliseconds		
• Geometry Errors			
• Object Plane/			
- Scan Angle Distortions	0.016%		
• Image Plane/			
- Scan Angle Distortions	0.016%		
- Bow Tie Distortion			
- Vehicle Yaw Error	530×10^{-6} Radians		
• Geometry Distortions			
• Orbit Inclination Skew	0°	9°-90°	
• Earth Rotation Skew	0°	5°-0°	
• Scan Time Skew	0°	0.021°-0°	
• Orbit & Local Terrain			
- Altitude Error	0 Meters	500 Meters	30 Meters*

*With Stereo Processing

E. 4.1.1- Minimum Overlap Requirement

The minimum overlap factor acceptable on the EOS program for adjacent (non-consecutive) swaths is a function of how rapidly a fully corrected map of a given area must be available after original data acquisition.

At the equator, the creation of a contiguous set of UTM 15' charts from the basic tapes can be obtained in a number of operational ways.

One of the principle operational goals would be the ability of the data reduction system to generate a full set of UTM 15' charts without having to merge the data from adjacent tapes. This can be achieved at all latitudes unequivocally if the % overlap meets or exceeds: (See Figure E. 4-7)

$$\% = \frac{15 \text{ N Mi.}}{\cos \text{ (inclination)}} \cdot \frac{1}{\text{swath width}}$$

For a 100 n. mi.: Swath width, this becomes

$$\% = \frac{15}{(0.985)\ 100} = \sim 15\%$$

For latitudes farther north, the 15' UTM width is less than 15 N. Mi. and the equation becomes

$$\% = \frac{15 \text{ N. Mi. } \cos \text{ (lat.)}}{\cos \text{ (inclin.) X swath width}}$$

which can be tabulated as follows:

Swath Width	Latitude 0°	25°	48°
100	15%	13.4%	10%
125	12%	11 %	8%

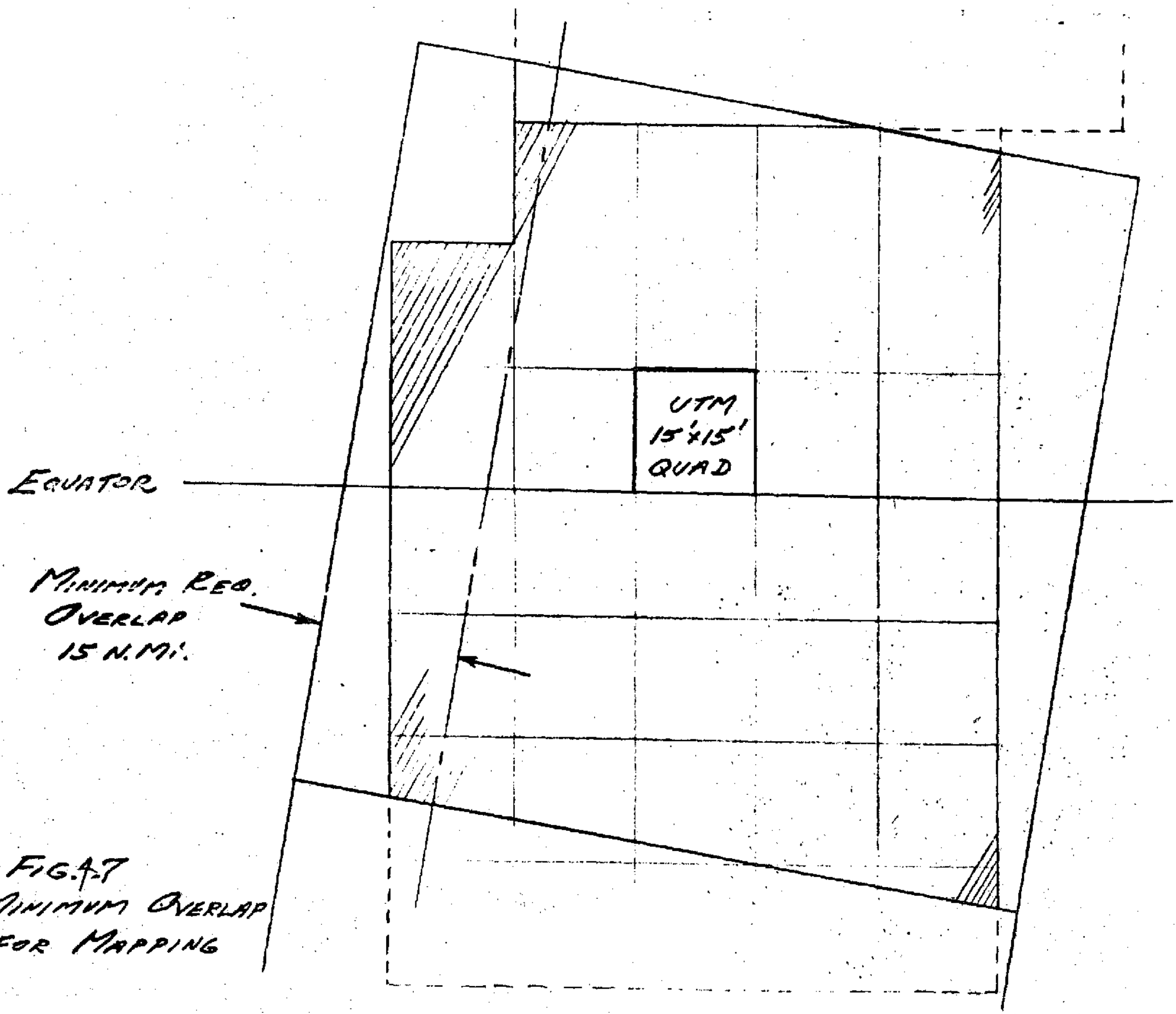

FIG. 4-7
MINIMUM OVERLAP
FOR MAPPING

The above situation would hold true indefinitely if the spacecraft was operated in an orbit exhibiting an exact overlay of subsequent orbits.

If an orbit is chosen such that the orbit path does not repeat exactly in a small integral number of days, allowing a ± 50 n.mi. displacement at the end of one 17 day cycle for example, the overlap factor becomes much less important. Then, the 15' UTM charts not obtainable from the tapes generated during the first 17 day orbital cycle are by necessity available during the second cycle.

In the absence of clouds, the overlap factor is no longer of consequence except to ensure absence of voids and to allow sufficient overlap for visual matching of adjacent uncorrected imagery. This should be achievable with as little as 2% overlap. Taking into account a 50% chance of significant cloud cover in any 15' UTM area and a probability of a completely clear UTM of about 10%, approximately one year would be required to collect a complete set of types from which a complete set of UTM 15' charts could be created containing a minimal amount of cloud and without having to perform any tape merging.

Of course the orbit retrace cannot be allowed to wander continuously, the longtime average orbit must retrace exactly and have a specific inclination to remain annsynchronous. However, allowing the retrace to go from an overcorrected 50 n.mi. error to a drag induced 50 n. mi. on the other side can allow a relatively long time between orbit makeup activities without incurring a mission penalty.

Local altitude perturbations in the orbit due to various mass anomolies and terrain features can also cause errors in the maps of a significant amount at the 30 meter performance level. At the extreme scan angle for the 100 n mi scanner at 680 KM nominal altitude, an altitude error of only 220 meters will result in a mapping error of one resolution element. This is well within the local terrain variations found frequently in CONUS and worldwide and is of the order of the systematic errors in the orbit. Removal of the terrain errors in the absence of stereo coverage would only be by reference to ground control points (located on the specific hill of interest) or other material. The establishment of such local ground control points would involve a survey team in the field and would be prohibitively expensive. With stereo or pseudostereo coverage, available throughout the CONUS if ± 50 n mi orbit repeat wander is allowed, correction of ± 30 meters can be achieved using standard stereo techniques. The variation in local terrain altitude will become the dominant error in the data reduction system (especially if a wide angle TM is used) as the flight program matures and the system begins serving the more difficult users -- the small farms located in rolling countryside for example. Thus as the system matures, the requirement for stereo will increase and orbital drift during data acquisition will become desirable.

E. 4.2.1 Candidate Scanning Techniques

As a result of a series of sponsored point designs for the Thematic Mapper followed by a similar series aimed at a High Resolution Pointing Imager, a very large range of possible optical imaging techniques were considered as indicated in Figure E 4-8. The pushbroom electronic technique can also be described as a linear image plane scanner although its implementation is somewhat different than the others in this family.

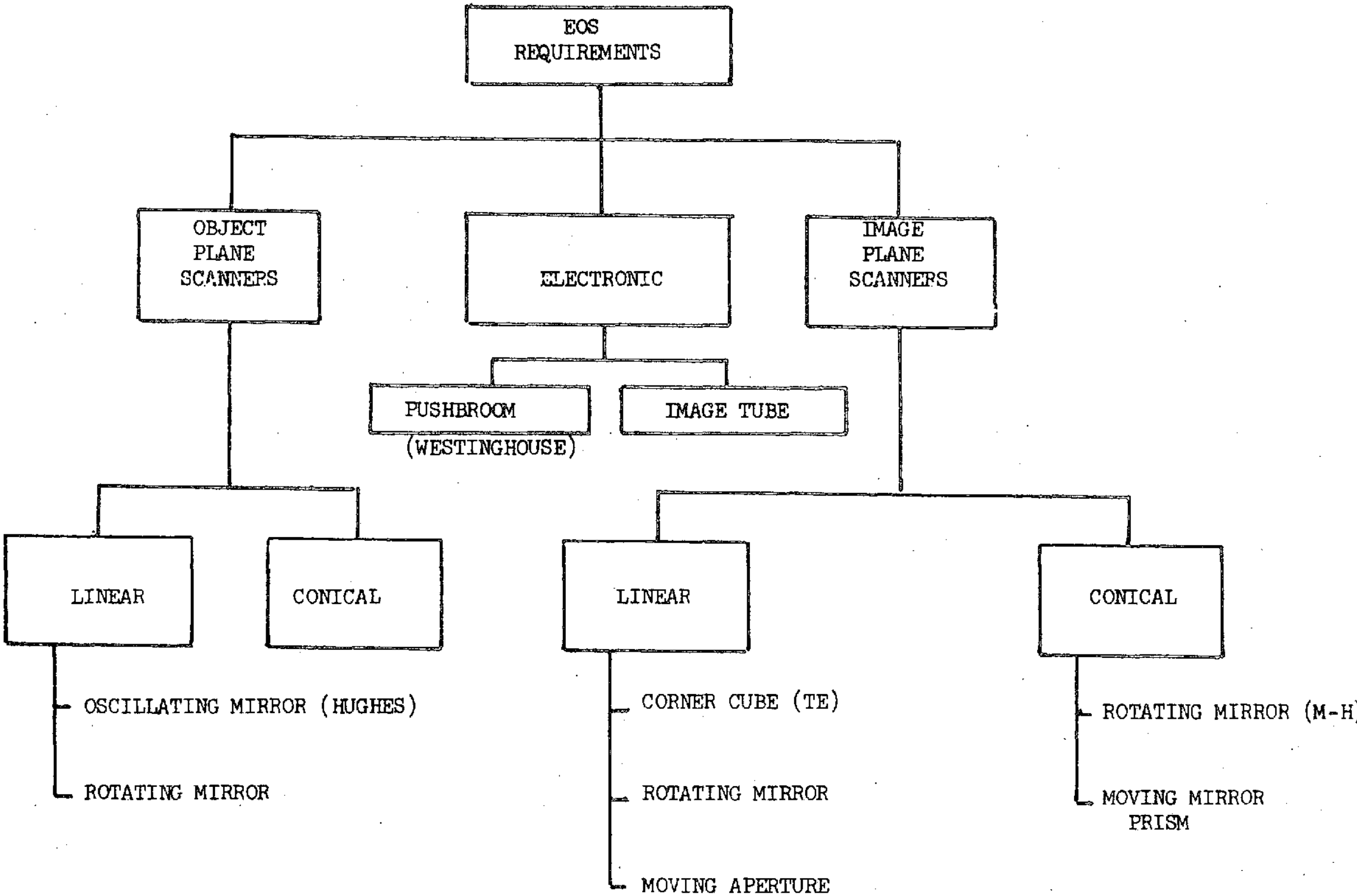

SCANNER SYSTEMS

Fig. 4-8 Scanner Systems

Each of these scanner types are capable of meeting the EOS requirement. It is the secondary considerations which must be used to evaluate their relative utility, reliability, and difficulty to produce and use (cost).

Of primary importance before proceeding is to point out that the title linear scanner may be misleading. Such a scanner may scan a geometrically straight line under optimum conditions but generate a temporaly non-linear output data stream which is difficult to process. Conversely, the conical scan may generate a temporaly linear data stream while scanning a circular arc on the geoid.

Furthermore, the scan patterns on the geoid are only truely linear or circular when the scanner reference axis passes directly through the nadir of the sensor. This is a very difficult constraint. In addition, most of the preferred scanner configurations employ multiple detector arrays. Under such circumstances only one of the detectors of a linear scanner can scan through the nadir and produce a geometrically straight scan on the geoid, all other detectors must scan an arc resulting in the familiar bow-tie effect.

Thus, as a practical matter, one should not attach too much significance to the term linear as used here. Except for a local user or a user only requiring cursory knowledge, all of the scanner-spacecraft combinations evaluated will require computer computation prior to reconstruction of the imagery in final form. The amount of computation required is a strong function of the performance of altitude control system.

Telescope Concepts:

The principle advantages of an object plane scanner relative to an image plane scanner are two. First, the object plane scanner only requires a very small image plane field of view, about 1/32° (specifically the size of the detector array) and is therefore. easier to correct optically.

The image plane scanner must image an area as large as the area to be scanned. This difference is quite significant in the TM (image field of $\sim 15°$) and any up rated TM (image field reaching ~ 30-$40°$). Second, correction for such wide fields of view in a fast telescope become quite difficult and, as a minimum, adds to the number of surfaces in the optical path, an area where image plane scanners are already at a disadvantage.

In the case of the HRPI, the offset pointing requirement further accentuates the difference in computational complexity required to handle the linear versus conical scanners and the need for excellent alignment of the sensor reference axis to the nadir point.

Scan Distortions:

For a linear scanner with a negligible pitch and yaw misalignment, offset around the roll axis results merely in an increase in the bow tie effect and the loss in resolution according to the cosine law in the direction of the flight vector and the cosine square law perpendicular to the flight vector. No voids are caused and if desired, certain detectors which are providing redundant data due to overlap can be ignored. A pitch or yaw error causes the bow tie pattern to be unsymmetrical causing some complications in the data reduction.

For conical scanners, offset can be accomplished in one of two ways: changing the sector of the arc usually scanned to one including the desired offset or by offsetting the reference axis so the desired area falls within the area desired. In the first method, the scan geometry is unchanged except with relation to the flight vector. The processing algorithms required are changed little. In the second method, the entire scan geometry changes to a series of ellipsoidal segments containing considerable overlap scan to scan, complicating the processing considerably.

In the variable sector scanner vehicle pitch and yaw errors are almost insignificant causing a small displacement of the total field of view. In the displaced reference conical scanner, they add additional minor terms to an already complex algorithm.

Inertial Impact:

All of the mechanical scanners involve motions having an inertial impact on the spacecraft most of these involve continuous rotary motions. It is anticipated that the scanners will run continuously once orbit is achieved. Therefore, the principle transient effect is a momentum transfer during initial startup, and the principle steady state effect is one of gyroscopic coupling of any torquing to the vehicle caused by the attitude control system. The proposed linear object plane scanner has adopted a nutating rather than a continuous rotating mirror. This scheme avoids a gyroscopic effect but introduces a continuous vibration at about 10 hertz and harmonics thereof which must be accounted for and isolated.

Pointing Errors:

The size and performance of the Thematic Mapper is such that a review of previous practice with regard to establishing the sight line of the instrument with respect to the Nadir, is suggested.

In a great many earlier NASA missions, the instrumentation was relatively small physically and the angular resolution relatively course compared to the accuracy readily available from the guidance system.

The above considerations have led to the practice of considering the vehicle an optical bench to which the guidance package and instruments were physically aligned prior to launch. If necessary, the actual instrument alignment to the Nadir after launch could be calibrated out,(a rather coarse absolute accuracy) by manually examining the imagery. It was not difficult to design the vehicle (the optical bench) for adequate rigidity and temperature stability due to the coarse resolution involved.

The above procedure was abandoned some years ago in high performance military camera systems for a number of reasons.

First, the relatively large "telescopes" employed must be mounted in a statically determinate manner to avoid the introduction of forces causing defocussing of the camera system. Such determinate mounting makes it difficult to maintain tight alignment to the attitude reference through the intervening optical bench (the spacecraft in this case). Furthermore, as the angular pointing accuracy goes up, it becomes more difficult to achieve the desired rigidity of the spacecraft without a weight and/or design cost penalty.

Similarly, the difficulty of guaranteeing thermal stability to the degree desired during design becomes more costly.

Calibration by ground control points is still a means of establishing the actual pointing angle over a relatively short segment of the mission duration. However, it suffers from at least three drawbacks:

1. It will require human intervention into the data processing system of a high volume operationally oriented information system.

2. It will require at least quarterly recalibration during the mission life until the stability of the calibration is demonstrated as the required frequency of recalibration is established.

3. The calibration results will not be available in a timely manner, hours after data acquisition, to allow preparation

of "final" maps by the data processing system as part of its on-line operation.

A further complication, in terms of aligning the instrument to the guidance package through the vehicle structure, arises when the instrument must be removable as a module for resupply or maintenance by shuttle. Designing a simple latching mechanism while maintaining the desired alignment accuracy, probably in tandem with the determinate mount, will be a difficulty and a cost.

The preferred solution to the alignment task is to mount a pointing reference directly on the instrument. This accomplishes a number of things:

1. It allows the instrument and the reference to be aligned to each other at the subsystem level where smaller packages and shorter distances are involved.

2. It allows the spacecraft to be designed without as demanding requirements as rigidity and thermal stability, contributing to a low cost design.

3. It makes the spacecraft design independent of the particular payload carried, leading to a more general purpose spacecraft.

4. It considerably simplifies the spacecraft system integration problem since no alignment benches and or pathways need be provided as part of the AGE.

5. It eliminates entirely the need for human intervention in the data processing system after launch, both in the field establishing ground control points, and at the data center reviewing the imagery.

The cost savings associated with items 2 through 5 will normally far exceed the cost of mounting an additional star tracker on the instrument (as an instrument mission peculiar item) assuming integration of the sensor into the spacecraft system is not too difficult.

In terms of integrating the IMP star-tracker into the EOS spacecraft, the additional cost is remarkably low.

In the EOS baseline design, the system employs a common bus communications system between all system elements and the on-board computer and all elements communicate by way of the computer. Thus the star-tracker in the guidance and control module doesn't communicate directly with other elements of the guidance system. Instead, it is addressed and corresponds with the computer only.

In such a system, see Figure 4-8a, the introduction of an IMP star-tracker (and a backup to the main unit) is quite simple. The computer merely addresses one star-tracker or the other as desired. Of course, it must have the correct star map for each tracker in storage if it is assumed they have somewhat different optical axes. If they have similar axes and fields of view, only one map is required.

The IMP star-tracker would be addressed through the TM command and telemetry multiplexer wherein adequate capacity is available. Thus it would be replaceable as part of the TM package, Figure 8b.

The use of an IMP star-tracker would allow the exact line of sight of the instrument to be transmitted to the ground with an instantaneous accuracy of one IFOV or better in real time, far better and more current than the average value obtained by ground control points. The accuracy of the on-board reference system in the baseline would be on the order of ± 6 IFOV at best.

Therefore, it is recommended that a star-tracker (auxiliary to the main star-tracker) be mounted directly on the TM and communicate with the on-board computer through the TM multiplexer. If possible, the two star-trackers should have parallel optical axes and be otherwise identical to simplify the on-board computations.

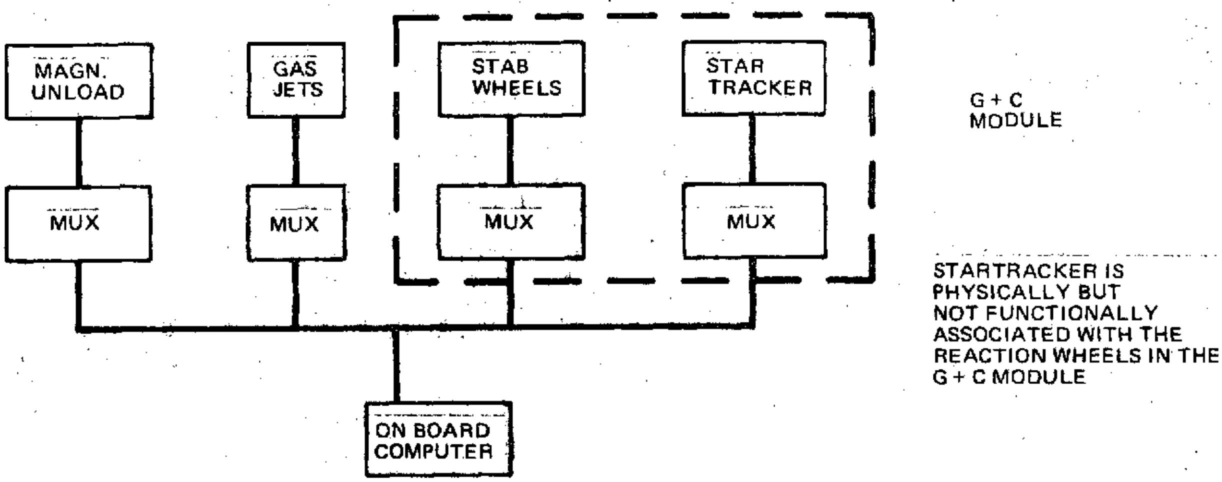

CURRENT GUIDANCE CONFIGURATION

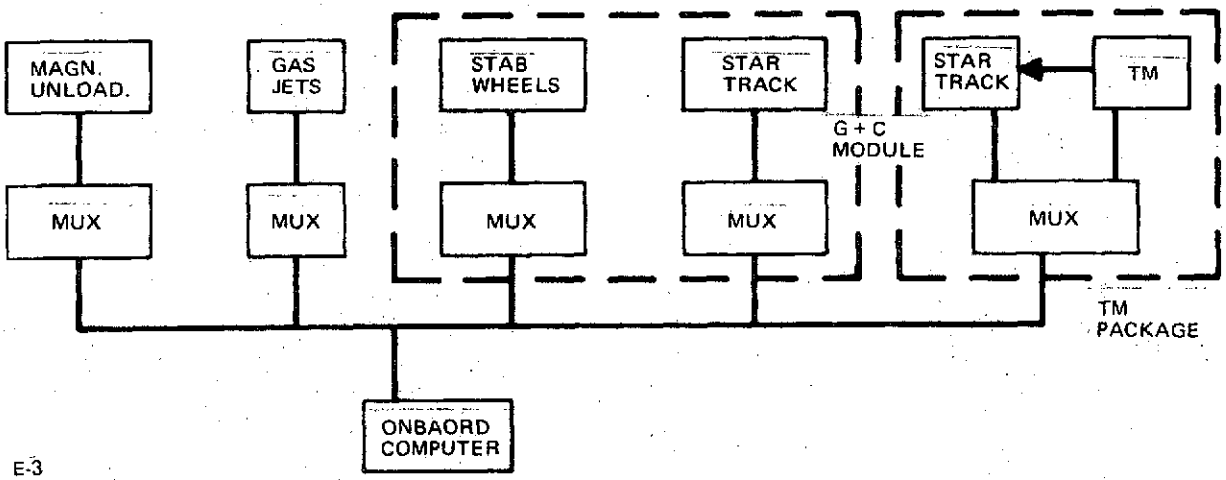

E-3

Fig. 4-8a Recommended Configuration From Instrument Data Handling Viewpoint

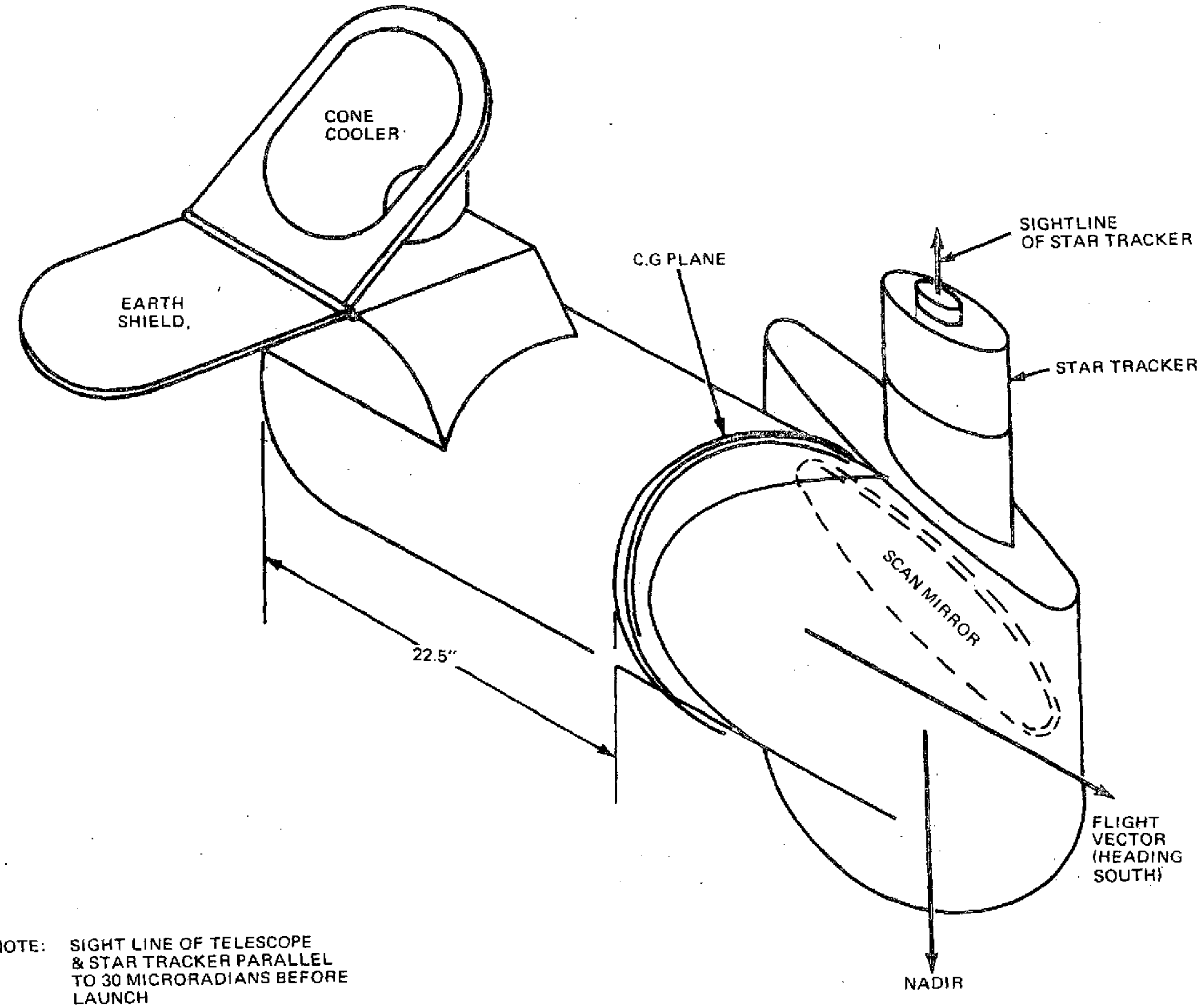

NOTE: SIGHT LINE OF TELESCOPE & STAR TRACKER PARALLEL TO 30 MICRORADIANS BEFORE LAUNCH

Fig. 4-8b

Whereas the HRPI is intended to achieve a higher ground resolution, it need not achieve the mapping accuracy of the TM. It need not carry its own star tracker, calibration is available conveniently by comparing the TM and HRPI imagery of the same scene.

Instrument Size:

All of the point designs considered for the TM were found to achieve similar optical system and sensor performance. Thus, they all required an aperture of about 19" at the 914 KM altitude to achieve the desired radiometric performance. Approximately 600 pounds was required as a weight allocation for each of the designs. The weight allocation was found to be proportional to the square of the altitude as is common in such instruments. Thus, at the preferred altitude, 680 km, a weight of about 350 pounds is to be expected, Fig. 4-9.

Scan Efficiency:

The mechanical image plane scanners typically exhibit a lower scan efficiency before vignetting than the object plane scanner. However, the object plane scanner exhibits a poorer temporal linearity as the scan efficiency is increased. A scan efficiency of between 70% and 80% can be expected in the final TM design with linearities better than 3 parts per 1,000. (Pixel location errors of up to 500 meters in the raw data).

If an extended swath TM is chosen for flight, the scan efficiency of image plane scanners will drop precipitously unless a significant weight penalty is incurred, Fig. 4-10.

HRPT Designs:

Each of the mechanical scan TM's were configured to a HRPI. The resolutions were increased at the expense of field of view and MTF. Therefore, the size and weights remained relatively fixed. In one case,

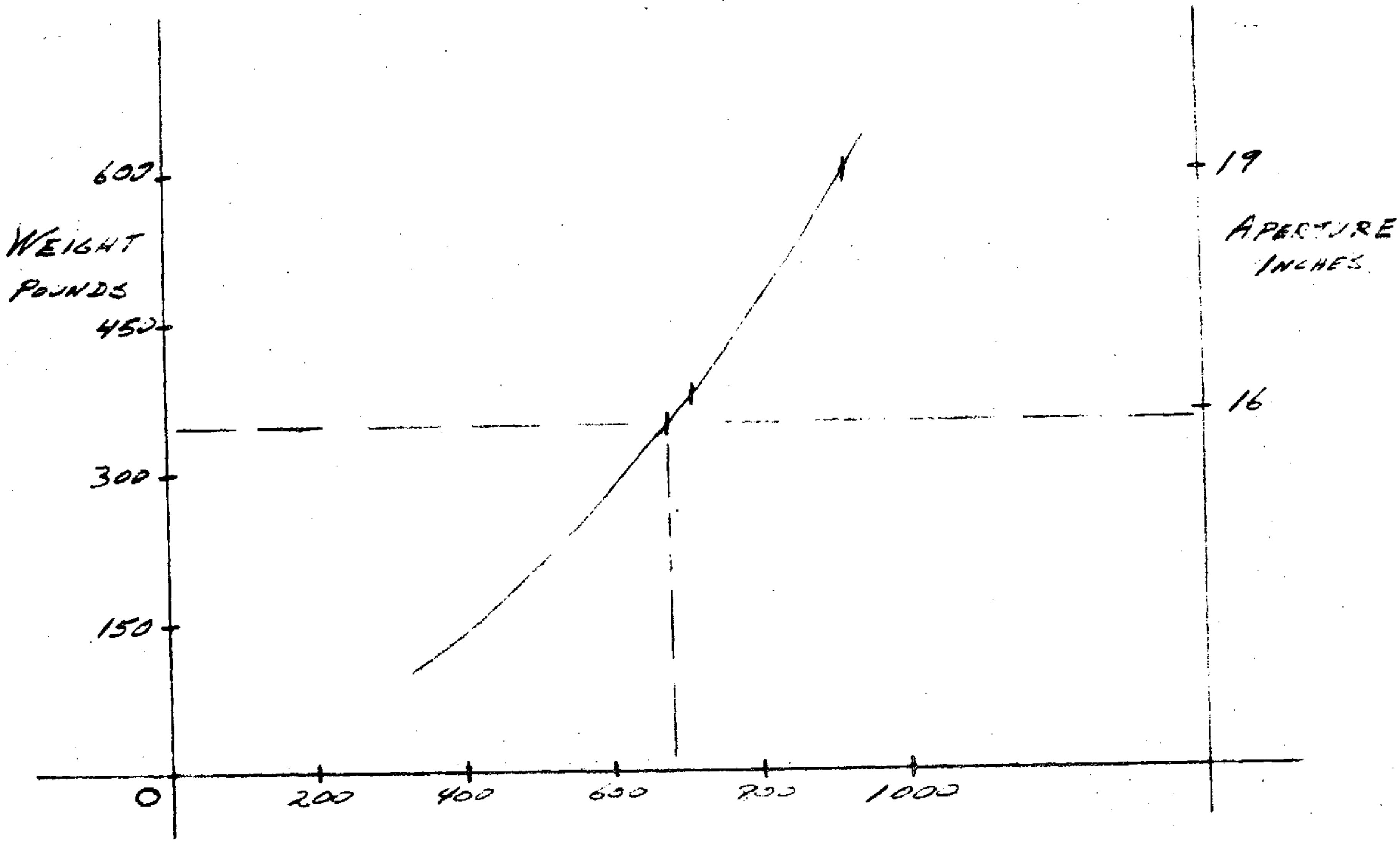

Fig. 4-9 Instrument Wt. vs Orbit

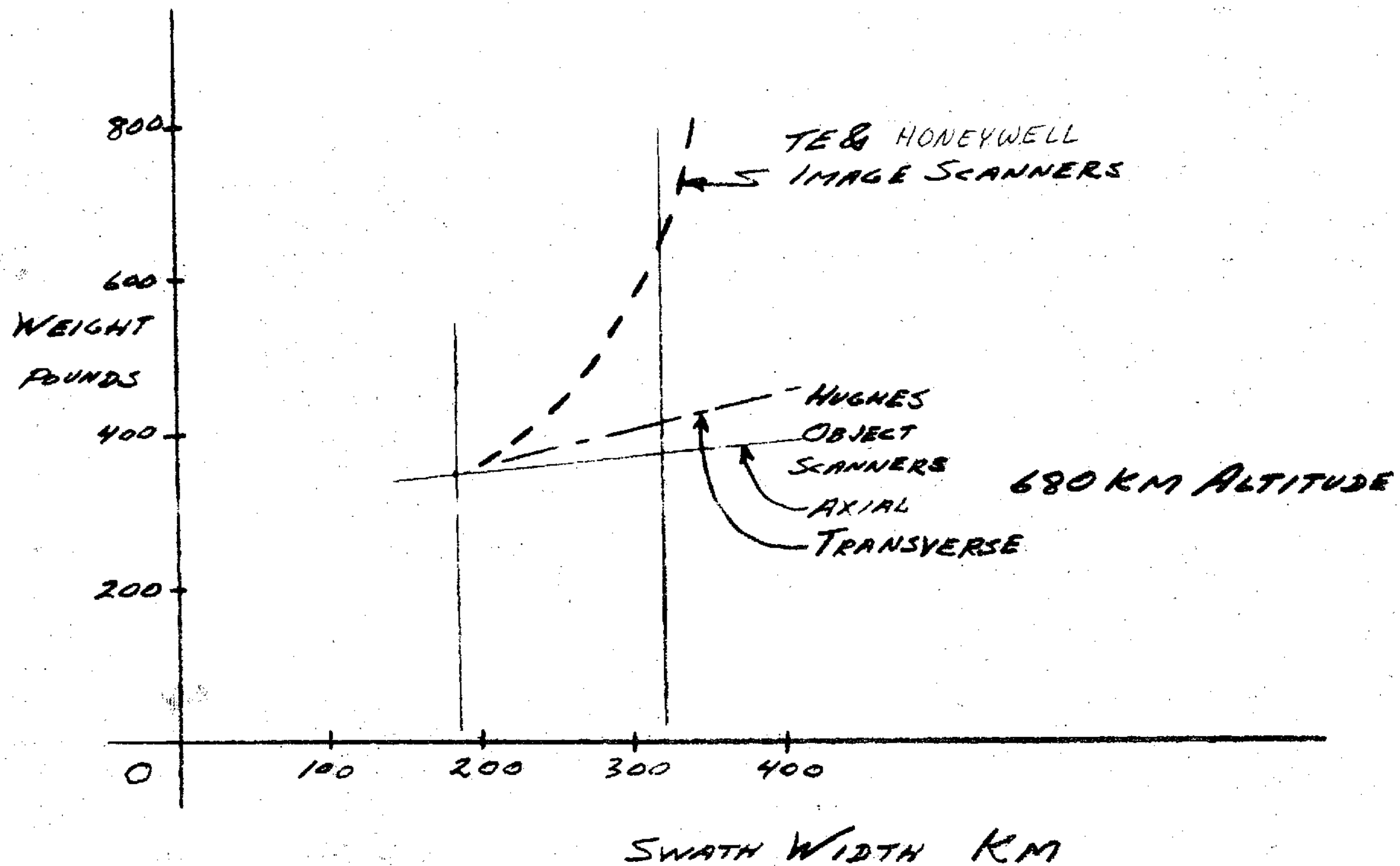

Fig 4-10 Instrument Weight Vs Swath Width

a pointing mirror was added, in two cases the entire instrument was redesigned to roll about the roll axis. Both satisfactory modifications involving less than 50 pounds. Where a major part of the instrument is rolled, an additional penalty of about 20 pounds is incurred in order to provide momentum compensation. Internal compensation is preferred over reliance on the ACS due to the desirability of pointing the HRPI rapidly and minimizing the settling time following pointing to ensure adequate capability for acquiring data from targets at similar latitudes on a single pass.

The electronic push broom HRPI was originally designed with a faulty optical system. When corrected, the total weight of this and the other HRPI's will all approximate 400 pounds (including momentum compensation) for the 680 KM Orbit.

GROWTH VS YAW ERRORS

All of the linear scan HRPIs and the extended swath TM's place a heavier requirement on the spacecraft yaw accuracy as the extreme scan angle is increased. In the absence of adequate yaw control, the required ground processing increases in complexity.

DESIGN COMPATIBILITY

Based on the current state of instrument design, each of the mechanical scanner suppliers is offering a pair of scanners, one TM and one HRPI, based on a single structural package. Therefore, considerable design cost could be saved by acquiring both instruments from the same supplier.

E.2.4.2.2 Candidate Detector Systems

All of the point designs choose the same detector type for band 7 and there is little choice for detectors for band 5 and 6. The area where choices remain is in bands 1 to 4.

For band 7, Mercury Cadmium Telluride operating at 100° Kelvin is the detector of choice. No other detector is known to meet the requirements at a temperature achievable with a passive cooler.

For band 5 & 6 a similar selection can be made. Indium Antimonide, though requiring cooling, has a very low internal power dissipation and represent a very small load to the cooler. By using a cooled filter immediately in front of the cell, a very good inherent S/N can be achieved. Whether this performance can actually be achieved is highly dependent on the design of the preamplifier used since due to the low impedance of the detectors, the circuit is usually preamplifier noise limited.

The performance in band 6 is generally found to be marginal in all of the point designs and the suggestion appears repeatedly that band 6 be combined with band 5 in order to provide generally higher performance. User requirements must be examined before taking this step.

In the visual region of bands 1 to 4 is where the most significant choices are required. In earlier programs, photo-emissive photo-multiplier tubes were by far the best performers, particularly when used in the multiple internal reflection mode. Recently, the solid state silicon technology has clearly surpassed even the new GaAs target PMT in the long wavelength band 4 and as better and better preamplifiers are designed it will also surpass PMT's in band 3. Hughes Figure 4-11 , has indicated in their HRPI point design that the number of silicon diodes for band 1 (the most challenging) is only 2-2.5 times the number of PMT's required, a very acceptable number except for the bow-tie errors encountered. These calculations were made for room temperature devices. TE corporation has introduced the idea of cooling the detector preamps to about 200°K in order to eliminate (reduce) the mostsignificant noise contributors. This leads to an improvement of about 1.6:1, nearly that needed to overcome the advantage of PMT's illustrated by Hughes.

Though the absolute superiority of silicon cells over PMT's may be argueable for some time, they exhibit nearly adequate performance and offer a number of significant advanteages.

1. They are considerably smaller and lighter.

2. They are a great deal cheaper and easier to space qualify. As time goes on the use of PMT's in industry will continue to drop causing their cost to increase further.

3. They are much simpler to interface to the optical system.

4. They offer growth potential both in single cell performance but also in integration of the signal from multiple cell arrays.

By modifying Figure E. 4-11 taken from the Hughes point design to reflect cooling, the use of about 20% more silicon cells than PMT's results in a design of comparable performance for the two cases. The use of even a few additional silicon cells is feasible and leads to an inexpensive improvement.

Of even more significance, is the growth potential available with silicon technology. If an increase in sensitivity is desired, the silicon cell arrays for each band, which at the moment are one dimensional, can be changed to two dimensional and longer signal integration can be obtained for each pixel by

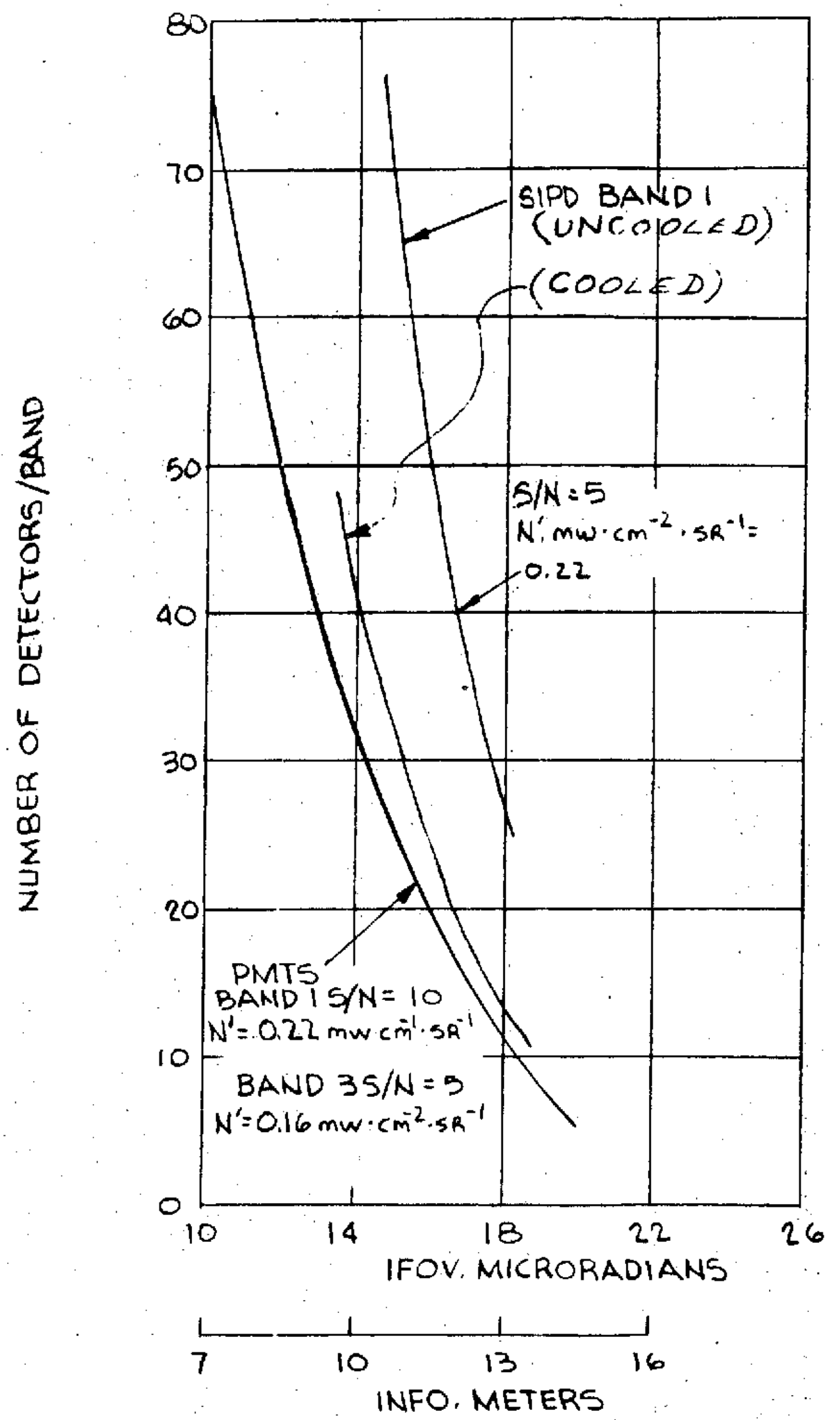

E-6

Fig. 4-11. Number of Detectors Required vs Resolution

GRUMMAN

TRADE STUDY REPORT

TITLE	TRADE STUDY REPORT NO.
	WBS NUMBER

employing "delay integration", (a technique which is intrinsically incompatible with oversampling which is discussed elsewhere). This is the technique suggested in the Hughes HRPI design. The technology to accomplish this improvement is already available in early form from several military space programs.

It is recommended that an all solid state detector package be utilized on both the TM and HRPI, utilizing a slightly larger aperture if necessary to achieve the necessary S/N ratio, that provision be made for cooling the band 1-4 detectors and preamplifiers to 200°K, and that provision be made for retrofitting two dimensional sensor arrays for each spectral band in the future.

E. .4.2.3 Output Data Formats

The total data rate out of each of the optical instruments is in the 100 megabit per second region, and is initially generated as approximately 100 individual analog channels. The choice of the method of transmitting this data and assimilating it for transmission are primary as is the question of the location of the interface between the instruments and the data transmission system.

The output data rate of the instruments is proportional to:

the scan width

the IFOV (Reciprocal Squared)

the scan efficiency (reciprocal)

the number of bands

the number of samples/IFOV

the number of bits/sample

the vehicle altitude ($\sqrt[6]{h}$)

E.4.2.3.1 Scan Efficiency

In all candidate instruments, a scan efficiency of between 70% and 80% is predicted. At 80% efficiency, it is not deemed useful to add a buffer on board the spacecraft to equalize the data flow and lower the data rate. With the cost of a data channel rising at the fourth root of the bandwidth, it is much cheaper and more reliable to raise the bandwidth rather than add a large on board, high speed Buffer.

E.4.2.3.2 Scan Linearity

Because each of the candidate linear scanners exhibits a temporal distortion in its scan there is a tendency to want to correct this prior to transmission in order to make it easier on the ground station. In the present image plane linear scanner, the error is due to the Earth's curvature. The error is small and predictable, since it is trigonometric. The object plane linear scanner as currently breadboard exhibits temporal scan nonlinearities of a higher order which are repeatable but not as well behaved. By operating the scanner in a closed loop mode, its temporal linearity can be brought to a residual error which is also trigonometric.

These remaining trigonometric errors are sufficiently small that the radiometric quality will not be affected. However, the error in true ground position still amounts to tens of pixels at the edge of the scan. Removal of these residuals can be accomplished in two ways; by sampling the detectors on board assynchronously and then clocking out the samples synchronously, or by sampling and transmitting the samples synchronously and correcting the errors along with the other geometric errors of pointing in a single correction process using a product matrix in the computer. This latter approach is by far the better one. It leaves the on-board equipment all synchronous and as simple as possible. To alleviate any problem in case of failure of the scanner feedback loop, it is proposed to transmit a scan error code on a per pixel basis on a routine basis. Therefore the result of a loop failure can be corrected on the ground, at least at the main station, with only a small reduction in throughput.

E.4.2.3.3 Offset Scanning

An additional problem appears in the case of a HRPI at high aspect angles. The bow-tie effect may become large enough to effect both the radiometric accuracy of the data and the amount of overlap in the imagery, (approaching 25% or $\frac{1}{4}$ of all detectors). Correction of this effect on board is complex requiring both a scan rate and scan duty cycle change. A preferred correction is to correct the radiometric data on the ground for not only scan angle effects but also for atmospheric column effects. Similarly, the geometric data can be corrected by the simple expedient of blanking out data from one of each pair of overlapped detected channels or by averaging.

In all of these cases, the preferred data handling approach involves synchronous sampling with a fixed clock.

E.4.2.3.4 Orbit Altitude Corrections

Consideration of a variable clock must be looked at from one other perspective, the possibility of an incorrect orbit injection. An error in the mean altitude and/or orbit ellipiticity could result. These errors are correctable with the basic orbit adjust system and are therefore unlikely unless a major malfunction causes a gross error which will necessarily result in a non sun-synchronous orbit and a compromised mission. For mean altitude errors of less than 50 kilometers, the data can be radiometrically corrected without resorting to a variable clock and the geometric errors amount to approximately 1 IFOV per stripe. There seems to be little chance of an altitude error of sufficient magnitude to justify a scan rate which is variable in flight.

Using the 185 KM swath width, 30 microradian resolution TM at 680 KM as a reference, and employing 15 detectors in each band except 7 where 5 are used, (15/5 is chosen rather than 16/4 in order to better accomodate the LOGS mode of operation). The time to move from one pixel to the next is approximately 6.72 microseconds.

E.4.2.3.5 Data Sampling Rate

An area of significant importance in the trade study is that involving the number of data samples to be transmitted per IFOV. As will develop below, specification of this ratio has a number of very important system ramifications:

1. It has a very significant operating cost impact amounting to millions of dollars per year.
2. It can have a significant impact on the accuracy of the radiometric data particularly at low radiance levels.
3. It can effect the fidelity of the reproduced imagery from a "resolution" and edge response point of view.
4. It can have a major impact on the growth potential of the overall system design selected.
5. There is a historical precedent in the developmental ERTS system which may or may not be relevant to the design of an operational system such as EOS.

Each of these impacts; cost, performance, and philosophical must be examined closely in arriving at an optimum system design.

Definitions

Because of the complexity of this study area, certain background and definitions are appropriate before proceeding.

For the types of instruments being considered here, using a row(s) of discrete continually integrating sensory cells whose field of view is being continually swept across a (relatively) stationary scene, the spatial performance is best described in a different manner for the along the row and the along-scan direction.

Therefore, the following definitions will be adopted:

	Along Scan	Along Row
The image response of the telescope	I_{ts}	I_{tr}
The image response of a single sensor cell	I_{ds}	I_{dr}
The image response of the sensor array	I_{as}	I_{ar}
The image response of any filter prior to sampling	I_{fs}	I_{fr}
The image response of the sampling system of the A/D converter	I_{ss}	I_{sr}
The image response of the reconstruction printer	I_{rs}	I_{rr}

In the above table, it is generally a good approximation that the system image response from the input to a given interface is described by the RMS sum of the image responses prior to that interface. Although the telescope itself is not quite Gaussian in image response, the central limit theorem is complied with after summing at least three image responses, i.e., prior to sampling and certainly after sampling. Thus the RMS sum is justifiable.

In the EOS system, the image response $I_{sr} = 0$ since no sampling is done along the row except that due to the geometry of the array I_{ar}. For the non-CCD TM configurations, $I_{as} = 0$. Also $I_{fr} = 0$ since the analog filtering provided does not affect the data in the along the row direction.

To conform to earlier definitions on the EOS program, the instantaneous field of view (IFOV) of the instrument is given by

$$IFOV_s = \sqrt{I_{ts}^2 + I_{ds}^2 + I_{as}^2 + I_{fs}^2}$$

$$IFOV_r = \sqrt{I_{tr}^2 + I_{dr}^2 + I_{ar}^2 + I_{fr}^2}$$

and

$$IFOV_s = IFOV_r = IFOV$$

by specification.

The overall system performance can best be described by the system field of view (SFOV) given by

$$SFOV_s = \sqrt{\sum I_{-s}^2} = \sqrt{IFOV_s^2 + I_{ss}^2 + I_{rs}^2}$$

$$SFOV_r = \sqrt{\sum I_{-r}^2} = \sqrt{IFOV_r^2 + I_{rr}^2}$$

Generally, the system design will call for

$$SFOV_s = SFOV_r$$

however, this is difficult to achieve if $IFOV_s = IFOV_r$. It requires

$$IFOV_s^2 + I_{ss}^2 + I_{rs}^2 = IFOV_r^2 + I_{rr}^2$$

This can be achieved by degrading the reconstruction equipment (making $I^2_{rr} = I^2_{rs} + I^2_{ss}$) for the effect of sampling or by increasing the sampling rate to make I_{ss} approaching zero. Alternately the above equation can be an inequality resulting in an assymetrical output capability.

$$SFOV_s \neq SFOR_r$$

An alternate approach is to hold

$$SFOV_s = SFOV_r$$

and relax the requirement that

$$IFOV_s = IFOV_r$$

then any individual image response can be modified to optimize overall system.

By referring to Figure 4-12a, it can be seen that the data to be transmitted is presented to the array in parallel. Furthermore, the discrete position of the array causes its output to be phase sensitive. The frequency response function is statistical in nature rather than unique as illustrated in Figure 4-12b. Thus, whereas the overall image response of the system along the row is unique in a sense, its frequency response is not. Thus, an IFOV specification is probably most appropriate.

For the along the scan direction, a similar result is obtained but due to a different process. The overall system response is obtained as a result of a number of processes as indicated in Figure 4-12c. The data is presented to each cell in serial fashion, each cell sees portions of two data points simultaneously for a major portion of a sampling interval. This results in an output signal which is highly dependent on the sensor cell size relative to the imagery. For a bar pattern of the same pitch as the sensor maximum dimension, the high frequency content of the signal is greatly attenuated. The signal is then usually band limited further to minimize the noise content of the signal regardless of source, Fig. 4-12d.

The above signal is now sampled for purposes of transmission by digital means. The frequency of sampling has a distinct impact on many aspects of the system. Technically, its principle impact is on the fidelity with which a repititive pattern on the ground, at limiting resolution, is reproduced.

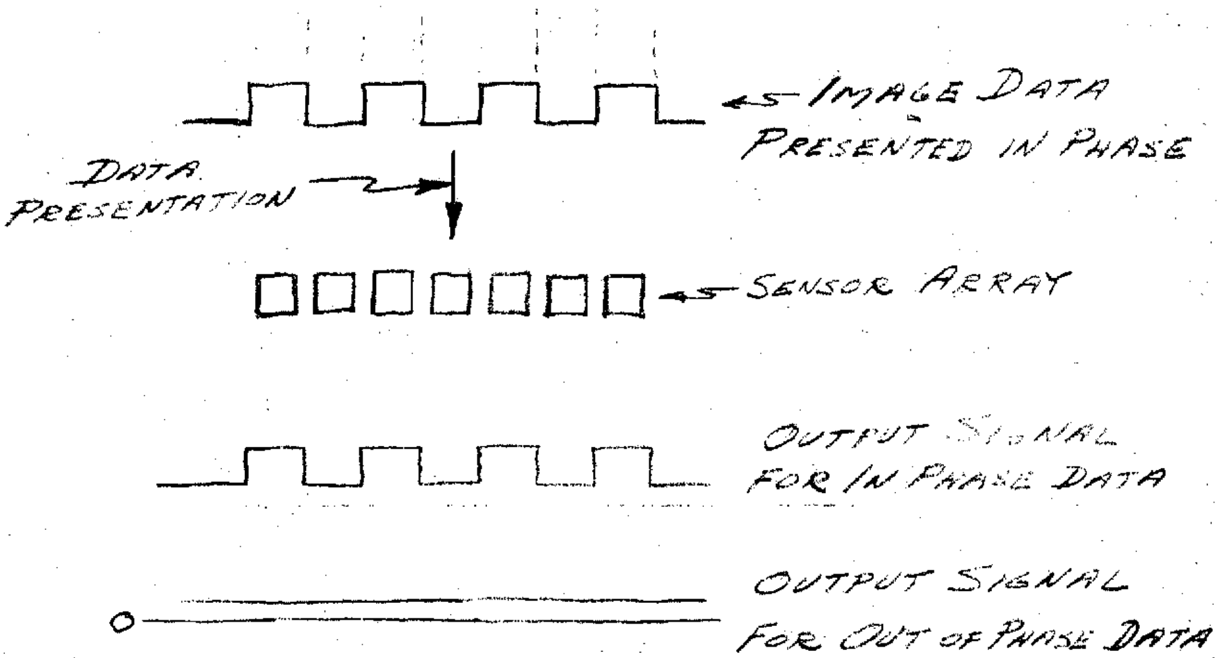
IMAGE DATA
PRESENTED IN PHASE
DATA
PRESENTATION
SENSOR ARRAY
OUTPUT SIGNAL
FOR IN PHASE DATA
OUTPUT SIGNAL
FOR OUT OF PHASE DATA

E-7

Fig. 4-12a

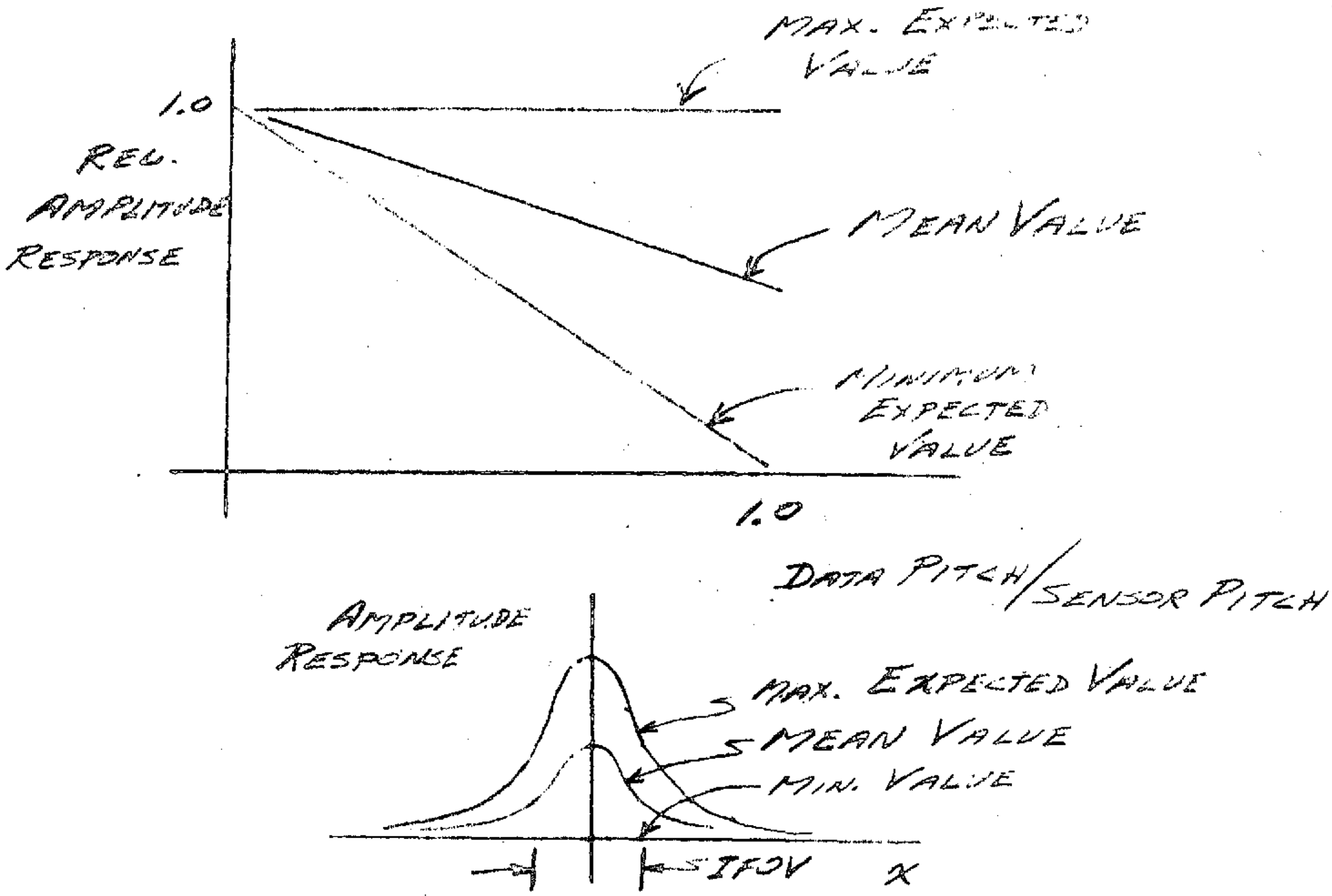
MAX. EXPECTED VALUE
1.0
REL. AMPLITUDE RESPONSE
MEAN VALUE
MINIMUM EXPECTED VALUE
1.0
DATA PITCH/SENSOR PITCH
AMPLITUDE RESPONSE
MAX. EXPECTED VALUE
MEAN VALUE
MIN. VALUE
IFOV
x

E-8

Fig. 4-12b

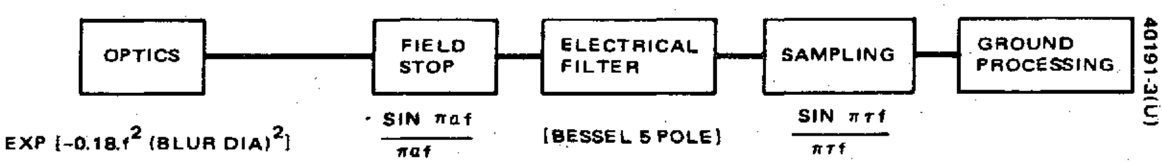

E-9

Fig. 4-12c Discrete Detector Analysis

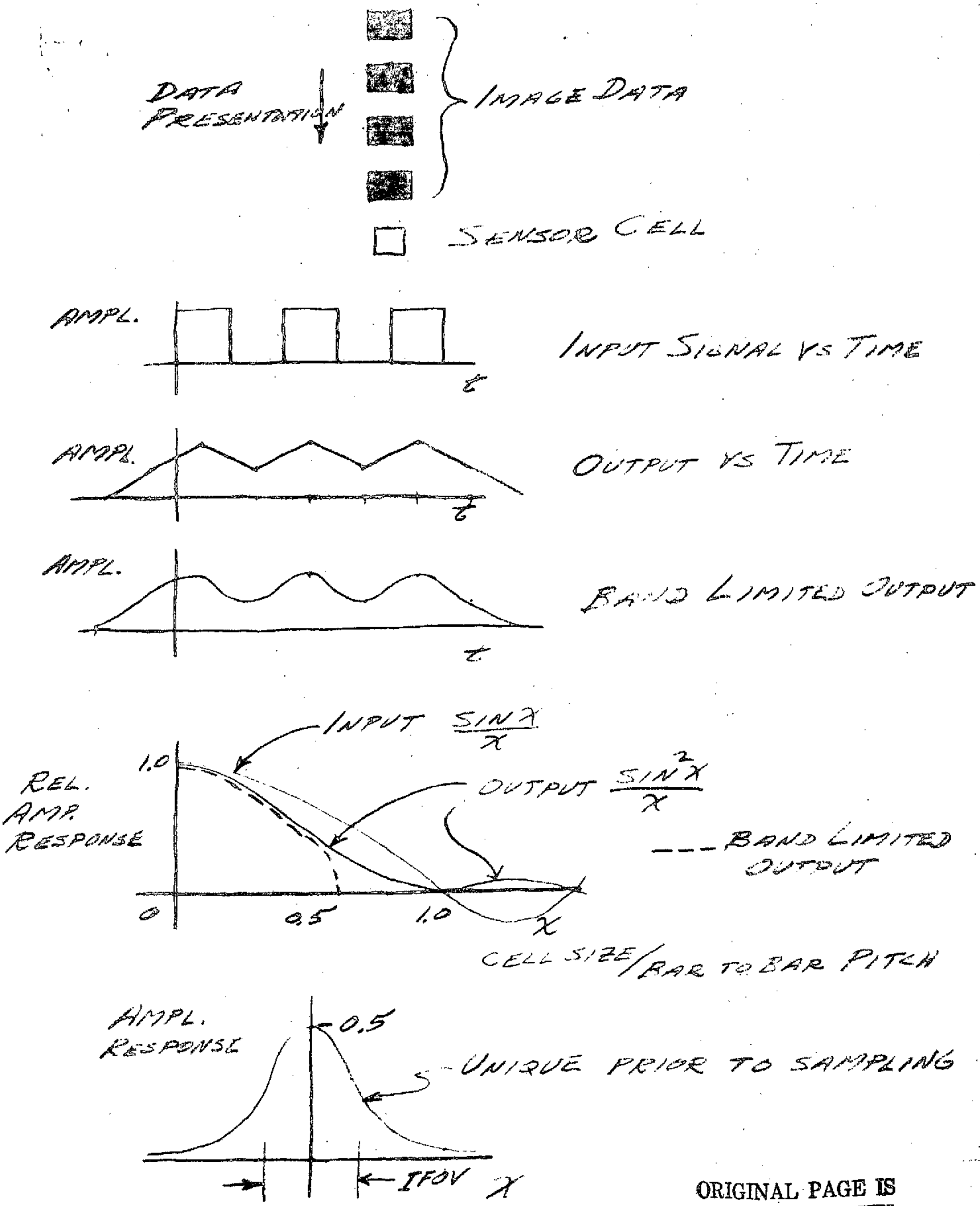

E-10

Fig. 4-12d

ORIGINAL PAGE IS OF POOR QUALITY

Shannon, when working with one dimensional audio signals, that two samples per cycle at the limiting resolution was adequate to reconstruct a long periodic pulse train. It is not adequate to reconstruct a short train because of inadequate phase information. Aliasing will frequently result in such a case.

Kell later showed that in commercial television, a poor analog to the current problem in terms of both scene content, scanning method and scene to scene integration, that 2.8 samples per cycle was a good statistical choice for TV broadcast purposes employing a virtually noise free signal (and certainly not a photon noise limited system). This criteria was developed boased on average scene content and was measured by using a long multi-line wedge target.

In modern military photo-transmission systems, an even stricter criteria is employed. It is required that only a few short parallel bars at or near limiting resolution be reproduced faithfully without aliasing or drop-outs(i. e. retaining the phase information). This criteria generally requires at least four samples per cycle.

In each of the previous applications, the absolute brightness levels associated with the data is of little concern, geometric detail is of greater concern.

For the land resources mission of interest here, a criteria different than any of the above may be appropriate. Clearly, the absolute radiance levels of the data is of greater interest. Furthermore, with the availability of data from multiple spectral bands simultaneously, the differential radiance data is of considerable interest-particularly if it is of adequate quality. Quality in this mission seems based much more strongly on signal to noise ratio than on fine spatial resolution.

Therefore, the criteria for this mission is clearly different than for those annotated above.

Cost Impact

The principle cost impact related to the sampling ratio is a straight forward one involving the cost of processing the additional data points related to a sampling ratio greater than 1.0. This additional cost falls into one or both of two categories:

1. For a map of 1.6 samples per IFOV in one direction and only 1.0 in the other, as in the NASA baseline, the total number of data cells is 1.5 times that of a map of 1.0 by 1.0 samples per IFOV.
2. The cost of recomputing a 1.0 by 1.0 samples per IFOV from the original 1.5 by 1.0 map.

The cost of data processing associated with the correction of the imagery, as received at the main station, into a fully corrected map is a major system cost. As shown elsewhere in this report, the cost of processing each map is between $36 and $92 based on 1.0 by 1.0 samples per IFOV. The cost of processing a 1.5 by 1.0 map is 50% higher as illustrated in Figure 4-12e.

Since this cost is an operating cost, it is highly dependent on map volume. Figure 4-12f shows data from the ground data processing report of this study modified to illustrate the cost of processing these maps as a function of sampling ratio.

Note the significant cost of raising the sampling ratio. The differential cost, also plotted on this chart, far exceeds the entire cost of operating the MOCC for a relatively few TM maps per day. Furthermore, the savings involved in using a 1.0 by 1.0 sampling ratio rather than the baseline can save $20 million dollars over a five year interval, a significant portion of the total system cost.

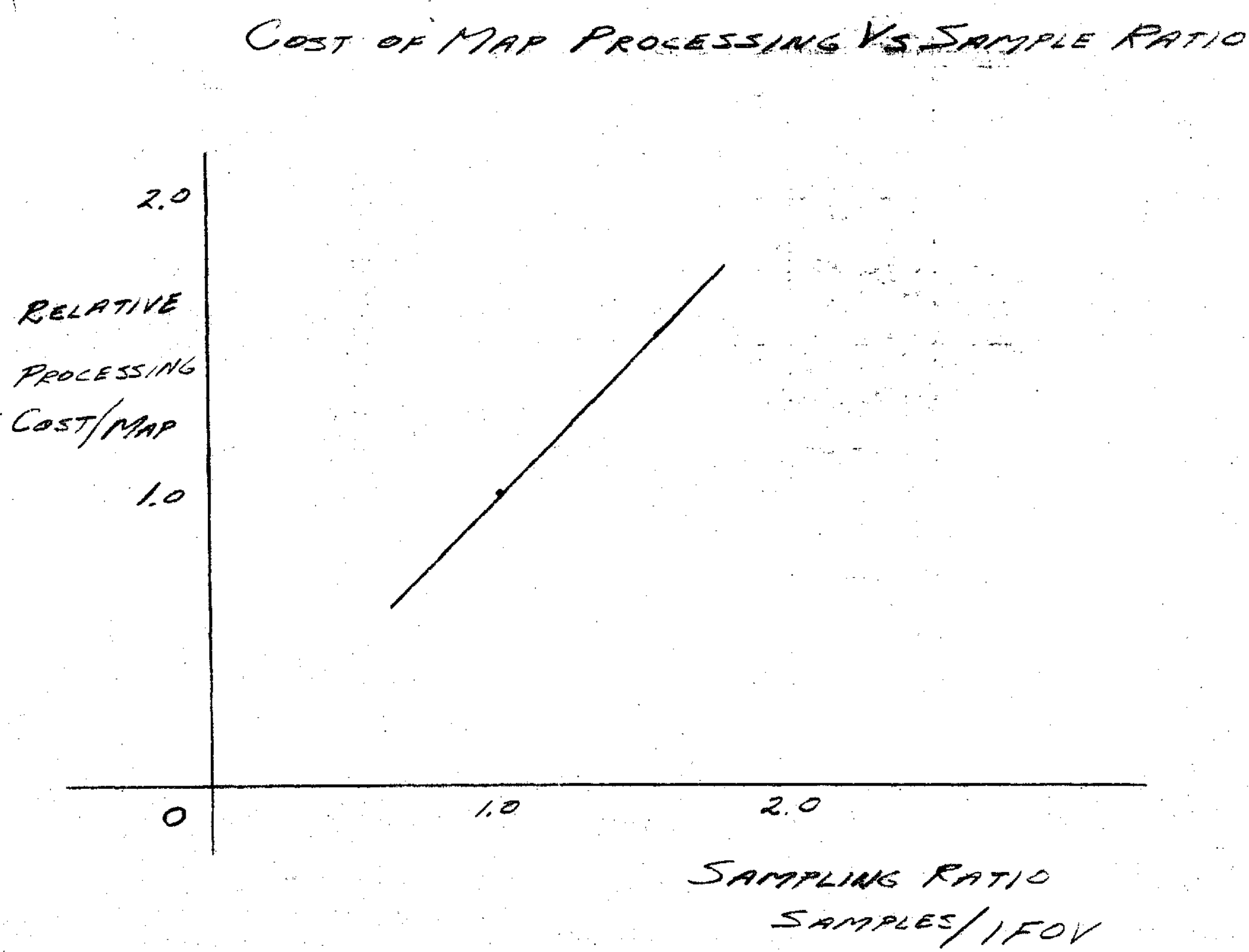

Fig. 4-12e Cost of Map Processing Vs Sample Ratio

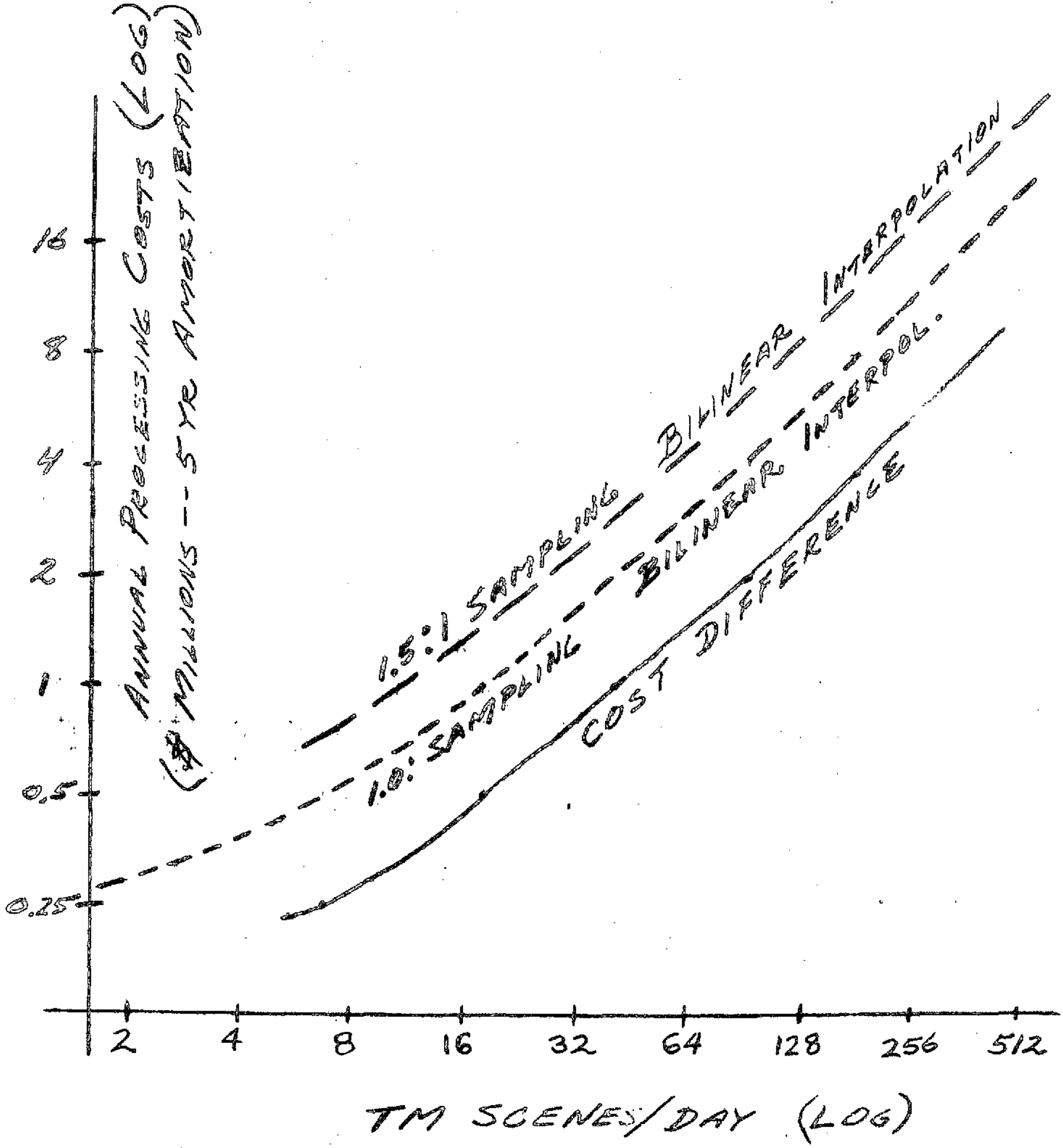

ANNUAL PROCESSING COSTS (LOG)
($ MILLIONS -- 5 YR AMORTIZATION)
16
8
4
2
1
0.5
0.25
1.5:1 SAMPLING BILINEAR INTERPOLATION
1.0:1 SAMPLING BILINEAR INTERPOL.
COST DIFFERENCE
2
4
8
16
32
64
128
256
512
TM SCENES/DAY (LOG)

E-12

Fig. 4-12F

If after generating a fully corrected 1.0 by 1.5 sample map, it is desired to generate a one data point per IFOV map, a 1.0 by 1.0 sample ratio map, two avenues are possible.

First, the corrected 1.5 by 1.0 map could be further processed to give the desired map at relatively little additional cost(about 25% since no geometric correction is involved) and probably no change in radiometric quality.

Alternately, a special purpose processer could be used to eliminate the extra data points on the original tapes prior to reprocessing into a 1.0 by 1.0 map at the cost originally quoted.

MAP COSTS STARTING FROM A RAW 1.5 by 1.0 MAP

Map	Nearest Neighbor	Bilinear
1.5 by 1.0	$54	$138
1.0 by 1.0	36	92
Both maps	67-90*	172-230*

* lowest number by use of special purpose processer. Higher number is by reducing 1.5 by 1.0 map to 1.0 by 1.0

Sampling vs Spatial Fidelity

There are two principle technical aspects to be considered in selecting the sampling ratio. First, the impact on the S/N ratio of the data(radiometric) and second, the impact on the spatial fidelity of the imagery along the scan defined more specifically as the effect on the point image spread function (or its integral, the edge response).

For a noise limited system, the effect on the radiometric quality of using a different sampling ratio is quite straight forward and depends on whether the noise is of detector origin or photon origin. Figure 4-12g illustrates the two conditions for the case of a uniform intensity level at the input (the large area case). The differential signal to noise ratio between two adjacent resolution elements is considerably poorer due to the loss of response at high spatial frequencies.

As seen from the figure, in areas of low intrinsic radiance, the quality of the radiometric data will be impacted by a sampling ratio significantly greater than 1.0, everything else being equal.

The effect on the spatial quality is not so direct since the point spread function due to scanning is convolved with several other spread functions of similar value. Thus referring back to Figure 4-12c, it is seen that the total spread function and MTF is the composite due to four elements;

1. the optics
2. the field stop or sensor cell
3. an electrical filter
4. the sampling process

The sampling process involves a statistical process not unlike that described in Figure 4-12a above. The resulting MTF is phase sensitive and not unique, it is as shown in Figure 4-12h. The probability distribution associated with this process appears to be flat so that the mean MTF is descriptive.

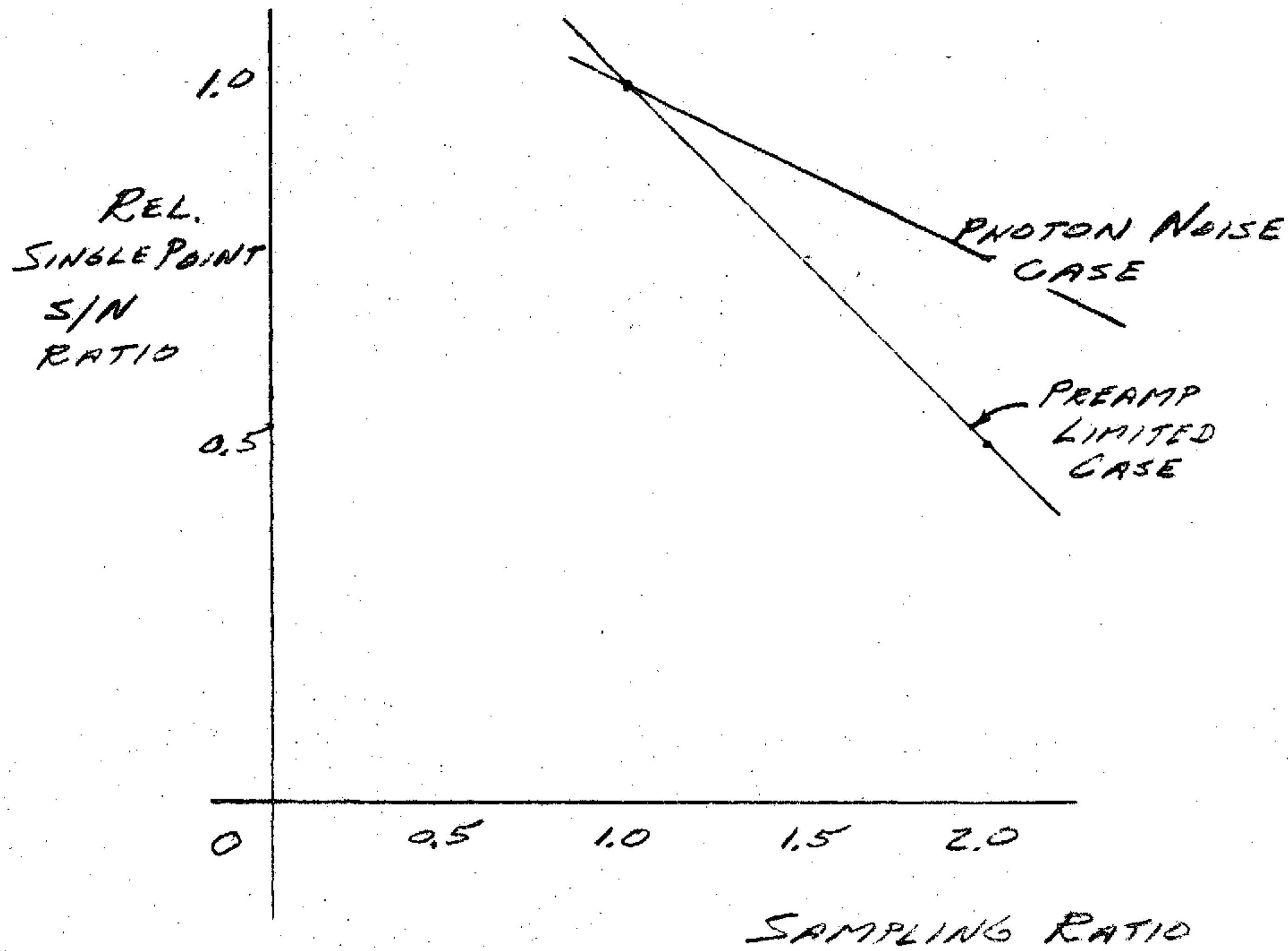

1.0
0.5
REL.
SINGLE POINT
S/N
RATIO
PHOTON NOISE
CASE
PREAMP
LIMITED
CASE
0
0.5
1.0
1.5
2.0
SAMPLING RATIO

Fig. 4-12g

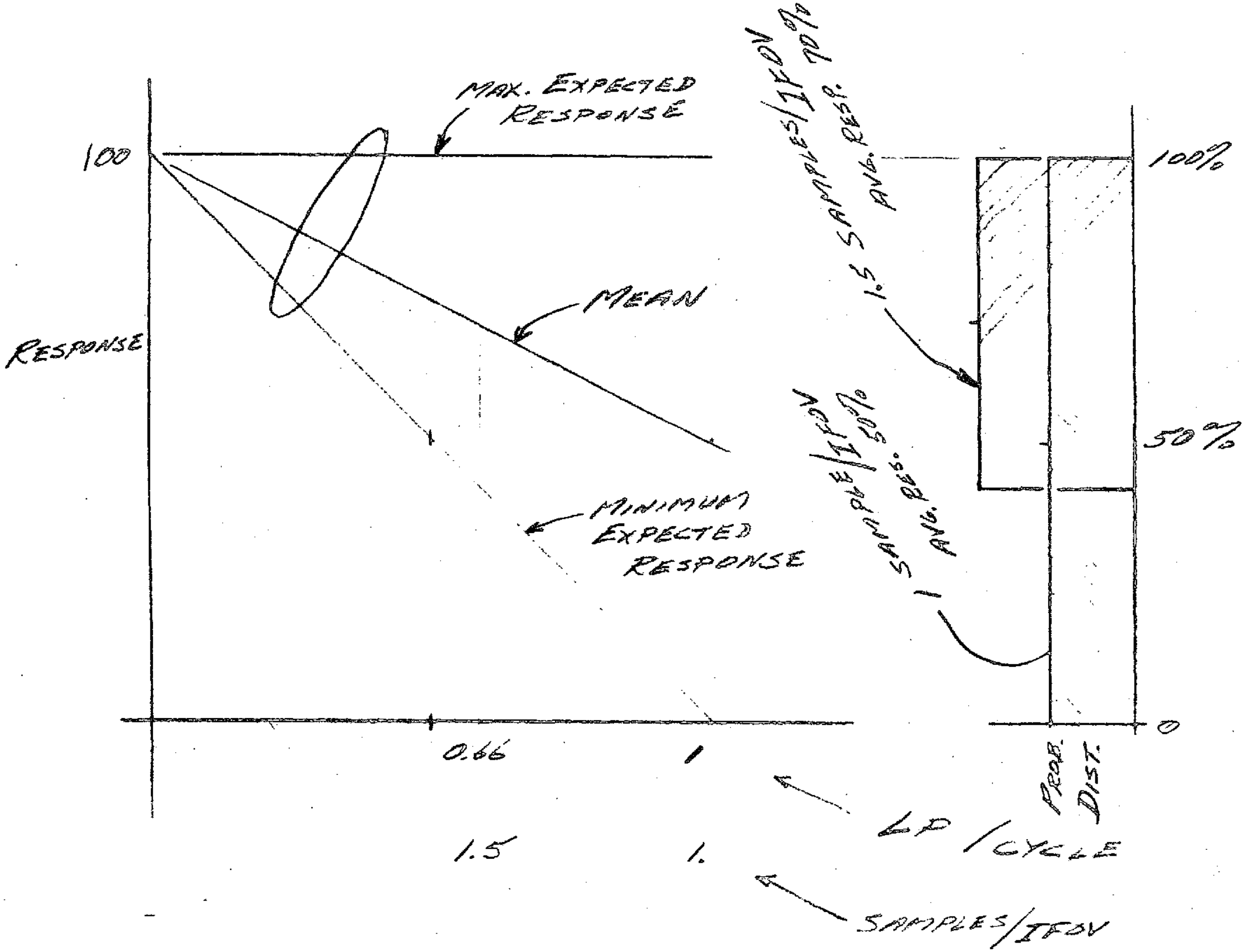
MAX. EXPECTED RESPONSE
100
RESPONSE
MEAN
MINIMUM EXPECTED RESPONSE
1.5 SAMPLES/IFOV AVG. RESP. 70%
1 SAMPLE/IFOV AVG. RES. 50%
100%
50%
0
0.66
1
1.5
1.
LP/CYCLE
SAMPLES/IFOV
PROB. DIST.

Fig. 4-12h

Figure 4-12i illustrates graphically the system costs as they relate to the sampling ratio and the MTF due to sampling. Note the sampling ratio, the data rate, and the cost of ground data processing are all shown on a common scale as a function of the sampling MTF. The average MTF due to sampling is seen to drop from 71% to 50% as the sampling ratio goes from 1.5 to 1.0. However, this is not the system MTF.

Looking again at our equation for the image response of the system, and neglecting the effect of the ground reconstruction equipment.

$$SFOV_s = \sqrt{IFOV_s^2 + I_{fs}^2 + I_{ss}^2}$$

$$\text{and} \quad SFOV_r \quad \sqrt{IFOV_r^2} = IFOV_r$$

Looking at the above figures in tabular form and using a baseline IFOV expressed as 30 meters ground resolution $(I_{fs} \ll IFOV_s + I_{ss})$,

	IFOV	SAMPLE SIZE	SFOV	COMMENT
1. Along Row	30^M	—	30^M	Baseline
2.	37^M	—	37^M	Larger Detectors
3. Along scan	30^M	21^M	37^M	1.5:1 sampling
4.	21^M	30^M	37^M	1.0:1 sampling

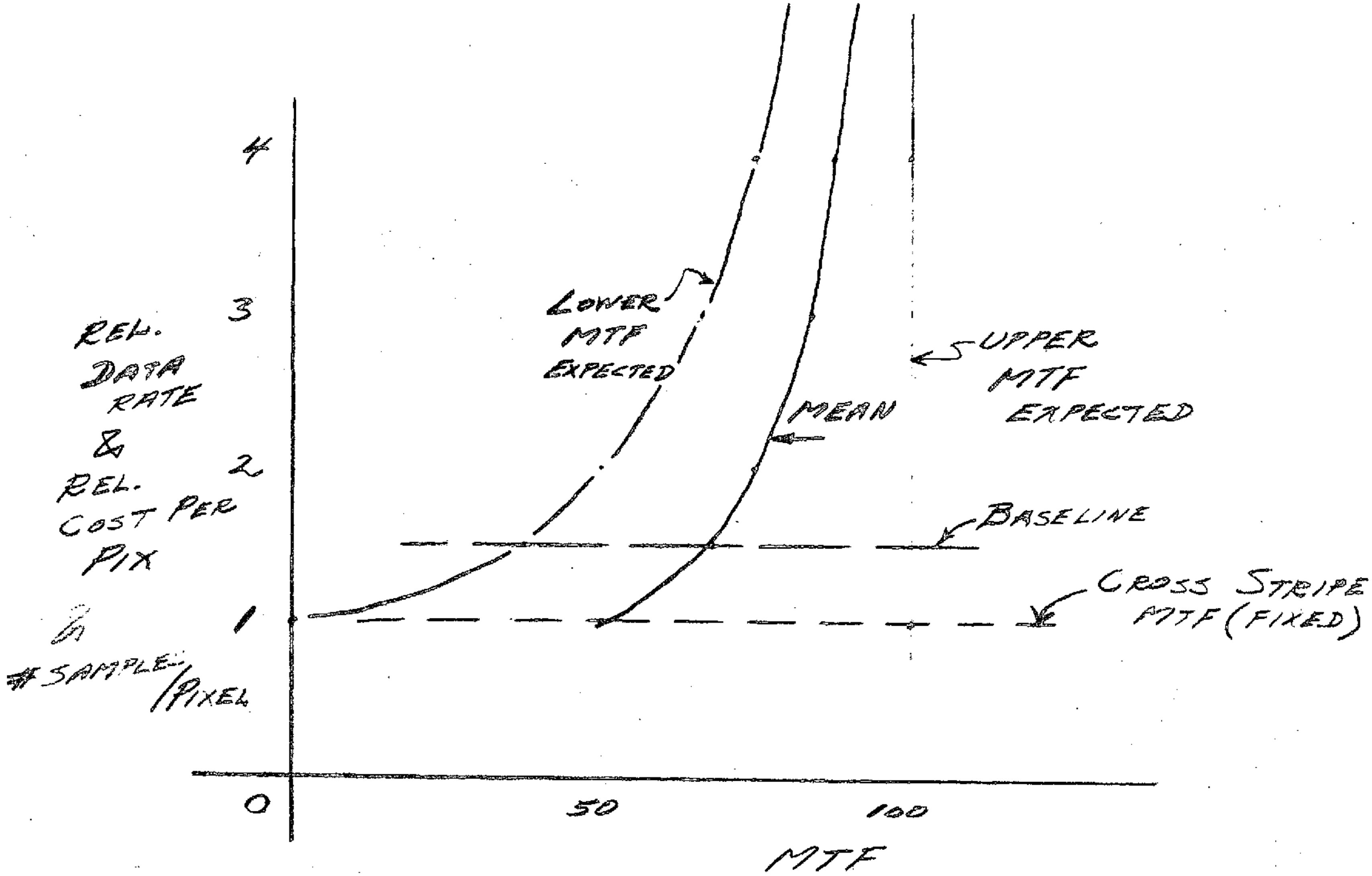

Fig. 4-12i Cost Trade Vs One Dimensional MTF (Due to Sampling Only)

Note the baseline system - (line 1 and 3) provides 30 meter system resolution in one direction and 37 meters in the other. An alternate design, lines 2 & 4 would provide 37 meters in both directions. This design would improve the along scan $IFOV_s$ by reducing the size of the detector cells in this direction by 1/3 and degrade the $IFOV_r$ slightly by increasing the detector size by 25%. The net effect on cell size would be small, a reduction in area by 16.5%, resulting in only a minor loss in S/N performance.

The design of the optical system would not be modified in any way, unless it was easy to increase the aperture by 8% -- less than 1" -- to regain the above signal to noise loss.

There is another method of achieving a 37 meter system response without reducing the along scan cell size (at least not so much). This involves departing from conventional gaussian analyses and using an electrical filter with a response which rises with frequency until system cutoff is approached. Such a pre-emphasis filter is capable of providing an increase in the instrument MTF prior to sampling at little cost and no performance penalty.

The filter should be of zero phase shift design since the other apertures in the signal chain cause a non-phase shifted roll-off in response.

Such a filter when analyzed in conjunction with the other apertures as a group does not introduce any undesirable ringing or other artifacts. In fact, it is normal engineering practice in photo transmission to introduce even more pre-emphasis prior to image reconstruction in order to remove the blurring and contrast reduction effects of the reproducer <u>and</u> telescope.

Figure 4-12j indicates how Hughes achieved the same instrument MTF <u>after sampling</u> in their HRPI point design while reducing the data rate to 76 Mbs.

Because of the considerable operating cost savings realizable and the lack of any significant performance penalties, it is recommended that:

1. The instrument be specified for an assymmetrical IFOV.

2. That the along scan instrument IFOV be specified as approximately 1/2 of the cross scan value by using rectangular sensor cells or aperture stops (the telescope response remains symmetrical).

3. That the sampling interval be chosen to have an equivalent sample size equal to 3/4 of the system field of view (SFOV) and 1.5 times the along scan $IFOV_s$.

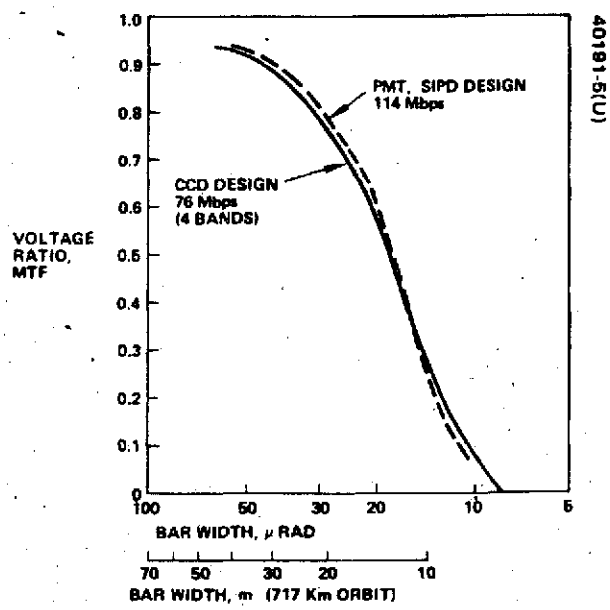

E-16 Fig. 4-12j MTF (Including Sampling) For CCDS and Conventional Detectors

The annual dollar savings in the ground data processing facility can reach or exceed $2 million per annum through this choice.

The recurring cost penalty associated with this recommendation would be at worst 1/8 of the above savings, about $0.25 million per launch because of the increase in telescope aperture size of about 1".

No performance penalty is anticipated as far as the imagery is concerned. On the contrary, as discussed elsewhere, the use of the suggested sampling ratio is compatible with the introduction of the new CCD technology at a later date. This can provide a growth of 10:1 in system radiometric sensitivity, providing a considerable increase in the systems performance at high latitudes and during the winter months.

Thus the question arises as to how the raw data should be encoded for transmission, by dividing the maximum dynamic range into a large number of linearly spaced increments no larger than the finest grey level change, by dividing the range non-linearly into a number of levels which are finer at the lower radiometric levels, or using a linear division which is switchable to provide the best of both capabilities. The choice comes down to two; whether to use 6 or 7 bit encoding, and whether to use linear or non-linear amplitude encoding. A parameter effecting these two choices is whether or not the dynamic range chosen can be varied on command. Figure 4-13 illustrates the possibilities.

The best choice of these options is to use 6 bit encoding in a linear mode with a command switchable dynamic range.

The data interface between each instrument and the data transmission system is of considerable concern due to the susceptability of the signals to degradation at this point.

Another aspect of the interface relates to the ground data reduction. It is desirable for the data emanating from the ground processing system to have output words from each spectral band which relate to a given pixel to be transmitted as a group. To accomplish this, the spatial relationship between the various detectors must be known. Since the field of view of the various detector cells associated with each spectral band are not necessarily identical, or even physically relatable except through calibration, it is important that a specification be placed on the instruments in this area. This will then allow relatively simple processing on the ground to generate the desired sample grouping.

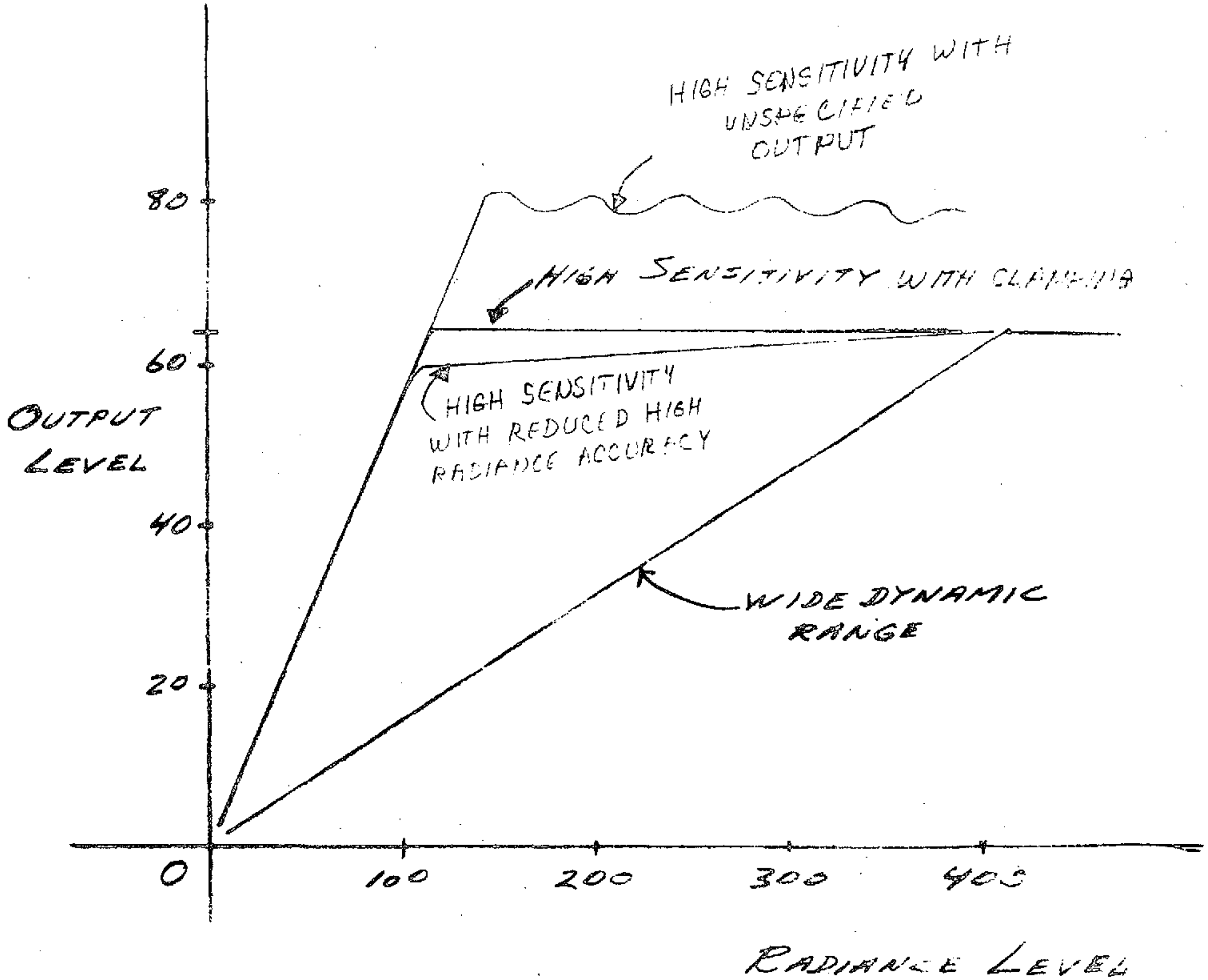

E-17

Fig. 4-13 Signal Level Transformation

In one of the point design instruments, both the east to west and west to east scan are used for data acquisition, in an attempt to keep the scan efficiency high. This causes a problem in data reconstruction since most recorders, particularly the cheaper optomechanical types, involve a continually rotating drum or optical system to recreate the scan. Generally, these recorders are also unable to record multiple data streams in parallel, such as are mandatory in the type of sensors anticipated for EOS. Because of the need to convert multiple parallel data streams into a single serial stream of higher data rate, it is anticipated that all stations, even LCGS users will record all of the data prior to reconstruction. If the data is recorded, only a slightly more complex memory system is required to turn the data from every other scan around than to merely change it from parallel to serial form. Therefore, the question of unidirectional versus folded output data is not of major significance to this study.

E.4.2.3.6 Data Encoding Accuracy

The expected dynamic range of imagery to be scanned by the TM and HRPI is relatively wide. However, the quality of the data within this dynamic range is variable; at relatively low radiance level which are of primary importance, the data is both of low contrast and of low signal to noise ratio. The low contrast calls for small steps between adjacent digital grey levels. The low S/N ratio indicates only coarse steps are needed on a pixel by pixel basis. However, large area integration may be a useful method of data analysis by some users to overcome this poor S/N ratio.

In the high radiance regions on the dynamic range, there is little information of critical value to the land resources related users. However, there could be a secondary output of the system of interest to the meteorology community if adequate contrast discrimination is available.

The above considerations all suggest encoding the overall dynamic range to seven bits or more and possibly providing this level of encoding over a selectable region of the overall dynamic range.

The cost impact on the ground data system of processing 7 bit versus 6 bit encoded data was examined. The computer system envisioned is expected to process the data in 8 bit Bytes. Thus even with one parity bit within the Byte, there is no cost impact with regard to computer cost.

With no operating cost impact to sway the choice, the non-recurring cost impact was examined. The use of seven bits instead of six bit encoding will have an impact on the system data rate and therefore could impact the data link costs. The increase in data rate will be 16%. This is less than 0.5 Db and should not impact the cost of the data link or ground stations.

The remaining question is then whether to use linear or non-linear amplitude encoding and whether or not to encode the entire and/or selectable portions of the dynamic range of the input imagery.

The best answer to the above choice is to rely on the actual experience being gained on the ERTS program. There is preliminary information indicating that the use of a switchable dynamic range A to D converter is and would be a useful feature. There is also preliminary information that the ERTS design may have a high sensitivity mode of the type illustrated in the upper portion of Fig. 4-13; saturation has been evident in some imagery due either to inadequate dynamic range in the electronics prior to the A to D converter or in the A to D converter itself.

Based on the above experience, the instrument dynamic range specification should probably be expanded to improve on the ERTS capability by controlling the output for over-range radiance inputs.

E.4.2.3.7 Data Interface

In reviewing the instrument-data link interface with the point design contractors, there was unanimous desire on their part to redefine this interface from that in the baseline. This desire was prompted by a number of considerations.

1. Merely mounting another supplier's encoder within the instrument did not alleviate the difficult grounding problem associated with 80-100 analog output signals.

2. Maintaining crosstalk and ground loops at a sufficiently low level to justify 7 bit encoding following an analog interface would also be difficult if two suppliers are involved.

3. Any synchronous noise detected in the output would probably not be detected until late in the program and it would be difficult to ascertain responsibility in this area.

These are very significant technical considerations which involve a significant design risk to the program and the contractors if an analog interface is desired between the instrument and the data link.

From the system design viewpoint, a second consideration is worthy of notice. A higher system reliability can be obtained if the data from the instruments do not pass through any common processor elements on their way to the two independent data outputs, the main data link and the LCGS link.

Thus, the concept of encoding all of the output data from an instrument into one serial bit stream and then stripping out a portion of the data for the LCGS user is a poor design from a reliability viewpoint.

A superior design, even at the cost of some prime power, would employ a separate low speed A to D converter for each spectral band to provide an output to both the main and LCGS processing system in parallel.

Following the above approach, failure of the main A to D converter cannot cause loss of the system. Failure of one A to D converter would only cause loss of one band of data; failure of the main data processor would cripple but not defeat the system. Failure of one or more modes of the LCGS processor would cause more inconvenience than loss since the data would still be available to LCGS users by alternate means from the main ground station's.

Whether the data emanating from the A to D converters is passed to the data processors in parallel or serial form is still open to analysis. It is colored considerably by the state of the art at the time of design freeze. In general, the use of a parallel wire digital interface leads to maximum flexibility in the data processors, the LCGS data rate need not be synchronously related to the main data link. It also avoids any data skewing problems which might arise with multiplexing multiple serial bit streams. However, the wire count at this interface, through reduced from the analog case, would still be close to fifty wires instead of the eight or so of a serial interface (including scan sync data).

It is recommended that the instrument-datalink interface occur after A/D conversion and it is suggested that a parallel wire interface, one set for each spectral band, be considered, all other things being equal. This recommendation is made primarily on reliability, data quality and ease of system integration considerations.

E 4.2.3.8 Data Grouping

(see Page 4-41 for text)

As indicated above, the linear point design scanners exhibit a scan non-linearity with time which is a complex function of the scanners basic non-linearity and the curvature of the earth. The scanner error predominates in a 185 Km swath scanner and is on the order of 3-10 parts per 1000 or on the order of 18 to 60 pixels per scan. This amount is sufficient to have a significant impact on the data management system, both from a radiometric and geometric point of view. The error in the object plane scanner is currently larger than for the image plane scanner, but the error is discontinuous in the image plane scanner making correction more difficult. Both corrections, if done on board the spacecraft, involve a servo loop with a drift interval during which a correction must be estimated. Correction of this error requires measurement of the error and prudence requires transmission of the error signal to the ground whether or not correction on board the spacecraft is attempted. Since the signal will be transmitted in any case and the added circuitry is a reliability consideration, the principle correction procedure should be ground based.

A special consideration applies if the linear object plane scanner is used in the high scan efficiency mode. The error between the east to west and west to east mode are not equal or symmetrical, implying that a quick look for LCGS printout without correction will result in significant missmatch between adjacent stripes. Because of this, the supplier of this scanner should be encouraged to linearize his scan employing a fail safe design which does not add additional elements to the data streams (correction of the scan mirror motion itself).

E. 4.2.4 CANDIDATE POINT DESIGNS

E. 4.2.4.1 COMPARATIVE EVALUATION

During the course of this study, each of the TM point design contractors developed an electro-mechanical HRPI point design and provided additional specific data concerning their TM designs. Hughes also submitted an alternate TM design based on the results of their HRPI design. This material provided the basis for a re-evaluation of the sensor designs. This re-evaluation will be treated along the following topical lines:

1. Volume, Weight, Power, Reliability
2. Scan Non-Linearity and its Consequences
3. Scan Rate Adjustability
4. Scan Efficiency and Buffering (or Spooling)
5. Synchronism of Scan Control and System Clock
6. Offset Pointing Mechanisms for HRPI
7. The Thematic Mapper Radiative Cooler
8. The Pushbroom HRPI
9. Wide-Swath Thematic Mappers
10. Possible TM-HRPI Combinations

The discussion of electromechanical HRPI designs and electromechanical TM designs is properly combined here because the individual instrument designers have used the same basic optical, mechanical and electronic technology in the HRPI as in the TM. A number of efforts in basic scan and detector technology have been pursued which are reflected in the latest design proposals. Also there have been very recent efforts to increase the swath coverage of the TM to satisfy certain user demands. On the latter point no formal documentation is available. Therefore, the discussion must revert again to basic technical differences in approach to design.

VOLUME, WEIGHT, POWER, RELIABILITY

It was somewhat mistakenly assumed during the early Phase A effort that it would be impractical to expand an object plane scanner represented by the ERTS MSS to fulfill the resolution and other performance objectives of the EOS Thematic Mapper. Because of this assumption, an early emphasis on the development of image plane scanners was evident.

Subsequently Hughes showed that the maximum feasible aperture size compatible with a nutating flat diagonal mirror was larger than previously thought, that it was in fact above 19 inches in diameter.

This result and the results of the image plane scanner studies showed that both the object plane and the image plane approach was feasible for the EOS mission, particularly the baseline situation, i.e., a scan angle of $\pm 6^{\circ}$ from an altitude of 915 KM. At lower mission altitudes, the image plane scanners find it more difficult to maintain the same ground swath width, i.e., $\pm 7.5^{\circ}$ at 680 KM to give 185 KM ground swath. When the requirements are raised to $\pm 20^{\circ}$ or more, it may well be that the single optical head image plane scanners have been eliminated from the competition.

Assuming that the performance specifications for the TM or HRPI can be met equally well the competition among instrument approaches resolves to one of volume, weight, power and reliability. In fact, some performance differences may arise within the range of presumably acceptable values, in such areas, for example, as scan linearity. It is also true that the competition in volume, weight and power has developed mostly in connection with a Delta launch, and as of fairly recent date. It is probably fair to say that this effort is largely an attempt by the image plane scanner instrument designers to at least match the first-cut lighter-weight object plane scanners (both TM and electromechanical/ HRPI).

General Optical Discussion - At this point the general optical similarities and differences pertinent to the subject of volume, weight and power may be reviewed. The object plane scanner (Hughes) uses the Ritchey-Chretien optical design with approximately 20% central obscuration of the entrance pupil by the secondary mirror. It is relatively straightforward to design a compact instrument around this optically symmetric system. Very good paraxial optical performance out to a large fraction of a milliradian is available as instantaneous field coverage of the so-called stripe (15 to 60 detectors in an array along flight direction). The use of the object field scan mirror makes it unnecessary to go beyond the paraxial coverage. (Fig. 4-14a)

The two image plane scanners (Honeywell and TE) make special use of the uncorrected spherical focal surface of a purely spherical primary mirror. These spherical surfaces are concave away from the primary mirror and thus provide a natural match to a rotary scan mechanism mounted behind the focal plane. By proper scaling, the scanner can be made to scan the image plane concentrically resulting in an output signal which is temporally linear with respect to a flat object plane. Once the exact altitude of the EOS spacecraft is known, the scaling can be adjusted to compensate for earth curvature as well. This would result in a perfect output signal with regard to the temporal position of the data versus its true earth position (assuming no pointing error).

The Honeywell scheme uses an off-axis, and, therefore, conical scan to pick off a zonal annulus of the sphere. The Te approach picks off a great circle annulus through the intersection of the main axis with the sphere. Because of the complete lack of an actual axis of symmetry in the spherical mirror it is still possible to correct to paraxial tolerances for either the Honeywell or Te approach. The aft-Schmidt approach of a corrector mirror following the first focus is used in both cases. However, in the Te case an entrance pupil immobilization device (the ICC) preserves the entire geometry of paraxial correction, whereas it is only approximated in the Honeywell approach. Consequently, the entrance pupil of the Honeywell instrument oscillates in position with scan angle, whereas the Te instrument pupil does not.

A good idea of utilization of pupil can be gleared from the entrance pupil outlines shown in Fig. 4-14b ENTRANCE PUPILS. The rocking action of the Honeywell pupil is illustrated in terms of the extreme scan positions.

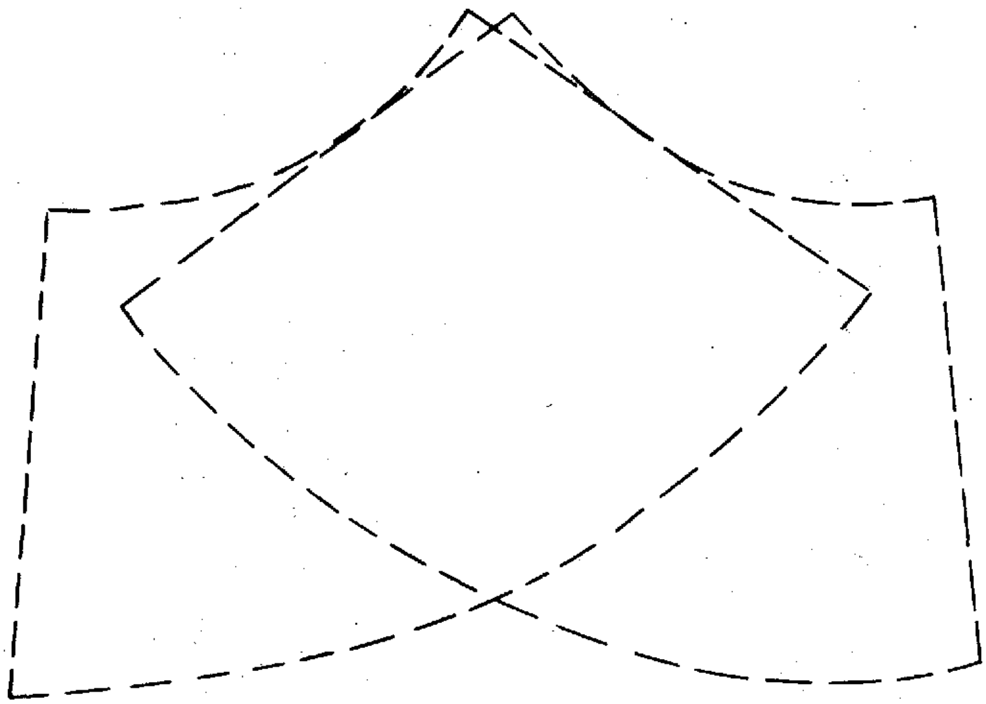

HONEYWELL
SCALE ¼"=1"

E-19

Fig. 4-14a Entrance Pupils

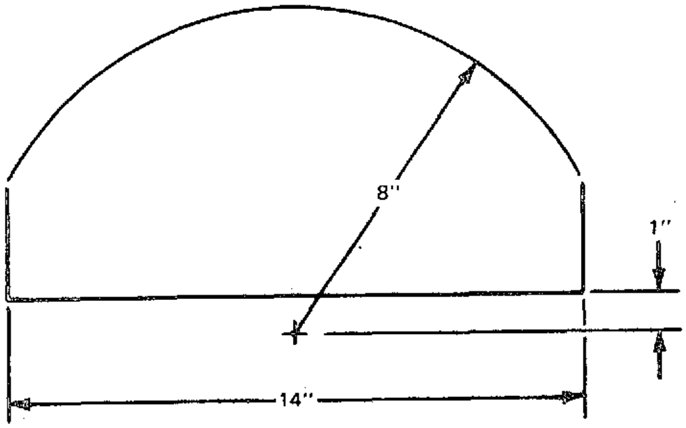

TE – TM

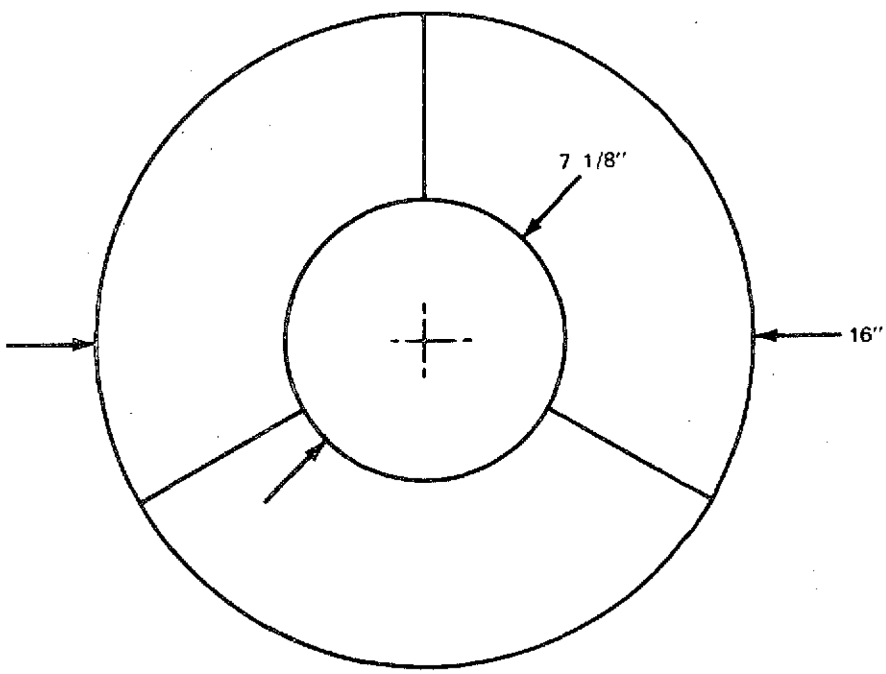

HUGHES TM

E-18 Fig. 4-14b Entrance Pupils

This motion gives rise to an excess projected area requirement of 30% or more which is reflected in added weight and volume of the instrument. In all cases there is fixed obscuration, central in the case of the Hughes and assymmetric in the Te. Large fixed obscuration tends toward an inefficient packaging, partly due to the fact that it is not possible to realize all the light-gathering potential associated with a given f/number of optics.

Balanced against this trend toward inefficiency in the Honeywell package is the compactness of the scan wheel compared to the bulk of the Te scan wheel. The bulk and weight of the scan mechanism in the Hughes scanner also compares unfavorably with the compactness of the Honeywell scan wheel, but the effect here is far over-balanced by the optical efficiency of the Hughes package.

Further revision of design by Te related to a lower f/number primary mirror and changes in scan wheel placement resulted in a less efficient-looking pupil as shown in Figure 4-15.

The electromechanical HRPI design problem called forth the supreme effort on the part of all to conserve weight to the point where the instrument could be considered for Delta launch. This effort reflected back into revised estimates of Thematic Mapper weight and configuration which were formalized by Te, and to a certain extent by Hughes, but not by Honeywell Radiation Center.

The efforts to conserve weight in TM or HRPI (or both have taken the following forms:

1. Proposed substitution of beryllium optics for some glass reflective optics.

2. Structural light-weighting with some changes in materials possible.

3. Proposed increased efficiency in visual and near-IR silicon detectors through new detector and preamplifier technology and through proposed cooling of both to 200°K.

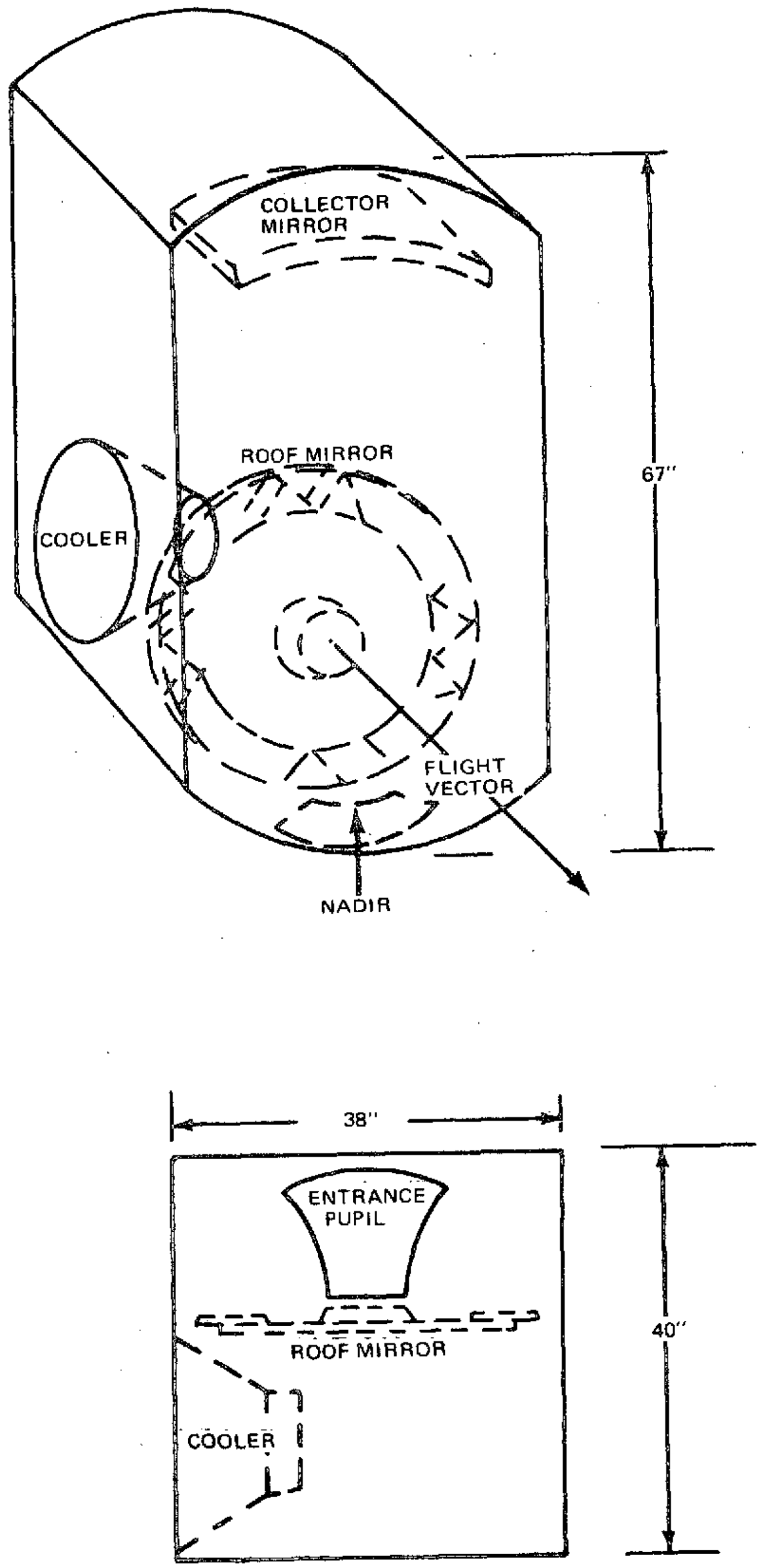

Bottom View

E-20

Fig. 4-15

The original Honeywell Thematic Mapper Point Design referred variously to weights of 600 lbs (specified limit) and 450 lbs. We have been informed by Honeywell that an extensive study of light-weight possibilities was made very early in the EOS program based on the breadboard design. It is stated that the situation then, as now, is that the Thematic Mapper could be a 350 lb. instrument with all beryllium optics, for example, as well as certain other light-weight structural modifications. The question as to why it was not proposed formally as such is answered in terms of funding, primarily, but also in terms of lead time.

In a similar vein the Te Company has reviewed the Thematic Mapper Point Design and come up with a much lighter weight arrangement with no offset pointing capability, a different orientation (see Fig. 4-16), an increased detective efficiency based very largely on the use of a special cooled silicon photodiode detector combined with a cooled preamplifier of special design.

This latter suggestion on the part of the Te Company deserves special attention since the extra burden of cooling the silicon detector arrays and associated preamplifiers to 200°K is fairly trivial. The Te Company has issued a formal report on the subject (previously referenced) entitled DETECTOR AND INPUT FET CHARACTERISTICS AT REDUCED TEMPERATURE. It is based upon laboratory tests of the British TI BF 805 FET used with a UDT silicon photodiode. It is largely on the basis of the resultant gain in signal-to-noise ratio over a 300°K detector-preamplifier that Te proposes lower collecting areas for the specified signal-to-noise ratio in the various spectral bands for the silicon detector. The improvement can be discussed using data provided by Te for the HRPI design. It is to be noted that the other sources of noise do not greatly exceed the so-called "photon noise" which is actually noise inherent in the signal. For the "photon noise" limited case the signal-to-noise ratio is a function of the square root of the aperture area, whereas for the electronic noise-limited case it is a function directly of the area. The actual case may be intermediate.

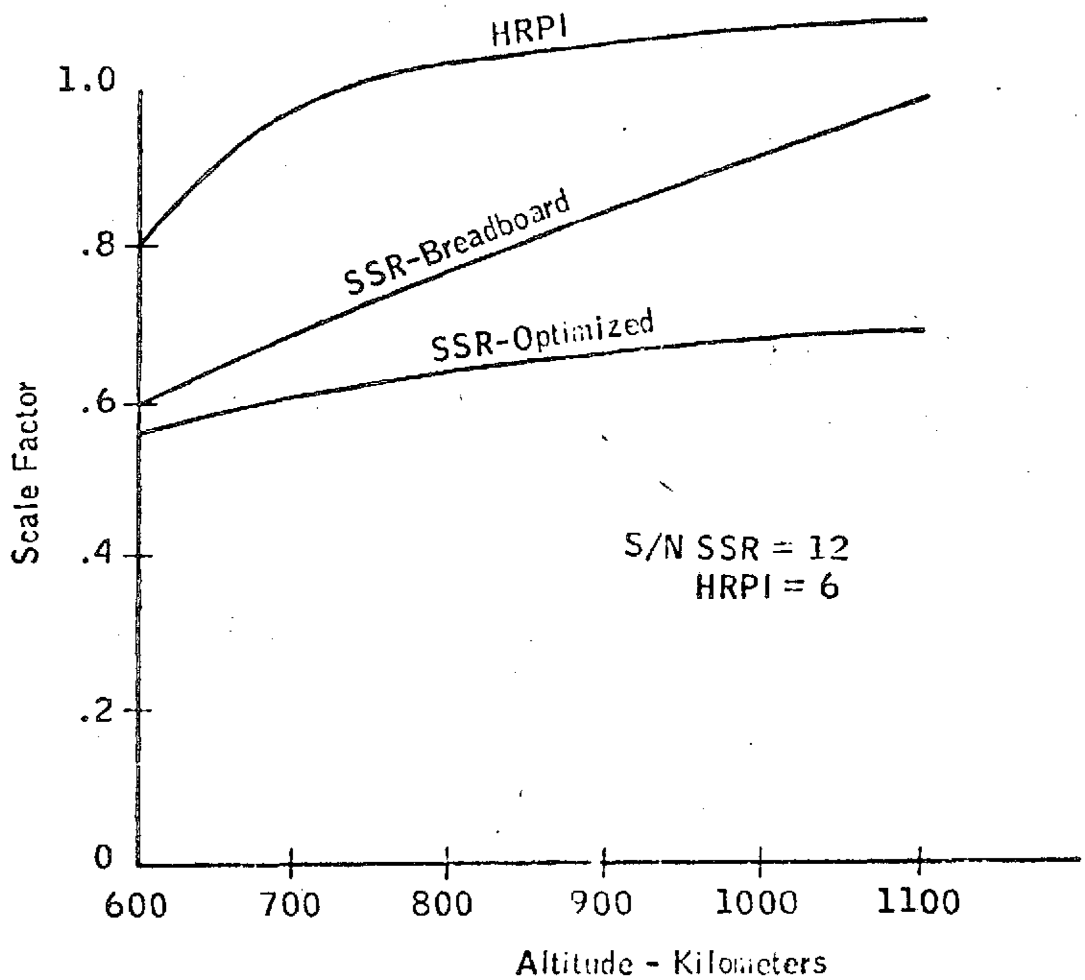

E-21 Fig. 4-16 **Scanner Size vs Altitude**

Table 3 intimates a gain in signal-to-noise ratio of 1.6 by cooling to 200°K. The gain due to changing to the parallel BF 805 FET in the first place seems larger, about 2.4. Assuming that this special combination of detectors, electronics and cooling provides a 3:1 gain in signal-to-noise ratio the implication on sizing of collector aperture is that a collecting area between 33% and 60% of the originally proposed area should be adequate. Assuming that the figure is about 50% the linear diameter or comparable dimension would only need to be 70% of the original. This type of analysis is one input to the evolution of "scaling factors" which Te has proposed to apply to the original Point Design. Another input is the effect of decrease in altitude, e.g. from 915 Km to 700 Km. Figure 22 Scanner Size vs Altitude is reproduced from a Te document. The scale factor applies to linear dimensions and Table 4 also reproduced from the same Te document indicates that only 450 CM^2 collecting area is needed at the original 914 Km altitude compared to a scale 1.0 value of 800 CM^2. At the lower altitude of 700 Km the required collecting area comes down to 293 CM^2 which according to another Te tabulation is that of a Thematic Mapper weighing less than 300 lbs.

These analyses are not regarded as yielding anything better than an "educated guess" at this time. Figure 4-17 TOTAL SYSTEM WEIGHT AS FUNCTION OF SCALE FACTOR is also reproduced from Te with the thought that the weights shown for a scale factor of 1.0 may actually be more representative of probable achievement.

It should be obvious that any technological breakthrough of appreciable magnitude in this area will be used by other instrument designers competitive to Te; and that the advantage, if realized, is transitory. The Te Company is to

Table 3 TM Optimized Scale Factor

$$A_c \text{ (Scale = 1)} = 800 \text{ cm}^2$$

h (km)	A_c (cm^2)	Scale Factor
600	249	.558
700	293	.605
717	311	.623
800	323	.635
900	336	.648
1000	364	.675
1100	371	.681

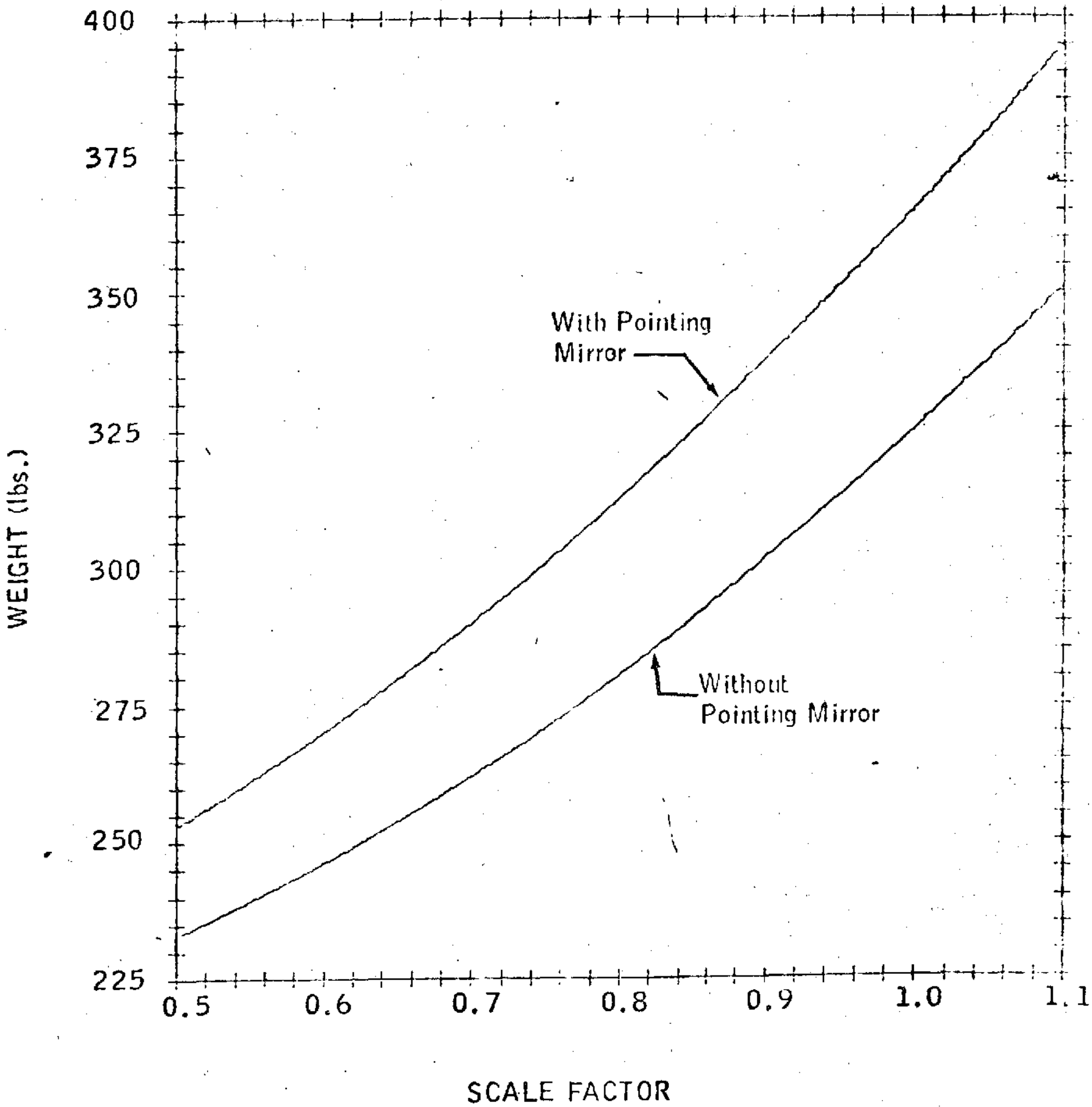

E-22

Fig. 4-17 **Total System Weight as Function Of Scale Factor** be credited with considerable initiative in the exploration of this area of improvement.

In conversation with Te it develops that the application of similar electronic and cooling design to the near infrared and thermal infrared spectral channels of the Thematic Mapper show promise of substantial, but less dramatic, improvement of signal-to-noise ratios at given aperture sizes.

Signal-to-noise problems encountered by Hughes in the design of the electromechanical HRPI were solved by the use of a mosaic of 270 CCD detectors, 18 in stripe height and 15 detectors along each scan line direction. These detectors are used in a time-delayed integration mode thus markedly reducing the noise bandwidth. Honeywell Radiation Center decided to increase the number of detectors to 80 per-band (stripe height) and to substitute photovoltaic detectors for reverse biased photodiodes.

It is not felt that the CCD technology has been proven completely adequate at this time for radiometric work. It should be noted that it is considered necessary by Hughes to insert a 300 electron artificial bias (The fat zero) to overcome noise. It is equally true that the new detector-preamplifier technology proposed by Te must be objectively examined.

The general previous and current progress in solid state detector technology, particularly in silicon, seems to obviate the need for the use of photomultiplier tubes with the complications of high voltage. Photomultiplier tubes still maintain an edge in performance in the "visual" bands (1, 2 and 3) since they are photoelectron-noise limited. Since quantum yield as well as dark current are important factors and the quantum yield in band 4 is much better for silicon detectors the silicon holds the edge in band 4. It is believed that silicon compactness and reliability are factors of sufficient weight to actually supplant all the photomultipliers.

Scan-Non Linearity and Its Consequences

One of the chief criticisms of the Hughes TM Point Design has been the double non-linearity of scan angle with time - one linearity function for trace and another for re-trace. Statements made by Hughes representatives and reproduced in this report under the Support Summary have been to the effect that this non-linearity can be removed completely to all practical purposes by a mechanical design modification. This must be proven in hardware, of course. The Te Company has emphasized the issue of exacting scan angle linearity with time in the interest of reducing ground processing, providing good quick maps to LCGS and reducing the overhead burden in the data link. In theory the Te scan principle of the roof wheel achieves excellent linearity. If non-linearities do ensue in spite of theory it would be because of inability to maintain the exacting alignment of components called for. Again the situation cannot be completely clarified without thorough (including environmental) testing.

The Honeywell Radiation Center lays claim to a very uniform conical scan, but it is not linear in the ordinary sense. The impact on data processing has been further examined by this company as represented in a report entitled CORRECTION TO CONICAL SCAN DATA USING A LOW COST GROUND STATION, included in the Support Summary. It is very difficult to assess the impact of conical scan on processing of HRPI offset pointing data. However, a rather subjective judgment at this time is that it is not practical when considered against more viable alternatives in the Pushbroom HRPI or other HRPI designs.

Scan Rate Adjustability

The Te Company has been a long-standing advocate of in-orbit scan rate adjustment for purposes of accommodating to the oblateness of the earth and to errors in altitude to injection or orbit adjust. Investigation into the latter orbital errors seems to indicate a very small error, not worth serious concern, unless there is a failure of some kind. Investigation into earth oblateness errors is based on the well-confirmed flattening of 1/298.5. Figure 4-18 shows the effect over the CONUS latitudes of interest. The angular rate (V/H) value derived for a mid-CONUS latitude will not be more than $\pm$ 1/2% in error for CONUS latitude extremes. Design for use of TM and HRPI over the whole earth would dictate attention to the point. Considering the need for bench adjustment to suit fabrication tolerances and possible in-orbit adjustment for partial failures, it is deemed worthwhile in the TM to add the capability, however.

In the HRPI with extensive offset pointing, the maintenance of a constant scan rate will generate overlap and wasted transmitted information as well as extensive correction at LCGS without adequate facilities. The growth of the ground resolution element with offset pointing is illustrated in Fig. 4-19 for both the along scan and cross-scan directions. The growth across scan (so-called low-tie effect) results in overlap between stripes.

A growth of 25% (to 1.25) results in an overlap between stripes of 4 IFOV for 16 detectors per stripe and 20 IFOV for 80 defectors per stripe. In comparison the earth oblateness (1/2% of error) would result in underlap or overlap

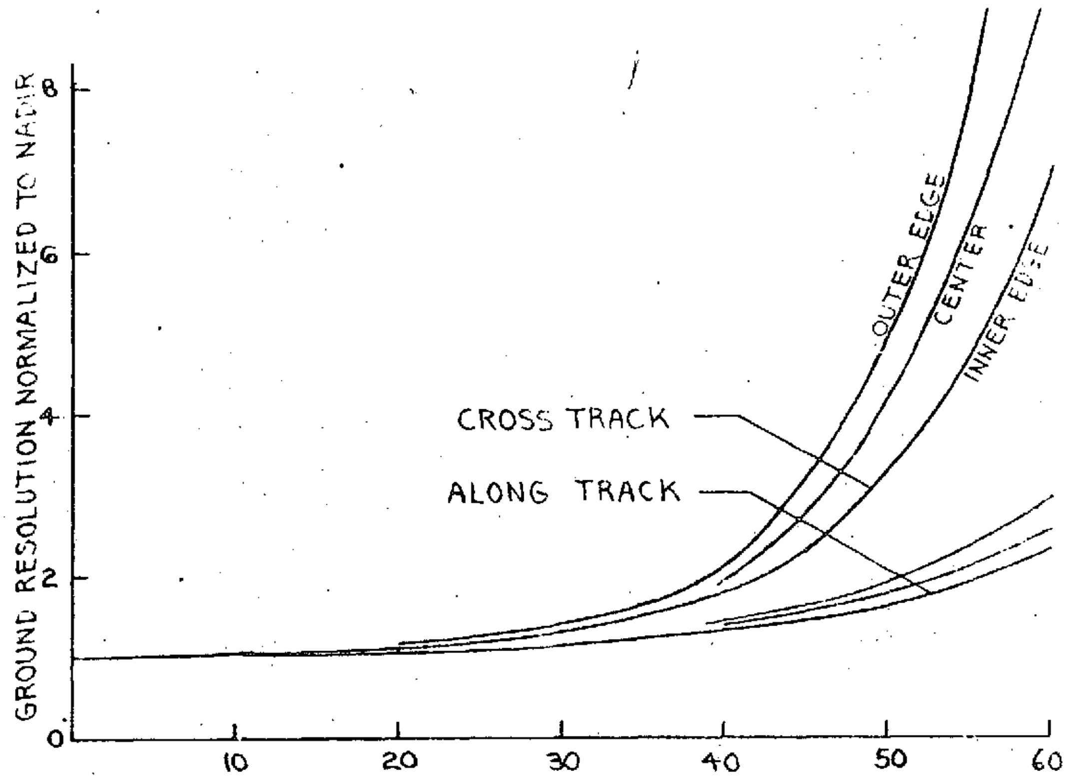

Fig. 4-18 Effect of Earth Oblateness on Stripe Overlap

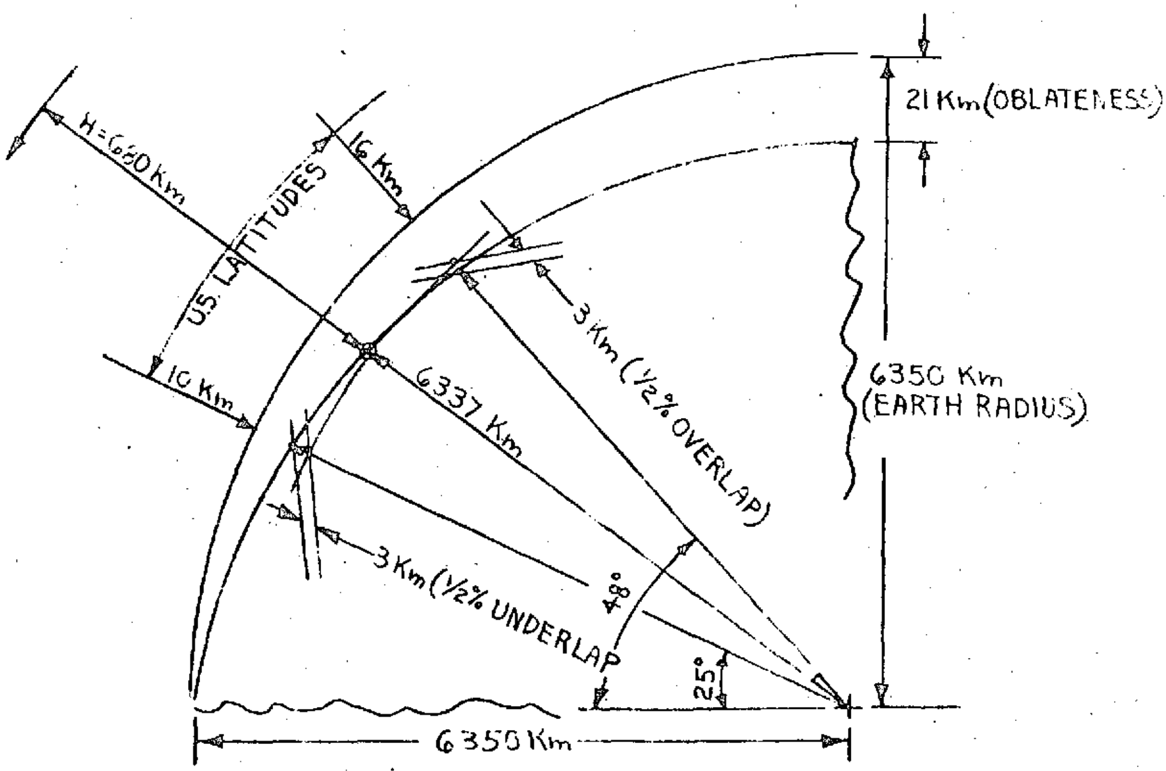

Figure 4-19 Offset Angle-Degrees

of only .4 IFOV for 80 detectors. With proper setting of rate of scan as a function of offset angle the HRPI maps should be directly useful to LCGS although still containing distortion.

The Te Company has presented its closed-loop servo control of the scan wheel in both TM and HRPI Point Designs. The Honeywell Conical Scanner also has similar potential. However, the use of the conical scan concept for HRPI will not be simplified so easily for the production of useful LCGS maps.

The Hughes Aircraft Co. has not presented in any detail in the Point Designs for HRPI or for TM the mechanism for scan rate control of the oscillating mirror. However, it is understood that formal documentation of a support effort on this matter is being prepared. In the meantime attention is called to our support summary quoting Hughes as saying that it is technically feasible over the rates required without serious impact on scan linearization.

One consequence of incorporating an adjustable scan rate in the TM and HRPI designs is that it permits flexibility in the choice of orbit altitudes. If the advantages of a change in altitude become apparent after the fabrication is started the change is still practical.

Scan Efficiency and Buffering (or Spooling)

The only scan technique which can yield a perfect (or 100%) duty cycle is the electronic scan (e.g. pushbroom). The duty cycle in the MSS is about 45% because the scan mirror is not used in re-trace to generate data. This low duty cycle has the effect of adding communications burden in terms of peak bit rate. On the proposed Hughes TM and HRPI the use of re-trace will bring the duty cycle to about 85%. Since the residual 15% is not fully required for overhead the peak bit rate could be reduced by buffering.

The Honeywell S-192 scanner on SKYLAB constitutes a space precedent for the use of buffering for this purpose. Honeywell has not proposed it for the TM or HRPI Point Designs because it appeared unnecessary under the development guidelines.

The Te Company has difficulty reaching even 74% with the roof wheel approach. It turns out that a more compact package can be designed by sacrificing scan efficiency. Buffering assumes more importance in this case. Therefore, the Te Company has treated the subject more than Hughes or Honeywell. Fig. 4-20 is reproduced from the Te HRPI Point Design Report. It shows the use of integrated circuit random access memory modules for simultaneous read-in and read-out. Under the support arrangement Te was asked for an estimate of weight and power for TM and HRPI. The answer (by telephone, to be confirmed) was that 25 lbs, 35 in.^{3} and 6 watts form the logistics for a C-MOS System. Costs are admitted to be high.

The Honeywell Radiation Center was also queried on this point in view of SKYLAB experience. A preliminary estimate on weight alone was 30 lbs. A point on reliability was made by Honeywell because of the large number of parallel lines required (as evident from the Te schematic).

In all fairness the "compact" Te designs should probably consider an extra 30 lbs for buffering (or spooling as it is called by Te). However, a very beneficial effect would ensue for the communications and data system in general if this buffering were to apply to all designs.

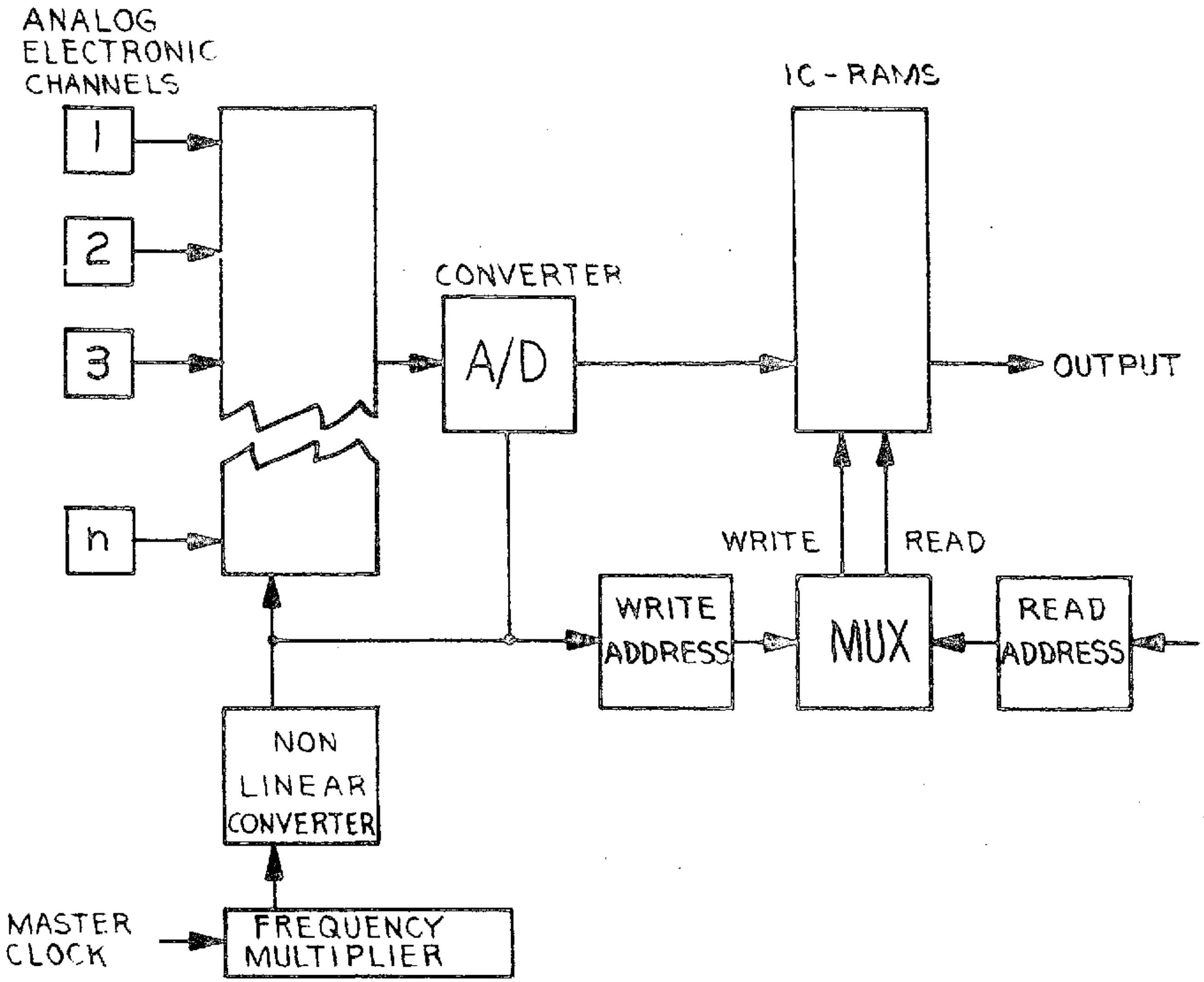

Fig. 4-20 Spooling Schematic (TE) Adapted to Photogrammetric Processing

Synchronism of Scan Control and Data Flow with System Clock

With fixed scan rate there is minimum difficulty in synchronizing with the system clock, although the clock frequencies usually mentioned are not high enough to provide direct control of the A to D conversion. The exactitude of scan control required necessitates a high quality frequency converter and firm locking to the master clock dictates common harmonic relationships for locking comparison at discrete frequencies. Variable rate control, as advocated particularly for HRPI, carries the implication that this locking at discrete frequencies may become a substantial task.

The Te Company has been the advocate of adjustable scan rate and Fig. 4-21 is reproduced from the Te HRPI Point Design to illustrate the modified phase-lock loop which was proposed. It will be noted that there is no closed loop shown with the master clock itself in respect to the frequency multiplier. The importance of the locking probably depends strongly on the reliability of the "frequency multiplier". It is apparent also that the change in scan rate control may upset the relationship between the output of the scanner and the "MOMS" control of A - to D conversion and multiplexing. This is particularly true for the HRPI where we may be dealing with the possibility of a 2/3 nadir scan rate at extremes of offset.

No schematic of this adjustable rate control is presently available from Hughes, although the matter has been discussed on the telephone. As presently understood Hughes is proposing essentially open-loop control of the scan mirror simply by furnishing a variable pulse rate to the usual mirror control mechanism.

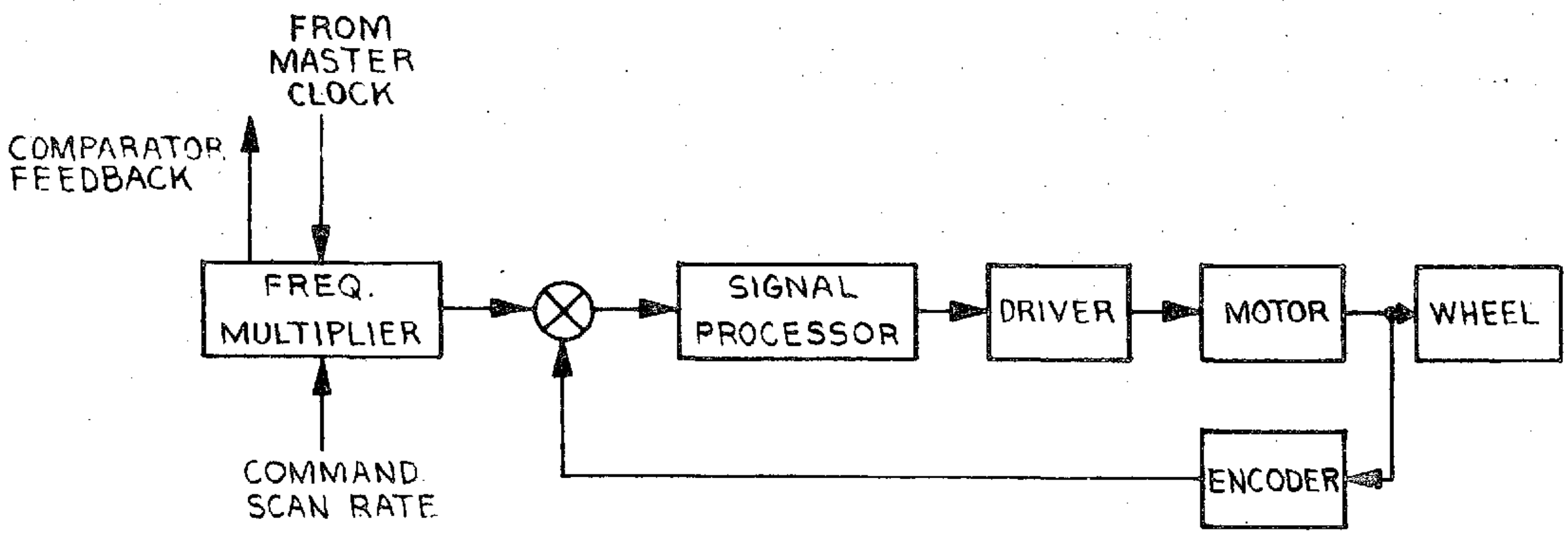

Fig. 4-21 Schematic of Phase-Lock Loop Control (TE) with Added Feedback to Master Clock

Presently Hughes has no continuous encoder to propose (in line with the optical encoder on the Te scan wheel) although the statement is made that one is under development. On the other hand it is understood that Hughes is proposing essentially closed loop control of frequency changing by providing harmonically related pulses for feedback comparison to the master clock.

The matter of how to handle the correlation of A - to D conversion with the variable scan rate has been discussed with the Te Company, and a possibly viable suggestion ensued. If the number of samples per specified angular IFOV in the analog data is allowed to vary in inverse proportion to the scan rate a fixed frequency of conversion can be used for both TM and HRPI, and therefore, a fixed frequency interface with "MOMS" can be preserved. Put another way this means a variable angular "pixel" size along the scan direction. However, the variability for the TM would be minimal since it is not anticipated that ordinary circumstances (e.g., good orbit control) would necessitate changing TM scan rate. For example this could be designed and held very close to 30 meters resolution at any given altitude. The variability normally expected for HRPI, however, would result in a variable sampling angle projected on the ground as a function of offset angle. Up to 1.5 samples per HRPI IFOV angle would result at 45° offset. This could be used in the direction of preserving cross track (along scan). ground resolution at the expense of signal-to-noise ratio for each sample, although not affecting the overall signal-to-noise level for the radiometric map as re-constituted on the ground.

The buffering system shown in Fig. 4-20 was designed for filling gaps in each scan cycle rather than providing storage to accommodate changes in the number of scans per unit time. It cannot be used to accommodate to changes in scan rate. However, the suggestion made here would help implement the scheme. The Control over the A-to-D converter would be a rather direct function of the spacecraft master clock, as would the control over read-out. Vice-versa the buffer storage probably could provide a cushion for minor delays in the data system. Certainty of accurate retrieval of ground data should be increased.

It should be noted that the suggestion is in the direction of simplification of data handling especially for LCGS. The ground scale along scan (cross-track) is determined in the individual pixel, whereas the ground scale in the cross-scan (along track direction) is preserved in the height of the stripe. It is true that the swath width on the ground (cross-track) would be variable with offset, but this is not serious and was anticipated in any event. The still un-corrected geometric distortion in the HRPI data is illustrated in Fig. 4-22

There naturally has to be some recording and transmission of scan control data (along with the A-to-D control) to properly identify the data. In the case of extremely linear scan (possibly Te) the recording is minimal, but for non-linear scan sufficient points must be recorded on the time base to identify the function completely.

<u>Offset Pointing Mechanisms for HRPI</u>

At this time the only HRPI design suggestion (or Point Design) which retains the original concept of an internal flat diagonal mirror is the Te electromechanical HRPI. The Hughes electromechanical scanner HRPI is rotated as a whole. The design incorporates a 45° mirror for optical folding to implement this capability, thus

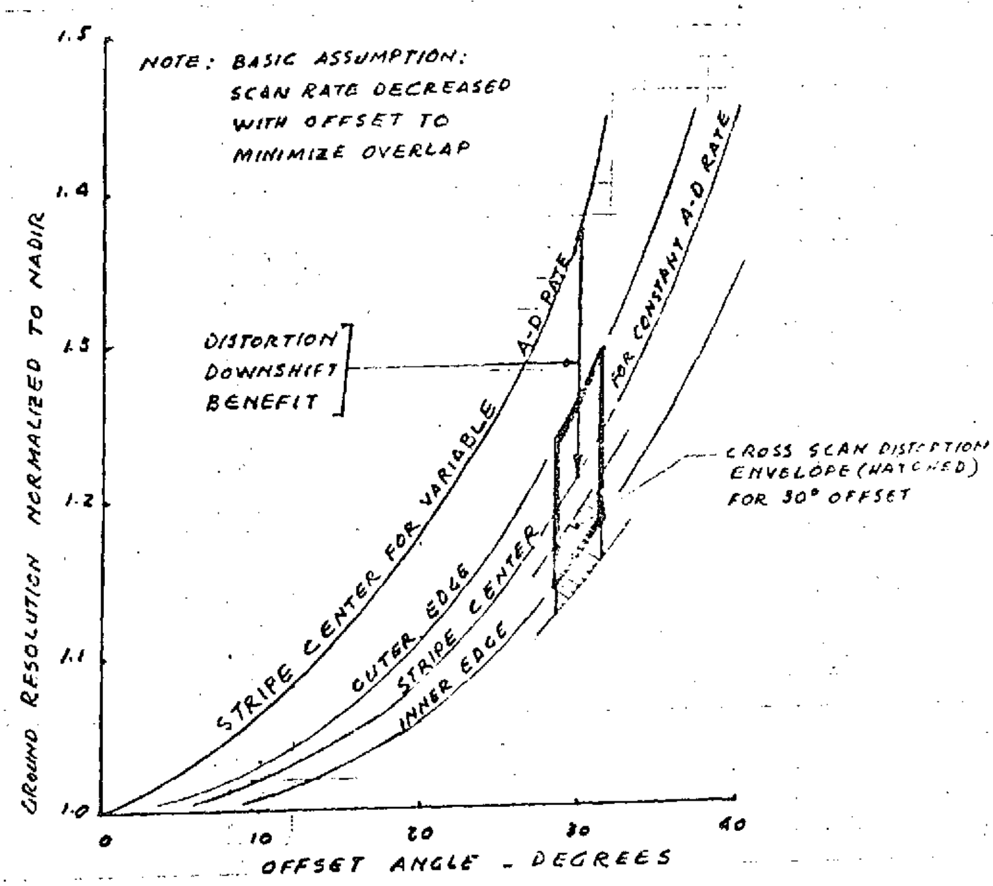

Fig. 4-22 **Benefit to HRPI Offset Pointing Ground Distortion Due To Constant A-D Sampling Rate**

E-23

making it close to a "cube" package. The Honeywell HRPI proposal involves rotating all parts of the sensor except the primary mirror. Without rather exceptional pre-loaded bearings the focus would not remain constant at the detector plane. However, it is stated that tolerances can be held. The Westinghouse HRPI rotation as shown in this report is whole-sensor about the optical axis.

The possible advantages for the Te HRPI in this respect is the slewing speed. Without internal momentum compensation the mirror can be offset 45° in 1.5 minutes without serious impact on the attitude control system. The angular read-out capability should be at least equal to any other although the Te HRPI Point Design does not describe the encoding process.

The Thematic Mapper Radiative Cooler

Originally the Hughes TM design alone gave comprehensive coverage of design of the radiative cooler. Honeywell Radiation Center proposal includes an A.D. Little radiative cooler at present. The Te Company originally treated the cooler as possibly GFE. Honeywell has supplied by short memorandum certain amplifying details including the sensitivity of performance to launch time-of-day. The Te Company has supplied a design concept entitled THEMATIC MAPPER RADIATION COOLER which it is claimed will provide adequate detector cooling between 8 AM and 4 PM orbits. Back -reflection of unwanted radiation and vignetting baffles are utilized to maximum advantage. Analysis of the presence of solar arrays in the field must be performed, but as yet has not been accomplished. The design concept appears to be important.

The Pushbroom HRPI - Fig. 4-23 shows a hypothetical Pushbroom HRPI in a whole-sensor gimballing configuration for offset pointing. The resemblance to the

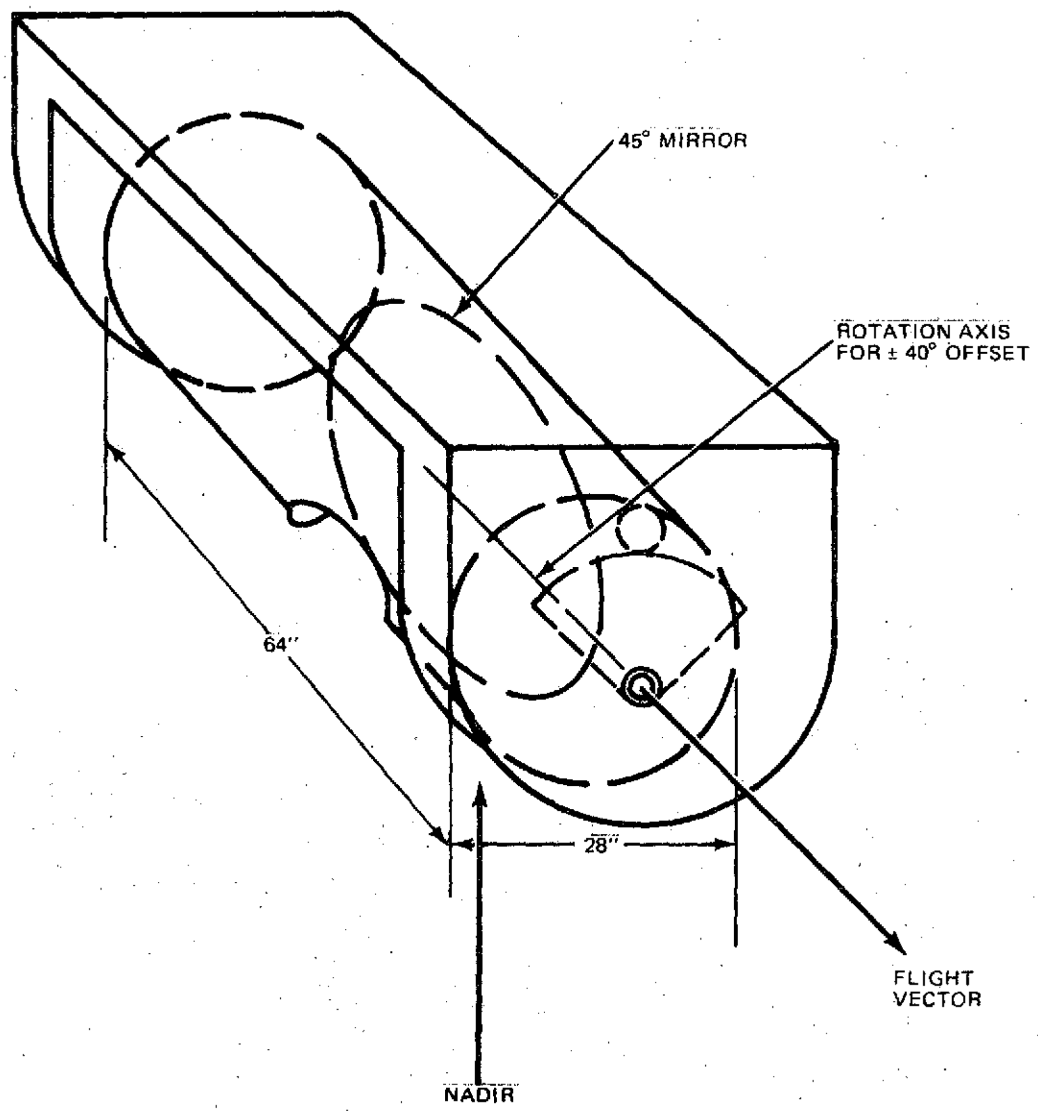

E-24 Fig. 4-23 **Push Broom HRPI (Parallel to Flight Vector)** packaging of the Hughes HRPI in a cradle is purposeful at this time since an estimate is on hand for this type of mount and control of a similar package. After discussion with Westinghouse a weight estimate of 250 lbs for the sensor is offered. The sensor includes a fixed 45° diagonal mirror as shown. Using the Hughes estimate (approximately) of 70 lbs for the cradle structure and drive a total of 320 lbs is arrived at. As nearly as we can determine at this time the scanner will offer signal-to-noise ratios which are equal to, or slightly better than the electromechanical HRPI configuration shown by Hughes, which is also based upon self-scanned arrays although CCD-type in the Hughes design and digital-type in the Westinghouse design.

It is of interest to compare the use of these arrays in the pushbroom and electromechanical scanner. At a rate of 6790 meters/sec the 10 meter ground element is traversed in 1.48 milliseconds. In order to avoid impairment of MTF by convolution with image smear MTF the integration period may be restricted to .15 milliseconds. For a 4800 detector array with stripe rate adjusted for contiguity the noise bandwidth would be the same for 480 detectors working full time. This compares to 270 detectors in the Hughes CCD matrix of the delayed integration HRPI scheme. Assuming equality in performance between the Hughes CCD matrix and the Westinghouse arrays, the signal-to-noise ratio for equivalent optical performance should be slightly better for the Westinghouse Pushbroom. A comparison has not been attempted, but could be performed on the basis of the optics of the Westinghouse Point Design.

On the basis of data furnished by Westinghouse, however, it appears that noise superiority cannot be claimed by Westinghouse over the Hughes CCD detectors.

However, there are probably inherent spectral uniformity advantages in the Westinghouse-type detectors as illustrated in Fig. 4-24. The Westinghouse data on their arrays has been reported as follows:

In Band 1 (.5 μm to .6 μm) the input to cells .0009 in. x .0007 in. required to equal noise level in HRPI operation is 1.3 microjoules/meter^2. At a quantum yield of 6 photoelectrons per 10 photons this is equivalent to saying that the charge input to equal noise is 670 electrons.

Wide Swath Thematic Mappers

While no formal documentation is available at this time to Grumman, efforts have been followed with Hughes, Honeywell and Te to arrive at TM configurations for 300 Km to 500 Km swath. The results seem to be about as follows:

As indicated previously in this report, the Hughes Object Plane Scanner TM approach lends itself to wide angle scan easiest of all. For coverage of 320 Km the TM ± 7.5° must be enlarged to ± 13.2° referred to nadir. To cover 500 Km the angle must be still further enlarged to ± 20°. The angular excursion of the scan mirror remains at reasonably modest values of ± 6.6° for 320 Km and ± 10° for 500 Km. Without changing the number of detectors per stripe height the noise bandwidth increases by a factor of about 1.8 for 320 Km and about 2.7 for 500 Km. If the number of detectors is changed in these proportions, respectively, the noise bandwidth stays the same and the system performs as well as the Point Design TM. The mirror control, including linearization of scan, is not beyond the technical bounds already considered by Hughes, including necessary changes, if any, in mirror oscillation rate.

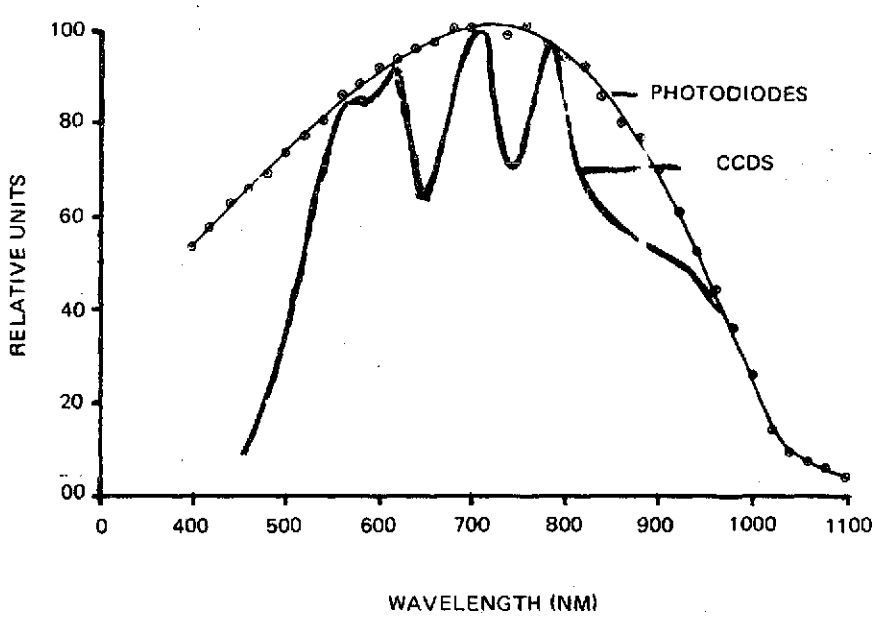

E-25

Fig. 4-24 **Spectral Response**

GRUMMAN

TRADE STUDY REPORT

TITLE	TRADE STUDY REPORT NO.
	WBS NUMBER

The Honeywell effort to reconfigure within the 36" x 72" TM envelope for 500 Km, 30 meter resolution proved unsuccessful, it is understood a 600 lb instrument capable of 50 meter resolutions within this envelope appears to be possible.

Te Company has advised that a new design concept for utilization of the roof wheel was evolved. This includes use of double entrance pupil. In each pupil half a portion of the diagonal mirror is located. The portion in one pupil is oriented at a slight angle of inclination to that in the other half. This feature, is said to enable the scanner to splice together two separate swaths, one coming from each pupil half. It is predicted by Te that the 30 meter resolution over 490 Km swath could be accomplished about 500 lbs. weight and within an envelope of 40 in. x 36 in. x 72 in. The orientation must be similar to enable incorporation of the diagonal mirror. The capability of performance within this limited envelop depends strictly on the achievement of close to photo-electron noise limited performance from cooled silicon photodiodes and cooled parallel/FET preamplifiers.

PREPARED BY	GROUP NUMBER & NAME	DATE	CHANGE LETTER
H. Hallock/J. Halajian			REVISION DATE
APPROVED BY			PAGE 4-101

GRUMMAN

TRADE STUDY REPORT

TITLE	TRADE STUDY REPORT NO.
	WBS NUMBER

There is a design trade to be made with regard to the method of spectral band separation. In all three TM point designs, the thermal band (7) is separated spatially in the focal plane from the other bands. Beyond this point, there are basic differences.

The Honeywell design employs a spectrometer behind a single aperture stop to generate signals for bands 1-6 which are all in perfect registration.

The Hughes design employs a relatively small assembly of prisms and apertures in a single mask to provide a fixed spatial separation which can easily be accounted for in later data processing. Hughes, as a result of their HRPI point design efforts, has also proposed the use of a single photo-detector assembly for bands 1-4 which would be fabricated on a single integrated circuit substrate resulting in minimal mechanical complexity and excellent long term registration. Furthermore, the design provides a charge coupled device (CCD) of about 18 elements in place of each individual detector of the conventional design. These individual elements are illuminated in sequence by a given ground element and by accumulating the charge generated from each element related to a given ground element by time delay integration (TDI) a gain in S/N of about 4x is obtained.

The Te design employs a spectrometer similar to Honeywell.

From both a mechanical complexity and long term stability point of view, the TE design appears least desirable.

PREPARED BY	GROUP NUMBER & NAME	DATE	CHANGE LETTER
			REVISION DATE
APPROVED BY			PAGE 4-102

The Te and Honeywell designs are clearly superior from the stability of registration point of view.

The Hughes design offers besides simplicity and good long term stability, growth potential through the introduction of a CCD/TDI array at the focal plane to provide increased instrument sensitivity. An area of considerable concern as a result of the point designs, there is a general belief that higher S/N ratios should have been required at the low irradiance limits specified to the point design contractors. The CCD/TDI technique could easily provide this.

E. .4.2.4.2 Comparative Evaluation of TM

Figures 4-25 through 4-27 illustrate the three TM configurations examined in greatest detail (several earlier designs are obsolete). The Hughes version shown is a alternative of their HRPI design. It employs a folding arrangement which leaves the main telescope aligned to the flight vector.

The Honeywell unit also exhibits this overall alignment. These designs were carried forward to allow interchangability in the spacecraft design until actual acquisition of one design as the flight instrument freezes the configuration.

The TE design employs a transverse package which may be difficult to get onto a Delta launch vehicle when finally developed. Therefore, packaging of this unit in our spacecraft designs was not stressed.

None of these versions include mechanical offset pointing but emphasizes lowest weight achievable within the specification.

Figure 4-28 illustrates the expected instrument weights as furnished to us by the vendors (under a variety of conflicting ground rules involving flight weight options, titanium vs aluminum structure and the uses of INVAR) and our estimate of the weights to be expected of the units without incurring large cost penalties. The trends clearly show the weight growth with altitude and the advantage of the object plane scanner at lower altitudes where a wider scan angle is required. At the 680 KM altitude, all of the instrument types could be flown on the Delta.

Figure 4-29 attempts to estimate the relative cost of the various

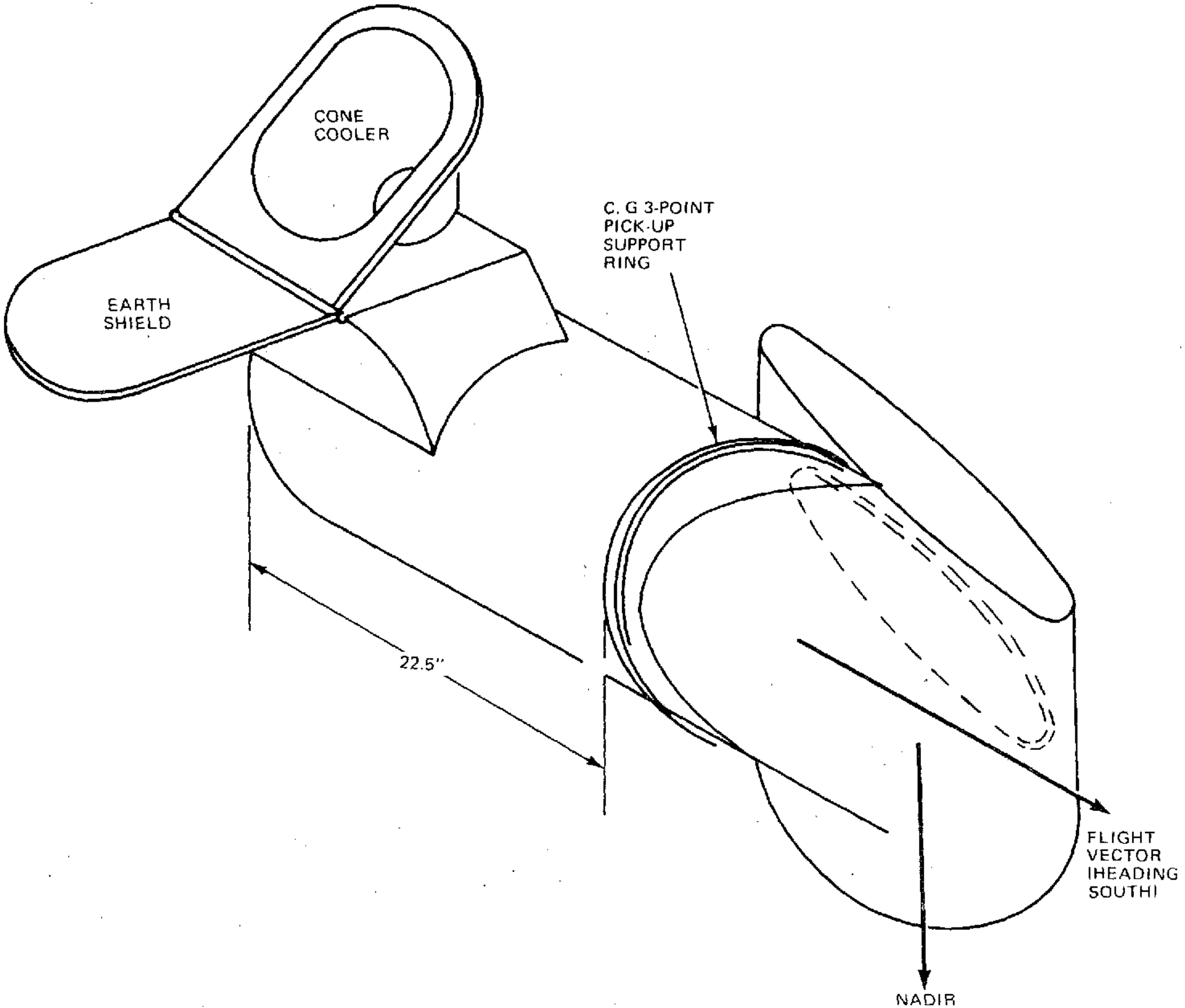

Fig. 4-25 **Hughes (Axial) TM**

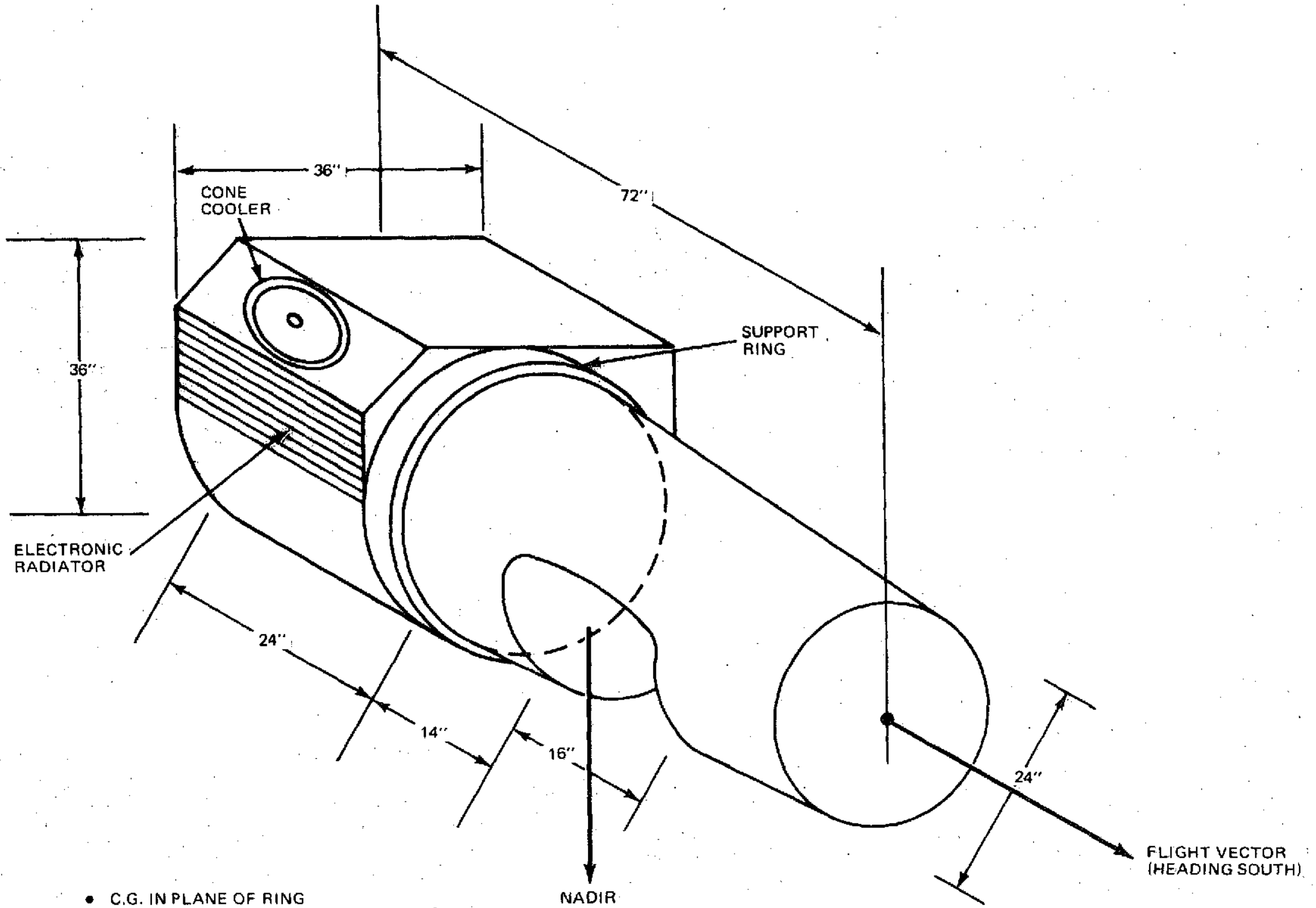

- C.G. IN PLANE OF RING
- THREE PICK–UP POINTS AROUND RING
- INSTRUMENT WEIGHT = 450 LBS NOMINAL
  CAN BE REDUCED TO 350 LBS
- ASSUMED ORBIT: 0930

Fig. 4-26 Honeywell Thematic Mapper

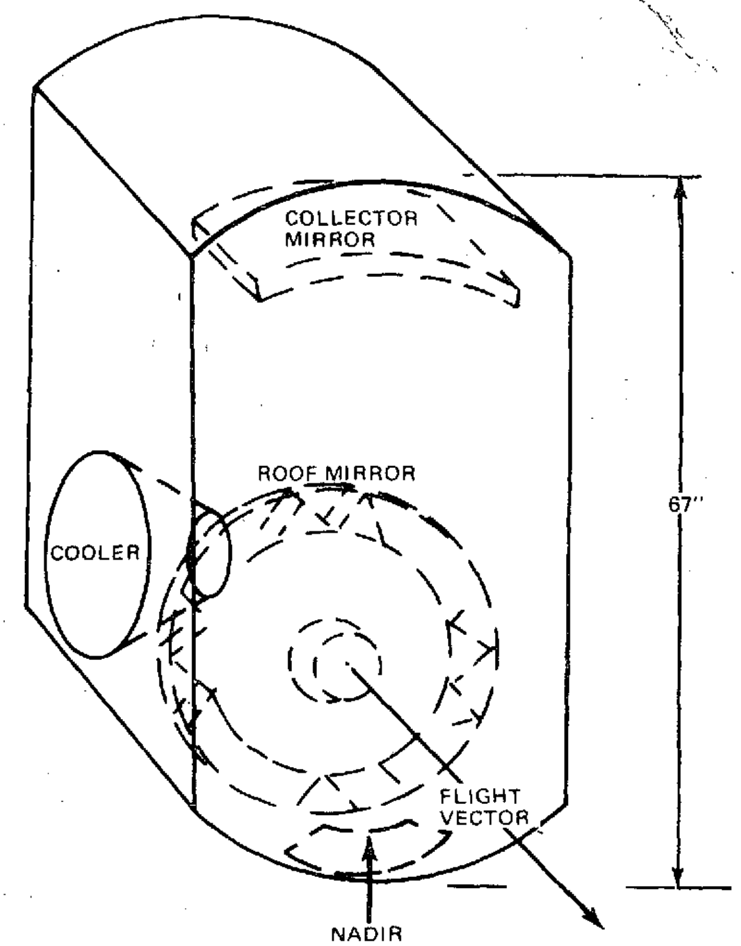

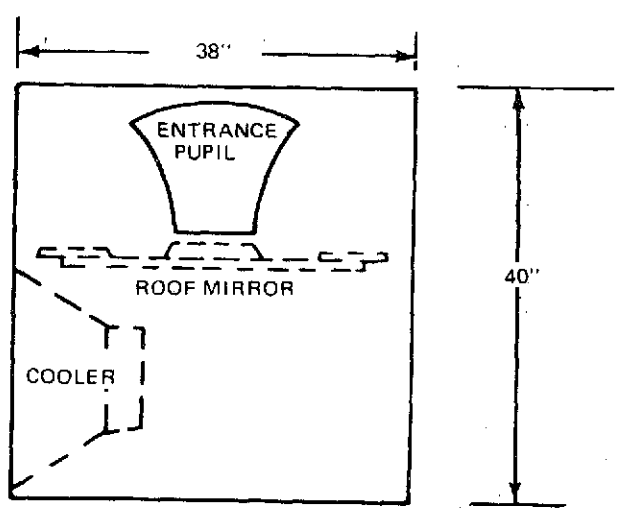

Bottom View

E-28

Fig. 4-27 TE TM

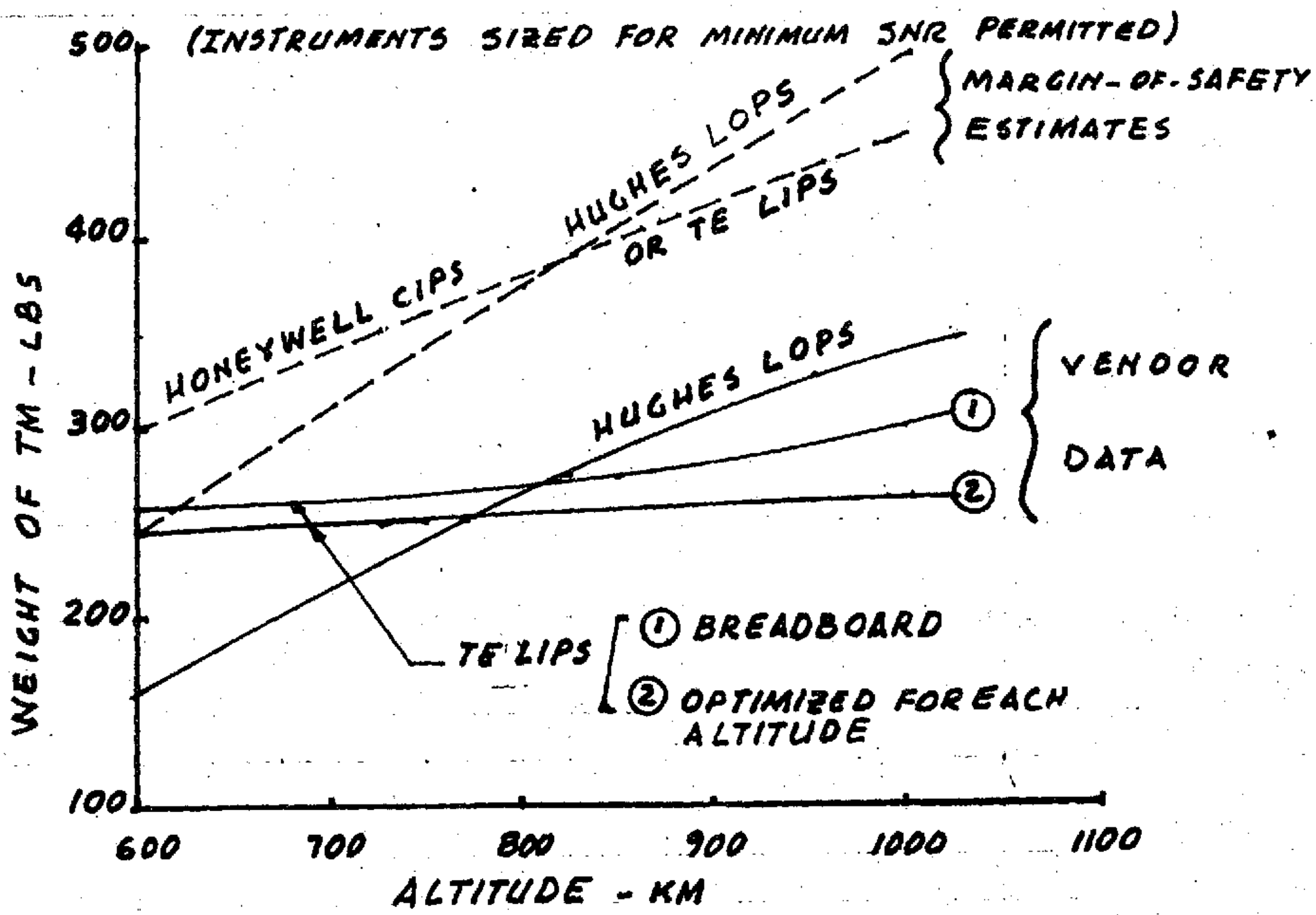

E-29 Fig. 4-28 Anticipated 185KM TM Weight as Function Of Altitude

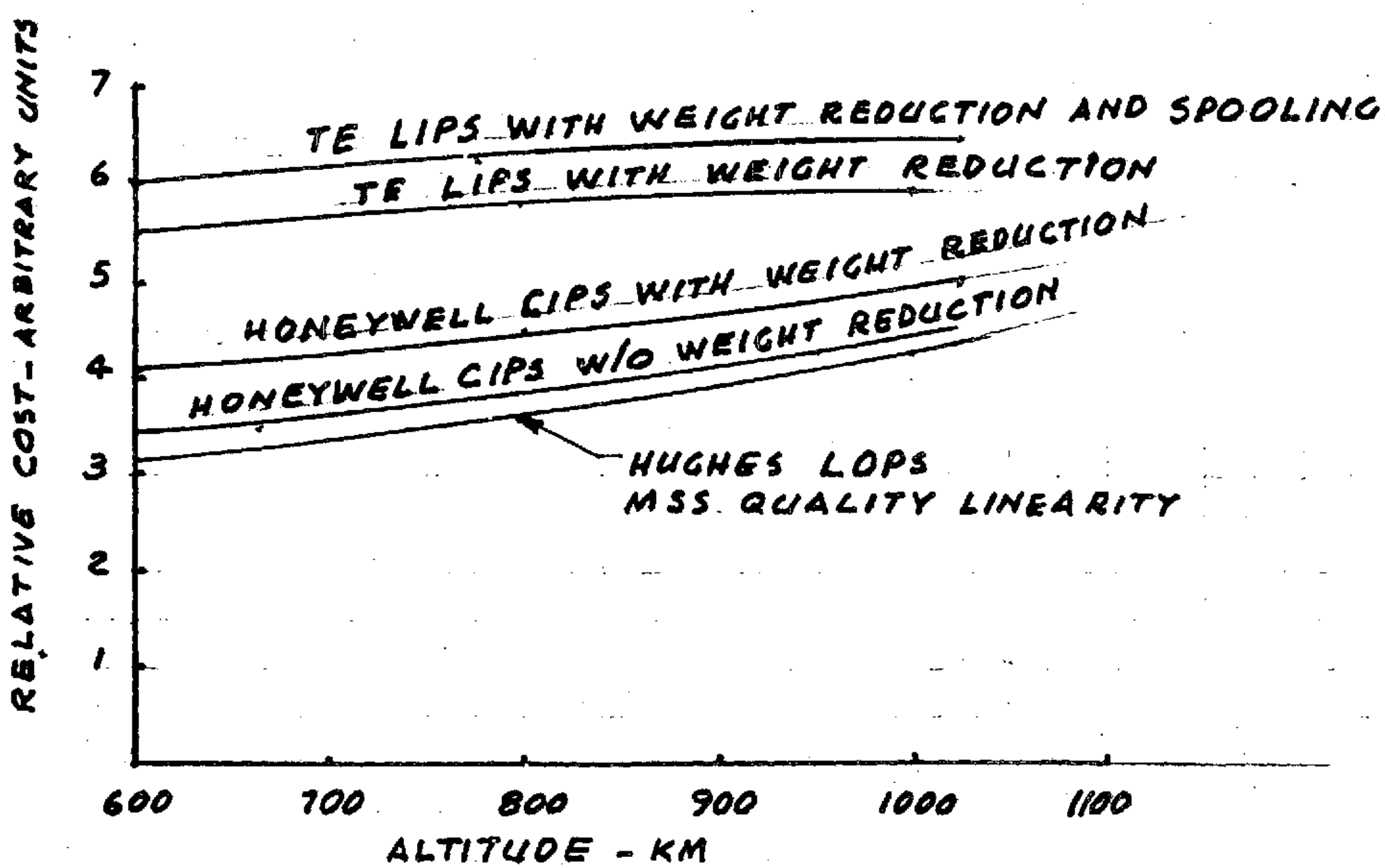

 Fig. 4-29 Anticipated Intrinsic Cost – Diffulty Trends For 185 KM TM

instruments based on their current state of development and the relative difficulty of the design.

Figure 4-30 exhibits the significant improvement in sensor performance achieved in the TE design through cooling of the detectors in the visual band. This feature is employable in all of the designs and has been assumed in all other considerations.

Figure 4-31 considers what is probably the second most important trade (after weight vs altitude) in the instrument area. The utility of the TM improves rapidly with swath width, particularly in the absence of the HRPI on early flights. Shorter repeat cycles are the principle advantage with more timely stereo coverage being bonus. Note the significant advantage of the object plane scanner in this area.

E. 4.2.4.3 <u>Comparative Evaluation of HRPI</u>

Figure 4-32 through 4-36 illustrate the various HRPI configurations supplied as a result of the point design and support contract efforts.

The Hughes design is identical physically to their TM design except for elimination of the cooler outer cone. The unit is gimballed about its roll axis by means of a towel rack which is integrated into the vehicle support structure.

The Honeywell design is also virtually identical externally, except for a larger aperture on the nadir side. This is needed to accomodate the internally rotating telescope used to obtain offset. This design employs about 60% commonality with the corresponding TM design.

The TE design is basically the same as the TM physically except for the addition of the pointing mirror and consequent rotation of the package 90° on the spacecraft (an interface cost penalty).

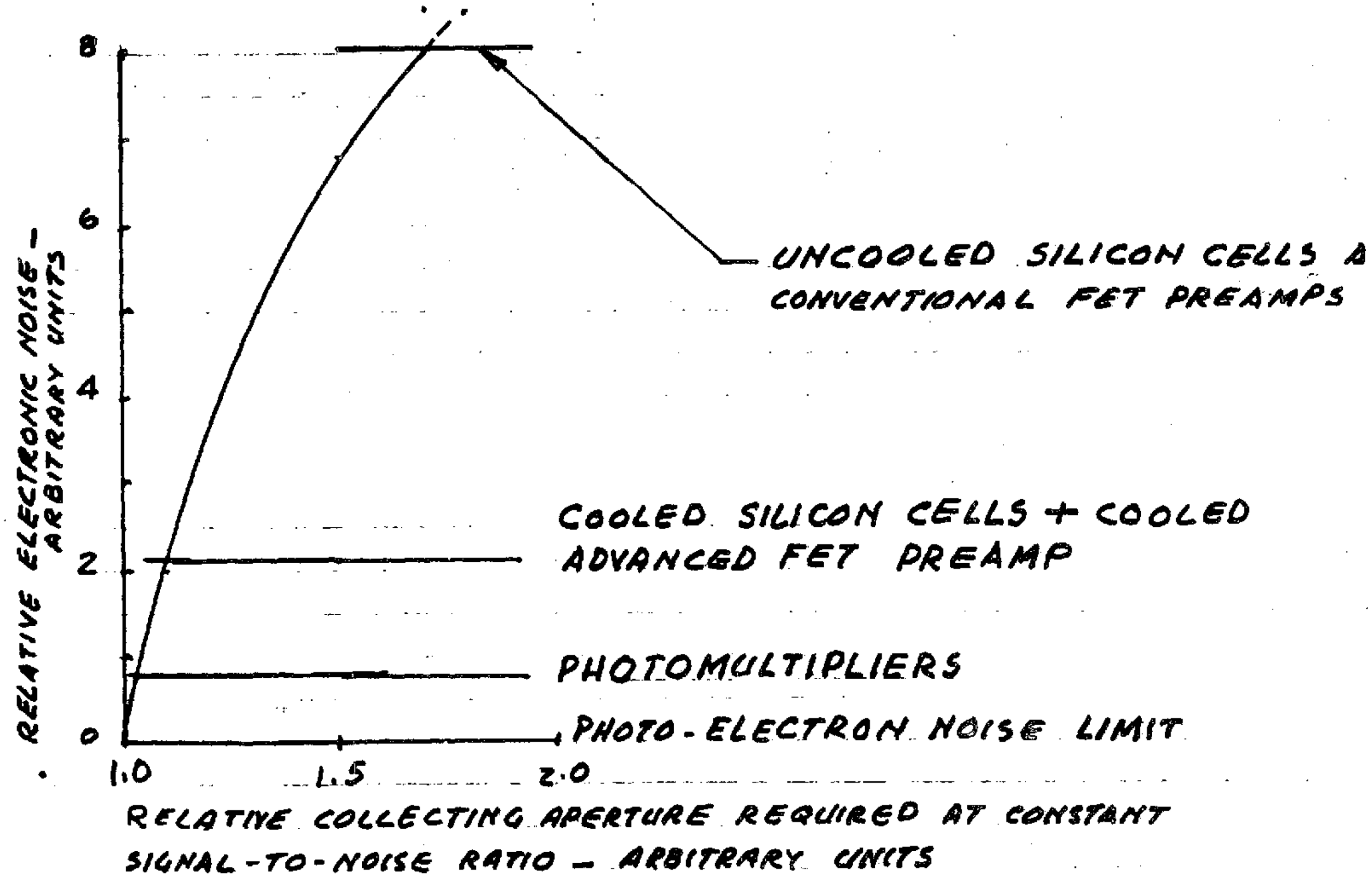

Fig. 4-30 The Conservation Of Size B Electronic Noise Reduction

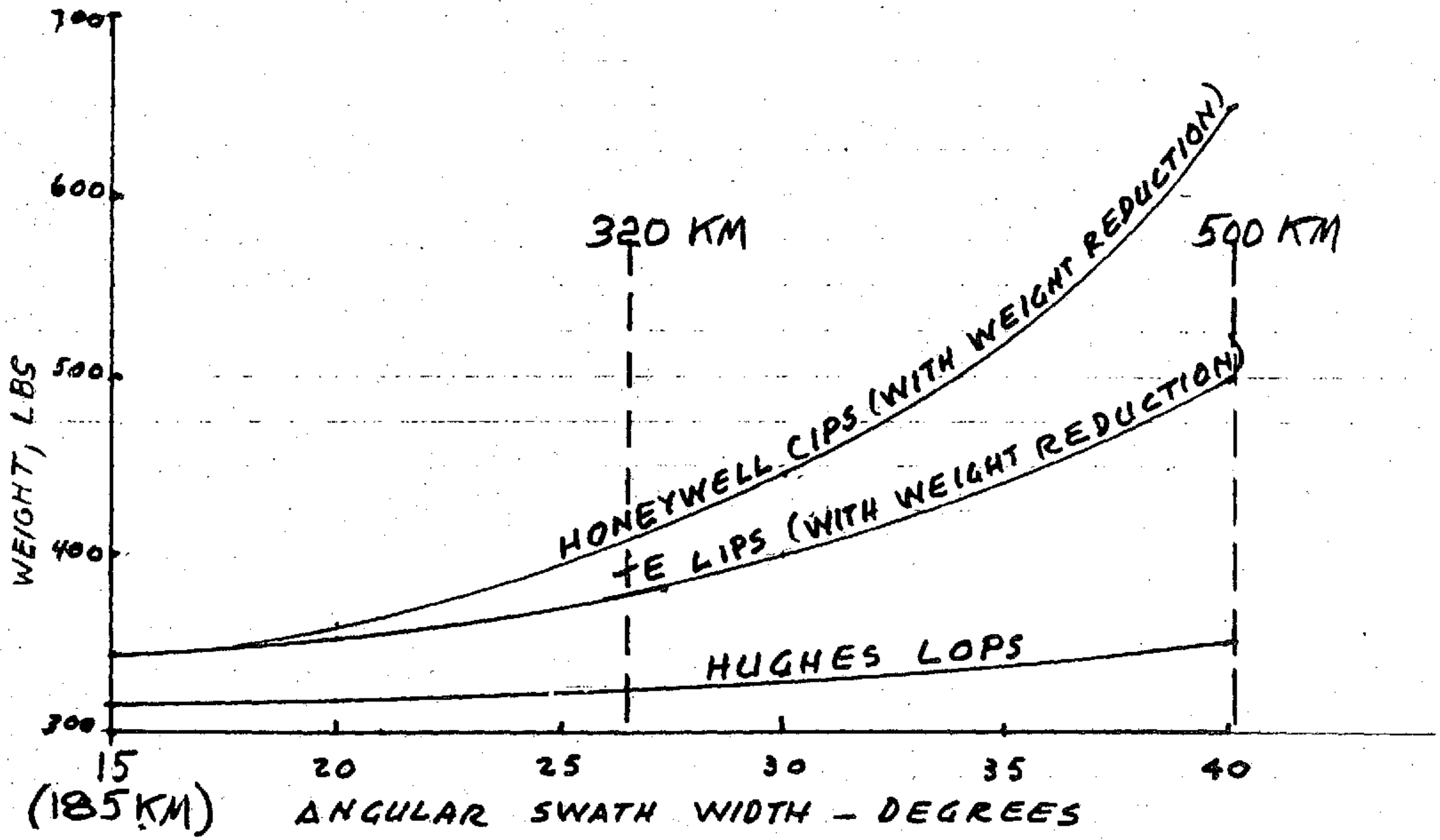

Fig. 4-31 Anticipated Growth of TM Weight with Swath Width for 30M Resolution at 680 KM Altitude

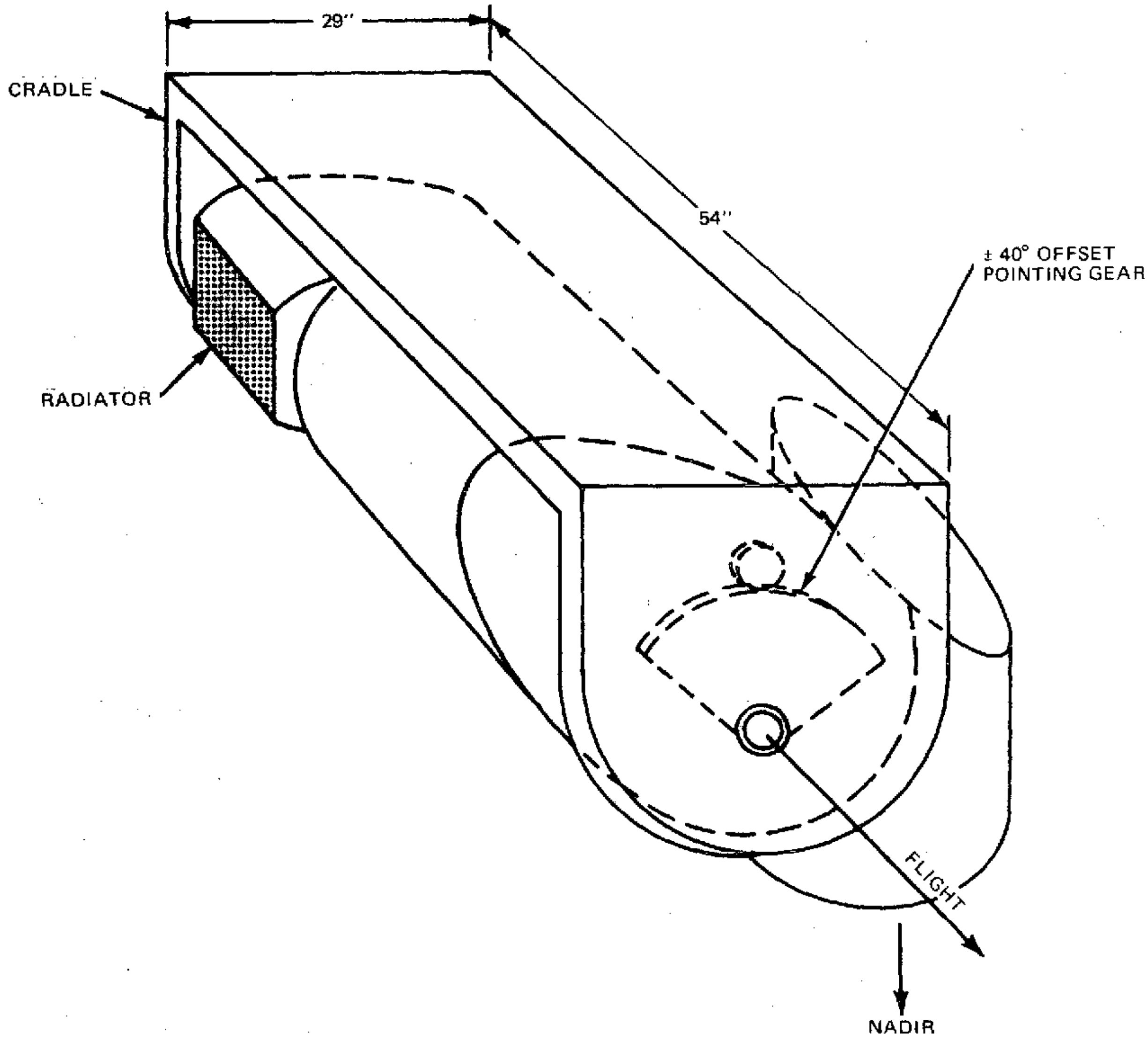

E-33

Fig. 4-32 Hughes HRPI

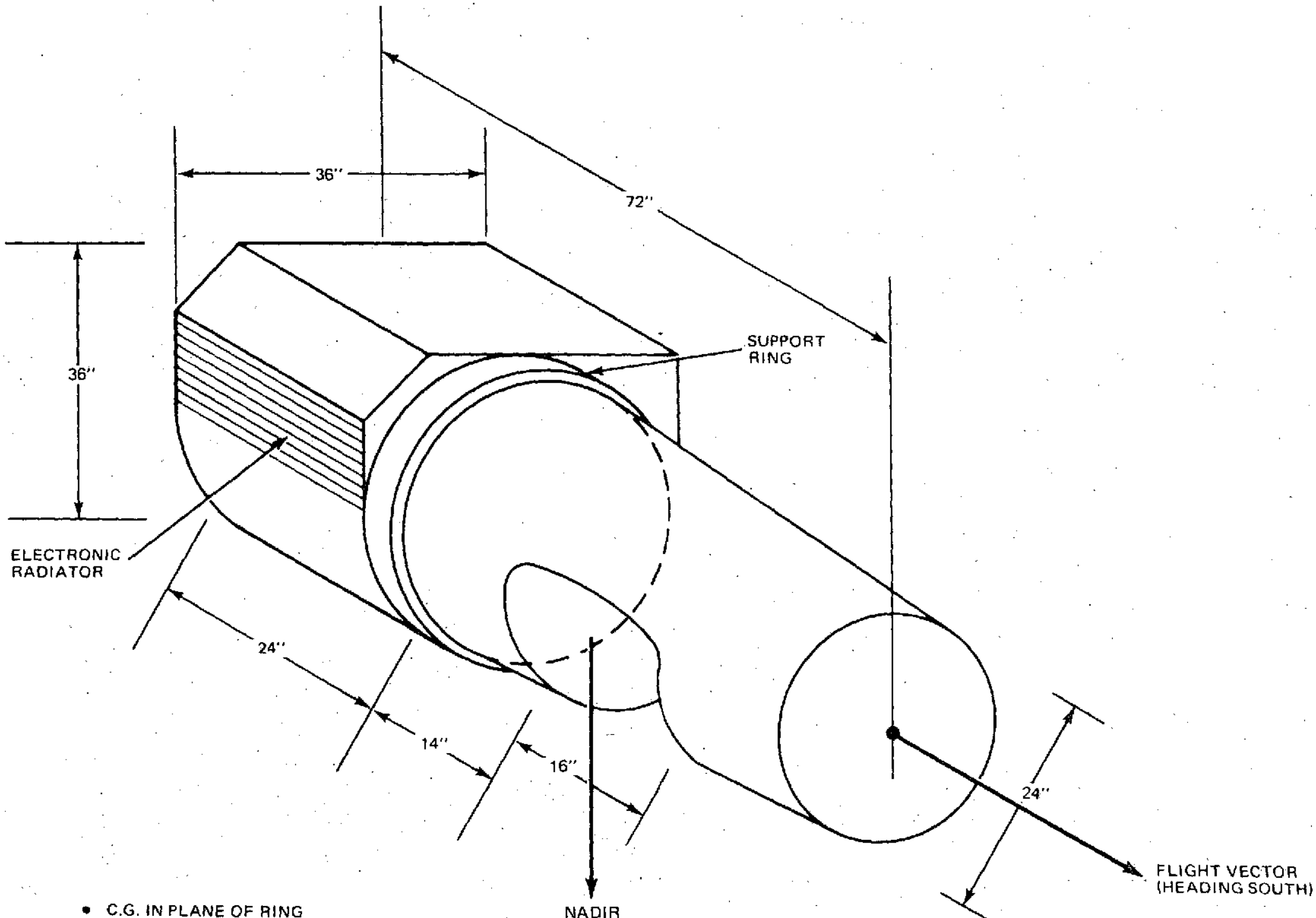

- C.G. IN PLANE OF RING
- THREE PICK-UP POINTS AROUND RING
- INSTRUMENT WEIGHT = 450 LBS NOMINAL
  CAN BE REDUCED TO 350 LBS
- ASSUMED ORBIT: 0930

Fig. 4-33 **Honeywell HRPI**

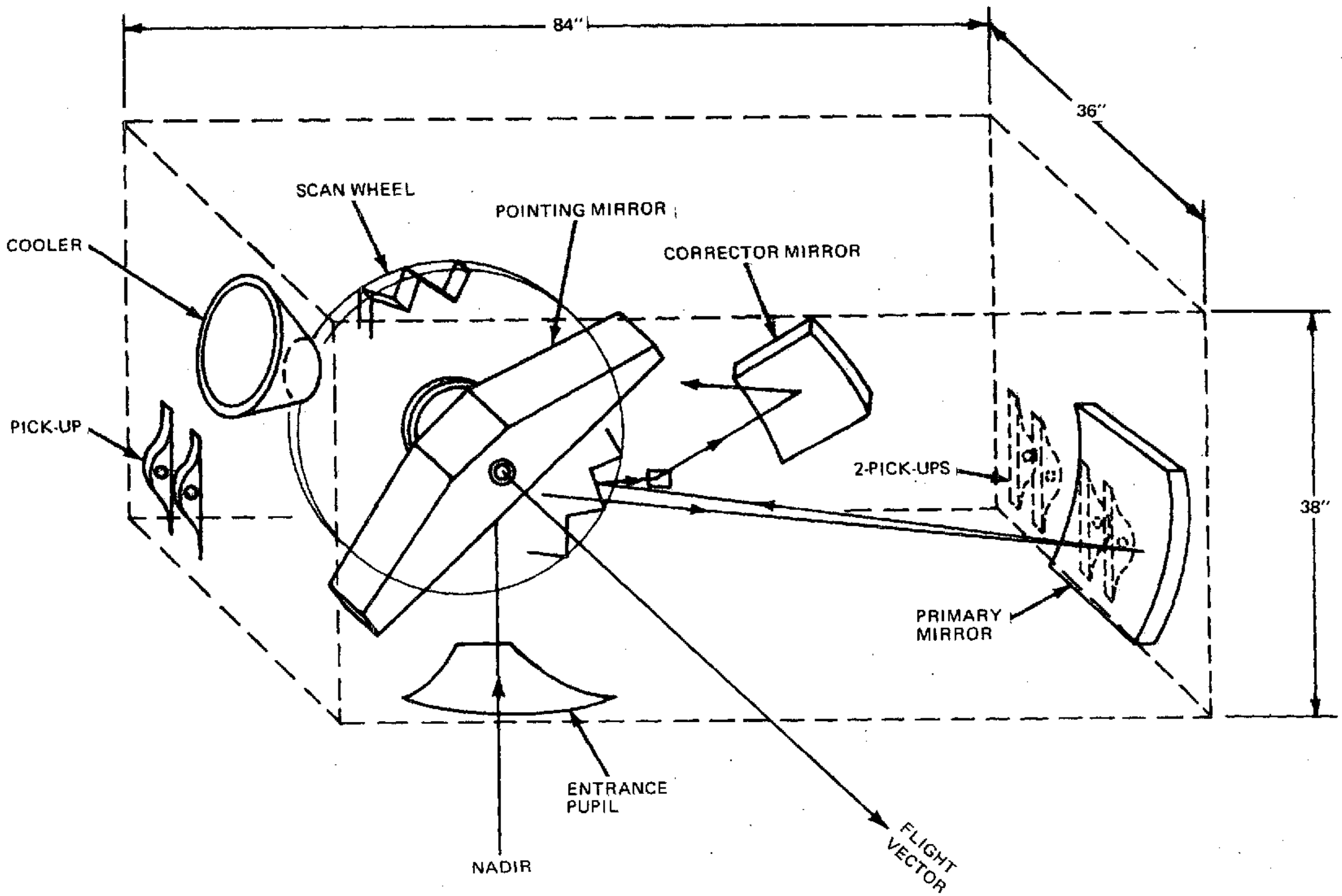

E-35

Fig 4-34 TE–HRPI

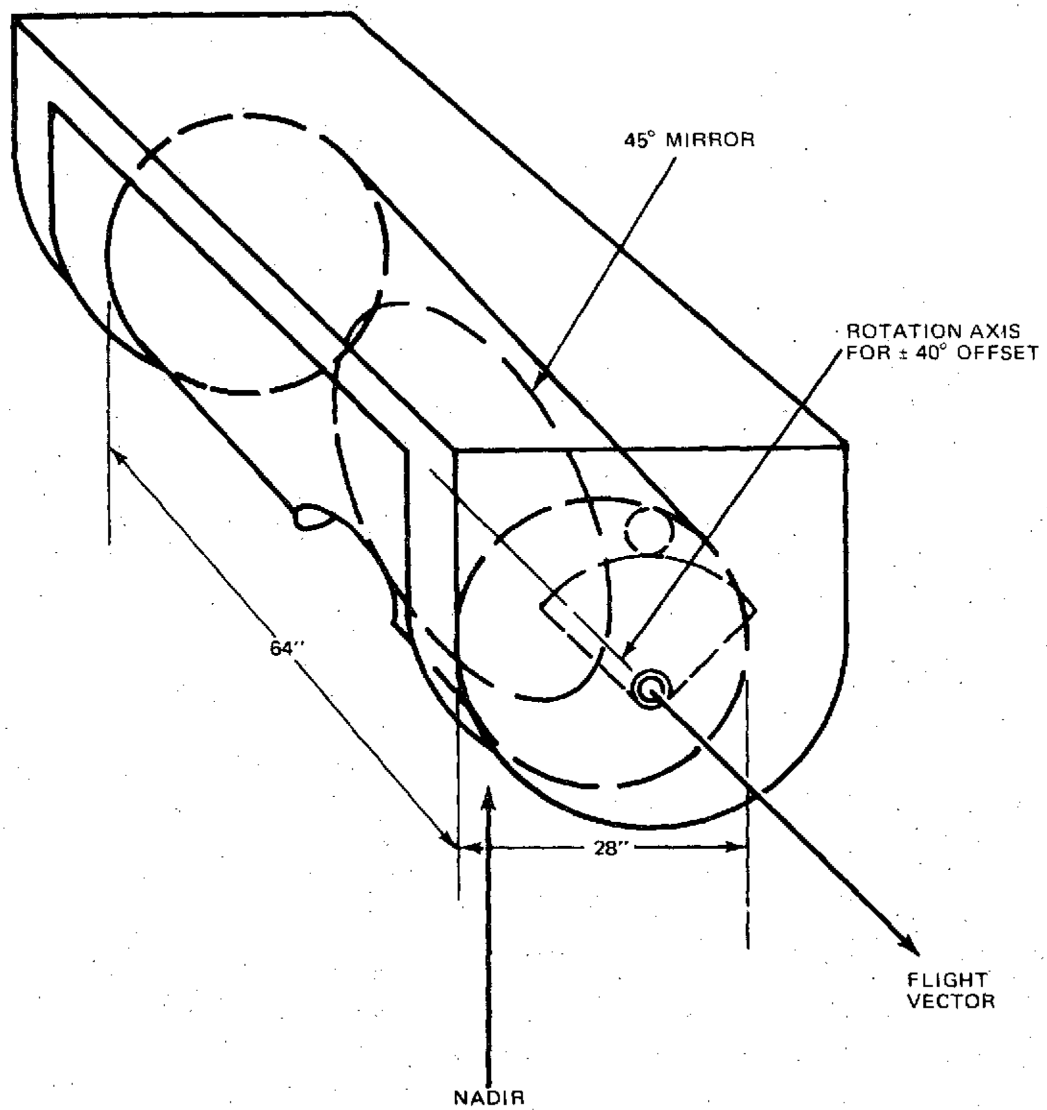

E-36 Fig. 4-35 **Push Broom HRPI (Parallel to Flight Vector)**

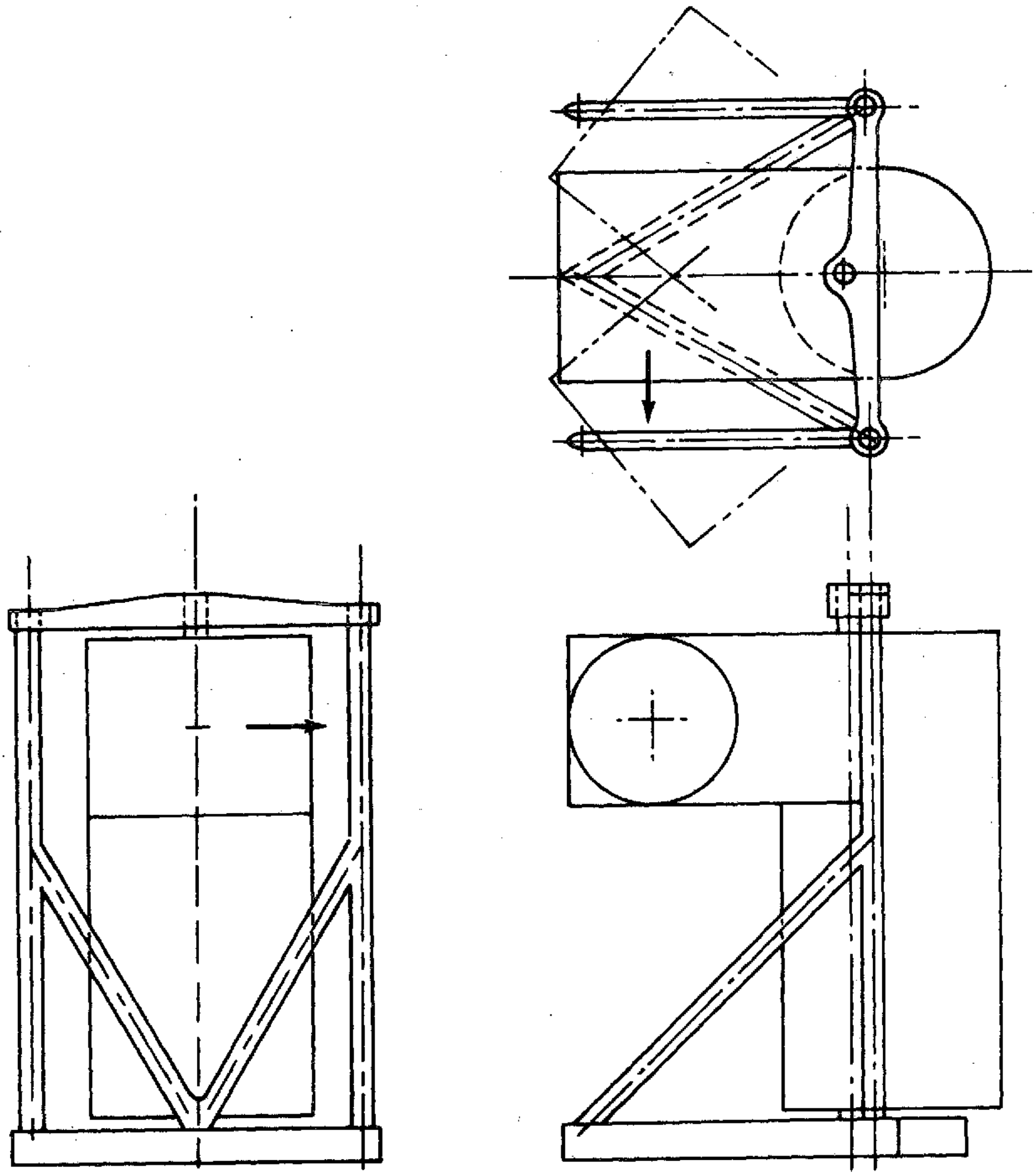

E-41 Fig. 4-36 HRPI Mounting Assembly

The Westinghouse pushbroom all electronic HRPI is expected to take the form illustrated i.e, using an external axle to rotate the entire package. The similarity to the Hughes package is large.

Note that three of the four designs can be considered physically interchangable as far as the spacecraft accomodations are concerned. Only the TE package is unique.

Figure 4-37 illustrates the expected weights for these various designs as a function of altitude ($\pm 30^{\circ}$ scan), here again the object plane scanner approach is the lightest of the electro-mechanical units, only the pushbroom HRPI would be lighter, and simpler.

Figure 4-38 provides a course indication of costs for several of the designs based on data supplied to us. It would be expected that the Honeywell design would fall between the Hughes and Te approaches.

All of these designs could be employed on the Delta vehicle at the 680 Km altitude.

E. 4.2.5 Preferred Baseline Design

Many considerations must be evaluated in defining a preferred point design and several levels of definition are involved.

During the course of this study, several point designs evolved which are significantly different from those specified in the original work statement. Furthermore, the requirements of the program expanded particularly with regard to ground coverage (500 Km vs 185 Km).

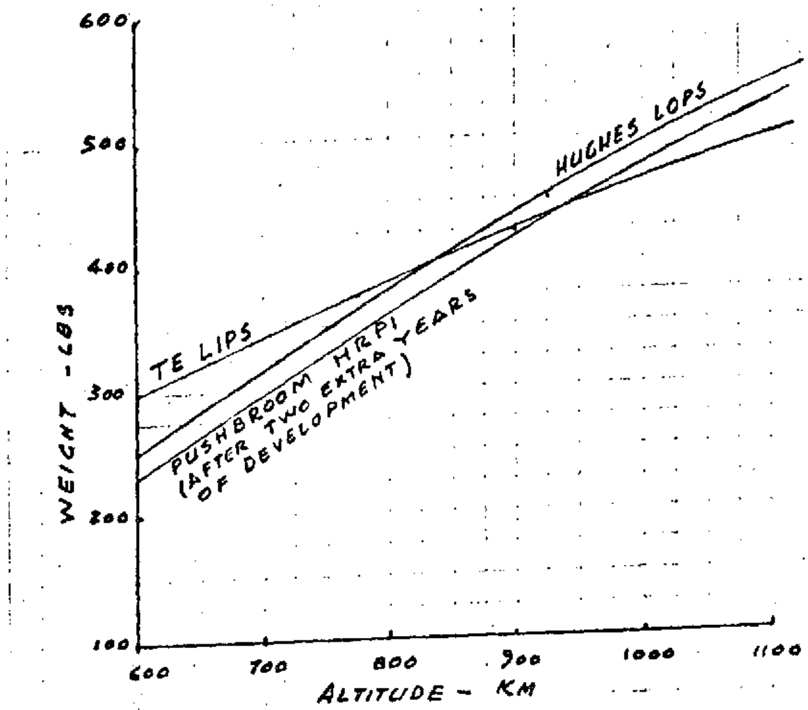

E-37

Fig 4-37 Anticipated HRPI Weights as Function of Altitude

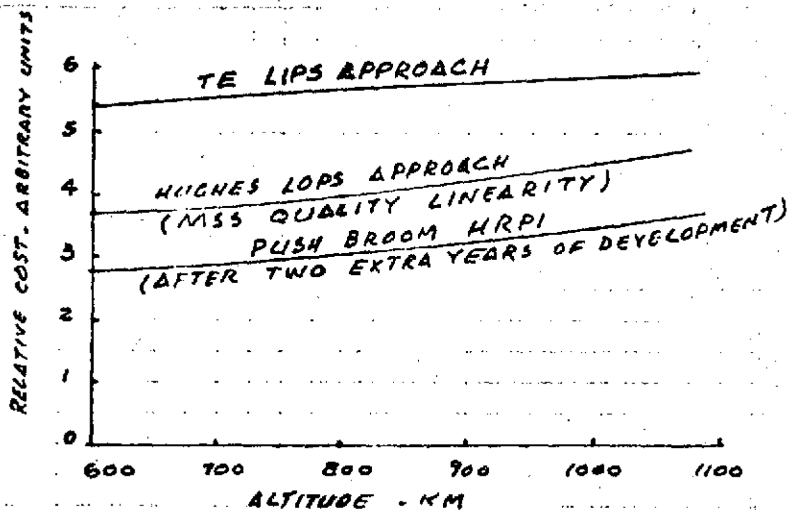

E-38

Fig 4-38 **Anticipated Cost-Difficulty Trends for HRPI**

The preferred point design configuration is based primarily on the following considerations:

1. Overall instrument capability
2. Performance growth
3. Previous hardware qualification
4. Development risk
5. Simplicity of interfaces
6. Compatibility with mission options

7. Cost

The preferred configuration for both the TM and the HRPI is an on-axis telescope design with the optical axis parallel to both the flight and lauch vectors employing an object plane scanner based on a nodding mirror.

The preferred aperture for the 680 Km orbit is 40.5 cm to make maximum use of similar design hardware and to insure adequate S/N ratio performance with solid state detector technology.

The preferred mechanical design of the HRPI (Figure 4-46) consists of an L-shaped cylindrical package mounted on an axle at the CG providing pointing perpendicular to the flight vector of up to $\pm 40^{\circ}$ when required. The support of the axle at one end includes momentum compensation mechanism as well. as a redundant indexing mechanism capable of providing 2° increment pointing and a maximum time to point of twenty (20) seconds including any settling time.

This configuration is shown in Figure 4-39 wherein the supporting framework is attached through latches to the vehicle when required for resupply purposes, and provides mounting area for the necessary electronics packages.

Figure 4-40 illustrates the preferred TM design, which is the same as for the HRPI with two principle exceptions:

1. The axle is omitted and the package is supported at the spacecraft end by a single thrust pad at the axle (CG) location and by two points at opposite sides of the opposite end in a determinate configuration.
2. A low temperature cooler, 100°K, is provided to provide the necessary operating temperature for the thermal detectors.

The size and weight of the TM with respect to the spacecraft, and the criticality of optical alignment internal to the telescope and with respect to the vehicle indicate a three point mounting of the instrument different from that called out in the point design specifications is desirable. A larger separation between the mounting points is desirable from both an alignment and vibration point of view. Elimination of structural stresses induced into the instrument calls for a determinate mount, a configuration in which no stresses can be introduced into the instrument from its mounting structure.

The preferred design also has provision for mounting and aligning a fixed head star tracker directly on the TM. By employing such a configuration, it is possible to uncouple the vehicles structural stability from the instrument pointing accuracy equation without causing any operational or other design difficulties, particularly if the star tracker communicates with the on board computer by means of the TM telemetry and command encoder.

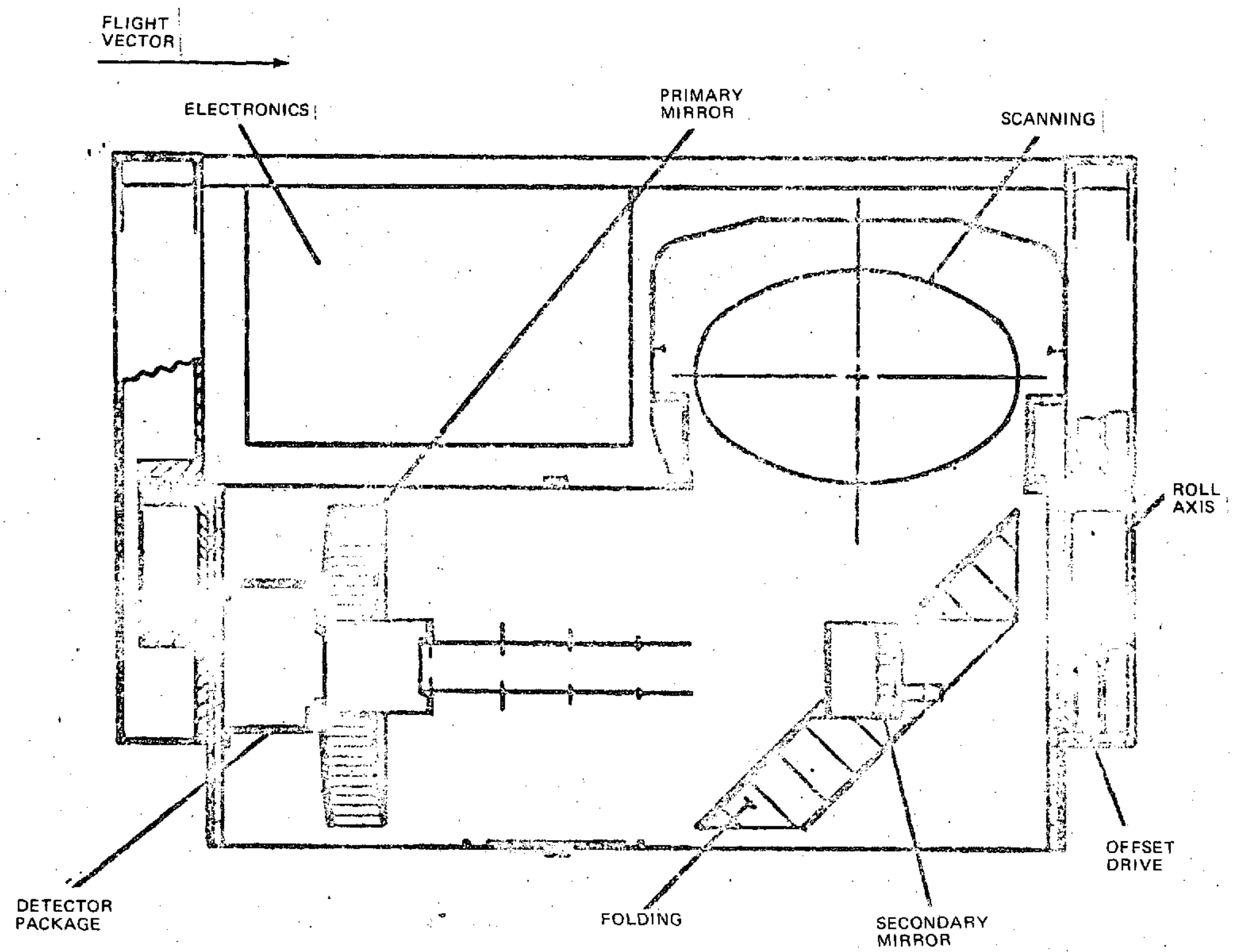

Fig. 4-39 Preferred HRPI

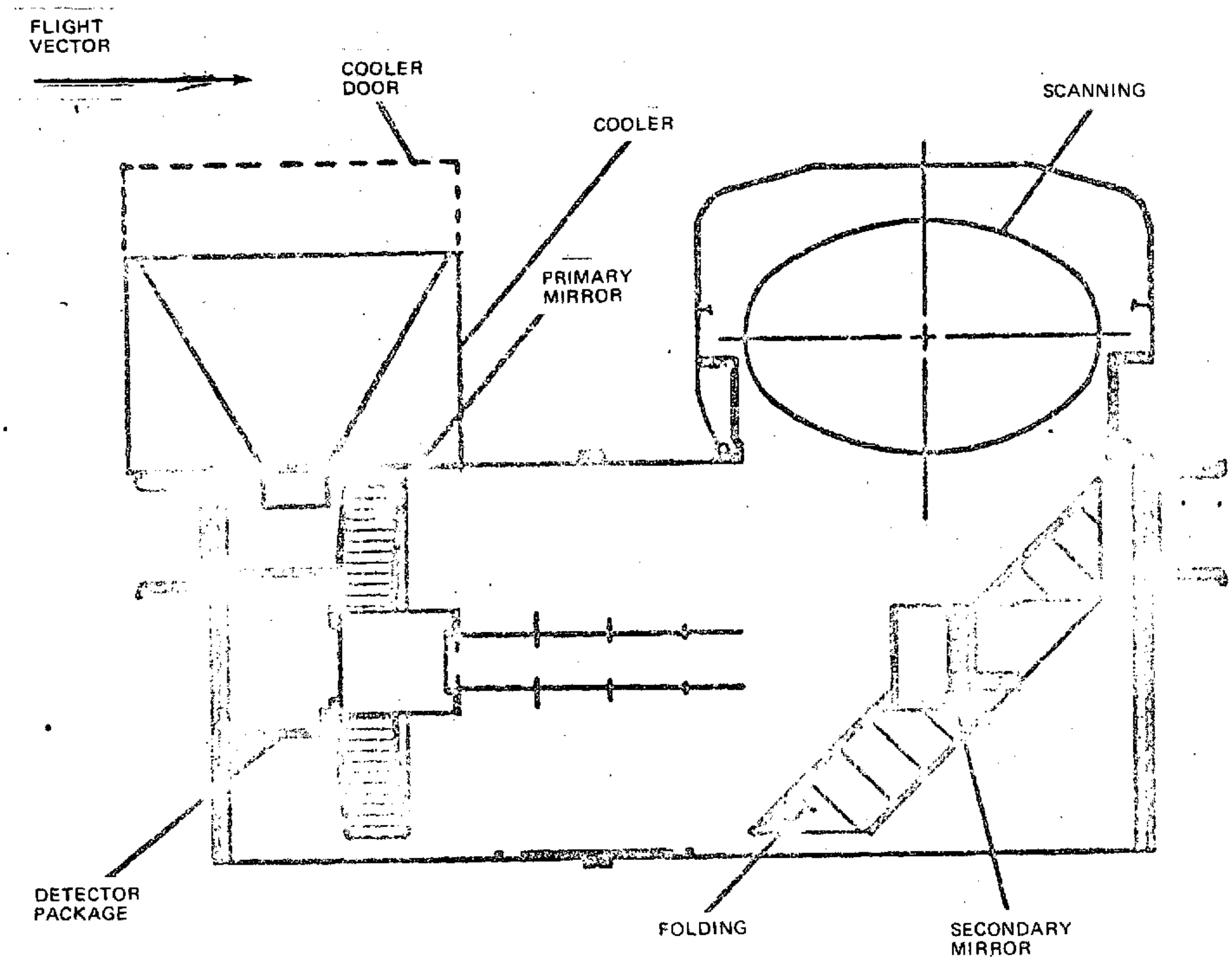

ORIGINAL PAGE IS
OF POOR QUALITY

E-40

Fig. 4-40 Preferred TM

E. 4.2.6 Optimized TM Configuration

During the preceding evaluation's, it became quite clear that the baseline TM performance was underutilized from the system point of view, scanning as it was only a $\pm 5.5^{\circ}$ field at 915 kilometers altitude.

As the system design progressed, the optimum altitude was lowered to 680 kilometers resulting in a scan angle of $\pm 7.7^{\circ}$ for a fixed 185 kilometer swath wdith. This angle began to challenge the image plane scanners but had little effect on the object plane scanner.

In fact the object plane scanner mirror was only nutating over one half this angle or $\pm 3.9^{\circ}$, an almost un-noticeable range. Clearly the utility of the design could be raised considerably by increasing the scan angle. This would provide three things:

1. More timely coverage of a wider area.
2. A higher repeat frequency for a single vehicle system at a given altitude.
3. A shorter time before revisit in the CONUS latitudes.

In addition a greater degree of stereo coverage would be available in a given time interval for when the ground processing system begins trying will produce maps of area of rough terrain where local ground elevations will be needed.

4.2.6.1 Swath Width

As shown in the orbit altitude studies, the next logical swath width was found to be 330 kilometers, $\pm 13.7^{\circ}$. For the object plane scanner this angle (the mirror operates at one-half of it) is still small and there is a negligible weight or size growth to provide this capability. What is involved is a minor change in the stray light baffle and a 12cm increase in the distance from the main telescope to the scanning mirror, as shown in Figure 4-41.

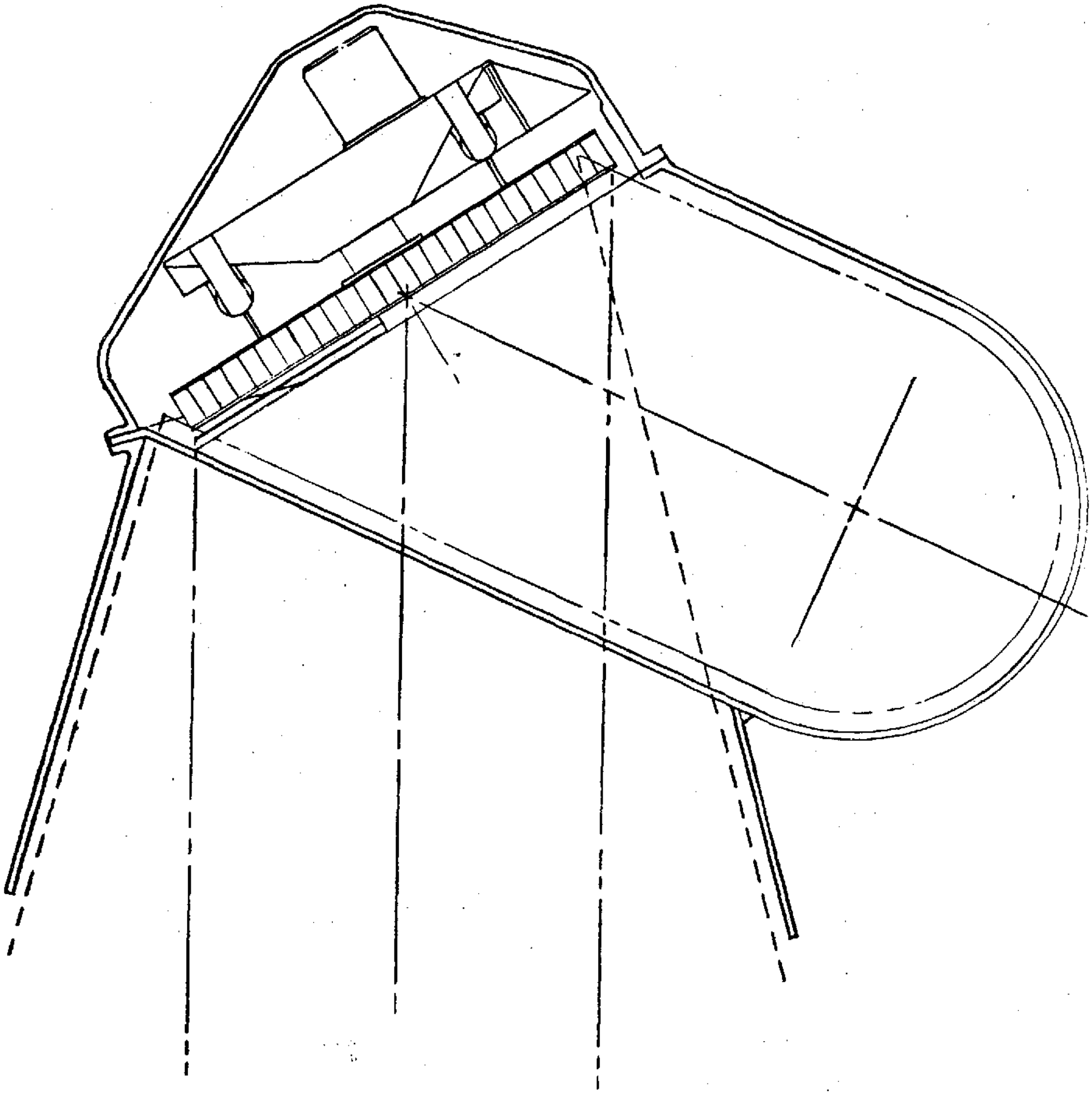

E-42

Fig. 4-41 Optimized TM Configuration

The increase in swath width at the same ground resolution does involve a growth in output data rate and a worsening of the bow-tie problem.

The data rate required is now handled by employing more detectors. During the early EOS missions where a HRPI is not planned to be carried anyway a regrouping of the data interface is used to accommodate the higher data rate over the same data link. In this case, bands 1 to 4 are transmitted at a total data rate of about 70 megabits/second on the in-phase channel of the quadraphase transmitter and channels 5 to 7 and the synchronization and housekeeping data also at a total data rate of 70 megabits/sec, are transmitted on the quadrature channel.

The bow-tie effect is still well within reason as shown in Fig. 4-42, amounting to an overlap of less than 6 meters at the edge of the field compared to contiguous coverage in the center.

The use of additional detector calls in an optimized scanner leaves the scan mirror velocity unchanged and the scan angle increased resulting in a lower scan mirror frequency. This frequency would be approximately 2/3 of the baseline frequency or about 5-3/4 cycles per second. No significant difficulties are expected in system design due to this lower scan frequency, in fact most of the pertinent distortions and vibrations are reduced with a reduction in scan frequency.

The effect of the atmospheric path is still negligible for scan angle change from $\pm$ 7.7° to $\pm$ 13.7° and no correction for sun angle change within the scanned swath is deemed necessary.

Therefore an optimized TM for the EOS mission is characterized as a 16" aperture object plane scanner aligned with the telescope parallel to the flight vector, weighing approximately 350 pounds, and scanning a $\pm$ 13.7° field. The

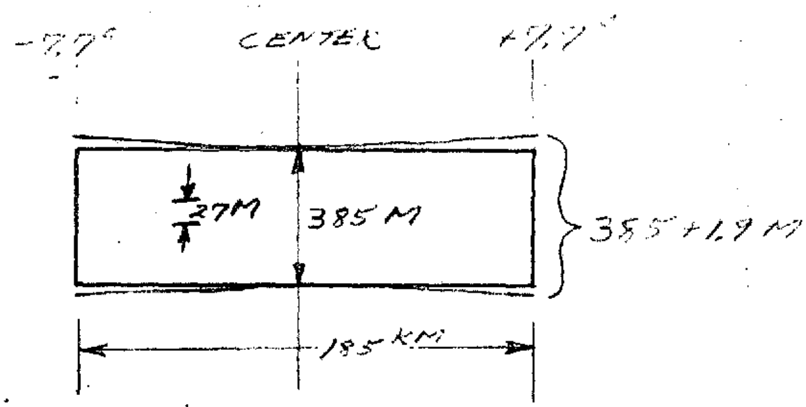

BASELINE TM STRIPE
(14 DETECTORS)

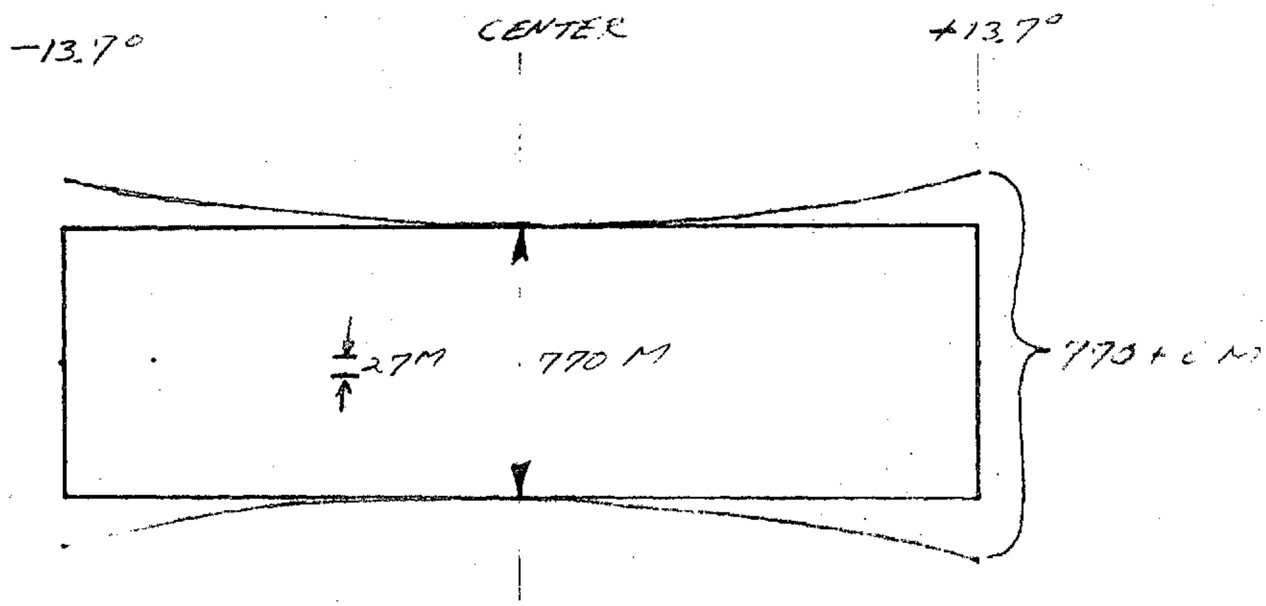

OPTIMIZED TM STRIPE
(28 DETECTORS)

REF: HUGHES SSR POINT DESIGN, PG 2-2

E-43

Fig. 4-42 TM Stripe Comparison

ORIGINAL PAGE IS
OF POOR QUALITY

unit provides a total output data rate of 140 megabits per second divided into eight channels, one for each of the spectral bands plus a synchronization channel.

When flown at 680 nautical miles, the unit provides a 30 meters ground resolution at the signal to noise ratio and radiance levels of the point design specification.

4.2.6.2 MSS + HRPI EMULATION

During the early EOS missions, there is a need to provide a backup for the operational MSS. Furthermore, it would be useful to evaluate the desirability of the HRPI concept. The advanced TM developed above along with the on-board data processing equipment related to the LCGS provides a unique capability in this area.

By proper selection of the data output options from the instrument and data processor, the following capabilities can be achieved.

1. A complete and faithful emulation of the 5 band MSS (either standard or wide format) for transmission to DOI,
2. A pseudo HRPI signal providing a 30 meter resolution over a continuously selectable 35 kilometer swath of the total 330 kilometer field of view.
3. The prescribed selection of LCGS outputs.

Any one of these signals can be made available at the data processor output simultaneously with the normal 30 meter resolution output. They would be transmitted over the LCGS data link to DOI or other user as appropriate.

Thus a full MSS backup and a pseudo-HRPI capability are achieved at minimum cost and complexity.

When flown at 680 Km altitude, it is currently planned to maintain the MSS resolution at 80 meters IFOV in order to maintain the output data rate and ground data formatting unchanged. Using the current 1.5:1 sample ratio on the MSS, a system field of view of 100 meters is obtained for the MSS at an in scan sample size of 54 meters.

If the TM specification is adjusted only slightly, to a sample size of 27 meters instead of 30 meters, and the detector cell size increased proportionately, the TM will still provide a system FOV of 37 meters while delivering an output data stream which can easily be processed to emulate an MSS.

Specifically, every pair of samples from the TM would be summed and divided by 2 to obtain the appropriate along scan sample size and then the values obtained from each group of three detector cells would be summed and divided by 3 to provide an 80 meter sample in the cross scan direction, this is illustrated in Fig. 4-43 (If 18 detectors are used in the TM, this results in a 6 detector equivalent output identical to the MSS). The least significant bit of the 7 bit code of the TM is deleted to form the 6 bit MSS emulation code.

As mentioned earlier, by employing an object plane scanner as the basic design, a HRPI can be obtained as a minor modification of a production TM. Such a change involves:

1. A change in the sensor array to achieve the desired resolution.
2. A change in the scan mirror rate and scan angle.

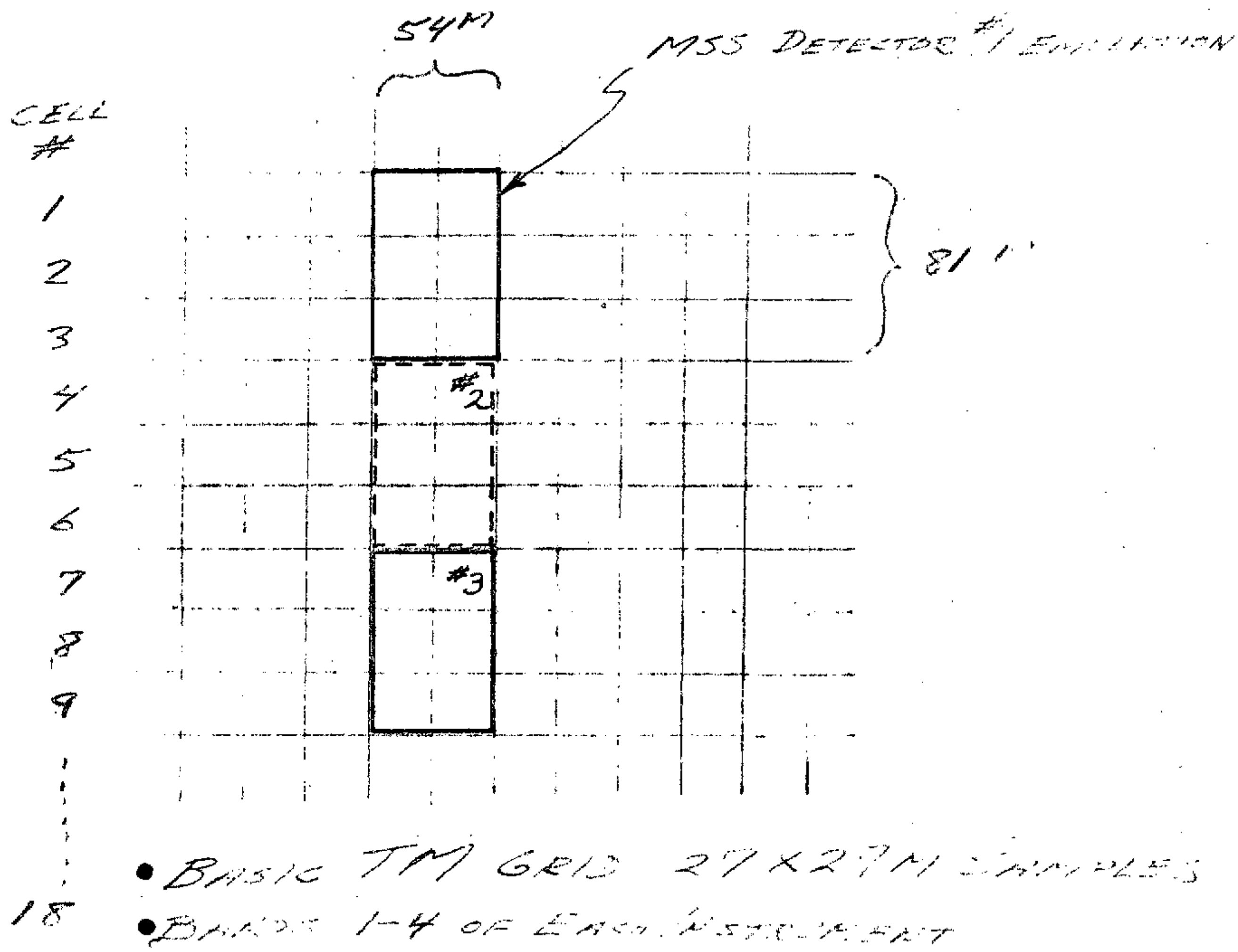

- BASIC TM GRID 27 X 27M SAMPLES
- BANDS 1-4 OF EACH INSTRUMENT
- SIMILAR PATTERN [illegible] BANDS

E-44 Fig. 4-43 TM-MSS Sampling Grid to Obtain MSS Emulation

ORIGINAL PAGE IS OF POOR QUALITY

3. Mounting of the entire unit on an axle
4. Deletion of the passive cooler for bands 5 through 7.
5. Minor reharnessing of the detector amplifier assembly.

These changes can be accomplished at a minor cost compared to a new instrument development if provided for in advance.

4.2.6.3 Growth Potential

As a product improvement during the life of the program, the object plane scanner offers two further features:

1. The ability to incorporate short CCD arrays in the focal plane and employing delay integration ot achieve increased S/N ratio data or lower minimum radiance levels of about 8:1.
2. The ability to incorporate long CCD or similar electronically scanned arrays in a pushbroom mode of operation by disabling the scan mirror. Assuming the state of the art is raised to that expected before implementation, the expected performance improvement in minimum radiance level would exceed 100:1 over the individual detector approach.

The conversion to a pushbroom instrument with the field of view of the HRPI ($\pm$ 2°) would actually require replacement of the focal plane sensor package by a new package including not only the pushbroom sensor circuitry but also a field corrector element to achieve adequate resolution (MTF) over the required field. The Ritchey-Chretian optical configuration, most likely to be used here, has on many occasions been corrected to achieve this field of view at much higher

MTF than required here, for film camera applications.

Alternately, if the above correction appeared too expensive, a Schmidt corrector assembly could be considered but this would probably require refiguring of the main optics.

4.2.6.4 Summary

In summary, an advanced TM has been defined which:

1. Provides a 3:1 improvement is ground resolution over the ERTS program and a significantly better repeat frequency.
2. Offers a utility and cost effectiveness of 3:1 or greater over the baseline
3. Offers a complete MSS emulation in order to backup the MSS during early missions
4. Offers a pseudo-HRPI output simultaneous with its normal output for development of the HRPI concept and/or requirement.
5. Can be modified in production to obtain a flight model HRPI at a nonrecurring cost of about ½ the recurring cost of a TM.
6. Offers a growth potential in minimum radiance requirement for adequate data quality of from 8:1 to 100:1.
7. Can service a large variety of LCGS users with various output data formats.

GRUMMAN

TRADE STUDY REPORT

TITLE	TRADE STUDY REPORT NO. 5
DATA OPERATIONS	WBS NUMBER

See Report No. 3, Section 6.5

PREPARED BY	GROUP NUMBER & NAME	DATE	CHANGE LETTER
			REVISION DATE
APPROVED BY			PAGE 5-1

SYSTEM TRADE
STUDY NO. 6

GRUMMAN

TRADE STUDY REPORT

TITLE	TRADE STUDY REPORT NO.
ACS/CPF TRADEOFF	6
	WBS NUMBER 2.1.2.5

Purpose:

To determine the level of ACS pointing and stability accuracy and its associated ground processing requirements which result in the lowest total program cost.

Summary:

The objective of the ACS/CPF (Attitude Control System/Central Processing Facility) tradeoff is to determine the performance requirements for the ACS which result in the lowest program cost, where the program is a selected schedule of missions and the cost is computed for the ACS plus the CPF.

ACS/CPF costs have been computed for a matrix of twelve combinations: four ACS performance requirements for each of three programs.

For each of the three programs, the ACS performance requirements resulting in the lowest ACS/CPF cost was determined.

Conclusions and Recommendations:

The ACS configurations resulting in lowest ACS/CPF cost over complete mission programs are the baseline ($\pm$ 0.01 deg accuracy, $\pm 10^{-6}$ deg/sec stability) and low-cost ($\pm$0.05 deg accuracy, $\pm$ 5×10^{-6} deg/sec stability). For the projected EOS Missions consisting of A (MSS, TM, DCS, EROS), A' (MSS, TM, DCS, EROS), B(TM, HRPI, DCS, EROS, C(2 TM, HRPI, SAR, DCS), D(SEABAT B), and E (TIROS O), the stipulated experiment pointing accuracy and stability requirements are 0.01 deg and 2×10^{-6} or 10^{-6} deg/sec, except for SEASAT B, which is either 0.01 or 0.1 deg pointing accuracy. In addition, the requirements for synchronous altitude missions are expected to be more stringent than those at low altitudes; and the solar maximum and possibly other inertial-type missions could require 0.01 deg pointing accuracy and 10^{-6} deg/sec stability. Thus it is important to have as high a performance as possible to attain flexibility for meeting varying mission requirements, while simultaneously minimizing cost. Thus it is recommended that the baseline ACS configuration be used since a significant increase in flexibility is obtained at no additional cost.

PREPARED BY	GROUP NUMBER & NAME	DATE	CHANGE LETTER
G. A. Zetkov	493 Control Systems	7/16/74	
			REVISION DATE
APPROVED BY J. Fragola			PAGE 6-1

Cost and Performance Data Summary:

The preferred ACS performance requirements as a function of discrete values of ACS/CPF program cost is given in the Table below.

PROGRAM	ACS/CPF COST $ M	PREFERRED ACS PERFORMANCE REQUIREMENTS	
		Attitude Accuracy deg	Angular Rate Accuracy deg/sec
1	8.4	± 0.01	± 10^{-6}
2	20.2		
3	40.9		

The curves of ACS/CPF cost versus ACS configuration are shown in Fig. 6-1.

6.1 Assumptions

- Three program mission models

  - Launch date, missions, and types of instruments

Three programs (low-cost, baseline, and expanded capabilities) for both a development phase (1979-1983) and an operational phase (1983-1990) were constructed and are summarized in Tables 6-1 and 2. The tables show the times at which a spacecraft is launched and its operation terminated, its mission, and the types of instruments aboard.

  - Instrument data rate and volume

Tables 6-1 and 2 also show the data option used as designated by the letter A B or C and defined in Table 6-3. Each data option has the same instrument set, TM and HRPI. The variation in the data transmission results from the use of either Direct Data, Direct Data plus Wide Band Video Tape Recorder, or Direct Data plus transmission via the Telemetry Data Relay Satellite.

o Errors in ACS, Ephemeris, Instrument, Instrument/ACS Alignment, Earth Model, and Final Pixel Location

Assumptions for errors are given in Table 6-4. The final error for pixel location is specified to attain temporal registration. The three sets of ACS errors describe the ACS performance requirements. Corresponding to each of the three ACS performance requirements and to the fixed errors in ephemeris, earth model, and transfer alignment, there is a CPS which is capable of achieving the specified pixel location error.

6.2 Configurations and Costs for Three Types of ACS with Costs Computed over the Three Programs

Corresponding to the three ACS performance requirements as given in Table 6-4, three ACS configurations were constructed as shown in Table 6-5. The hardware costs for the three ACS configurations are shown in Table 6-6 on a component and spacecraft basis. The manpower costs for these three ACS configurations are shown in Table 6-7. The hardware and manpower costs are combined as shown in Table 6-8. The number and type of spacecraft in the three types of spacecraft are shown in Table 6-9. Using Tables 6-8 and 9 the ACS program costs were computed and are summarized in Table 6-10. The results of Table 6-10 are plotted in Fig. 6-2.

The ACS weights for three ACS configurations are given on a component basis in Table 6-11 and on a component and spacecraft basis in Table 6-12. The results of Tables 6-10 and -12 are plotted in Fig. 6-3 to relate ACS program costs to ACS hardware weight for the three programs and the three ACS configurations.

6.3 Configurations and costs for three ground data processing systems corresponding to the three types of ACS with costs computed over three programs

6.3.1 Cost per scene for correcting thematic mapper images

TITLE	TRADE STUDY REPORT NO. 6
ACS/CPF TRADEOFF	WBS NUMBER 1.2.1.2.5

1. Introduction

The EOS (EARTH OBSERVATORY SATELLITE) Satellite will contain scanning type sensors that collect and return to processing stations digital image data in several spectral bands. The thematic mapper (TM) is one of these multispectral sensors and this particular instrument covers six visible and one IR band with a resolution of 30 meters on the surface of the earth, in its visible bands. For satellites in near-polar orbit, so that ground tracks of the S/C are approximately north-to-south, the scanning of the earth is accomplished by rotating a mirror in the west-to-east direction. The light reflected from the earth (for the visible bands) is collected by a bank of N contiguous detectors (aligned approximately north-to-south) so that N scan lines are collected during each sweep of the mirror. Typically, each sweep covers a 185 Km swath (east-west dimension) on the surface of the earth. Scanning is precisely synchronized with S/C velocity so that adjacent sweeps are exactly contiguous. During each sweep, the light detectors in the sensors are sampled at equi-spaced time intervals (equal-time or ET sampling) so that a TM scene can be thought of as a digital image made up of 8633 pixels (picture elements) in each of 6166 lines. The image contains approximately 53 x 10^6 elements where each element is a 6-7 bit word (signifying one of 64 or 128 brightness values).

Several factors contribute to geometric imperfections in the images collected by the sensor and, although our primary concern here is with S/C attitude errors, it is necessary to mention some of the other sources of error so as to put ACS-caused errors in proper perspective. The ultimate use of the sensor data is to produce photo maps, typically on a scale of one-to-one million, of a 185 by 185 Km scene viewed by the sensor. Such a map, which may be in the form of a digital tape, will have its individual lines precisely aligned with lines of latitude on the surface of the earth, and the rows of pixels will be precisely aligned with lines of longitude. A slight west-east scale expansion will be experienced if a UTM (Universal Transverse Mercator) projection is used to map the earth onto a flat surface.

If one envisions the earth as having latitude and longitude lines painted on it and then considers how this "grid" is viewed by the sensor, it is clear that the grid will not appear rectangular, or regular, to the sensor. First, the S/C orbit (which is selected to be inclined slightly from a polar orbit) does not allow the S/C nadir point to follow a north-south line (a line of longitude). Even if the S/C were in a true polar orbit, the earth rotates under the scanner so that in the 27 seconds required to collect a scene, a skew would be imparted to the grid. Finally, even if the S/C orbit, pointing (attitude), and the sensor scanning were perfect, there are other possibly second-order effects that contribute additional distortion to the grid. Such effects would include earth curvature and earth obleteness.

In addition to these natural effects, there are certain characteristics of the system itself that contribute their own distortions to the grid. The S/C orbit

PREPARED BY	GROUP NUMBER / NAME	DATE	CHANGE LETTER
L. Palmer (CSC)		6/26/74	
			REVISION DATE
APPROVED BY J. Fragola			PAGE 6-4

will not be known precisely so that the exact point on the earth that the sensor is viewing at any instant of time may be displaced from where it is predicted to be. Attitude errors about the pitch and roll axis of the S/C manifest themselves in approximately the same way. Finally, the scanning itself may be imperfect so that the contiguous elements within each scan line do not represent equal-angle (EA) views of the scene.

All of these factors combine to distort the hypothetical grid which is viewed by the sensor and the major job of the geometric-correction phase of ground processing is to estimate this grid and to relate it to the data that was actually taken. By knowing the grid in relationship to the data, one can then resample the original data to produce the desired image. In general, this resampling requires the generation by interpolation, of picture elements in between those that were actually taken by the sensor.

With this background, we can now concentrate on the effect of attitude control system errors on the geometric correction of the images. We emphasize that even with a perfect ACS, certain corrections must be made to the data and these operations are significant from the standpoint of the amount of digital processing that must be done. However, as the ACS becomes poorer, in the sense that it allows larger errors in pointing, a point will be reached where the effect of these errors begins to affect the processing - e.g., more complex correction algorithms must be used, or more operations must be performed on the individual pixels. For even greater ACS errors, the necessary corrections may actually dominate the processing load. We will attempt to find these break points in the following although the latter case (ACS errors dominate the processing) may result when the ACS is so poor that the system is practically unusable.

The analysis will proceed in the following steps. In Section 2, we define "ACS errors" and give a range of values for both static and dynamic errors which should cover the range that might be considered for EOS. In Section 3, we show the impact of these errors on the TM scenes. We will consider the errors that might manifest themselves during one complete pass over CONUS, which might include 15 scenes. In Section 4, we show generally the processing that must be performed to geometrically correct the TM data. It is important that this processing be described in such a way that the impact of ACS-caused errors is clearly evident. Finally, in Section 5, we relate processing complexity to the processing steps and then go further and relate dollar costs to the processing that must be performed on one TM scene. Conceptually, if it costs $\$C_N$ to process one TM scene with an absolutely perfect attitude control system, we want to examine the total cost

$$\$C_T = \$C_N + \$\Delta \qquad (1)$$

where $\$\Delta$ is a function of ACS accuracy. To examine the relationship in (1) the major options to be considered are:

Processor Configuration

1. Completely General Purpose Computer(s), GP option
2. Special-Purpose Hardware to do as much of the processing as possible, referred to as SP option.

Availability of ACS Error Data

1. Not available
2. Accompanies the video data in each scan line

These four cases will be considered as options, and within each ACS errors will be the major parameter.

2. Assumptions about the ACS and the resultant errors

The intent of this section is to define very precisely what we mean by errors in attitude and to make the necessary assumptions about the statistics of these errors. Also, we will state our assumed ranges for static pointing and attitude rate errors.

The assumed geometry is shown in Fig. 6-4a. We assume that the scanner is aligned perfectly and executes pure rotation, sweeping out equal angular increments per unit time, about the roll axis of the S/C. The yaw axis of the S/C is assumed to be aligned perfectly with the center of the earth when there are no pitch or roll attitude errors.

The control system is depicted in simplified form in Fig. 6-4b. The instantaneous pointing of the S/C is determined by making use of external references (stars, the sun, and possibly the earth) and internal inertial references. We assume that these references periodically supply error signals to the ACS which indicate errors in angular alignment. These error signals are denoted in Fig. 6-4b as e_θ, e_ϕ, and e_ψ denoting errors in radians about the roll, pitch, and yaw axes, respectively. Generally, these error signals will include noise that is incurred in sensing the reference in addition to any misalignment betwen the actual S/C pointing and the desired pointing indicated by the reference. If we denote the reference noise as e_R, which we will assume to be zero-mean Gaussian and independent from sample to sample with standard deviation σ_R, we can denote the errors in actual spacecraft pointing as

$$\mathrm{VAR}\{E_\theta\} \cong \mathrm{VAR}\{E_\phi\} \cong \mathrm{VAR}\{E_\psi\} \cong \sigma^2 \Delta\omega_n / 4\zeta \qquad (2)$$

Where Δ is the basic sampling interval (interval at which the reference is sampled) and a second-order control system is assumed which is characterized by the undamped natural resonant frequency ω_n and damping factor ζ. The relationships in (2) are approximations since cross-coupling between the three spacecraft axes is neglected and also the control system parameters (ω_n, ζ) may not be the same for the three axes. Note that the actual pointing errors in (2) are primarily a function of the control system bandwidth ω_n; for larger values of ω_n, the control system responds more rapidly to the reference but it cannot average, or reduce, the input noise as effectively.

In Fig. 6-4c we show typical time histories of the S/C attitude errors E_θ, E_ϕ and E_ψ where each angle is expressed in radians. These angles change slowly with time with a correlation time that is roughly equal to the time constant (τ) of the control system ($\tau = 1/\omega_n$). For example, if ω_n = 1 radian/second, then the fluctuations in the time histories would experience significant changes only about once per second. These errors are assumed to be zero-mean Gaussian random variables with variances given by (2).

As the attitude angles fluctuate with time, we can identify a rate of change of S/C attitude and also the errors $E_{\dot\theta}$, $E_{\dot\phi}$ and $E_{\dot\psi}$ with respect to the normal values of these rates. Spacecraft rates should be approximately zero about the roll and yaw axes and precisely the orbit rate ($\dot\theta_o$ = $2\pi/100$ rad/min) about the pitch axis. With the assumption of a second-order control system, we can approximate the rate errors as

$$\mathrm{VAR}\{E_{\dot\theta}\} \cong \mathrm{VAR}\{E_{\dot\phi}\} \cong \mathrm{VAR}\{E_{\dot\psi}\} \cong \sigma_R^2\, \Delta\, \omega_n^3/4\zeta \qquad (3)$$

so that the variance in the rate error is approximately equal to ω_n^2 times the variance of the angular error.

The foregoing is an overly simplified view of the actual ACS operation. In practice, the operation may be changed from an external (star-tracking) to an internal (gyro) reference at the beginning of each image-taking pass. For our purposes, we must interpret several specification values in a form that will be suitable for the analysis to follow. The three specified accuracies are (See Fig. 6-5)

1. Rate error averaged over 30 minutes, $\equiv \dot\sigma_{30°}$
   As shown in Fig. 6-5a, this measure specifies the maximum allowable departure of the average angle rate from its nominal value (zero for roll and yaw and $\dot\theta_o$ for pitch) <u>when the average is taken over a 30 minute interval</u>. This measure can be *very* misleading when applied to shorter, say 30 second, intervals.

2. ATTITUDE ERROR - σ_{static} ; this parameter is interpreted as the static pointing error, measured in microradians which exists at the start of a satellite pass. In switching to a "hold" mode of operation, the ACS system attempts to maintain this initial pointing with absolutely no change over the remainder of the pass. To do so, of course, it must maintain zero rate error (or if rate error was zero to start with, it must not allow any acceleration).

3. ATTITUDE JITTER OVER 30 SECONDS - $\sigma_{0.5}$
This parameter is shown in Fig. 6-5b where we now observe the angle-versus-time record over 30 second time intervals and specify the maximum allowable change in angle over these intervals.

Note that the jitter requirement can be more meaningful in terms of the individual TM images than the long-term requirement. If jitter is specified as one arc second (4.85 μradians) over 30 seconds then the maximum allowable rate is 0.1616 μrad/sec over this interval.

In Table 6-13, we list the assumed values of attitude and attitude rate errors corresponding to the definitions noted above.

3. The impact of ACS errors on the TM scenes

We can now apply the numbers in Table 6-13 to the individual TM scenes to determine the distortion caused by the fact that the S/C is pointed incorrectly or is moving as the scenes are taken.

Several time intervals are of interest and these are depicted in Fig. 6-6. Clearly, the S/C cannot move enough to produce any degradation over the sample or the sweep time. However, over the duration of one scene, the rate errors can integrate to produce significant displacements in the pixels of the image.

The static pointing error, σ_{st}, yields errors on the surface of the earth of 30 meters for a 44 μradian pointing error about the pitch or roll axis. For static errors about the yaw axis, the outer pixels in a scene will be displaced only .09 meters for each μradian error. Assuming a 50 meter (3σ) orbit error in both the along-track and cross-track directions, we obtain a worst-case circular error in initial pointing of

$$\sigma_p = \left[16.6^2 + [0.68\ \sigma_{st}]^2 + 16.6^2 + [0.68\ \sigma_{st}]^2 + [0.092\ \sigma_{st}]^2\right]^{\frac{1}{2}}$$

$$\sigma_p = \left[551 + 0.9332\ \sigma_{st}^2\right]^{\frac{1}{2}} \text{ meters} \quad (4)$$

where σ_{st} is now expressed in microradians. The four values in Table 6-13 for σ_{st} give the following pointing errors:

σ_p	EXPANDED	BASELINE	LOW COST	DEGRADED
Meters	41.1	170	842	4211
Pixels	1.37	5.65	28	140

We can now summarize the four cases for both static and dynamic errors by computing a displacement over the time interval T as

$$\sigma_{Dyn} = \left[(0.68\sigma_T\,T)^2 + (0.68\,\sigma_T\,T)^2 + (0.092\sigma_T\,T)^2\right]^{\frac{1}{2}}$$

$$= 0.966 \;\; T\,\sigma_T \text{ meters (T in seconds, } \sigma_T \text{ in } \mu\text{rad/sec)} \qquad (5)$$

where σ_T is the rate error averaged over the interval T . To obtain σ_T for T = 400 seconds (the pass duration) we use

$$\sigma_{400\text{ sec}} = \left[\frac{30 \text{ minutes}}{400 \text{ sec.}}\right]^{\frac{1}{2}} \cdot \sigma_{30\text{ minutes}} = 2.12\;\sigma_{30\text{ minutes}}$$

A general comment about the numbers in Table 6-14 is that dynamic errors will have very little effect on the images. This, of course, is due to the extremely precise rate control that has been assumed even for the "degraded" system.

4. Steps in the processing of a single scene

In this section, we will outline the processing that must be performed in a single scene of TM data ($6\frac{1}{4}$ bands). Generally, the processing can be divided into three categories;

I. Calibration, including radiometric correction and one-dimensional line-scan correction.

II. Geometric correction including two-dimensional resampling of the data to correct for all sources of distortion. This step excludes, however, the location of ground-control points (GCP's)

III. Identical to II except that GCP's are first found in the image so that the resampling grid can be estimated more accurately.

We will assume that scenes are corrected to the maximum precision possible. Therefore, we will be concerned with all three types of processing. Within each type, certain operations are performed independently on each pixel in each band; certain others are common to two pixels in one scan line (different operations are not required for the bands); and finally, some operations are performed only once for the complete scene. The individual steps, and the above mentioned commonalities are noted in Table 6-15. To process all bands in one scene, therefore, assuming $N_{pix} = 5.3 \times 10^7$, for a GP processor, we obtain

Type I Processing

$$O_I = 5.3 \times 10^7 \left[6.25 \;\; (1) + 1 \; (2)\right]$$
$$= 4.37 \times 10^8 \text{ operations/scene} \qquad (6)$$

Type II Processing (No ACS data, nearest neighbor interpolation)

$$O_{II} = 6.0 \times 10^4 \; N_{GP} + 5.3 \times 10^7 \left\{ 1. \, (2) + 6.25 \, (8) \right\} \text{ Opns/Scene} \qquad (7)$$

Type III Processing

$$O_{III} = 10 \left[1 + 10 \, (M/32)^{\frac{1}{2}} \right] \left[L - M + 1 \right]^2 \cdot N_{GCP} \quad \text{Opns/Scene} \qquad (8)$$

L = Size of search area in pixels

M = GCP size in pixels

We see that O_I is a constant; O_{II} is a function of N_{GP}, whether or not ACS data is available, and the interpolation algorithm; and O_{III} is a function of N_{GCP}, M, and L. We assume the following values for these parameters for the different situations shown in Table 6-14.

	NO ACS DATA				WITH ACS DATA			
Parameter	Expanded	Baseline	Low Cost	Degraded	Expanded	Baseline	Low Cost	Degraded
N_{GP}	64	100	225	400	36	64	100	225
N_{GCP}	4	9	25	64	2	4	9	25
M	100	100	100	100	100	100	100	100
L	120	160	380	1500	106	136	268	940

Total operations for the GP cases (with and without ACS data) are listed in Table 6-16.

5. Estimates of processing costs

To estimate processing cost for one TM scene, it will be necessary to assign a dollar cost to the operations performed on each TM scene. For the GP approach, we will do this by simply equating one machine operation to $\$10^{-8}$. Note that this is equivalent to a "charge" of approximately $200 per hour on a machine capable of 5×10^6 million operations per second (5 Mips). This equivalent charge is low by 1974 standards by approximately 3-to-1, but we assume that it is reasonable for the EOS time frame. Using this cost relationship, the totals in Table 6-16 can be converted to dollars by multiplying by 10^{-8}. These results are plotted in Fig. 6-7. For the ACS accuracies specified for the baseline and expanded capability systems, the cost to process one TM scene is independent of ACS errors and is determined only by the interpolation algorithm used in the two-dimensional resampling.

For the low cost system, with static pointing errors of 872 μrad (28 pixels) and rate errors of 0.8 μrad/sec over 30 seconds, a noticeable increase in processing cost is incurred. Stated as a percentage, the increase is less for the situation where the more complex interpolation algorithm is used. For the "degraded" system where ACS errors become 5-to-1 larger than for the low-cost case, processing cost increases rapidly. This increase is not as rapid if ACS data is available to be used in the grid computation. For the GP approach, processing cost is dominated by the Type II processing, specifically by the two-dimensional resampling/interpolation.

To consider the impact of special-purpose (SP) processors we assume as a benchmark, that the SMS line-stretcher* cost $700K for one unit. This device handles input data at a 38Mbps and produces output data at a rate of approximately 2 Mbps. The SMS processes 1 visible channel with 8 detectors/channel and 2 IR channels which (together) give one-quarter the resolution of the visible channels. As an approximation, the SMS produces $1\frac{1}{4}$ bands with 14,500 lines and 15,000 pixels/line for 2.7×10^8 pixels per scene. Such a scene is collected in approximately 20 minutes. Assuming 6 bits/pixel, SMS yields an average data rate of 2 Mbps.

For EOS, a scene is collected in 30 seconds. For the low cost system, however, only 20 scenes per day are collected so that the peak data rate (100 Mbps, approximately) can be averaged over a 16 hour day to give an average rate of

$$R_{avg} = 100 \text{ Mbps} \times \frac{20 \times 0.5}{960} \cong 1 \text{ Mbps}$$

Therefore for 20 scenes/day, the type I processing for EOS will be assumed to be performed in a device that is slightly less expensive than the SMS line stretcher. At 400 scenes/day, however, the average rate becomes 20 Mbps which we will assume is considerably more expensive (not 20:1 more expensive, however). For the type II processing, we really have no good benchmarks. We will, therefore, make some arbitrary estimates assuming that the two dimensional interpolation is considerably more complicated than the type I processing. Finally, for both devices we assume a five year system life so that both the type I and type II processes can be reduced to a "cost" per scene. These numbers are summarized in Table 6-17.

We have not tried in Table 6-17 to distinguish between the interpolation algorithms used in the type II processing. Note that these costs, themselves, reflect an increase in cost per scene in moving from the expanded-capability to the low-cost system simply because the SP processors for the former case processes 20 times the minimum data at only a four to six to one increase in cost. To remove this variation, we assume a cost of $40/scene for the types I and II processing where grid computation is excluded in the latter (the first part of Eq (7)).

*Synchronous Meteorological Satellite - Synchronizer/Data Buffer Design Plan, October 1971, prepared by Westinghouse Electric Corporation, for Goddard Space Flight Center under Contract NAS-S-21574.

The cost trend is then shown on Fig. 6-7 as a dotted line. For a degradation in ACS errors of 5:1 from two low-cost values, processing costs again become dominated by GCP location and rise abruptly. For the baseline system, however, the costs (Bilinear interpolation assumed) is lower than for the GP approach.

6. Summary and conclusions

As indicated earlier, the ACS accuracies assumed for the expanded capability, baseline, and even the low-cost systems have very little impact on processing costs for the TM data. Costs are determined, almost entirely, by the two-dimensional sampling/interpolation of the data. For ACS accuracy that is degraded 5:1 from the low-cost option, giving initial pointing errors of 140 pixels (one sigma) and rate errors of 4 μrad/sec (average rate over 30 seconds), the ACS errors have a significant impact on processing. This impact is dominated by the cost of GCP location - primarily the fact that GCP search areas must be widened but also because more GCP's must be found in the scenes. The impact is less, but is still significant, if ACS error data is available to assist in computing the resampling grid.

Until the ACS system is analyzed or cumulated in more detail, so that time histories of the pointing are available, a more detailed analysis of the problem cannot be made. It appears that the baseline attitude control system being considered is completely adequate insofar as TM image distinction is concerned.

6-3.2 Cost per program for correcting images

Information in Tables 6-1, -2 and -3 is condensed to form Table 6-18, to show the processing requirements as a function of program phase and size. The cost per scene for the TM was given in the previous section. To obtain the cost per scene for the HRPI, the TM cost per scene will be multiplied by the following factor:

$$k = \frac{\dfrac{(\text{Scene area})\ (\text{No freq. bands})\ (\text{bits/pixel})\ (\text{samples/pixel})}{(\text{pixel area})}\ \text{HRPI}}{\dfrac{(\text{Scene area})\ (\text{No freq. bands})\ (\text{bits/pixel})\ (\text{samples/pixel})}{(\text{pixel area})}\ \text{TM}}$$

Using the data given in Table 6-3, the factor is

$$\frac{\dfrac{(48 \times 10^3 \times 185 \times 10^3)(4)\ (7)\ (1.0)}{(10 \times 10)}}{\dfrac{(185 \times 10^3 \times 185 \times 10^3)\ (6\ 1/16)\ (7)\ (1.0)}{(30 \times 30)}} = \frac{48}{185} \times \frac{30^2}{10^2} \times \frac{4}{6.0625} = 1.54$$

The cost for TM and HRPI is then estimated to be 2.54 times the cost of TM alone.

The data of Table 6-16 is multiplied by 10^{-8} \$/machine operation to obtain Table 6-19, showing the cost per TM scene for the general-purpose computer. Using Table 6-19, (nearest neighbor interpolation only), the factor 2.54 for the cost of TM and HRPI relative to that of TM only, and Table 6-18, the cost per program was computed and is shown in Table 6-20.

6.4 Total costs for the three ACS/GPS combinations over the three programs

The costs for the ACS over the three programs as given in Table 6-10 and for the CPF over the three programs as given in Table 6-20 were summed. The results are shown in Table 6-21.

The portion of Table 6-21 for the total program (development plus operations) and for ACS data included was used to construct Fig. 6-8. By inspecting Fig. 6-8, the least-cost ACS/CPF combination for each of the three programs results when ACS configuration 1 is used. Fig. 6-9 was obtained in a similar fashion, but in this case, cubic convolution interpolation was used without ACS data. Inspecting Fig. 6-9, the lowest-cost ACS/CPF results when the baseline configuration is used for the expanded capabilities program and when the low-cost ACS configuration is used for the other two programs.

Fig. 6-8 is repeated in Fig. 6-10, except that ACS Configuration 0 has been added, so that the minimum-cost point in each curve is more clearly indicated. ACS Configuration 0 has an accuracy and stability 5 times less than ACS Configuration 1 (0.05 deg, 5×10^{-6} deg/sec).

To show the decrease in cost of ground processing with increase in cost of the ACS for ACS Configurations having lesser and lesser performance, Fig. 6-11 was constructed. The net cost, shown by the dashed line shows that the least-cost is associated with ACS Configuration 1, but the cost of ACS Configuration 2 (baseline) is so close to that of ACS Configuration 1 (within the probable error of estimation) that either ACS Configuration 2 or 1 can be considered as the low-cost configuration.

The cost of ACS hardware and manpower as a function of the number of spacecraft is shown in Fig. 6-12A. The cost of the first spacecraft includes nonrecurring costs and is therefore larger than the cost of each subsequent spacecraft (recurring cost only). In Fig. 6-12B, the cost of ground processing for operations over a two year interval is shown. It is assumed that nearest neighbor interpolation, ACS data, and a general-purpose computer are used. The number of scenes per day applies to TM and HRPI simultaneously.

In Fig. 6-13, the cost of ACS recurring hardware and manpower is shown on the vertical axis. Additional costs incurred due to the ground processing of a number of TM scenes/day simultaneously with the same number of HRPI scenes/day are given in the curves. At 288 scenes/day TM plus 288 scenes/day HRPI, the cost of ACS Configuration 2 becomes equal to that of ACS Configuration 1.

Figure 6-14 is similar to that of Fig. 6-11, except that the variation in estimated ACS manpower costs have been removed from Fig. 6-14. In this case, the costs are lowest for ACS Configuration 2 (baseline).

When manpower costs are fixed for all ACS configurations at the level computed for ACS Configuration 2, as given in Table 6-8, the curves of Fig. 6-10 change slightly to that shown in Fig. 6-1. In this case, the minimum ACS/CPF cost occurs at an accuracy of 0.02 deg and stability of 2×10^{-6} deg/sec. However, the cost is practically constant for ACS Configurations 1 and 2 and in between. ACS Configuration 2 is thus preferred, because it provides the highest performance and permits the greatest flexibility for meeting varying mission requirements at no additional cost relative to the cost of ACS Configuration 1.

TABLE 6-1 PROGRAM FOR DEVELOPMENT PHASE

PROGRAM	MISSION MODEL	SPACE CRAFT NO.	LAUNCHED BY	LAUNCHED IN YEAR	OPERATIONS COMPLETED IN YEAR	RETURNED BY	RETURNED IN YEAR	MISSION	INSTRU-MENTS	DATA OPTION
1 (Low Cost)	12A	1A	Delta 2910	1980.5	1982.5	Shuttle	1983.5	LRM	TM, HRPI, DCS	A
2 (Baseline)	5	1A	Delta 2910	1979.5	1981.5	Shuttle	1983.5	LRM	TM, HRPI, DCS	A
		2A (DEMO)	Shuttle	1981.25	1981.3	Shuttle	1981.3	DEMO(1)	—	—
		2B(2)	Delta 2910	1982.5	1984.5	Shuttle	1984.5	LRM	TM, HRPI, WBVTR, DCS	B
3 (Expanded Capabilities)	1	1A	Titan 3B/SSB/NUS	1979.5	1981.5	Shuttle	1983.5	LRM	TM, HRPI, WBVTR, DCS	B
		2A	Titan 3B/SSB/NUS	1980.5	1982.5	Shuttle	1983.5	(3)	—	—
		3A (DEMO)	Shuttle	1981.25	1981.3	Shuttle	1981.3	DEMO	—	—
		3B	Titan 3B/SSB/NUS	1982.5	1984.5	Shuttle	1984.5	LRM	TM, HRPI, WBVTR, DCS	B

NOTES:

(1) Demonstration Flight: Demonstrate deployment, resupply, and retrieval. Include all ACS Modes Flight - lasts 6 days

(2) Spacecraft No. 2B is refurbishment of 2A.
Spacecraft No. 2C is refurbishment of 2B, etc.

(3) Mission is either
SOLAR MAX, SEASAT, OCEANOGRAPHIC, SEOS, or STELLAR

TABLE 6-2 PROGRAM FOR OPERATIONS PHASE

PROGRAM	SPACE CRAFT NO.	LAUNCHED BY	LAUNCHED IN YEAR	OPERATIONS COMPLETED & RETURNED BY SHUTTLE IN YEAR	MISSION	INSTRUMENTS	DATA OPTION
1 (LOW COST)	1B	SHUTTLE	1984.5	1986.5	LRM	TM,HRPI, DCS	A
	2	SHUTTLE	1986.5	1988.5	LRM	TM,HRPI, DCS	A
	3	SHUTTLE	1988.5	1990.5	LRM	TM,HRPI, DCS	A
2 (BASELINE)	1B	SHUTTLE	1984.5	1986.5	LRM	TM,HRPI, WBVTR,DCS	B
	3	SHUTTLE	1985.5	1987.5	(3)	—	—
	4	SHUTTLE	1986.5	1988.5	LRM	TM,HRPI, WBVTR,DCS	B
	5	SHUTTLE	1988.5	1990.5	LRM	TM,HRPI, WBVTR,DCS	B
3 (EXPANDED CAPABILITY)	4A	SHUTTLE	1983.5	1985.5	LRM	SAR	—
	1B	SHUTTLE	1984.5	1986.5	LRM	TM,HRPI, TDRS,DCS	C
	2B	SHUTTLE	1985.5	1987.5	(3)	—	—
	5	SHUTTLE	1986.5	1988.5	LRM	TM,HRPI, TDRS,DCS	C
	6	SHUTTLE	1987.5	1989.5	(3)	—	—
	7	SHUTTLE	1988.5	1990.5	LRM	TM,HRPI, TDRS,DCS	C

GRUMMAN

TRADE STUDY REPORT

TITLE ACS/CPF TRADEOFF

TRADE STUDY REPORT NO. 6

WBS NUMBER 1.2.1.2.5

TABLE 6-3 DATA OPTIONS FOR USE IN ACS/CPF TRADEOFF STUDY

ITEM		DATA OPTION A	DATA OPTION B	DATA OPTION C
INSTRUMENTS		TM, HRPI		
DATA TRANSMISSION		DIRECT DATA	DD + WBVTR	DD + TDRS
NO. GND. STATIONS		3		
PASSES/DAY OVER CONUS		3		
SCENES/DAY		TM 10 HRPI 10	TM 45 HRPI 45	TM 100 HRPI 100
SCENE DIMENSIONS, KM		TM 185 X 185 HRPI 48 X 185		
DETECTORS/BAND		TM 16 HRPI 4800		
RESOLUTION, METERS		TM 30 HRPI 10		
BITS/PIXEL		7		
SAMPLES/RESOLUTION		1.4		
BANDS		TM 6 1/16 HRPI 4		
DATA RATE, MBPS (WITH BUFFER)		TM 85 HRPI 90		
LEVEL OF PROCESSING*		STAGES I & II		
OUTPUT PRODUCTS, SCENES/DAY	HDDT	24	108	240
	CCT	7	15	56
	B & W PHOTO	36	108	360
	COLOR "	24	72	240
NO. OF FORMATS		2		

* Stage I: Calibration supplied with picture (radiometric, 1-dimensional line scan)

Stage II: Corrections for earth curvature & rate, UTM projection, and 2-dimensional sensor scan

PREPARED BY	GROUP NUMBER & NAME	DATE	CHANGE LETTER
G. A. Zetkov	493 Control Systems	6/14/74	
			REVISION DATE
APPROVED BY J. Fragola			PAGE 6-18

GAC 3711 3-72

TABLE 6-4 ERROR BUDGET

ITEM	VALUE		
Error, Pixel Location	0.5 Pixel Resolution, 1 σ		
Error, ephemeris	along-track 50 met 1 σ cross-track 30 met 1 σ radially 30 met 1 σ		
Error, earth model	10 met 1 σ		
Error, transfer alignment between ACS Startrackers and Instrument	21 μrad = 4.3 sec 1 σ equivalent to 15 met at 716 Km.		
Errors, ACS	Attitude Deg. 1 σ	Angular Rate Deg/Sec 1 σ 30 min	$\leq$30 sec
o Expanded Capability	0.002 (7.2 sec)	0.2 x 10^{-6} (2.6 sec/hr)	0.2x10^{-5}
o Baseline(NASA ACS spec for LRM)	0.01 (36 sec)	10^{-6} (13 sec/hr)	10^{-5}
o Low-Cost	0.05 (3 min)	5 x 10^{-6} (1.1 min/hr) (0.018 deg/hr)	5 x 10^{-5}

FIGURE 6-5. ACS CONFIGURATIONS

ITEM		ACS Configuration 1 Low-Cost	ACS Configuration 2 Baseline	ACS Configuration 3 Expanded Capability
Performance Requirements	Attitude, deg.	0.05	0.01	0.002
	Angular rate, deg/sec	5×10^{-6}	10^{-6}	0.2×10^{-6}
Components (Non-redundant System)	Coarse Sunsensor	2	2	2
	Digital Sunsensor	1	1	1
	Rate Gyro Assy (3 gyros & electr)	1	1	1
	Earthsensor(static)	1		
	Fixed-head Startracker		2	
	Gimbaled Startracker			1
	Magnetometer	1	1	1
	Signal Conditioner/ Analog Processor	1	1	1
	Reaction Wheel/Driver Assy (3 wheels)	1	1	1
	Magnetic Bars/Driver Assy (3 Bars)	1	1	1
	Jet Driver Assy (4 75-lb, 8 1-lb, 8 0.1-lb)	1	1	1
	Signal Conditioner/ MUX/Decoder Assy	1	1	1
	Bus Protection Assy	1	1	1

NOTES:
(1) An onboard digital computer is used in each configuration.
(2) Complexity Factors associated with ACS configuration are:

ACS Configuration	Complexity Factor
1 (low-cost)	0.8
2 (baseline)	1.0
3 (expanded capabilities	1.25

TITLE	TRADE STUDY REPORT NO.
ACS/CPF TRADEOFF	6
	WBS NUMBER 1.2.1.2.5

TABLE 6-6 ACS HARDWARE COSTS

Component	No on each Spacecraft			COST, $K														
				Non-recur			Recur			1 st Spacecr			Subsequent Spacecr		
Type	ACS Config			ACS Config			ACS Config			ACS Config			ACS Config		
	1	2	3	1	2	3	1	2	3	1	2	3	1	2	3
Coarse Sunsensor	2	2	2	5	5	5	2	2	2	9	9	9	4	4	4
Digital Sunsensor	1	1	1	10	10	10	40	40	40	50	50	50	40	40	40
Rate Gyro Assy	1	1	1	10	350	350	40	200	200	50	550	550	40	200	200
Earth Sensor	1	0	0	100	-	-	125	-	-	225	-	-	125	-	-
Fixed-head Startracker	0	2	0	-	40	-	-	43	-	-	126	-	-	86	-
Gimbaled Startracker	0	0	1	-	-	500	-	-	500	-	-	1000	-	-	500
Magnetometer	1	1	1	15	15	15	35	35	35	50	50	50	35	35	35
Analog Processor	1	1	1	150	150	150	150	150	150	300	300	300	150	150	150
Reactionwheel Assy (1)	1	1	1	20	20	20	130	130	130	150	150	150	130	130	130
Magnetic Bar Assy (1)	1	1	1	50	50	50	120	120	120	170	170	170	120	120	120
Jet Driver Assy	1	1	1	10	10	10	40	40	40	50	50	50	40	40	40
Signal Cond/MUX/DCD Assy	1	1	1												
Bus Protection Assy	1	1	1												
TOTALS →										1054	1455	2329	684	805	1219

Notes: (1) Size 1 (Smallest)

PREPARED BY	GROUP NUMBER & NAME	DATE	CHANGE LETTER
G. A. Zetkov	493 Control Systems	6/14/74	
			REVISION DATE
APPROVED BY J. Fregola			PAGE 6-21

TABLE 6-7 ACS MANPOWER COSTS

TASK	COST, $K														
	Non-Recur			Recurring			1st Spacecraft			Subsequent Spacecraft					
	ACS Config			ACS Config.			ACS Config.			Standard ACS Conf.			Demo ACS Conf.		
	1	2	3	1	2	3	1	2	3	1	2	3	1	2	3
Design ACS to satisfy mission spectrum	320	400	500				320	400	500						
Procure components for qualification	64	80	100				64	80	100						
Test components at vendor	32	40	50				32	40	50						
Support qualification tests on spacecraft	64	80	100				64	80	100						
Procure components for flight spacecraft				160	200	250	160	200	250	160	200	250	160	200	250
Perform acceptance tests on components at vendor				80	100	125	80	100	125	80	100	125	80	100	125
Integrate components into ACS module & test				54	67	84	54	67	84	54	67	84	54	67	84
Support system tests on spacecraft				80	100	125	80	100	125	80	100	125	80	100	125
Support flight (2 Yr operations (Demo				192 8	240 10	300 13	192	240	300	192	240	300	8	10	13
TOTALS							1046	1307	1634	566	707	884	[illegible]	[illegible]	[illegible]

TITLE ACS/CPF TRADEOFF

TRADE STUDY REPORT NO. 6

WBS NUMBER 1.2.1.2.5

TABLE 6-8 SUMMARY OF ACS HARDWARE AND MANPOWER COSTS

Category	COST, $M								
	1st Spacecraft			Subsequent Spacecraft					
				Standard			Demonstration		
	ACS Config.			ACS Config.			ACS Config.		
	1	2	3	1	2	3	1	2	3
Hardware	1.054	1.455	2.329	0.684	0.805	1.219	0.684	0.805	1.219
Manpower	1.046	1.307	1.634	0.566	0.707	0.884	0.382	0.477	0.596
Total	2.100	2.762	3.963	1.250	1.512	2.103	1.066	1.282	1.815
Refurbishment				0.250	0.302	0.421			

NOTES: (1) Cost of refurbishing spacecraft:

20% of total for subsequent standard spacecraft

PREPARED BY	GROUP NUMBER & NAME	DATE	CHANGE LETTER
G. A. Zetkov	493 Control Systems	6/14/74	
			REVISION DATE
APPROVED BY J. Fragola			PAGE 6-23

TABLE 6-9 NUMBER AND TYPE OF SPACECRAFT IN THE THREE TYPES OF PROGRAMS

PROGRAM	NUMBER OF SPACECRAFT				
	DEVELOPMENT PHASE			OPERATIONS PHASE	
	TYPE OF SPACECRAFT			TYPE OF SPACECRAFT	
	STANDARD	DEMO	REFURB.	STANDARD	REFURB.
1 (LOW-COST)	1	0	0	2	1
2 (BASELINE)	1	1	1	3	1
3 (EXPANDED CAPABILITIES)	2	1	1	4	2

TRADE STUDY REPORT

TITLE	TRADE STUDY REPORT NO. 6
ACS/CPF TRADEOFF	WBS NUMBER 1.2.1.2.5

TABLE 6-10 ACS PROGRAM COSTS, $M, HARDWARE PLUS MANPOWER

LOW-COST PROGRAM

PHASE	TYPE SPACECRAFT	NO. OF S/C	ACS CONFIGURATION 1 PER S/C	1 AMT	2 PER S/C	2 AMT	3 PER S/C	3 AMT
DEVELOPMENT	1st SPACECRAFT	1	2.100	2.100	2.762	2.762	3.963	3.963
	SUBSEQUENT STANDARD	0	1.250	0	1.512	0	2.103	0
	DEMONSTRATION	0	1.066	0	1.282	0	1.815	0
	REFURBISHMENT	0	0.250	0	0.302	0	0.421	0
	TOTALS			2.100		2.762		3.963
OPERATIONS	SUBSEQUENT STANDARD	2	1.250	2.500	1.512	3.024	2.103	4.206
	REFURBISHMENT	1	0.250	0.250	0.302	0.302	0.421	0.421
	TOTALS			2.750		3.326		4.627
DEVELOPMENT PLUS OPERATIONS	TOTALS			4.85		6.088		8.590

BASELINE PROGRAM

PHASE	TYPE SPACECRAFT	NO. OF S/C	ACS CONFIGURATION 1 PER S/C	1 AMT	2 PER S/C	2 AMT	3 PER S/C	3 AMT
DEVELOPMENT	1st SPACECRAFT	1	2.100	2.100	2.762	2.762	3.963	3.963
	SUBSEQUENT STANDARD	0	1.250	0	1.512	0	2.103	0
	DEMONSTRATION	1	1.066	1.066	[illegible]	1.282	1.815	1.815
	REFURBISHMENT	1	0.250	0.250	0.302	0.302	0.421	0.421
	TOTALS			3.416		4.340		6.199
OPERATIONS	SUBSEQUENT STANDARD	3	1.250	3.750	1.512	4.536	2.103	6.309
	REFURBISHMENT	1	0.250	0.250	0.302	0.302	0.421	0.421
	TOTALS			4.000		4.838		6.730
DEVELOPMENT PLUS OPERATIONS	TOTALS			7.416		9.184		12.929

EXPANDED CAPABILITIES PROGRAM

PHASE	TYPE SPACECRAFT	NO. OF S/C	ACS CONFIGURATION 1 PER S/C	1 AMT	2 PER S/C	2 AMT	3 PER S/C	3 AMT
DEVELOPMENT	1st SPACECRAFT	1	2.100	2.100	2.762	2.762	3.963	3.963
	SUBSEQUENT STANDARD	1	1.250	1.250	1.512	1.512	2.103	2.103
	DEMONSTRATION	1	1.066	1.066	1.282	1.282	1.815	1.815
	REFURBISHMENT	1	0.250	0.250	0.302	0.302	0.421	0.421
	TOTALS			4.666		5.858		8.302
OPERATIONS	SUBSEQUENT STANDARD	4	1.250	5.000	1.512	6.048	2.103	8.412
	REFURBISHMENT	2	0.250	0.500	0.302	0.604	0.421	0.842
	TOTALS			5.500		6.652		9.254
DEVELOPMENT PLUS OPERATIONS	TOTALS			10.166		12.510		17.556

PREPARED BY	GROUP NUMBER & NAME	DATE	CHANGE LETTER
G. A. Zetkov	493 Control Systems	6/14/74	
			REVISION DATE
APPROVED BY			PAGE OF
J. Fragola			

TABLE 6-11 ACS COMPONENT WEIGHTS

COMPONENT	WEIGHT, LB		
	ACS CONFIGURATION		
	1	2	3
Coarse Sunsensor	0.156	0.156	0.156
Digital Sunsensor	5	5	5
Rate Gyro Assy (3 gyros & electronics)	7.25 (LG100 Bendix)	15 (64 RIG Bendix)	15 (64 RIG Bendix)
Earthsensor (static)	45	—	—
Fixed-head Startracker (incl. electr.)	—	17	—
Gimbaled Startracker (incl. electr.)	—	—	50.1
Magnetometer	6.5	6.5	6.5
Signal Conditioner/ Analog Processor	—	8	8
Reactionwheel/Driver (3 wheels, Size 1)	(10 x 3 = 30) /-	(10 x 3 = 30) /4	(10 x 3 = 30 /4
Magnetic Bars/Driver (3 bars, Size 1)	10.2 x 3/ -	10.2 x 3/5.75	10.2 x 3/5.75
Jet Driver (4 75-lb 8 1-lb 8 0.1-lb)	—	4	4
Signal Conditioner/ Multiplexer/Decoder Assy	-/0.5/1.0	5/0.5/1.0	5/0.5/1.0
Electronics Assy(1)	13	—	—

NOTES: (1) Electronic Assy Includes

(1) Analog processor & conditioning of signals into analog processor
(2) Drivers for reactionwheels, magnetic bars, and jets
(3) Signal conditioning for signals into multiplexer and for signals out of decoder

TITLE	TRADE STUDY REPORT NO.	WBS NUMBER
ACS/CPF TRADEOFF	6	1.2.1.2.5

TABLE 6-12 ACS COMPONENT & SYSTEM WEIGHTS

COMPONENT	ACS CONFIGURATION 1			ACS CONFIGURATION 2			ACS CONFIGURATION 3		
	NO/ SPACECR	WEIGHT EA, LB	TOTAL WT.LB	NO/ SPACECR	WEIGHT EA, LB	TOTAL WT.LB	NO/ SPACECR	WEIGHT EA, LB	TOTAL WT.LB
Coarse Sunsensor	2	0.156	0.312	2	0.156	0.312	2	0.156	0.312
Digital Sunsensor	1	5	5	1	5	5	1	5	5
Rate Gyro Assy (3 gyros & electr.)	1	7.25	7.25	1	15	15	1	15	15
Earthsensor (static)	1	45	45	0	—	—	0	—	—
Fixed-head Startracker	0	—	—	2	17	34	0	—	—
Gimbaled Startracker	0	—	—	0	—	—	1	50.1	50.1
Magnetometer	1	6.5	6.5	1	6.5	6.5	1	6.5	6.5
Signal Conditioner/ Analog Processor	0	—	—	1	8	8	1	8	8
Reaction Wheel/Driver Assy (3 wheels)	1	30	30	1	34	34	1	34	34
Magnetic Bars/Driver Assy (3 bars)	1	30.6	30.6	1	36.35	36.35	1	36.35	36.35
Jet Driver Assy (4 75-lb, 8 1-lb, 8 0.1-lb)	0	—	—	1	4	4	1	4	4
Signal Conditioner/ MUX/Decoder Assy	1	1.5	1.5	1	6.5	6.5	1	6.5	6.5
Electronics Assy(1)	1	13.0	13.0	0	—	—	0	—	—
TOTALS			139.162			149.662			165.762

(1) Electronics Assy includes
- (1) Analog processor & conditioning of signals into analog processor
- (2) Drivers for reaction wheels, magnetic bars and jets
- (3) Signal conditioning for signals into multiplexer and for signals out of decoder

PREPARED BY	GROUP NUMBER & NAME	DATE	CHANGE LETTER
G. A. Zetkov	493 Control Systems	6/24/74	
			REVISION DATE
APPROVED BY J. Fragola			PAGE 6-27

TABLE 6-13

RANGE OF ATTITUDE AND ATTITUDE RATE ERRORS*

	EXPANDED CAPABILITY	BASELINE	LOST COST	DEGRADED
1. Rate Err. Over 30 Min. $\dot{\sigma}_{30}$ $\mu r/_s$, 1σ	3.5×10^{-3}	17.4×10^{-3}	87.2×10^{-3}	436×10^{-3}
2. Static Attitude Error σ_{ST} μradian, 1σ	35	174	872	4360
3. Jitter Over 30 Sec; $\sigma_{0.5/30}$ Expressed as μrad/sec, 1σ	32×10^{-3}	162×10^{-3}	808×10^{-3}	4.05

*Note that there is an approximate inverse square-root relationship between the one-sigma rate errors and the time intervals over which the measurements are defined. We will assume and use this relationship later to interpolate between 30 seconds and 30 minutes. The 30 second value will be assumed for intervals shorter than 30 seconds.

TITLE

ACS/CPF TRADEOFF

TRADE STUDY REPORT NO. 6

WBS NUMBER 1.2.1.2.5

TABLE 6-14

SUMMARY OF DISPLACEMENTS

IN PICTURE ELEMENTS FOR THE FOUR

ASSUMED CASES (ALL VALUES, ONE SIGMA)

SYSTEM	STATIC ERROR PIXELS	MAXIMUM ERROR OVER ONE SCENE, PIXELS (T = 30 SECONDS)	MAXIMUM ERROR OVER ONE PASS, PIXELS (T = 400 SECONDS)
Expanded Capability	1.37	0.03	0.095
Baseline	5.65	0.15	0.475
Low Cost	28	0.78	2.38
Degraded	140	4.0	12

PREPARED BY L. Palmer (CSC) | GROUP NUMBER & NAME | DATE 6/26/74 | CHANGE LETTER

REVISION DATE

APPROVED BY J. Fragola

GAC 3711 3-72

TABLE 6-15

SUMMARY OF PROCESSING STEPS AND ESTIMATES OF MACHINE OPERATIONS TO PERFORM EACH STEP

TYPE OF PROCESSING	DESCRIPTION OF OPERATION	BASIC UNIT THAT DETERMINES PROCESSING LOAD	MULTIPLICATIVE FACTOR*	MACHINE OPERATIONS PER BASIC UNIT**
I	Radiometric Correction Line Stretching	Each Pixel, Npix	6.25 1	1. 2.
II	Calculation of Re-Sampling Grid	N_{GP} (number of grid points)	- (grid is used for all bands in one scene)	6×10^4 opns w/o ACS Data 10^5 opns w/ACS Data
	Coordinate Computation for Resampling	Npix	1.0	2.0
	Actual Resampling Including Interpolation • Nearest Neighbor • Bilinear • Cubic Convolution	Npix	6.25	 8 25 60
III	Ground Control Point Location	N_{GCP} (Number of Control Points)	-points used for all bands in one scene	†

*Multiplicative Factor = 1 if computation is common for all bands; = 6.25 if the computation is different for each band.

**"Operation" defined as integer add.

† Assume sequential similarity detection (SSDA) so that number of operations is $10 \left[1 + 10 (M/32)^{\frac{1}{2}} \right] \left[L - M + 1 \right]^2$ where L is size of search area in pixels and M is the size of the GCP in pixels.

TABLE 6-16

TOTAL OPERATIONS/SCENE

FOR GP APPROACH

		NO ACS DATA			WITH ACS DATA		
		NN	BI	CC	NN	BI	CC
EXPANDED CAPABILITY	I	4.3×10^{8}	4.3×10^{8}	4.3×10^{8}	4.3×10^{8}	4.3×10^{8}	4.3×10^{8}
	II	2.7×10^{9}	8.4×10^{9}	2.0×10^{10}	2.7×10^{9}	8.4×10^{9}	2.0×10^{10}
	III	3.2×10^{5}	3.2×10^{5}	3.2×10^{5}	1.8×10^{4}	1.8×10^{4}	1.8×10^{4}
	TOTAL	3.1×10^{9}	3.6×10^{9}	2.0×10^{10}	3.1×10^{9}	8.8×10^{9}	2.0×10^{10}
BASELINE	I	4.3×10^{8}	4.3×10^{8}	4.3×10^{8}	4.3×10^{8}	4.3×10^{8}	4.3×10^{8}
	II	2.7×10^{9}	8.4×10^{9}	2.0×10^{10}	2.7×10^{9}	8.4×10^{9}	2.0×10^{10}
	III	6.2×10^{6}	6.2×10^{6}	6.2×10^{6}	1.0×10^{6}	1.0×10^{6}	1.0×10^{6}
	TOTAL	3.1×10^{9}	3.8×10^{9}	2.0×10^{10}	3.1×10^{9}	8.8×10^{9}	2.0×10^{10}
LOW COST	I	4.3×10^{8}	4.3×10^{8}	4.3×10^{8}	4.3×10^{8}	4.3×10^{8}	4.3×10^{8}
	II	2.7×10^{9}	8.4×10^{9}	2.0×10^{10}	2.7×10^{9}	8.4×10^{9}	2.0×10^{10}
	III	3.6×10^{8}	3.6×10^{8}	3.6×10^{8}	4.8×10^{7}	4.8×10^{7}	4.8×10^{7}
	TOTAL	3.5×10^{9}	9.2×10^{9}	2.1×10^{10}	3.2×10^{9}	8.9×10^{9}	2.0×10^{10}
DEGRADED	I	4.3×10^{8}	4.3×10^{8}	4.3×10^{8}	4.3×10^{8}	4.3×10^{8}	4.3×10^{8}
	II	2.7×10^{9}	8.4×10^{9}	2.0×10^{10}	2.7×10^{9}	8.4×10^{9}	2.0×10^{10}
	III	2.3×10^{10}	2.3×10^{10}	2.3×10^{10}	3.3×10^{9}	3.3×10^{9}	3.3×10^{9}
	TOTAL	2.6×10^{10}	3.2×10^{10}	4.3×10^{10}	6.4×10^{9}	1.2×10^{10}	2.3×10^{10}

NN = Nearest Neighbor Interpolation

BI = Bilinear Interpolation

CC = Cubic Convolution

TABLE 6-17

ASSUMED COST OF SP PROCESSORS FOR

TYPE I AND TYPE II PROCESSING

	DEGRADED/LOW COST 20 SCENES/DAY	BASELINE 90 SCENES/DAY	EXP. CAPABILITY 400 SCENES/DAY
Assumed cost of Type I processor	$500,000	$700,000	$2.0M
Cost per scene over 5 years	$13.60	$4.26	$2.73
Assumed cost of Type II processor (Bilinear Interpolation Assumed)	$1.0 M	$2.0 M	$6.0 M
Cost per scene over 5 years	$27.20	$13.00	$8.20
Total Cost/Scene (Type I & Type II)	$40.80	$17.26	$11.00

TABLE 6-18 PROCESSING REQUIREMENTS AS A FUNCTION OF PROGRAM PHASE AND SIZE

PHASE	PROGRAM	YEARS OF OPERATIONS	INSTRUMENTS	DATA OPTION	SCENES/DAY
Development	1 (low-cost)	2	TM, HRPI	A	TM 10 HRPI 10
	2 (baseline)	2	TM, HRPI	A	"
		2	TM, HRPI, WBVTR	B	TM 45 HRPI 45
	3 (expanded) (capabilities)	4	TM, HRPI, WBVTR	B	"
Operations	1 (low-cost	6	TM, HRPI	A	TM 10 HRPI 10
	2 (baseline)	6	TM, HRPI, WBVTR	B	TM 45 HRPI 45
	3 (expanded capabilities)	8(1)	TM, HRPI, TDRS	C	TM 100 HRPI 100

NOTES:

(1) The SAR was counted as a data option C. Spacecraft No. 4A with SAR operates simultaneously with spacecraft No. 3B for 1 year, and simultaneously with spacecraft No. 1B for 1 year.

TABLE 6-19

TM COST PER SCENE, USING THE GENERAL PURPOSE COMPUTER APPROACH

ACS CONFIGURATION	TYPE PROC.	COST PER SCENE $					
		Without ACS Data			With ACS Data		
		N/N	BL	C/C	N/N	BL	C/C
3 - (Expanded Capabilities)	I	4.3	4.3	4.3	4.3	4.3	4.3
	II	27.0	84.0	200.0	27.0	84.0	200.0
	III	0.0032	0.0032	0.0032	0.0002	0.0002	0.0002
	TOTAL	31.3	88.3	204.3	31.3	88.3	204.3
2 (Baseline)	I	4.3	4.3	4.3	4.3	4.3	4.3
	II	27.0	84.0	200.0	27.0	84.0	200.0
	III	0.062	0.062	0.062	0.01	0.01	0.01
	TOTAL	31.3	88.4	204.4	31.3	88.3	204.3
1 (Low Cost)	I	4.3	4.3	4.3	4.3	4.3	4.3
	II	27.0	84.0	200.0	27.0	84.0	200.0
	III	3.6	3.6	3.6	0.5	0.5	0.5
	TOTAL	34.9	91.9	207.9	31.8	88.8	204.8
0 (Degraded)	I	4.3	4.3	4.3	4.3	4.3	4.3
	II	27.0	84.0	200.0	27.0	84.0	200.0
	III	230.0	230.0	230.0	33.0	33.0	33.0
	TOTAL	261.3	318.3	434.3	64.3	121.3	237.3

NN NEAREST NEIGHBOR
BL BILINEAR
CC CUBIC CONVOLUTION

TABLE 6-20

COST PER PROGRAM, GROUND PROCESSING

PROGRAM		COST PER PROGRAM, $M							
		WITHOUT ACS DATA				WITH ACS DATA			
		ACS Configuration				ACS Configuration			
PHASE	NUMBER	0	1	2	3	0	1	2	3
Development	1 (low-cost)	4.85	0.65	0.58	0.58	1.19	0.59	0.58	0.58
	2 (baseline)	26.67	3.58	3.19	3.19	6.55	3.25	3.19	3.19
	3 (expanded capabilities)	43.64	5.86	5.22	5.22	10.72	5.32	5.22	5.22
Operations	1	14.55	1.95	1.74	1.74	3.57	1.77	1.74	1.74
	2	65.46	8.79	7.83	7.83	16.08	7.98	7.83	7.83
	3	193.93	25.9	23.2	23.2	47.7	23.6	23.2	23.2
Development Plus Operations	1	19.40	2.60	2.32	2.32	4.76	2.36	2.32	2.32
	2	92.13	12.37	11.02	11.02	22.63	11.23	11.02	11.02
	3	237.57	31.76	28.42	28.42	58.42	28.92	28.42	28.42

NOTES:

(1) For nearest neighbor interpolation

(2) Excludes cost of data products (tapes, photos)

TITLE

ACS/CPF TRADEOFF

TABLE 6-21 PROGRAM COSTS, $M, ACS +CPF

PROGRAM PHASE	PROGRAM NUMBER	WITHOUT ACS DATA				WITH ACS DATA			
		ACS CONFIGURATION				ACS CONFIGURATION			
			1	2	3		1	2	3
Development	1 (low-cost)		2.75	3.34	4.54		2.69	3.34	4.54
	2 (baseline)		7.00	7.54	9.39		6.67	7.54	9.39
	3 (exp cap)		10.53	11.08	13.52		9.98	11.08	13.52
Operations	1		4.70	5.07	6.37		4.52	5.07	6.37
	2		12.79	12.67	14.56		11.98	12.67	14.56
	3		31.4	29.85	32.45		29.10	29.85	32.45
Development Plus Operations	1		7.45	8.41	10.91		7.21	8.41	10.91
	2		19.79	20.20	23.95		18.65	20.20	23.95
	3		41.93	40.93	45.98		40.09	40.93	45.98

NOTES: (1) For nearest neighbor interpolation only.

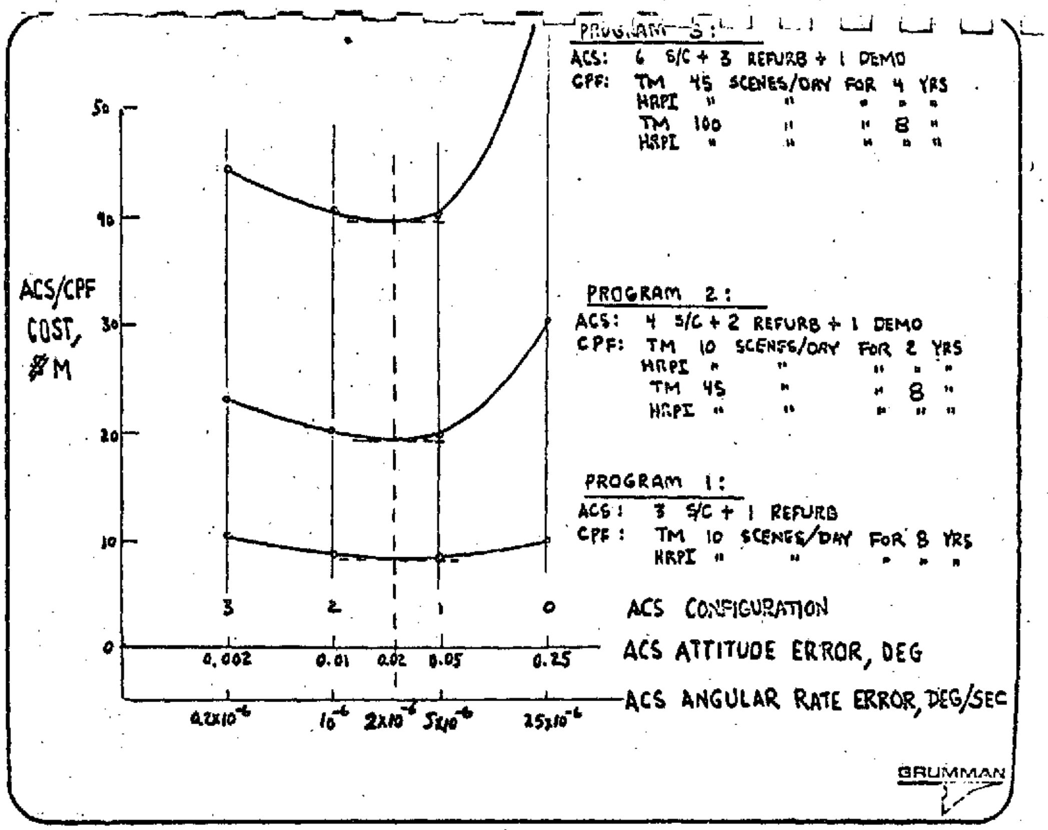

Fig. 6-1 ACS/CPF Cost vs ACS Performance

PREPARED BY: G. ZETKOV 493 CONTROL SYSTEMS 7/1/74 APPROVED BY J. Fragola

GRUMMAN

TRADE STUDY REPORT

TITLE	TRADE STUDY REPORT NO.
ACS/ CPF TRADEOFF	6
	WBS NUMBER 1.2.1.2.5

FIG. 6-2 ACS COSTS VS ACS CONFIGURATION & TYPE OF PROGRAM

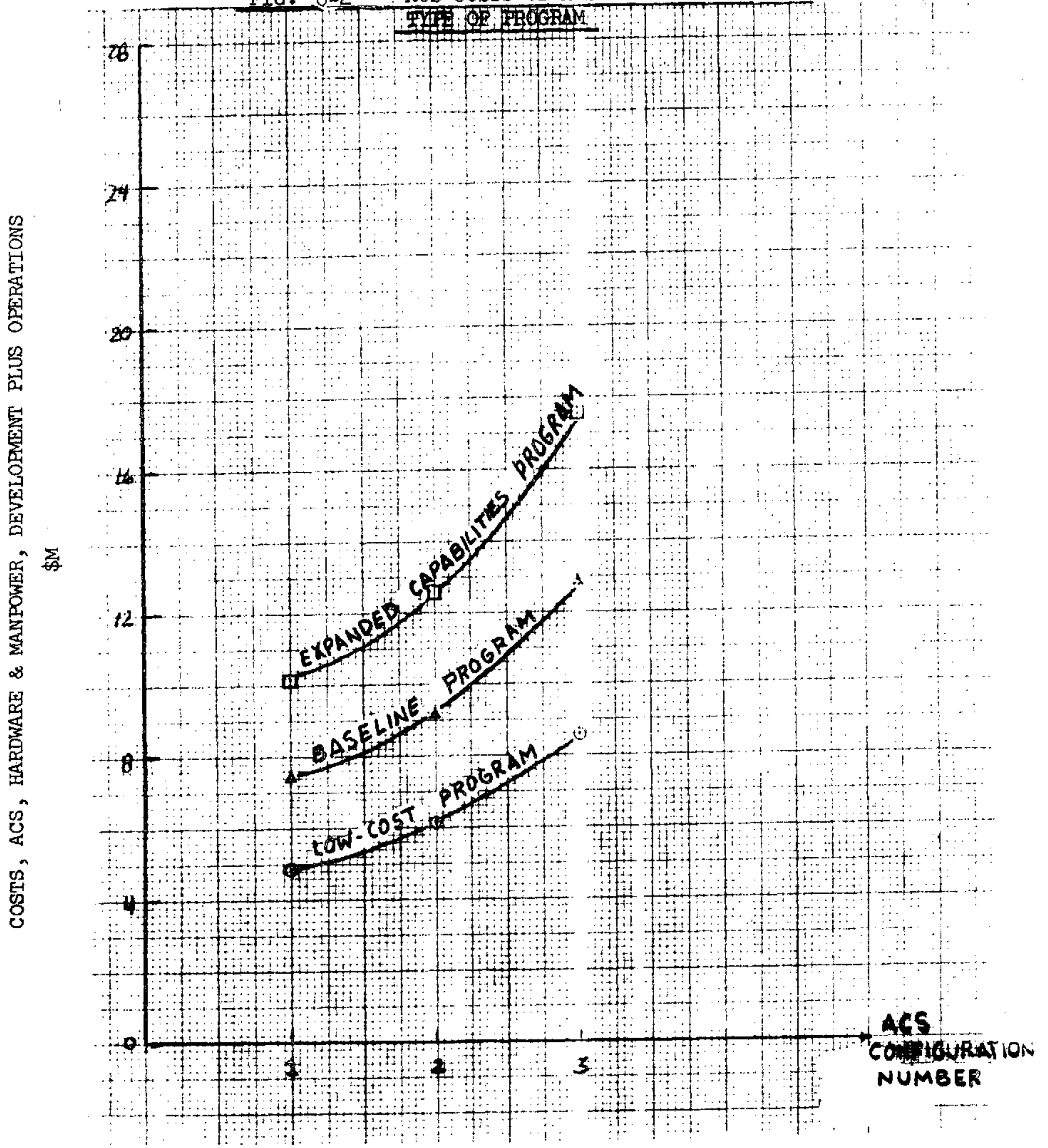

PREPARED BY	GROUP NUMBER & NAME	DATE	CHANGE LETTER
G.A. Zetkov	493 Control Systems	6/14/74	
			REVISION DATE
APPROVED BY J. Fragola			PAGE 6-38

*GAC 3711 3-72

GRUMMAN

TRADE STUDY REPORT

TITLE	TRADE STUDY REPORT NO. 6
ACS/CPF TRADEOFF	WBS NUMBER 1.2.1.2.5

Fig. 6 - 3 ACS COSTS VS ACS WEIGHT & TYPE OF PROGRAM

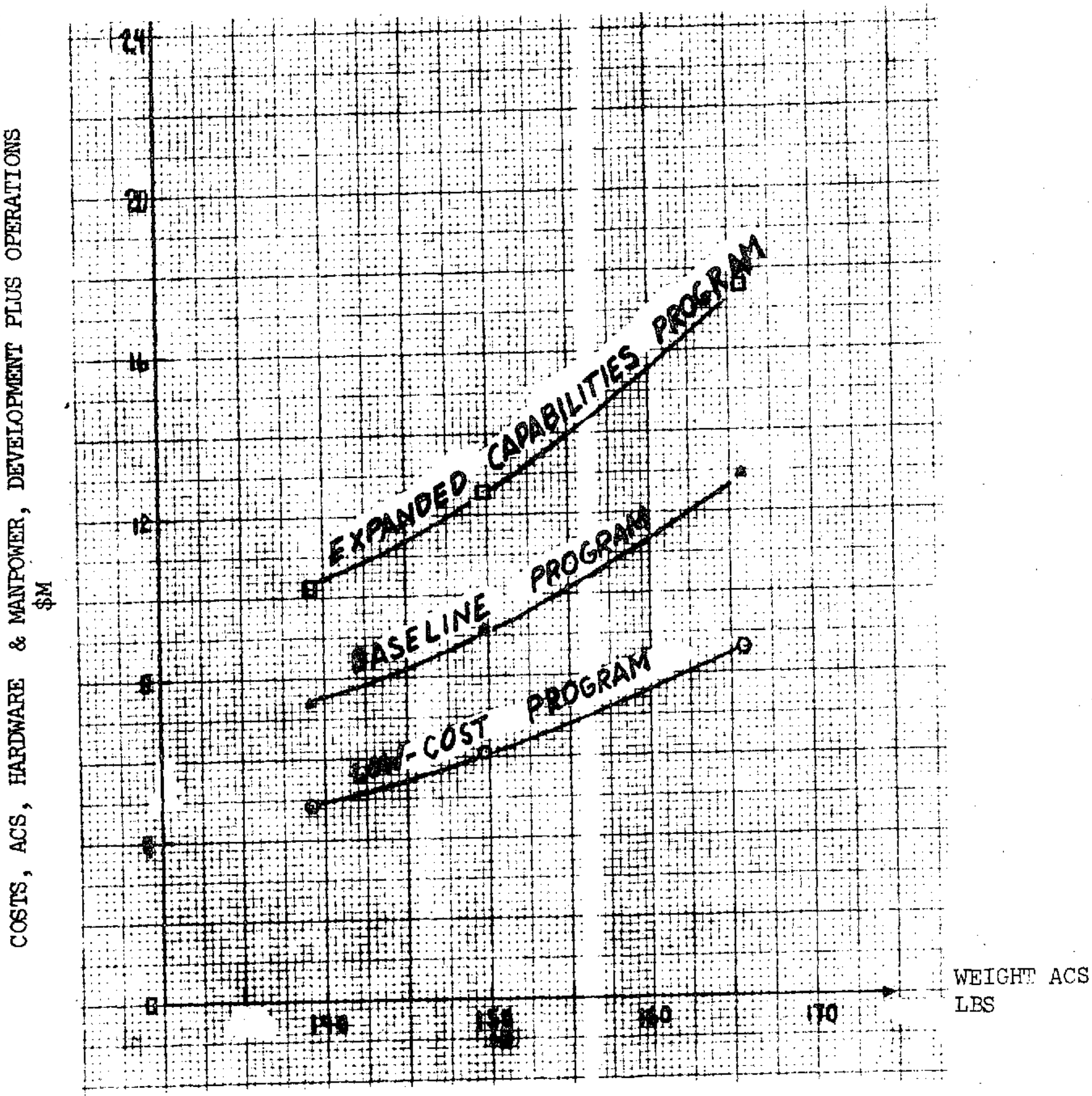

PREPARED BY G. A. Zetkov	GROUP NUMBER & NAME 493 Control Systems	DATE 6/14/74	CHANGE LETTER
			REVISION DATE
APPROVED BY J. Fragola			PAGE 6-39

GAC 3711 3-72

TITLE	TRADE STUDY REPORT NO.
ACS/CPF TRADEOFF	6
	WBS NUMBER 1.2.1.2.5

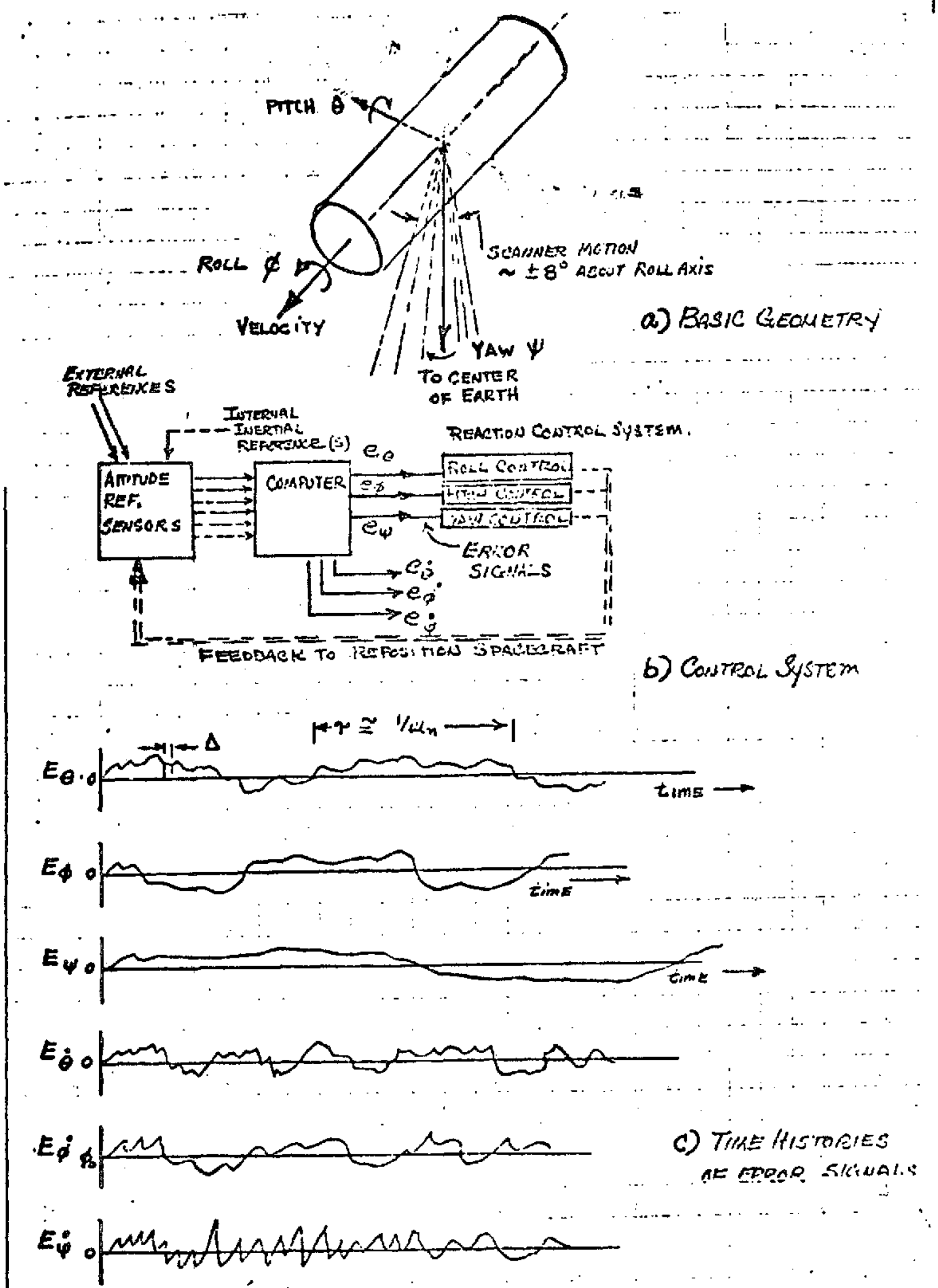

FIGURE 6-4 - DEFINITIONS RELATIVE TO ACS

PREPARED BY	GROUP NUMBER & NAME	DATE	CHANGE LETTER
L. Palmer (CSC)		6/26/74	REVISION DATE
APPROVED BY J. R. Fragola			PAGE 5-40

ORIGINAL PAGE IS OF POOR QUALITY

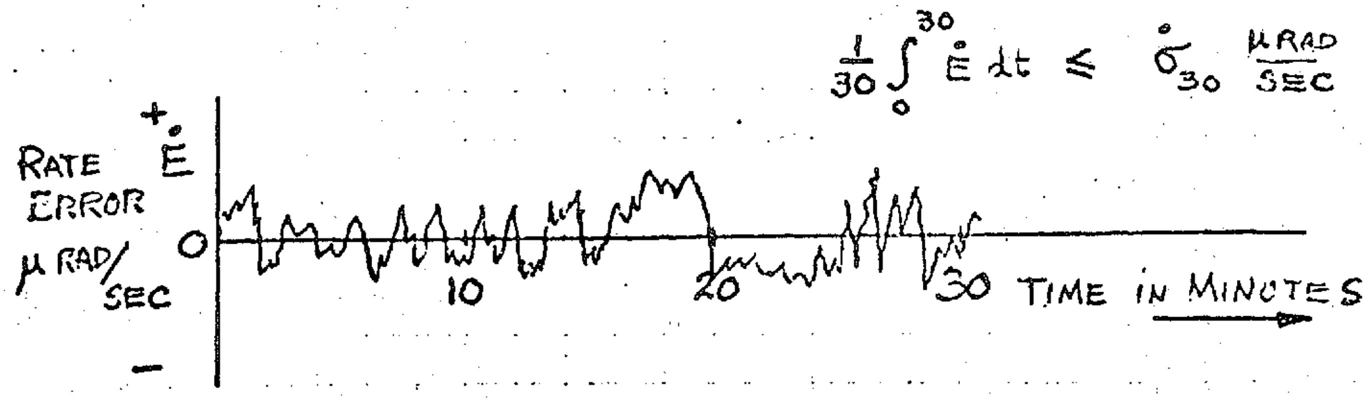

a) RATE ERROR AVERAGED OVER 30 MINUTES.

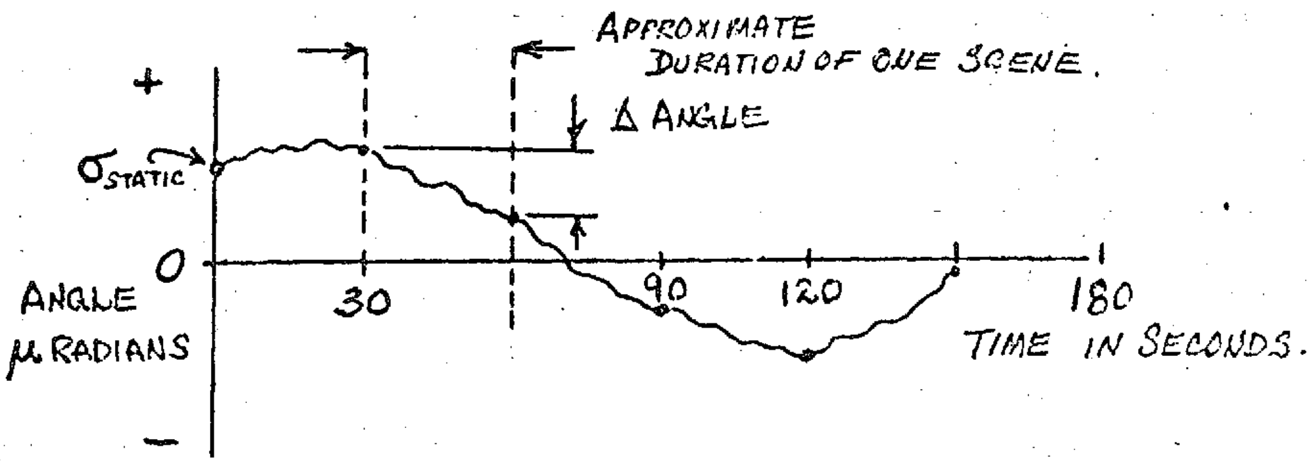

b) ANGULAR JITTER OVER 30 SECONDS.

ORIGINAL PAGE IS
OF POOR QUALITY

FIGURE 6-5 INTERPRETATIONS OF ACS ACCURACY REQUIREMENTS

GRUMMAN AEROSPACE CORPORATION

TRADE STUDY REPORT

TITLE	TRADE STUDY REPORT NO.	WBS NUMBER
ACS/CPF TRADEOFF	6	1.2.1.2.5

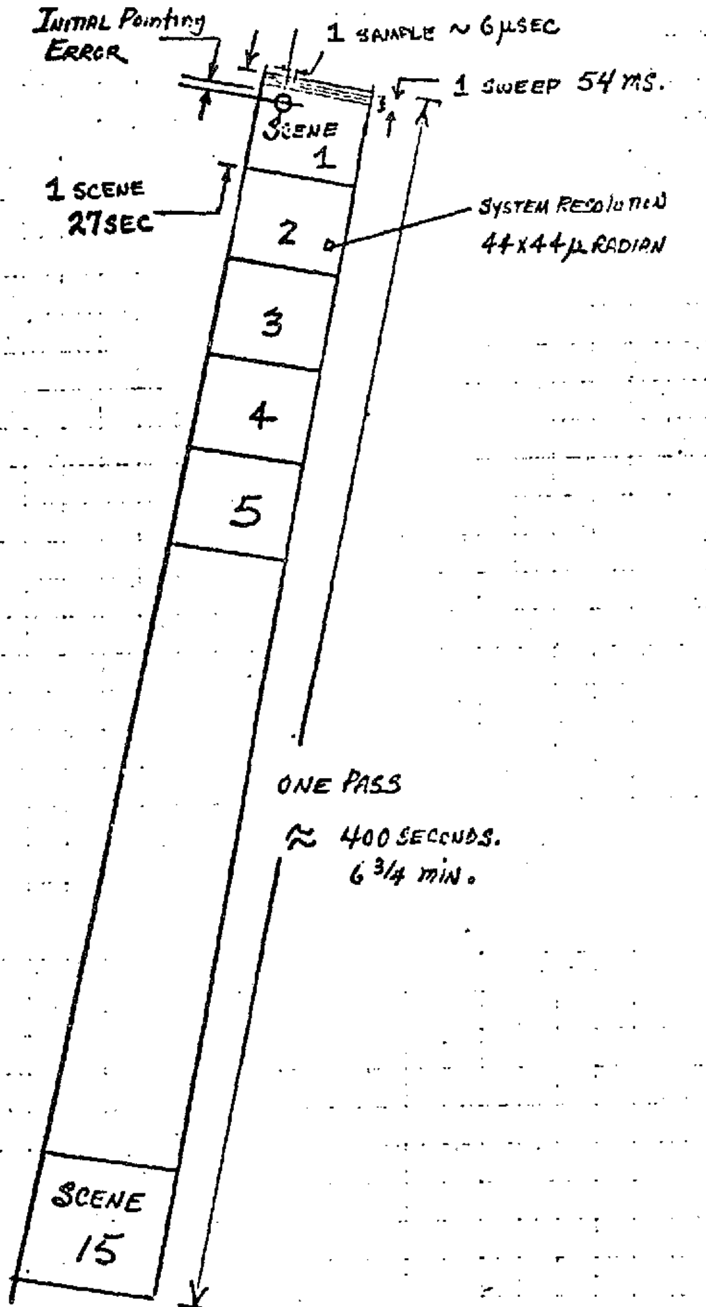

FIGURE 6-6 - TIME INTERVALS OF INTEREST DURING ONE PASS

PREPARED BY	GROUP NUMBER & NAME	DATE	CHANGE LETTER
L. Palmer (CSC)		6/26/74	
			REVISION DATE
APPROVED BY J. R. Fragola			PAGE 6-42

GAC 3711 3-73

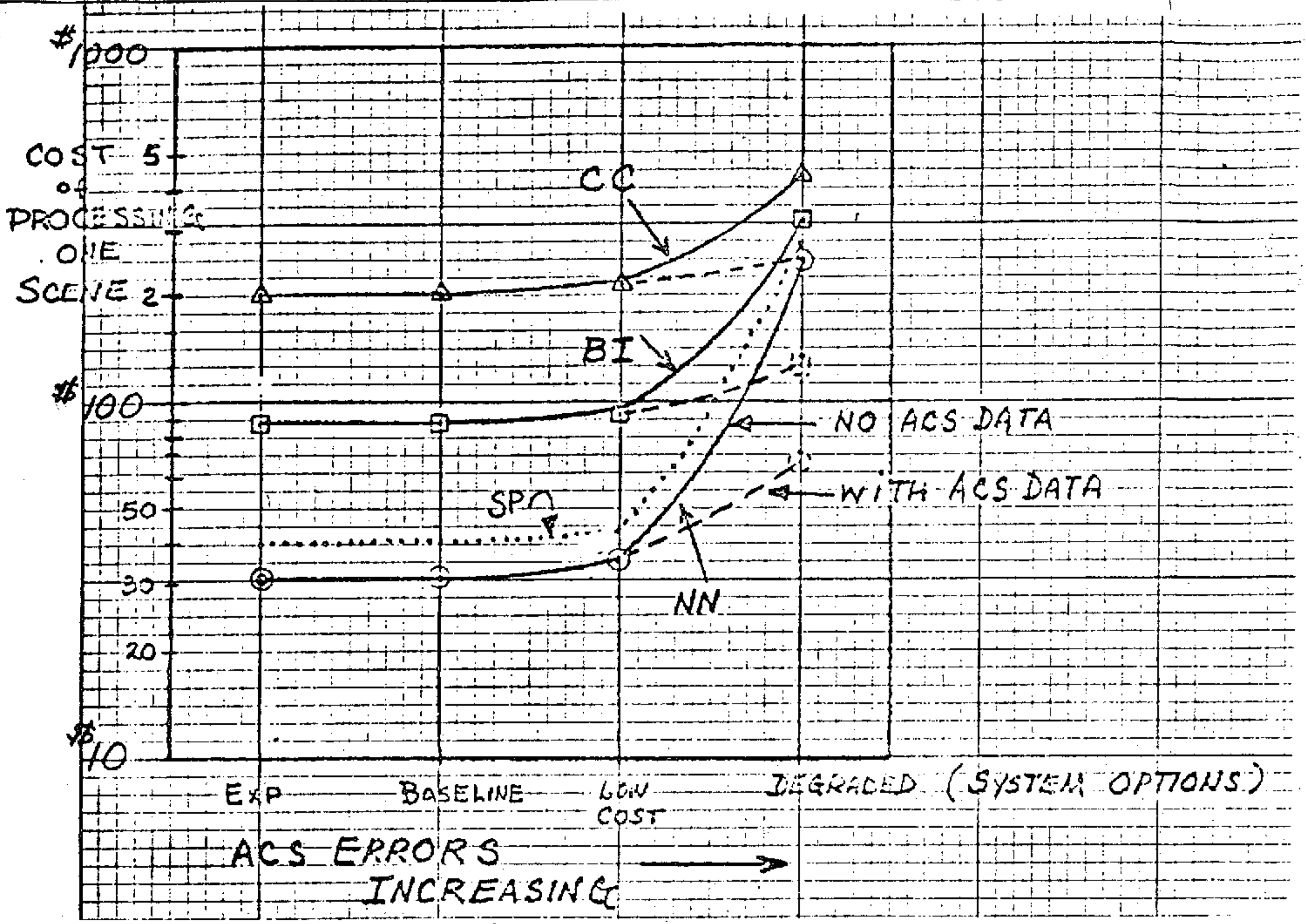

FIGURE 6-7 COST OF PROCESSING ONE TM SCENE VS. ACS ACCURACY - ASSUMES ALL PROCESSING BY GP COMPUTER

TITLE	TRADE STUDY REPORT NO. 6
ACS/CPF TRADEOFF	WBS NUMBER 1.2.1.2.5

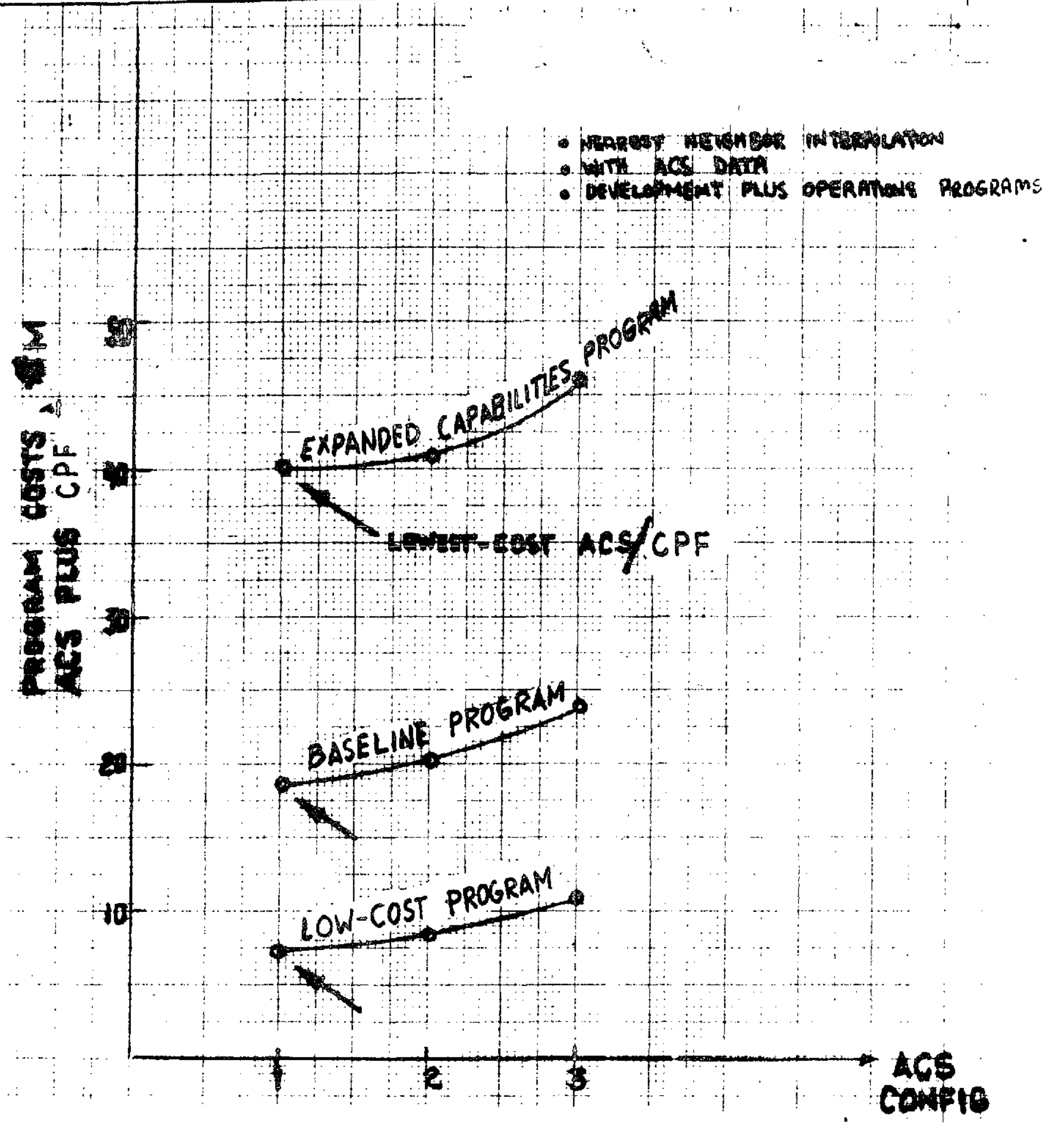

FIGURE 6-8 PROGRAM COSTS, ACS PLUS CPF, VS ACS CONFIGURATION

PREPARED BY	GROUP NUMBER & NAME	DATE	CHANGE LETTER
G. Zetkov	493 Control Systems	6/26/74	
			REVISION DATE
APPROVED BY J. Fragola			PAGE 6-44

GRUMMAN AEROSPACE CORPORATION

TRADE STUDY REPORT

TITLE	TRADE STUDY REPORT NO. 6
ACS/CPF TRADEOFF	WBS NUMBER 1.2.1.2.5

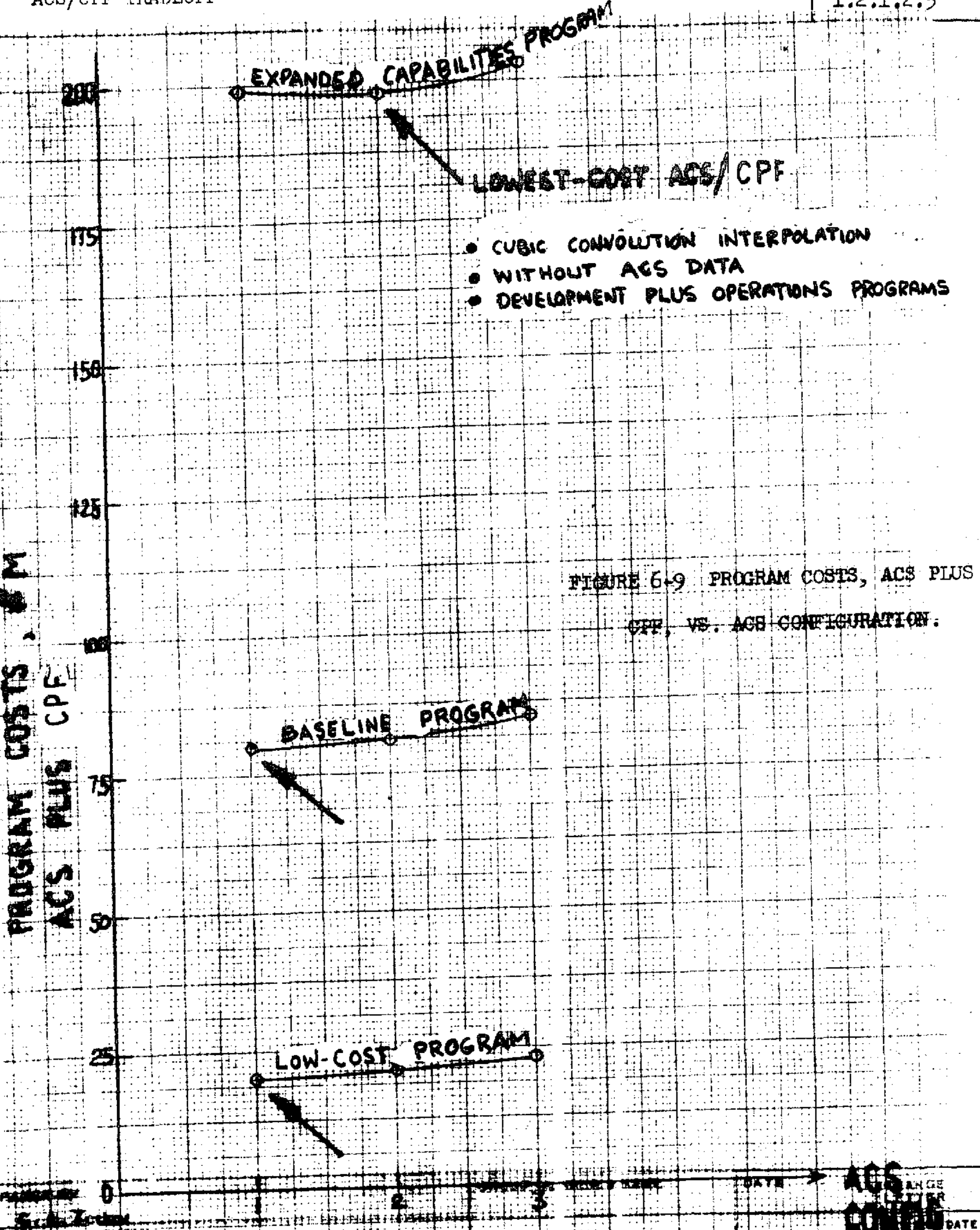

FIGURE 6-9 PROGRAM COSTS, ACS PLUS CPF, VS. ACS CONFIGURATION.

PREPARED BY		DATE	CHANGE LETTER
S. A. Zwerdling			DATE
APPROVED BY J. Fragola			PAGE 6-45

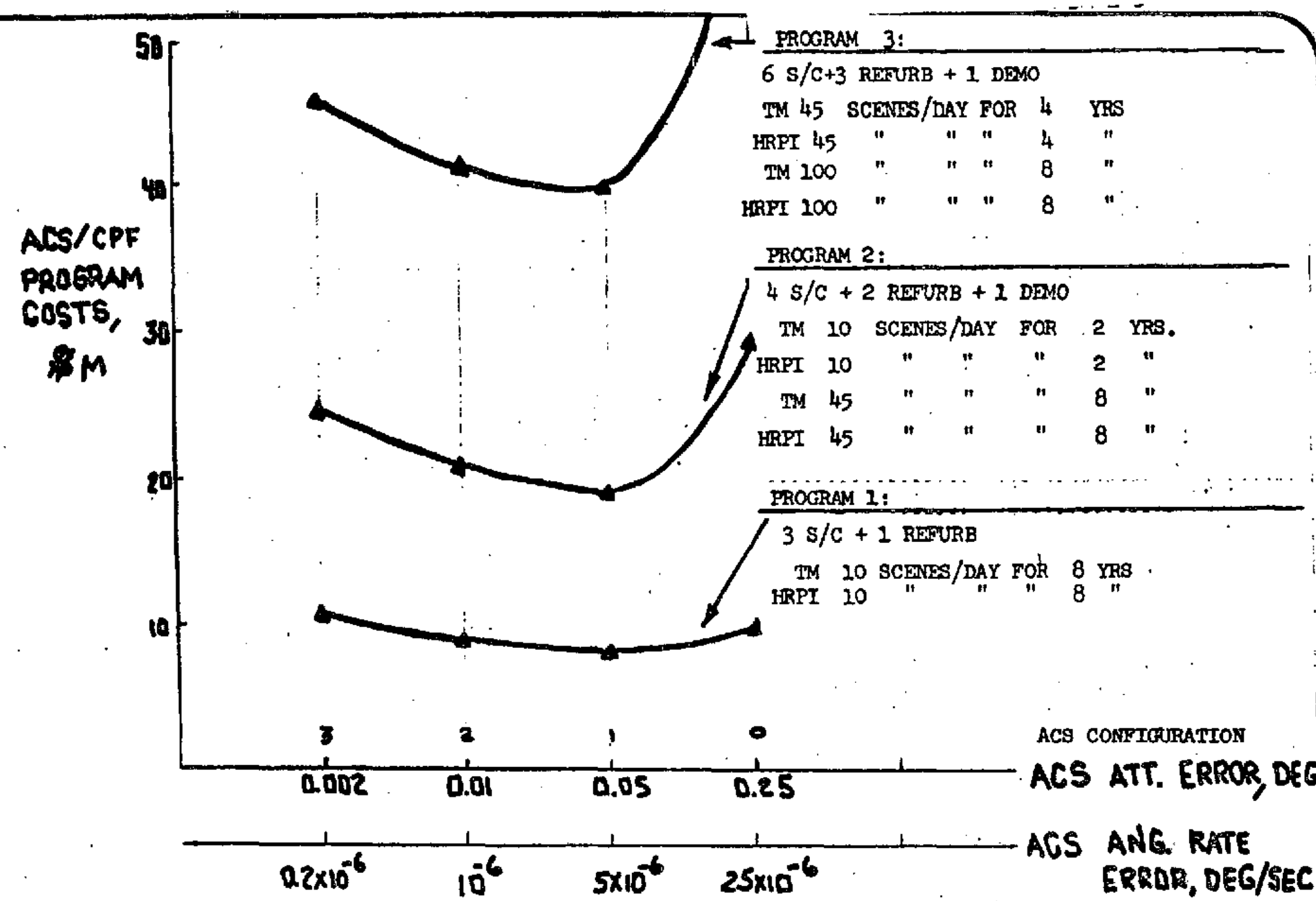

FIGURE 6-10

PROGRAM COST VS ACS PERFORMANCE

GRUMMAN

Prepared by G. A. Zetkov 493 Control Systems Approved by J. Fragola

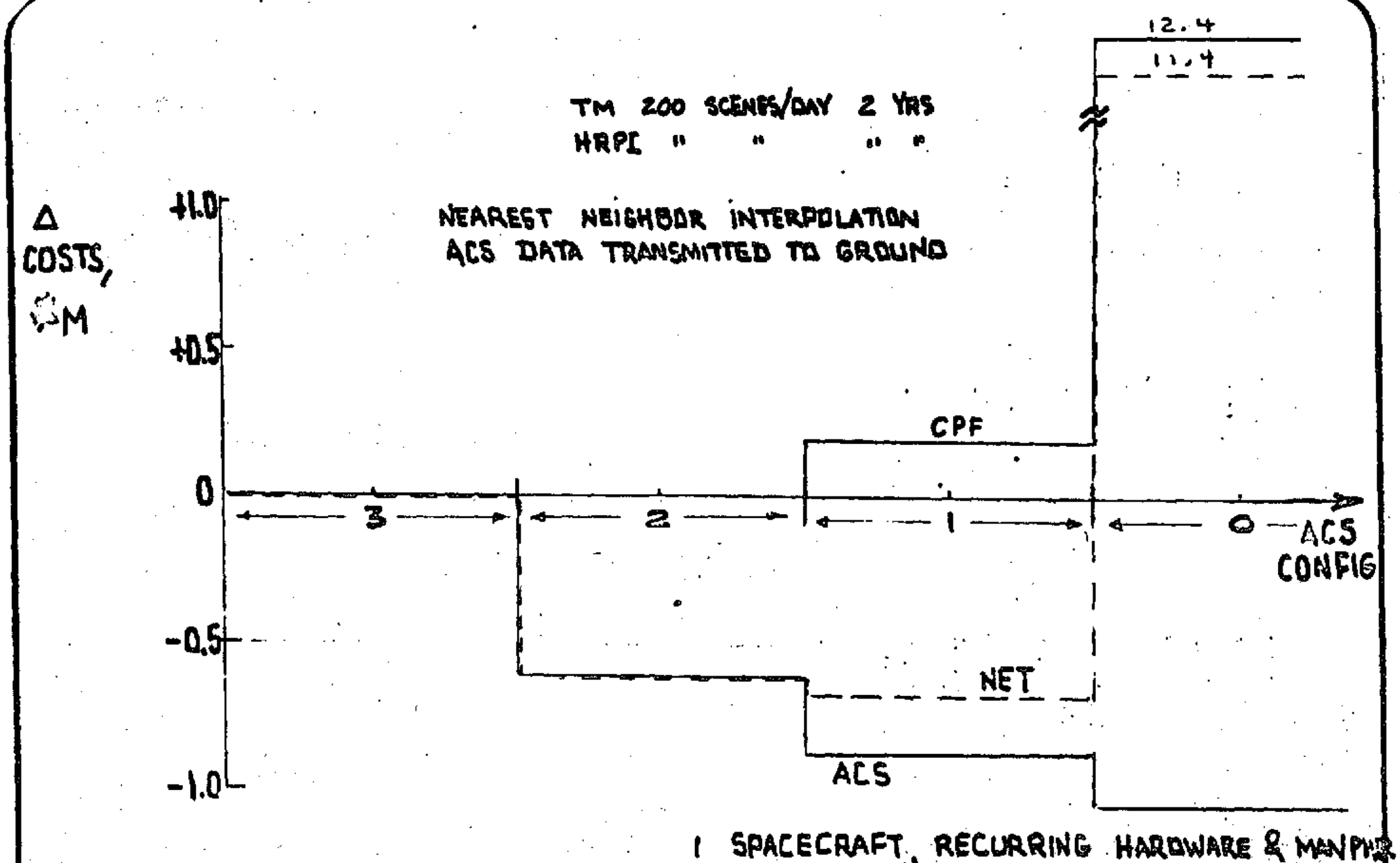

FIGURE 6-11

Δ COSTS VS. ACS CONFIGURATION

GRUMMAN

PREPARED BY G A. ZETKOV 493 CONTROL SYSTEMS 7/16/74 APPROVED BY J. FEAGOLA

TITLE	TRADE STUDY REPORT NO. 6
ACS/CPF TRADEOFF	WBS NUMBER 1.2.1.2.5

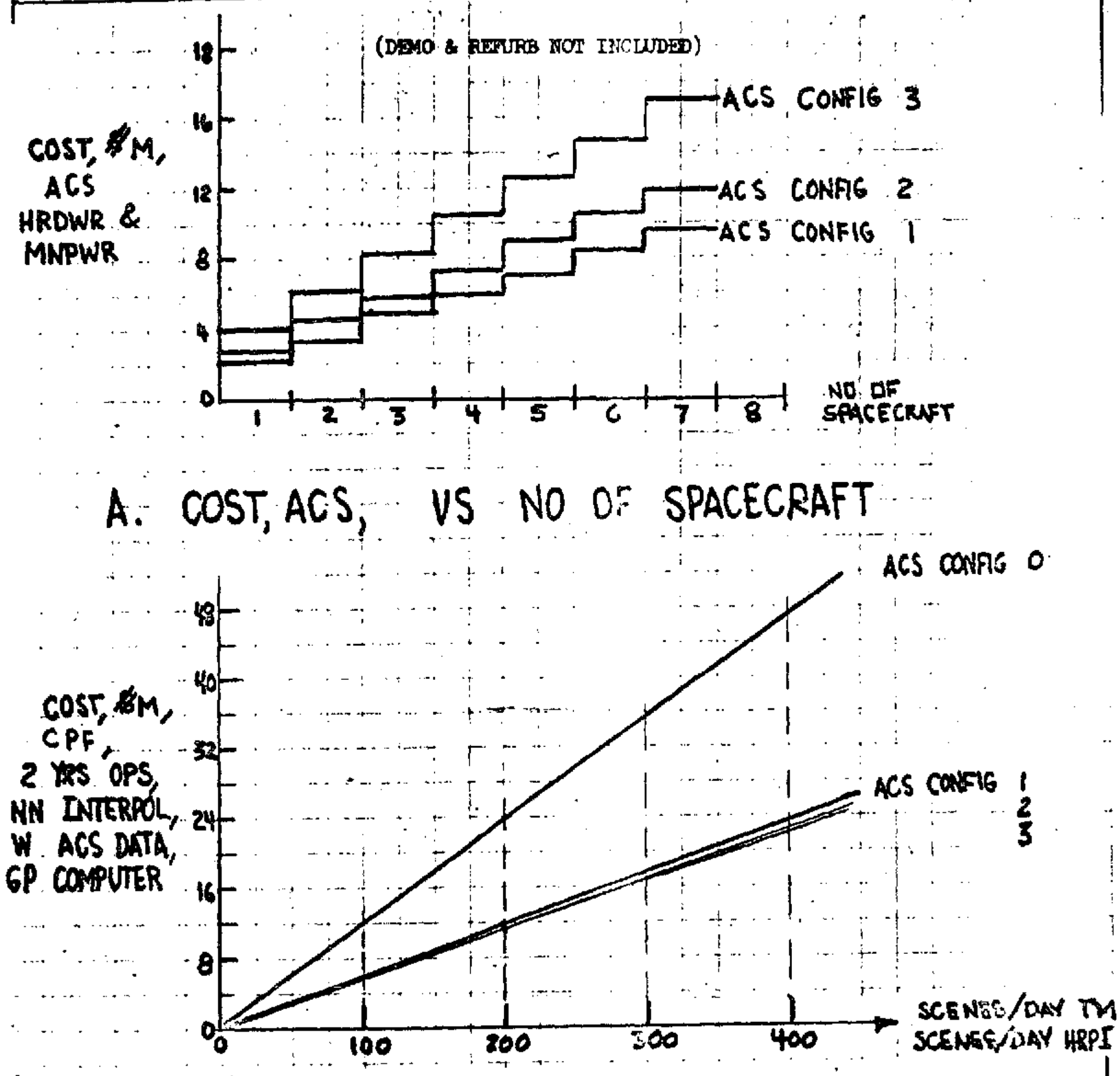

B. COST, CPF VS NO SCENES/DAY

FIGURE 6-12 COST VS SPACECRAFT OR SCENES/DAY

PREPARED BY	GROUP NUMBER & NAME	DATE	CHANGE LETTER
G. Zetkov	493 Control Systems	7/16/74	REVISION DATE
APPROVED BY J. Fragola			PAGE 6-48

TITLE	TRADE STUDY REPORT NO. 6
ACS/CPF TRADEOFF	WBS NUMBER 1.2.1.2.5

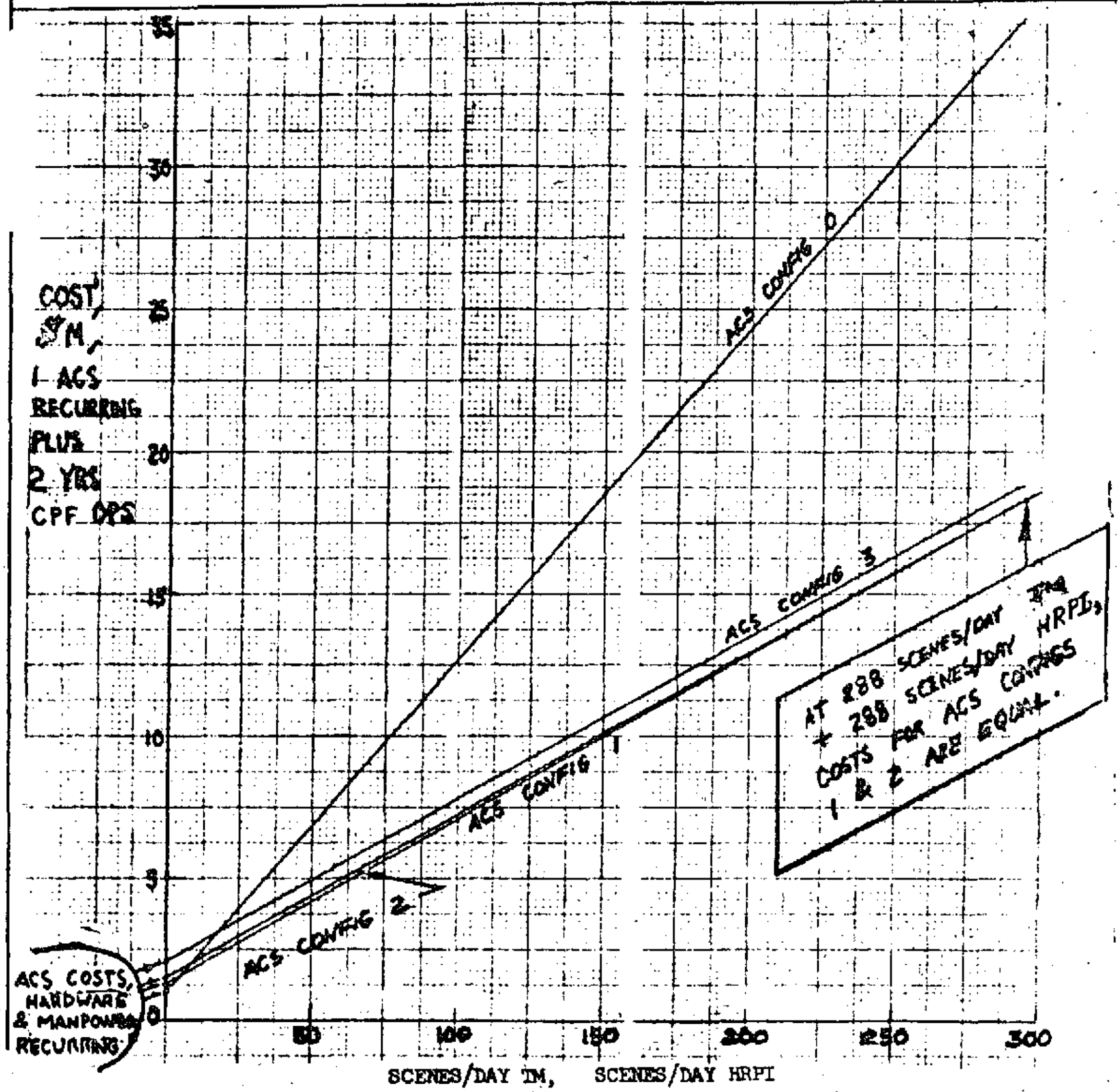

FIGURE 6-13, COST, ACS/CPF, VS SCENES/DAY

PREPARED BY	GROUP NUMBER & NAME	DATE	CHANGE LETTER
G. Zetkov	495 Control Systems	7/16/74	
			REVISION DATE
APPROVED BY J. Fragola			PAGE 6-49

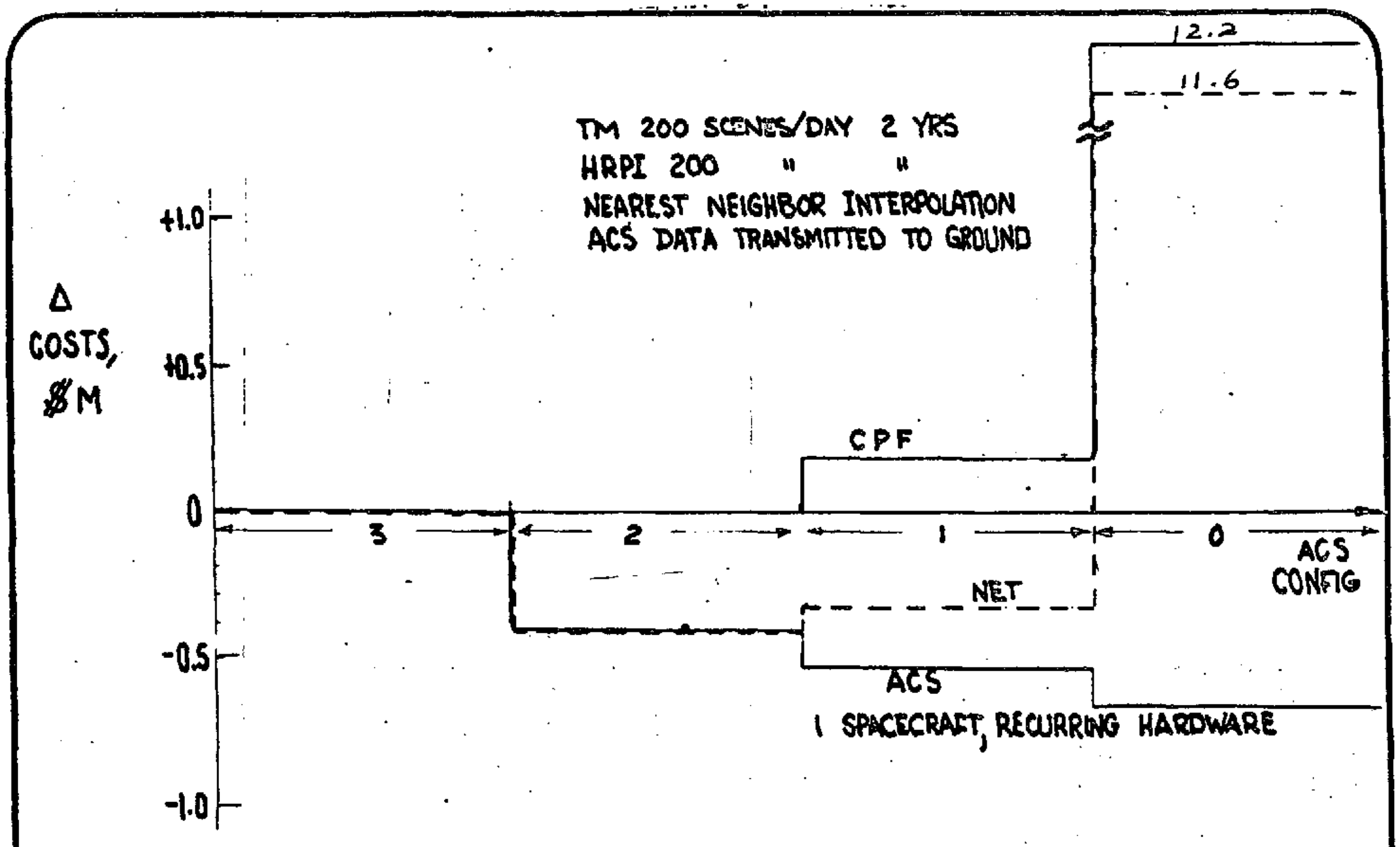

FIG 6-14 Δ COSTS VS. ACS CONFIGURATION

GRUMMAN

PREPARED BY G ZETKOV 493 CONTROL SYSTEMS 7/16/74 APPROVED BY J. FRAGOLA

SYSTEM TRADE

E. 7 SPACECRAFT AUTONOMY/HARDWARE VS SOFTWARE

PURPOSE

The study examines the allocation of system functions among the spacecraft computer, spacecraft hardware and groundbased computers in order to establish a preferred configuration from the points of view of cost, reliability, safety and function. A major incentive for such a study is the rapid advances made in the past few years in the versatility and reliability of space-qualified computers, as demonstrated by the OBP (On-Board Processor) of the OAO satellite, which imply that much of the spacecraft computation burden may be shifted to the spacecraft computer.

SUMMARY

The study considers each candidate function from the point of view of cost, reliability, safety and suitability of function. In general, any function which has a limited number of input parameters and has outputs which are used in the satellite is appropriate for on-board processing. The functional benefit of assigning these processes to the OBP results from the limiting of the number of parameters which require uplink transmission. The limited number makes parameter generation in the ground software simpler and reduces the number of transmission errors to be detected, rejected and retransmitted. The resulting software package, with approximately 23000 words of memory, is larger than the OAO software package, but still well within the 64000 word capability of the AOP (Advanced On-board Processor) design or of the other space-qualified computers considered for the satellite.

CONCLUSIONS & RECOMMENDATIONS

The use of an on-board computer for a large proportion of the EOS system functions can "off-load" the ground operations which were required for earlier programs, with substantial benefits in overall program cost. On-board accounting for time and image location, included in the downlink image data stream, can simplify ground indexing of the data and make the use of low cost ground stations dependent only on receiving the downlinked data.

Reliability of the spacecraft, once a committment to computer control is made, is not particularly affected by the size of the software package; any transfer of functions to software improves system reliability if the alternate approach has a reliability penalty.

Further studies are recommended to search out alternate software development approaches to reduce the cost associated with the EOS software. Basic study areas are:

- o Processor Versatility
- o Software Support System
- o Higher Order Language

Processor versatility refers to the capability of the instruction set of the computer to perform the detailed tasks desired by the programmer. The software sizing of this study is based on the use of the AOP instruction set; modification of the AOP arithmetic logic and test unit may permit significant reductions in the number of instructions (and thus cost of software development) required for some tasks. A typical example is the BRM (BRanch and Mark return location) instruction, which, for compatibility with the memory protect feature, requires all subroutine linkage to be stored in a remote unprotected area. Inclusion of a "return location register" in the processor, with "Branch to Return Register" and "Store Return Register" instructions would reduce the programming effort for each program or subroutine by two instructions, with corresponding savings in programming cost and in memory requirements. As the size of the software package increases, the savings may well surpass the additional hardware development costs.

The Software Support System is the tool with which the programmer prepares the spacecraft software. The baseline support system for the AOP is based on the METAPLAN system, and operates in a batch mode, which requires substatial "load and wait" operations. Conversion of the support systems to time share operation would permit interactive program, test, and edit functions at a programming station, with considerable time savings. Again, as the size of the software package increases, the savings may well surpass the system change costs.

Similarly, development of a compiler for the AOP to permit the use of a higher order language would reduce the programming effort required for a given function, with a penalty in memory required and running time. A major benefit would result if the higher order language chosen were one in which desireable software from other programs were available.

COST DATA SUMMARY

The cost of developing the software for the EOS can be visualized in the blocks shown below. Development of the software is split into two segments on the basis of the end use:

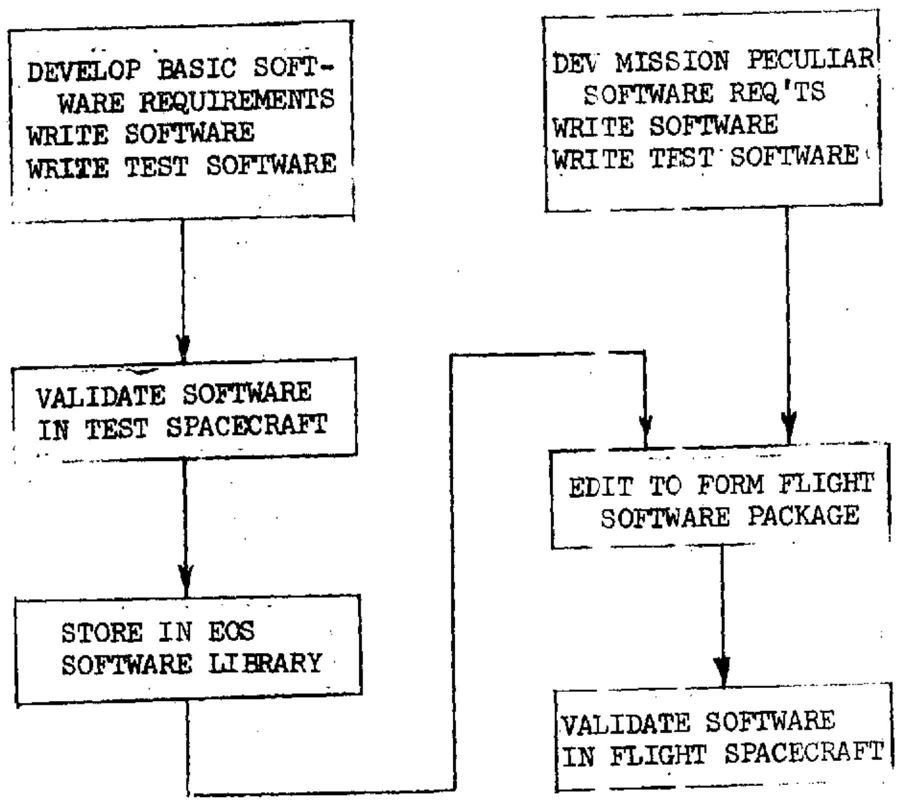

Basic Software is intended to be applicable to the software packages for all EOS spacecraft, and thus will be tailored to achieve compactness and broad compatibility. The Mission-peculiar software is intended for use with the spacecraft for a specific mission, and will contain the adaptations and additions to make the Basic Software function for the specific mission.

The non-recurring costs for the development of these software blocks are estimated:

Basic Block	12 Man-years
Mission-peculiar block	6 Man-years

Note that for mission-peculiar software, this cost is incurred for each new mission.

Validation of the Basic software is estimated to require an additional 8 man years. This process includes operation in a test spacecraft and the attendant testing and software rework. After validation, the Basic software will be available in the EOS library for use in the development of software for specific missions.

Editing the library version of the basic software in combination with the Mission-peculiar software will generate a spacecraft software package for the specific mission. This software link-editing is actually an internal step in the debug and rework process which leads to validation, and is not costed separately.

Validation of the spacecraft software is performed in the actual flight spacecraft computer, and includes the required de-bug and rework of the Mission-peculiar software. This process, including the link-editing required to produce the final software package, is estimated to require 4 man-years. Software maintenance of the validated software will be required to accommodate minor changes in hardware, modifications system requirements and repair of system and software bugs. This effort can be expected to continue from the installation of the software before launch through the operating life of the satellite.

7.1 SPACECRAFT AUTONOMY

Spacecraft Autonomy, for the purposes of discussion is defined as the performance by the spacecraft of system functions with no requirement for intervention by ground support facilities. There are obvious limitations to autonomy: For each function, either assurance from previous flight tests or suitable ground backup methods should be available, at least during the early operational stages. The level to which functions are assigned to the spacecraft rather than ground facilities must be selected with reference to the qualities of the resulting system:

- System costs
- System reliability
- System safety
- System function

System cost as a function of autonomy can be described in terms of fixed and recurring changes; the fixed costs of preparing a computer program to perform a specific function are perhaps twice as great for the satellite computer as for a ground computer, primarily because of the triple constraints of real-time operation, memory limitations, and running time limitations. The actual memory costs for a given function tend to be roughly the same since the lower memory costs of the ground computers are offset by the relatively large bulk of the compiler-generated programs. Recurring charges for operators and machine time for ground computers however, have no counterpart in the satellite computer; power and installation costs are fixed once a computer installation is established. As a result, any function which can be eliminated from the required ground computations results in an overall system cost saving.

System Reliability as a function of autonomy depends mostly on the susceptability of the data to transmission errors between the ground command source and the satellite command performance. For each function which requires up-or-down-link, the point in the functional flow path which requires the least frequent transmission of the least amount of data is the appropriate ground/satellite dividing point for maximum reliability.

Safety considerations, as far as the EOS autonomy is concerned, are limited to the possibility of operations which would endanger a Shuttle crew during a maintenance and resupply mission, or, in a different context, operations which would result in complete loss of the satellite. The completely "autonomous" failure mode in which the spacecraft seeks a stable but non-functioning attitude and awaits repair must not be compromised by either ground or satellite functions if safety considerations are to be met.

System Function is a matter of fulfilling the requirements of the overall system within the accepted tolerances. In the establishment of a given system design, some accommodation in the tolerances themselves may be required to achieve the optimum combination of system qualities.

7 Spacecraft Function Selection

This section considers the level of autonomy appropriate for a series of spacecraft functions. The functions chosen for examination are those which by their nature require interaction between ground and spacecraft.

Each function is described in terms of overall approach, options in autonomy level, and rationalization of a preferred approach. Implementation of the chosen approach is described in section 3.2.9.3 and is the basis for the software memory budget presented in section 3.2.9.4.

RGA Calibration Method

The RGA (Rate Gyro Assembly) contains three (or more) rate integrating gyros which measure the attitude changes of the spacecraft. Each gyro output is subject to errors of bias and scale factor which if uncorrected would lead to spacecraft attitude errors after some time of operation. The correction for bias and scale factor must be kept up to date during mission operations in order to keep attitude errors within tolerance.

Measurements of the attitude offsets can be made by ground operations in the following sequence:

1. Command (by uplink) a suspension of star-tracker attitude correction. This will permit gyro errors to build up in a recognizable pattern.
2. Analyze returned image data for build-up of pitch, roll or yaw offset error.
3. Compute appropriate calibration change for each gyro.
4. Command (by uplink) calibration changes.
5. Command (by uplink) resumption of star-tracker attitude compensation.

Aboard the spacecraft, a series of operations by the OBP (On-Board Processor) can detect and correct for gyro bias and scale error:

1. Collect star-tracker offset commands, determine long-term average attitude correction. Long-term error is symptom of gyro bias.

2. Compute appropriate calibration change for each gyro.

3. Change gyro calibration.

Although the fixed costs for the two methods are probably about the same, operating costs for the groundbased process have no counterpart in the on-board process: costs for full autonomy are less.

The system reliability of the two gyro calibration methods is approximately the same except for the possibilities of bad commands arriving at the spacecraft because of transmission errors: the autonomous system is slightly more reliable.

System safety is affected in either system if large-scale gyro corrections upset attitude control during maintenance or resupply processes: The non-autonomous system is slightly safer, since the control link may be more easily disabled than the OBP during maintenance.

System function during the ground-based calibration is degraded by the turn-off of the precision star-tracker reference and the build-up of attitude error. The autonomous method results in comparatively smooth changes which will be imperceptible from the experiment point of view: the autonomous system is functionally preferable.

STAR-TRACKER DATA HANDLING

The star-tracker of the EOS attitude control system provides the precision reference which permits precise pointing to a geometric vertical. Outputs of the tracker when an observable star is within its field are:

- o Lock-on signal
- o Star magnitude
- o X offset of the star from the central axis
- o Y offset of the star from the central axis

Ground utilization of the star-tracker data for precision attitude control requires:

1. Stable (rate gyro reference) control of spacecraft attitude as a background for star-tracker corrections
2. Downlink of star-tracker outputs with associated time-tags
3. Latitude and longitude of spacecraft computed for the times of sighting
4. Computation of direction of star sight
5. Identification of sighted star and evaluation of the errors of the sighting
6. Determination of pitch, roll and yaw components of the errors
7. Computation of attitude correction commands
8. Command (by uplink) to add correction to individual axes

The corresponding OBP process requires basically the same sequence of operations with the exception of the downlink of star sighting data and the uplink of correction commands. The OBP has the advantage of operating in real time so that star sightings which are too short can be abandoned without further handling, and so that corrections can be made while the attitude errors are still small. Problems of the star tables to be used will probably be solved differently in ground-based and on-board programs; advantage can be taken of the ground-based computer's size to permit the use of planet sightings for attitude reference. In the on-board programs, the star tables will omit reference stars in the ecliptic vicinity so as to avoid any possibility of associating planet sightings with actual stars. Sun and moon sightings are assumed to be avoided by shuttering the star tracker.

System costs for actual software are about equal for ground-based or on-board programs; operation of the ground-based system at the required rates, however, will require very nearly full time software support, with its attendant costs: costs for full autonomy are less.

System reliability for the two star-tracker methods is approximately the same except for the additional risk of bad data transmitted through the downlink or of bad corrections arriving at the spacecraft because of transmission errors: the full autonomous system is more reliable.

System safety is not affected by the star-tracker system.

The system function of the ground-based star-tracker data handling system is poorer than the on-board system because of the intermittent nature of the application of corrections. This drawback can be accommodated by transmission of the computed attitude misalignments to the data reduction facility for correction of the returned images. The system performance of the two approaches is equivalent if this additional cost and effort is accepted.

EPHEMERIS GENERATION

POSITION COMPUTATION

The functions of ephemeris generation and position computation are required to determine the position of the spacecraft at any instant. The ephemeris generation function, by multiple sightings and orbit modelling, determines the elements of the orbit at some (past) reference time, and the position computation function propagates these elements to determine the position at the desired instant. Each function, though highly analytic, must be fine-tuned by empirical methods to achieve the accuracy desired by the EOS dsign.

Emphemeris generation requires as a data source many sightings either of the spacecraft from known measuring stations or of surveyed landmarks or beacons from the spacecraft. Since observations from the spacecraft require either a landmark recognition instrument or a instrumented beacon network, ephemeris generation is not feasible for the current spacecraft program, since these support elements are not available. Thus ground computation of orbit elements is the preferred method, at least for the current program.

Position of the spacecraft is required for a number of functions which are also candidates for on-board operations:

- o Star-sighting data reduction
- o Experiment start and stop control
- o Downlink and uplink data transmission control

- o Experiment (HRPI) and antenna pointing
- o Experiment data tagging

Computation of the spacecraft position requires either solution of a multi-variable trigonometric formula or extrapolation by incremental integration of the position vector of the spacecraft under the influence of estimated perturbing forces. Either method requires initial data in the form of an array which contains the measured ephemeris information, and produces position estimates which approximate the true position within an error which increases as a function of time from the last array update. The rate of error buildup and the level of acceptable error determine the time interval permitted between array updates. For the ground computation system the next array update must await the next satellite sighting and ephemeris computation; for the on-board system, partial array update may be made as a function of horizon sensor data or of orbit sunrise or sunset timing error.

The cost of developing software for ground-based or on-board position computation is roughly equivalent, but the system operation of the ground-based method requires near-continuous manning with its associated costs: the costs for spacecraft autonomy are less.

The reliability of both systems is dependent upon the reliability of the ephemeris data with which it is fed: the two systems are equivalent.

System safety is not affected by the position computation function.

System function is slightly better with on-board computation since partial corrections between array updates are possible: the autonomous system is preferable.

ORBIT COUNTING

Orbit counting is the process of identifying the particular orbit which is current, as an identifier of housekeeping information and experiment data. It is actually a representative of a series of minor accounting tags which permit handling of spacecraft data on the ground.

Ground computations are handled on a batch basis. Continuity from the data of one batch to the next must be based on tape storage and playback. As a consequence, human errors in the collection and loading of accounting tags may occur.

On-board computations are performed on a real time basis. As a consequence, accounting tags such as orbit number are handled continuously as long as the computer remains active.

Cost, system safety and system function are not affected by the choice between on-board and ground-based orbit-count routines. The reliability of the onboard function is superior since it avoids the possibility of data loss due to human error: spacecraft autonomy is preferred.

ANTENNA STEERING

The wideband antennas for experiment data downlink require steering to align them with the ground antennas for satisfactory downlink gain.

Ground control of wideband antenna steering will require a sequence of steps:

1. predict the time and ground path of the next pass of the spacecraft over the ground station antenna.
2. prepare a sequence of spacecraft commands which will steer the antenna during the pass and turn the transmitter on and off
3. transmit the command sequence to the spacecraft through the command uplink
4. at the predicted time, the command handling routine of the OBP will issue the commands to the antenna drives and the transmitter

The on-board process for antenna steering requires a similar sequence of operations:

1. at intervals, the OBP will scan ahead along its ground track, checking for the values of latitude and longitude tabulated for ground receiving stations.
2. when an approaching ground station is found, the OBP compute and execute commands to steer the spacecraft antennae
3. when contact is made, turn on transmitters

As with the star-tracker service function, the major differences between on-board and ground-based computation are:

- o higher cost of ground-based operations
- o possible loss of control due to uplink command errors

7.3 Function Descriptions

The functions to be performed by the on-board computer of the EOS are listed in Table 7-1 under three general classifications:

- o Basic software,
- o Adaptable Basic Software,
- o Mission Peculiar Software

The classifications refer to the extent to which the library version of the software must be modified to be suitable for a specific EOS mission. Basic software, aside from program linkages and priority schedules, requires no modification from mission to mission, and thus can be link edited into a computer load tape with little expended manpower. Adaptable basic software, while it can be used in library form, may require more involved modifications for some missions. Mission Peculiar software will require complete programming effort in its preparation; for missions using common experiment packages, however, the library form of the sftware may be used on subsequent missions.

GRUMMAN

TRADE STUDY REPORT

TITLE	TRADE STUDY REPORT NO.
SPACECRAFT AUTONOMY/HARDWARE VS SOFTWARE	7
	WBS NUMBER 1.2.1.2.2

TABLE 7-1 SPACECRAFT COMPUTER FUNCTIONS

	FUNCTION	MEMORY (18-Bit Words)
BASIC	Executive	2100
	Self-Test	200
	Program Change	200
	Command Handling	4000
	Mode Control	800
	OPS Scheduling	1200
	Data Compression	400
	History	1000
	Sit Assessment	300
	Comp Dump	100
	Stabilization	800
	Position Comp	1600
	Sub-Sys Service	1800
ADAPTABLE BASIC	Downlink	800
	Guidance	300
	Sensing	800
	Pre-Launch Test	4000*
	Pre-Maneuver Test	600
	Syst. Monitor	800
	Syst. Troubleshoot	1200
MISSION PECULIAR	Experiment	400
	Exp Control & Maintenance	2600
	Antenna Steering	700
	Exp Data	600
	TOTAL	23300

* Uses command handling memory area

PREPARED BY	GROUP NUMBER & NAME	DATE	CHANGE LETTER
R. V. MacMillan	501 Software Dev.		REVISION DATE
APPROVED BY			PAGE 7-18

GAC 3711 3-72

A detailed breakdown of the size estimates for the individual functions of Table 7-1 is made in Section 7-4, with the elements tabulated by function rather than by library status.

The allocations of memory for the functions are made on a "bare-bones" basis; no allowance has been made for program growth or for defensive programming to allow for difficulties caused by bad inputs or incorrect data. Note that the 4000 words for pre-launch checkout is expected to occupy the command handling buffer area prior to launch, and will be overwritten by stored flight commands at launch time.

7.4 SOFTWARE BUDGETS

The functions of the on-board software have been divided into six groups for estimating purposes:

- Computer Support Functions
- System Support Functions
- Data Handling
- Spacecraft Operations
- Experiment Operations
- System Test

Each group is described in the following text, and the characteristics of the group members are tabulated in Table 7-2.

GRUMMAN

TRADE STUDY REPORT

TITLE

SPACECRAFT AUTONOMY/HARDWARE VS SOFTWARE

TRADE STUDY REPORT NO. 7

WBS NUMBER 1.2.1.2.2

TABLE 7-2 SOFTWARE MEMORY BUDGETS

FUNCTION	18-BIT WORDS	RUN TIME µSEC	REP RATE /SEC	µSEC/SEC
COMPUTER SUPPORT FUNCTIONS				
EXECUTIVE	2100	—	—	5017
SELF-TEST	200			
PROGRAM CHANGE	200			
SYSTEM SUPPORT FUNCTIONS				
COMMAND HANDLING	4000	200	60	12000
MODE CONTROL	800	200	2	400
OPERATION SCHEDULING	1200	120	10	1200

PREPARED BY R. V. MacMillan

GROUP NUMBER & NAME

DATE

CHANGE LETTER

REVISION DATE

APPROVED BY

*GAC 3711 3-72

GRUMMAN

TRADE STUDY REPORT

TITLE	TRADE STUDY REPORT NO.
SPACECRAFT AUTONOMY/HARDWARE VS SOFTWARE	7
	WBS NUMBER 1.2.1.2.2

TABLE 7-2 SOFTWARE MEMORY BUDGETS

FUNCTION	WORDS	RUN TIME	REP RATE	μSEC/SEC
DATA HANDLING				
DATA COMPRESSION	400	400	1	400
HISTORY	1000	5000	neg.	—
SITUATION ASSESSMENT	300	500	.2	100
EXPERIMENT	400	6000	.1	600
DOWNLINK	800	2000	neg.	—
COMPUTER DUMP	100	20-200000	neg.	—
SPACECRAFT OPERATIONS				
STABILIZATION	800	2400	10	24000
GUIDANCE	300	2400	.1	240
POSITION COMPUTATION	1600	20500	.01	205

PREPARED BY	GROUP NUMBER & NAME	DATE	CHANGE LETTER
R. V. MacMillan			
			REVISION DATE
APPROVED BY			PAGE 7-21

GAC 3711

TABLE 7-2 SOFTWARE MEMORY BUDGETS

FUNCTION	WORDS	RUN TIME	REP RATE	μSEC/SEC
(SPACECRAFT OPERATIONS CONTINUED)				
SENSING	800	6800	1	6800
SUB-SYSTEM SERVICE	1800	9500	.1	950
ANTENNA STEERING	700	1200	.01	7
EXPERIMENT OPERATIONS				
EXPERIMENT CONTROL EXPERIMENT MAINTENANCE	2600	2500	1	2500
EXPERIMENT DATA	600	1500	.1	150

GRUMMAN

TRADE STUDY REPORT

TITLE	TRADE STUDY REPORT NO. 7
SPACECRAFT AUTONOMY/HARDWARE VS SOFTWARE	WBS NUMBER 1.2.1.2.2

TABLE 7 -2 SOFTWARE MEMORY BUDGETS

FUNCTION	WORDS	RUN TIME	REP RATE	μSEC/SEC
SYSTEM TEST				
PRE-LAUNCH	(4000*)	NA	NA	NA
PRE-MANEUVER	600	1400	neg.	—
SYSTEM MONITOR	800	6200	.1	620
SYSTEM TROUBLESHOOT	1200	4100	neg.	—
TOTALS	23300			55189

*occupies command handling area before launch

PREPARED BY	GROUP NUMBER & NAME	DATE	CHANGE LETTER
R. V. MacMillan			
			REVISION DATE
APPROVED BY			PAGE 7-23

GAC 3711
3-72

Computer Support Functions

These functions are those which are required for the operation of the spacecraft computer. The EXECUTIVE schedules the running of other functions and supplies support subroutines such as trigonometric functions for the use of other programs The memory requirement for the Executive is taken as 10 percent of the memory required for the remainder of the software package, a typical proportion for single processor real-time computers. The Executive running time will actually consume all idle time of the processor, but the 10 percent proportion is used to permit comparisons. The associated self-test and program change routines, though of negligible size, are necessary for ground monitoring and control of the computer.

System Support Functions

The tasks of COMMAND HANDLING, MODE CONTROL and OPERATION SCHEDULING are self-explanatory; the allocation for Command Handling memory is made equal to a full "page" of computer memory in order to accommodate the maximum number of ground commands without having to change the page register. At three words per command, this permits storage of approximately 1300 commands. The command storage area will be unused before launch, permitting computer system test routines to occupy this area during prelaunch operations.

Data Handling

The Data Handling functions monitor and classify spacecraft data for ground monitoring of spacecraft operations. The DATA COMPRESSION routine provides a set of numbers to represent each stream of measurement values: maximum, minimum, mean and variance computed with a "Fading Filter" routine whose filter constant is chosen for the particular data. The HISTORY buffer accumulates time-tagged event codes generated by other routines to present a compact but detailed record of operational events since the last downlinked data transmission. The SITUATION ASSESSMENT routine evaluates data and classifies the status of the spacecraft for use by the MODE CONTROL function. EXPERIMENT is a routine allocated to examine spacecraft data for those engineering experiments which require only the spacecraft sensors for a source. The DOWNLINK function formats data for telemetry output, and initiates the clearing of the data compression and history files after each downlink transmission is completed. COMPUTER DUMP places selected portions of the computer memory on the downlink for ground examination.

Spacecraft Operations

The STABILIZATION routine provides the basic attitude control of the spacecraft using rate information from the RGA (Rate Gyro Assembly) and stabilization gains selected by the Mode Control Function. The GUIDANCE routine combines the error terms generated by the sensing function, and, depending on Mode Control, issues steering signals to the stabilization routine to permit precision control of spacecraft altitude.

The SENSING routines manage and extract data from the various spacecraft sensors to provide spacecraft attitude measurements. The SUB- SYSTEM SERVICE routines provide monitoring and operation of thermal, solar array, power and other spacecraft worker functions for specific hardware devices. The ANTENNA STEERING routine provides guidance commands for the steerable antennas.

Experiment Operations

The EXPERIMENT CONTROL and EXPERIMENT MAINTENANCE routines provide start up and run sequences for the experiments and monitor the experiment diagnostic outputs, taking corrective steps where necessary. The EXPERIMENT DATA routine provides the same services for the experiment data transmission system.

System Test

The PRE-LAUNCH TEST routines, loaded in the unprotected command buffer of the OBP, perform prelaunch readiness tests of all equipment which interfaces with the computer. Although the buffer area is limited to 4K words, a series of loads may be used to permit as many tests as are found appropriate. The fact that a minimum of external test equipment is required makes launch operations less complex. After completion of the tests, the buffer becomes available for normal command storage. The PRE-MANEUVER TEST verifies the proper status of all subsystems prior to orbit maneuvers, permitting ground evaluation of the status through examinations of the reply to a single command. The SYSTEM MONITOR provides continuous testing of spacecraft subsystems during otherwise idle time of the OBP. The systems tested are those which may be evaluated without disturbing the current tasks of the spacecraft. The SYSTEM TROUBLESHOOT function provides further test of the more critical subsystems when troubles are indicated either by the System Monitor or by ground examination of returned data. Each test is performed while a workaround routine takes over for the equipment being tested. In case of true failures, some of these workarounds may be utilized for continued mission operations.

SYSTEM TRADE
STUDY NO. 8

GRUMMAN

TRADE STUDY REPORT

TITLE	TRADE STUDY REPORT NO. 8
ELECTRONIC TECHNOLOGY	WBS NUMBER

See Report No. 3, Section 6.8

PREPARED BY	GROUP NUMBER & NAME	DATE	CHANGE LETTER
			REVISION DATE
APPROVED BY			PAGE 8-1